Regulation of the Protein Kinase C - Related Kinase Family

Peter Flynn

This thesis is submitted in partial fulfilment
of the requirements for the degree of

Doctor of Philosophy

University College
University of London

August 1999

Imperial Cancer Research Fund
44 Lincoln's Inn Fields
London
WC2A 3PX

ProQuest Number: 10631508

All rights reserved

INFORMATION TO ALL USERS
The quality of this reproduction is dependent upon the quality of the copy submitted.

In the unlikely event that the author did not send a complete manuscript
and there are missing pages, these will be noted. Also, if material had to be removed,
a note will indicate the deletion.

ProQuest 10631508

Published by ProQuest LLC (2017). Copyright of the Dissertation is held by the Author.

All rights reserved.
This work is protected against unauthorized copying under Title 17, United States Code
Microform Edition © ProQuest LLC.

ProQuest LLC.
789 East Eisenhower Parkway
P.O. Box 1346
Ann Arbor, MI 48106 – 1346

Abstract

Protein phosphorylation and its control by the action of protein kinases and phosphatases has been shown to play an essential role in signal transduction pathways and hence cell functions. More recent discoveries have implicated GTP hydrolysing enzymes and lipids; adding to the depth of complexity required for the balance and amplification of signals. The Protein Kinase C (PKC) family of kinases can be subdivided based on their requirement for Ca^{2+}, Diacylglycerol (DAG) and phospho-lipids. Previously, a PCR-based screen for novel PKC isoforms produced two new gene products, which were subsequently fully cloned: Protein Kinase C–Related Kinases (PRK 1 and 2). These were seen to be highly homologous to the PKCs in their kinase domains but had novel N-terminal regulatory regions. Their serine/threonine kinase activity was insensitive to both Ca^{2+} and DAG but was activated *in vitro* by limited proteolysis and polyphosphoinositides PtdIns(4,5)P_2 and PtdIns(3,4,5)P_3.

The aim of this thesis was to investigate the control of the PRKs. Initial work focused on the potential interaction between the PRKs and Small GTPases of the Rho family, and assessed what role such an interaction would have on the kinase's activity. A variety of *in vitro* techniques were used to characterise the site of contact on both the PRKs and the Rho proteins. The nucleotide-specificity of binding was also analysed. The definition of the Rho binding region within the PRKs novel regulatory region (Homology Region 1) suggested the GTPase disrupted an intramolecular, pseudo-substrate site interaction with the kinase domain. However, our data showed only a two-fold increase in the PRK's kinase activity when co-expressed in cultured cells with an active Rho. Nevertheless we were able to show translocation of PRK to early endosomes with RhoB overexpression and further that a hyperphosphorylated form of the

kinase existed within this sub-cellular compartment. This suggested that other components were involved in the control of the kinase.

On consideration of the similarities between members of the AGC kinase sub-families within the activation-loop, the involvement of the upstream kinase PDK1 in PRK activation was assessed. Co-expression studies in cultured cells allowed the definition of a Rho-dependent interaction between the two kinases and a three-way co-localisation of PRK, RhoB and PDK1 on early endosomes. An activation loop phosphorylation event was analysed using phospho-specific polyclonal antisera. *In vitro* and *in vivo* studies using both wild type and mutant PRKs demonstrated that this phosphorylation event was necessary for kinase activity. It has thus been shown that both Rho family GTPases and PDK kinases, which depend on the products of PI3-Kinase activity, are required for the cellular localisation and activation of the PRK sub-family of kinases.

Acknowledgements

Not wishing to sound like an award ceremony speech, there are many people to thank for their help and support over the last 4 years. Primarily I would like to thank Peter for his guidance, support and unbelievable enthusiasm. While saying 'TA very much' to all the members of the Lab. that I've worked with over the years I would especially like to mention Harry for his time, patience and wonderful singing voice, Ruth for her advise, Frank and Rudiger for being a constant source of amusement (and amazement) and thanks to Graeme Card for help with the HR1 structure. Outside of the Lab. I would like to thank those people that had to put up with my moods and habits, and my friends (you know who you are) for being a constant source of distraction. Finally, in true BAFTA-style, I'd like to thank my family for their constant support and confidence in me. Hope to see you all on the West Coast for a bit of healthy living.

Table of Contents

Chapter 1 - Introduction

Chapter 7 - Discussion

Appendices

List of Figures

Abbreviations

The abbreviations of both genes and their products will be given as they are mentioned within the text.

ADP	Adenosine 5'-diphosphate
ATP	Adenosine 5'-triphosphate
BSA	Bovine Serum Albumin
cAMP	Adenosine 3', 5'-cyclicmonophosphate
cGMP	Guanosine 3', 5'-cyclicmonophosphate
C. elegans	*Caenorhabditis elegans*
Ci	Curie
cpm	counts per minute
DAG	Diacylglycerol
DMSO	Dimethyl Sulphoxide
DNA	Deoxyribonucleic acid
dpm	dissintergrations per minute
DTT	Dithiothreitol
ECL	Enhanced chemiluminescence
EDTA	Ethylene diamine tetra-acetic acid
EGF	Epidermal Growth Factor
EGTA	Ethylene glycol-bis-tetra-acetic acid
FCS	Foetal Calf Serum
g	gram
GAP	GTPase Activating Protein
GDI	Guanine nucleotide Dissociation Inhibitor
GDP	Guanosine 5'-diphosphate
GEF	Guanine nucleotide Exchange Factor
GST	Glutathione S-Transferase
GTP	Guanosine 5'-triphosphate
GTPase	GTP hydrolase
HEPES	N-(2-hydroxyethyl)-piperazine-N'-(2-ethanesulphonic acid)
$Ins(1,4,5)P_3$	Inositol (1,4,5) trisphosphate
IPTG	Isopropyl-β-D-thiogalactopyranoside
kb	Kilobase
kDa	Kilodalton
LPA	Lypo-phosphatidic acid
M	Molar
m	milli
μ	micro
MAPK	Mitogen Activated Protein Kinase
MBP	Myelin Basic Protein
n	nano

p	pico
PA	Phosphatidic Acid
PAGE	Polyacrylamide Gel Electrophoresis
PBS	Phosphate Buffered Saline
PCR	Polymerase Chain Reaction
PC	Phosphatidylcholine
PS	Phosphatidylserine
PDGF	Platelet Derived Growth Factor
PH	Plecstrin Homology
PMA	Phorbol myristate acetate
PtdIns	Phosphatidylinositol
rpm	revolutions per minute
RTK	Receptor Tyrosine Kinase
S. cerevisiae	*Saccharomyces cerevisiae*
SDS	Sodium dodecyl sulphate
SH2/3	Src Homology domains 2/3
TBS	Tris-buffered Saline
Tris	Tris (hydroxymethyl) amino methane
v/v	volume / volume
w/v	weight / volume
X-Gal	5-Bromo-4-chloro-3-indyol-b-D-galacto-pyranoside

Chapter 1 - Introduction

1.1 Signal Transduction

The mode by which information is transmitted from the extracellular environment to the nucleus or protein machinery of the cell has been a subject of concerted research for several decades. The study of genetic mutations or viral genes that disrupt normal cell function coupled with the advent of molecular cloning technology has allowed the identification of a multitude of signalling molecules both in humans and lower organisms. An enormous amount of progress has been made towards the understanding of controlled events initiated by kinase and non-kinase proteins, GTPases, lipids and ions in these signalling events. However, it would seem that a more in-depth knowledge of the intricate communication between these elements is required prior to achieving truly effective methods of manipulating defective systems. As an introduction to this thesis some well characterised signalling mechanisms will be described with an attempt to highlight both the relevance to the present study and areas where the complete picture is unclear. Starting with brief descriptions of the general methods of signal transduction such as protein-protein interactions and the action of lipid second messengers; I will further describe the modes of small GTPase action and the regulation of serine / threonine kinases in greater detail.

1.2 Mechanisms of Signal Transduction

1.2.1 Protein - Protein Interactions

The direct interaction between the protein components of a signalling cascade is one of the primary modes by which information is transduced. The interaction may translocate specific enzymes to regions rich in substrate or directly activate them by disruption of an inhibitory complex. Conversely inhibitory interactions can keep pathways dormant or turn off active signals. Examples of such events are given below.

A variety of conserved domains have now been demonstrated to mediate interactions to related target sequences. SH2 and PTB domains specifically bind short stretches of sequence that contain phosphorylated tyrosine residues. The SH2 (Src Homology domain 2) domain was originally identified in the non-receptor tyrosine kinase Src, but these motifs have now been found in a wide range of signalling molecules, including PLC-γ, p120 Ras-GAP, SHP-2, the p85 subunit of PI3-kinase and the adaptor proteins such as Nck and Grb2 (reviewed by (Pawson, 1995)). The high affinity binding of SH2 domains to target sequences is specified by the phosphotyrosine itself and the residues C-terminal to it. There are four groups of SH2 domains based on target specificity (Sudol, 1998). PTB (p-Tyr-binding) domains generally recognise phosphopeptide motifs in which the phosphotyrosine residue is preceded by residues that form a β-turn and specificity is conferred by hydrophobic amino acids that lie five to eight residues N-terminal to the tyrosine. The insulin receptor substrate IRS-1 is an example of a PTB-containing protein (Pawson and Scott, 1997).

Src Homology 3 (SH3) domains were again originally identified in the Src proto-oncogene. Their binding sites consist of proline-rich peptides

approximately 10 amino acids in length. Studies using degenerate peptide libraries have indicated that SH3 domains have distinct binding preferences. These specificities are conferred by non-proline residues in the ligand (Pawson, 1995). Many proteins contain both SH2 and SH3 domains so enabling multiple interactions and complex formation. Several adapter proteins have been identified that contain multiple protein binding domains and act to link signalling molecules that contain one type of domain, examples being Shc, Grb2 and Nck. Other identified protein binding domains are, WW domains which are functionally related to SH3 domains and PDZ domains which are often present as multiple repeats in signalling proteins.

The most well characterised examples of complex formation due to these interaction domains is the recruitment of signalling proteins to the cytoplasmic domains of the growth factor receptor tyrosine kinases (RTK) or insulin receptors. Ligand stimulation of the growth factor RTK causes receptor dimerisation and transphosphorylation between the cytoplasmic catalytic domains on multiple tyrosine residues (reviewed by (Heldin, *et al.*, 1998)). The phosphotyrosines then act as a recruitment signal for a variety of signalling molecules which bind to the receptor scaffold at sites determined by the specificities of their SH2 domains. As illustrated in figure 1.1A, the resulting complexes initiate many signalling pathways. The recruitment of PI3-kinase via its p85 subunit results in a colocalization with activators and substrate, PtdIns(4,5)P_2. PLC-γ is also recruited and hydrolyses PtdIns(4,5)P_2 to inositol(1,4,5)trisphosphate and diacylglycerol which co-activate PKC via Ca^{2+} mobilisation and direct binding respectively. The adapter protein Grb2, which consists of one SH2 and two SH3 domains, binds either directly to the activated receptor or to the intermediate protein Shc via an SH2 domain and to the Ras nucleotide exchange factor Sos via an SH3 domain. The recruitment of Sos to the membrane results in Ras activation (see GTPase section of this Introduction). Negative regulators of signalling are also targeted to the

phosphorylated receptor: the Ras GTPase Activating Protein (GAP) contains two SH2 domains and its recruitment results in the inactivation of Ras; the tyrosine phosphatase SHP2 binds the receptor via two SH2 domains and may dephosphorylate it. The insulin receptor activation also leads to the recruitment of multiple downstream signalling molecules, however this is mediated through the scaffold proteins IRS-1 and IRS-2. These proteins interacts with the membrane through a Pleckstrin Homology (PH) domain (see below), and with the activated insulin receptor through a PTB domain (Pawson and Scott, 1997). The subsequent phosphorylation of the IRS-1 by the receptor results in target sites for the signalling molecules (see figure 1.1).

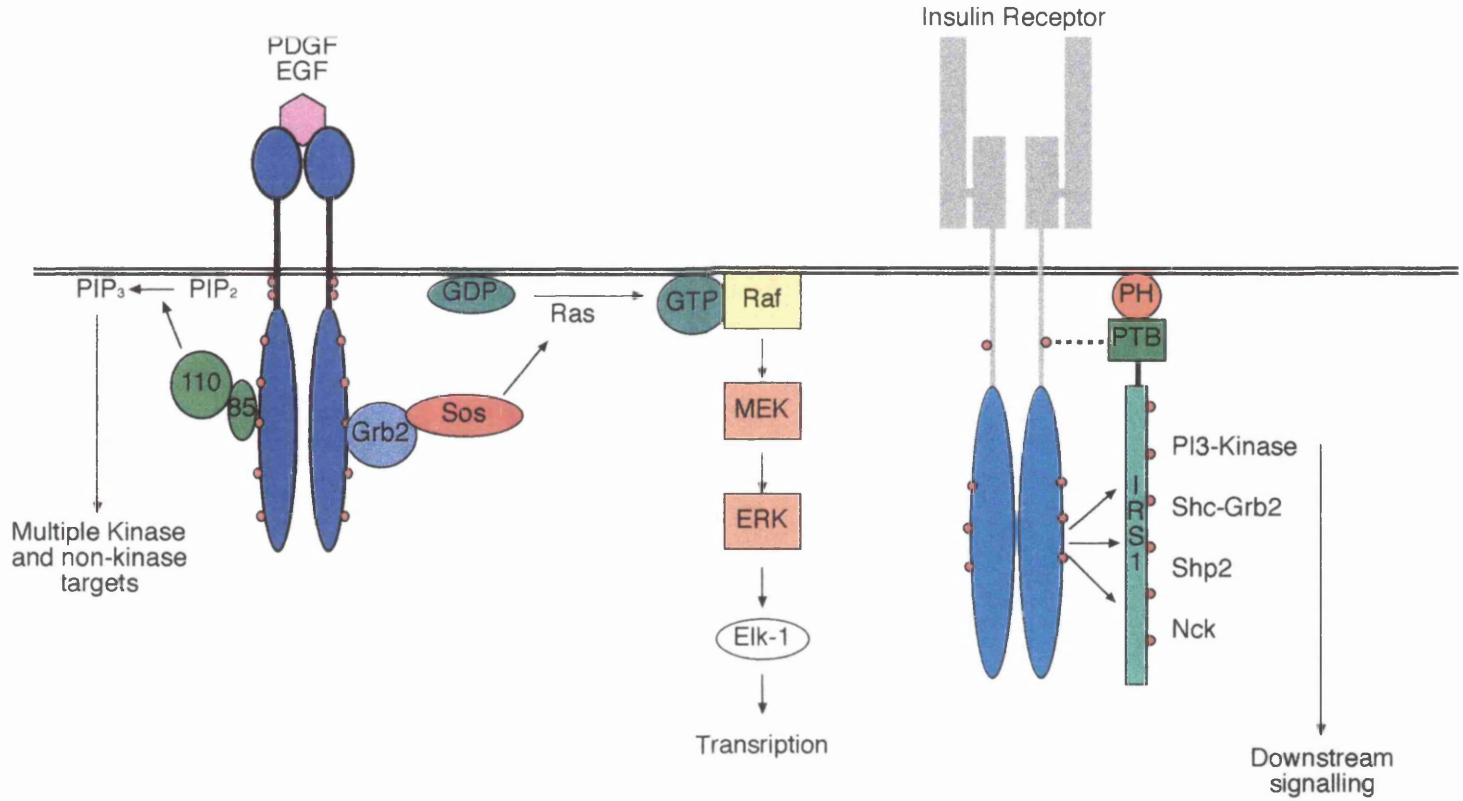

Fig. 1.1: Protein-Protein Interactions and Signal Transduction

An example of signalling complex formation through protein-protein interactions: the growth factor receptor tyrosine kinases directly recruit kinases and adapter molecules through phosphotyrosine-SH2 domain interactions, typified by the PI3-kinase interaction via its p85 subunit and the Grb2, Sos interaction. The resulting localisation of kinase and substrate or GEF and GTPase leads to the activation of multiple signalling events. The activated insulin receptor phosphorylates IRS-1 which is recruited via a PH domain interaction with the membrane and a PTB domain which binds to a specific phosphotyrosine on the receptor. Again SH2 domain proteins are recruited to the phosphorylated IRS-1 and downstream signalling events propagate.

1.2.2 Protein-Protein Interactions as Direct Activation Events

As discussed above the interactions between proteins can result in the translocation of enzymes to a site rich in substrate and activators. The activators may be specific lipids, protein kinases or GTPases. The exchange of GDP for GTP on Ras results in the recruitment of Raf-1 serine/threonine kinase to the plasma membrane. This translocation event was shown to be sufficient for Raf-1 activation (Leevers, *et al.*, 1994, Stokoe, *et al.*, 1994) and suggested that the only function of the kinase-GTPase interaction was to bring the former into contact with other membrane-localised activators. However, several lines of evidence point to a direct activational input from Ras into Raf-1, including the ability of a membrane-free complex of B-Raf and 14-3-3 proteins to be activated *in vitro* by Ras and the identification of Ras mutants that are able to interact with high affinity with Raf but not activate it (reviewed by (Campbell, *et al.*, 1998)). Ras is now known to interact with two distinct sites in the N-terminal regulatory region of Raf-1. The first site, referred to as the Ras binding domain (RBD), is between residues 51-131. The high affinity interaction with the RBD is required prior to the second contact which encompasses the conserved cysteine finger in Raf's cysteine rich domain (CRD). The CRD has also been implicated in interactions with other potential Raf activators; 14-3-3 protein and the lipids phosphatidylserine and ceramide (Morrison and Cutler, 1997). An interesting observation is that removal of the C-terminal kinase domain enables a Ras-CRD interaction to take place in the absence of Ras-RBD binding. Thus the CRD may well be masked by the kinase domain in the inactive kinase and the primary Ras interaction acts to open the structure allowing subsequent interaction events to take place. Other elements implicated in Raf-1 activation include 14-3-3 protein, lipids, tyrosine and serine/threonine phosphorylation events (Campbell, *et al.*, 1998). The active Raf-1 triggers the classical MAP kinase pathway which results in the transcriptional activation (Treisman, 1996).

1.3 Protein-Lipid interactions

As with protein-protein interactions lipids can facilitate both the translocation and activation of kinases involved in signalling net works. Several lipid binding domains have been identified each with affinities for specific lipid products, resulting in the complexity required for signalling systems.

1.3.1 C1 Domains

Several mammalian proteins contain C1 domains, most notably members of the classical and novel Protein Kinase C family (cPKC and nPKC). The domain sequence is defined by the presence of two zinc-fingers and mutation / deletion studies has shown the domain to interact with the tumour-promoting, PKC activators phorbol esters. Competition analysis has shown diacylglycerol (DAG) to interact with PKC at the same site (reviewed in (Mellor and Parker, 1998)). DAG is the lipid product of Phospholipase-C activity on PtdIns(4,5)P_2, and is a co-activator of the classical and novel PKCs (see below). Other proteins shown to contain a PMA-binding C1 domain include the Rac-GAP chimaerin, the Rac-GEF Vav and the protein kinase PKD.

1.3.2 C2 Domains

C2 domains are again found within the cPKCs along with many other proteins including synaptotagmins, phospholipases and GAPs (Ponting and Parker, 1996). The domain has been shown to confer Ca^{2+}-dependent phospholipid binding. Structural studies have suggested the Ca^{2+} interaction produces a conformational change which allows lipid headgroup binding (Mellor and Parker, 1998). The calcium independent PKCs and the PRKs contain C2-like domains that are missing residues required for Ca^{2+} binding. It is unclear whether these domains bind phospholipids even though several of the kinases containing them are seen to be lipid-activated (Palmer, *et al.*, 1995a).

1.3.3 Pleckstrin Homology (PH) Domains

Originally identified in pleckstrin, which is the major PKC substrate in platelets, PH domains are ~100 amino acid regions that have been shown to interact with both protein and inositol lipid targets, although their *in vivo* function is thought to be the binding of phosphoinositides. Over a hundred proteins have now been described to contain PH domains, with functions as diverse as serine/threonine and tyrosine kinases, GAPs and GEFs of small GTPases, lipid kinases, lipases and cytoskeletal components (Shaw, 1996). A common feature of many PH domain containing proteins is a membrane localisation requirement for function. The core structure of these domains is the same whereas three variable loops lie on a positively charged face, which has been shown to interact with both PtdIns(4,5)P_3 and the soluble Ins(1,4,5)P_3. To date the true specificity of the PH domains from most proteins remains unclear, although several have been shown to selectively bind PI3-kinase products over the much more abundant PtdIns(4,5)P_3 (Kavran, *et al.*, 1998). The membrane targeting and activation of two PH domain-containing kinases, PKB and PDK1 will be discussed later in this chapter.

1.3.4 FYVE Domains

The singly phosphorylated PtdIns3P has been seen to play a role in membrane trafficking and unlike the PtdIns(3,4)P_2 and PtdIns(3,4,5)P_3 is produced by the type III, Vps34-like kinases (see below). A specific domain target for this lipid has been identified in a number or yeast and mammalian proteins including the Early Endosomal Antigen 1 (EEA1), Vac1, a Rab effector involved in vesicle fusion and the PI5-kinases FAB1 and p255-PI5K. The crystal structure of the ~70 amino acid FYVE domain has recently been solved and displays a core secondary structure similar to the C1 domains (Misra and Hurley, 1999).

1.4 Signalling Intermediates

1.4.1 Intracellular Calcium

The modulation of the intracellular calcium concentration controls a wide variety of cellular and physiological processes. Rapid changes in cytosolic Ca^{2+} are produced by its regulated influx from the extracellular environment or release from intracellular stores. IP_3 is the major second messenger evoking Ca^{2+} release from intracellular stores and is a product of Phospholipase-C hydrolysis of PtdIns(4,5)P_2 (Berridge and Irvine, 1984). PLC-γ interacts with and is activated by growth factor receptor tyrosine kinases whereas PLC-β lies downstream of G protein-coupled receptors (Gawler, 1998). The soluble IP_3 interaction with its receptors results in a release of intracellular Ca^{2+} stores. The Ca^{2+} can co-activate cPKC isoforms along with DAG and phosphodiesterases via calmodulin.

1.4.2 cAMP Dependent signalling

The action of Adenylate cyclase converts ATP to cyclic Adenosine Mono-Phosphate (cAMP). This second messenger binds to the two regulatory subunits of cAMP-dependent protein kinase PKA that exists in an inactive state as a heterotetramer. The cAMP interaction results in the dissociation of the regulatory subunits, leaving the active catalytic subunits to stimulate downstream pathways. The action of phosphodiesterases cleave the 3' phosphate bond on the cAMP to give the inert AMP, resulting in the down regulation of the signal (Lehninger, 1988).

1.4.3 Lipid Second messengers

Diacylglycerol (DAG)

The agonist stimulation of most cell types results in a biphasic accumulation of DAG species. The initial rapid rise in polyunsaturated DAG, most notably 1-stearoyl-2-arachidonyl-DAG is due to the actions of phosphoinositide-specific PLC (β or γ), which hydrolyse PtdIns(4,5)P_2. The c/nPKCs are preferentially activated *in vitro* by these unsaturated forms of the lipid (Hodgkin, *et al.*, 1998). The signal is terminated by the action DAG-kinase which phosphorylates the DAG to produce PA, or the DAG-lipase catalysed deacylation of the lipid. The sustained phase of DAG accumulation mainly consists of saturated or monounsaturated DAGs derived from phosphatidylcholine (PC) (via the dephosphorylation of phosphatidic acid (PA) generated by phospholipase D (PLD) activity). PA generated by the action of PLD is required for LPA-stimulated stress fibre formation in PAE cells. The use of the *clostridium* toxin C3 has placed Rho GTPase downstream of PA on this pathway. A putative PC-PLC has been implicated in an alternative pathway for DAG production. However, a recent study has raised the possibility that sphingomyelin synthase, an enzyme that produces sphingomyelin and DAG from PC and ceramide, may be the *in vivo* target of a PC-PLC inhibitor (Luberto and Hannun, 1998).

Phosphoinositides

Phosphoinositides are 6-carbon rings linked by a phosphodiester bond to a glycerol backbone and hence to two hydrocarbon chains, the most common structures being sn-1-stearoly-2-arachidonyl (see figure 1.2A). The inositol ring can be specifically phosphorylated at either the 3, 4 or 5 positions producing a variety of lipid products. A schematic representation of these lipids and their routes of synthesis by specific phosphoinositide kinases,

phosphomonesterases and phosphodiesterases can be seen in figure 1.2B. Much of the work to define the specificities of the kinases and phosphatases has been completed *in vitro* and thus the true relative roles of these enzymes in the cellular system are assumed. However, there is convincing evidence that PtdIns(3,4,5)P_3 is synthesised in response to agonist stimulation by the action of type 1 PI3-kinase on PtdIns(4,5)P_2 (Hawkins, *et al.*, 1992, Stephens, *et al.*, 1991). Further, a lag in the agonist stimulated production of PtdIns(3,4)P_2 would suggest its production is predominantly via the action of 5-phosphatases on PtdIns(3,4,5)P_3. When the relative cellular levels of the lipids are compared it can be seen that the unphosphorlated phosphatidylinositol (PtdIns) is far in excess of all of the phosphorylated forms. While the single phosphorylated PtdIns3P is present at a constant level, possibly due to the kinase responsible for its formation being constitutively active (see below), both PtdIns(3,4)P_2 and PtdIns(3,4,5)P_3 levels are extremely low in unstimulated cells. The levels of these lipids rise within seconds of agonist stimulation of cell receptors suggesting a potential role in signalling processes (Stephens, *et al.*, 1993). Indeed both of these lipids are implicated in a variety of signalling processes including the translocation and activation of protein kinases and GTPase exchange factors. PtdIns(4,5)P_2 is another key signalling molecule both through its hydrolysis to IP_3 and DAG (Berridge and Irvine, 1984), and directly by its effects on the cellular cytoskeleton (reviewed in (Toker, 1998)). Its cellular concentration does not rise dramatically in response to agonist stimulation suggesting both that local increases in level are important and that the enzymes responsible for its production act to top up the pool of lipid rather than making it for immediate use. The recently characterised PtdIns(3,5)P_2 is seen to be constitutively produced in mammalian cells and its cellular levels in yeast increase dramatically on hyperosmotic shock (Dove, *et al.*, 1997, Whiteford, *et al.*, 1997). Further work in *S. cerevisiae* positively identified the product from the FAB1 gene to be the kinase responsible for its production from PtdIns3P (Cooke, *et al.*, 1998).

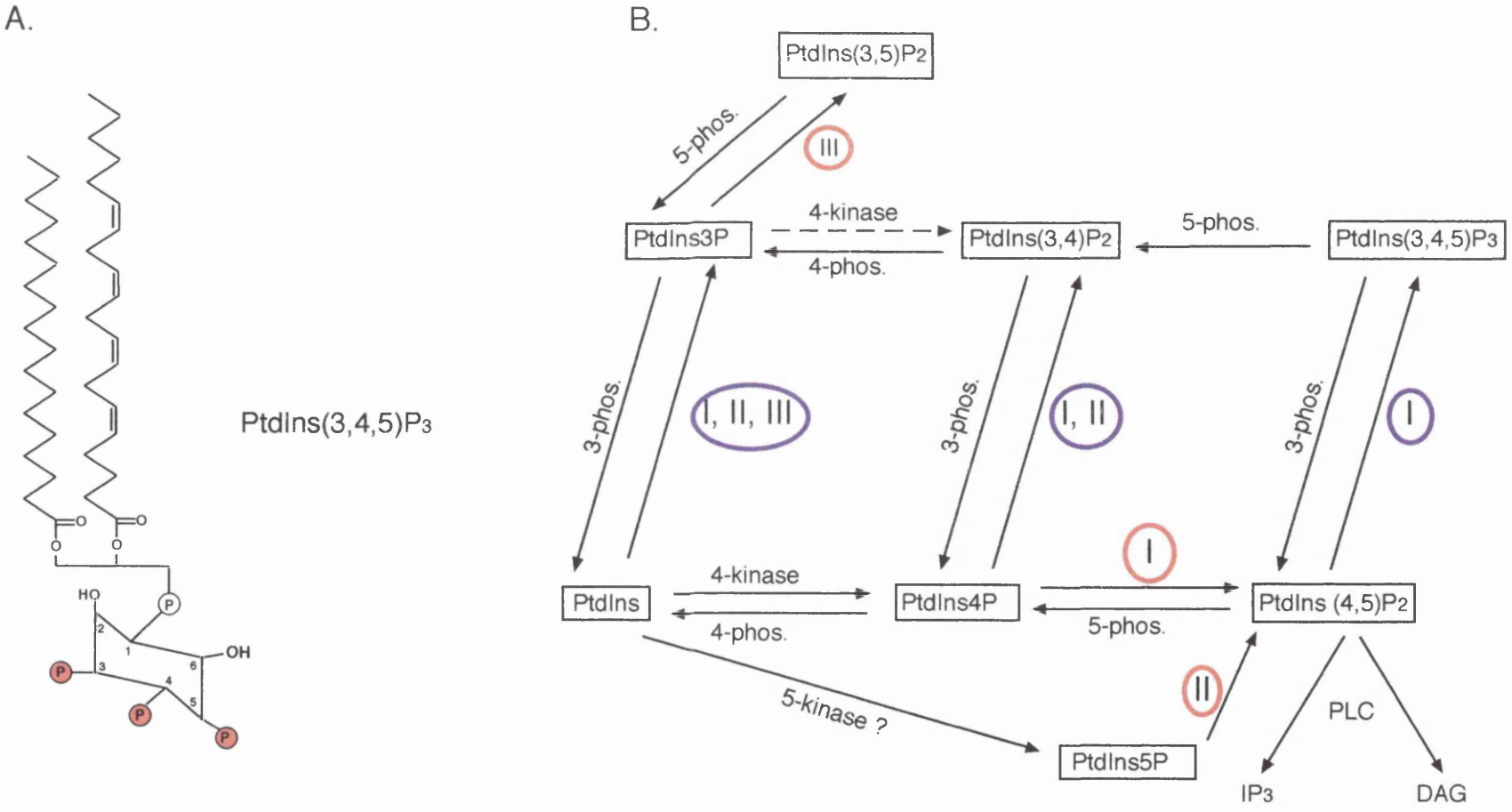

Fig. 1.2: Phosphoinositide Synthesis and Metabolism

A.) The structure of phosphatidylinositol (3,4,5) trisphosphate, with the relative positions on the inositol ring numbered and phosphate groups affected by kinase or phosphomonoesterase activity highlighted in red. The hydrocarbon tail shown is 1-stearoyl-2-arachidonyl; the most common naturally occurring form. B.) A schematic representation of the routes of phosphoinositide synthesis and metabolism. Many of the substrate specificities of the kinases and phosphatases have been described *in vitro* and thus may not represent the *in vivo* situation. PI3-kinases are denoted by type in purple circles and PI5-kinases are in red circles.

1.4.4 Phosphoinositide Kinases

1.4.4.1 PI4 and 5-kinases

The PI4-kinase activity can be stimulated by EGF treatment of fibroblasts and results in the formation of PtdIns4P from PtdIns. A PI4-kinase activity against PtdIns3P to form PtdIns(3,4)P_2 has also been described in platelets (Banfic, *et al.*, 1998). There are now over 10 gene products identified with PI4-kinase activity, including the two *S. cerevisiae* proteins Pik1p and Stt4p (Gehrmann and Heilmeyer, 1998).

There are now known to be 3 types of PI5-kinases, based on their biochemical properties. Type I and II both synthesise PtdIns(4,5)P_2 albeit by different mechanisms: the type I enzymes preferred substrate is PtdIns4P which it phosphorylates at the 5 position on the inositol ring (reviewed by (Anderson, *et al.*, 1999)). The type II enzymes have now been shown to phosphorylate PtdIns5P at the 4 position to form PtdIns(4,5)P_2 (Rameh, *et al.*, 1997). Thus a change in the nomenclature may be necessary. The type III enzymes are the previously mentioned FAB1-like activities that phosphorylate PtdIns3P to form PtdIns(3,5)P_2 (Cooke, *et al.*, 1998). While the mammalian homologue of FAB1 is yet to be characterised, an equivalent activity is seen in mouse fibroblasts (Whiteford, *et al.*, 1997).

1.4.4.2 PI3-kinases

The kinases responsible for phosphorylating the inositol ring at the 3 position so producing the second messengers PtdIns3P, PtdIns(3,4)P_2, and PtdIns(3,4,5)P_3 can be divided into three classes based on their substrate specificity (*in vitro*), structure and regulation.

Class I enzymes are functional heterodimers with a catalytic subunit of 110-130 kDa tightly bound to a regulatory subunit. This class of PI3-kinase catalytic subunits all contain a Ras binding domain, PI-kinase (PIK) region which is of unknown function, a regulatory subunit binding domain and a C-terminal kinase domain. They are divided further according to the adapter subunit they associate with: the 1a enzymes bind to 55-85 kDa regulatory subunits that contain two SH2 domains straddling the catalytic domain binding region. The p85 subunits also contain a single SH3 domain and a BCR-GAP domain. These regulatory subunits link the kinase to tyrosine kinase signalling pathways (Vanhaesebroeck, *et al.*, 1997). The only mammalian 1b catalytic subunit is p110γ which is regulated by the $\beta\gamma$-subunits of G protein coupled receptors (Stephens, *et al.*, 1997, Stoyanov, *et al.*, 1995). It is seen to bind to a p101 regulatory subunit that does not contain defined domains like the p55-85 adapters and the mechanism of its association with the heterotrimerics is unknown (Stephens, *et al.*, 1997). All of the class 1 enzymes can phosphorylate PtdIns, PtdIns4P and PtdIns(4,5)P_2 *in vitro* to form the three 3-phosphorylated products, as can be seen from figure 1.2B. However, their preferred substrate is PtdIns(4,5)P_2 *in vivo* (Stephens, *et al.*, 1991, Hawkins, *et al.*, 1992). Thus these enzymes are responsible for the rapid (within seconds) accumulation of the PtdIns(3,4,5)P_3 on RTK and G protein coupled receptor agonist stimulation which results in many of the mitogenic cellular responses. Although a recent study has also shown there to be a second phase of PI3-kinase products accumulated 4-7 hours after PDGF stimulation and these lipids are required for entry into S phase of the cell cycle (Jones, *et al.*, 1999).

Class II kinases are monomeric and larger than the class I enzymes, ~200 kDa. They are characterised as having a C-terminal C2 domain but this lacks the Asp residues critical for Ca^{2+} co-ordination, which would otherwise result in enzymes which bind lipid in a Ca^{2+}-dependent manner (Vanhaesebroeck, *et al.*, 1997). These enzymes are unable to use PtdIns(4,5)P_2 as a substrate *in vitro* but do

form PtdIns(3,4)P_2 and PtdIns3P from PtdIns4P and PtdIns respectively. These enzymes lack a Ras binding region. The PI3-kinase C2α has been demonstrated to be activated by insulin stimulation, although the mechanism for this action is unclear (Brown, *et al.*, 1999).

The class III mammalian enzyme bear homology to the S. cerevisiae PI3-kinase Vps34 the activity of which is seen to be vital for the vesicle mediated trafficking of soluble hydrolases from the Golgi to the vacuole. These enzymes only phosphorylate PtdIns to PtdIns3P (Volinia, *et al.*, 1995) so maintaining the pool of PtdIns3P required for vesicle transport (De, *et al.*, 1996). Both the yeast and mammalian enzymes associate with serine/threonine kinases that regulate both the lipid kinase activity and the cellular localisation of the Vps34 homologues (Vanhaesebroeck, *et al.*, 1997).

1.4.4.3 PI3-kinase Inhibitors

The elucidation of events downstream to PI3-kinase activity has been aided by the use of low molecular weight, cell permeable inhibitors. The fungal metabolite wortmannin binds irreversibly to the PI3-kinase catalytic domain and inhibits both the class I sub types as well as class III enzymes in the low nanomolar range whereas its IC_{50} for the Class II kinases ~2 orders of magnitude greater (Domin, *et al.*, 1997). Wortmannin is unstable in water and has been shown to inhibit the related PI4-kinase at concentrations greater than 100nM. LY294002 competes at the ATP binding site of Class I PI3-kinases and is an effective inhibitor in the 10μM range (Vlahos, *et al.*, 1994). It is less effective against the Class II kinases (Domin, *et al.*, 1997).

1.4.4.4 Phosphoinositide Phosphomonoesterases

Inositol 5-phosphatases

There are two subtypes of 5-phosphatase both of which remove a phosphate at the 5 position on the inositol ring: type I is only active against the soluble Ins(1,4,5)P_3 and Ins(1,3,4,5)$_4$ whereas the type II enzymes are active against lipid substrates and can be further divided into 3 subgroups. The GAP-containing inositol 5-phosphatases or GIPs have a C-terminal BCR-GAP domain which is also a feature of the p85 regulatory subunit of PI3-kinases. These enzymes are active against both the soluble and lipid inositols with positions 4,5 or 3,4,5 phosphorylated. The second subgroup is the SH2 domain containing inositol phosphates (SHIPs). These enzymes are only active against PtdIns(3,4,5)P_3 and the soluble equivalent and are the only members of the class to have been demonstrated to reduce the accumulation of PtdIns(3,4,5)P_3 *in vivo.* The third subgroup is the Sac domain containing inositol 5-phosphatases (SCIPs) which are identified by the presence of an N-terminal Sac domain homologous to that of the yeast Sac1p protein. There are two mammalian members of this family one of which, synaptojanin is active against both PtdIns(4,5)P_2 and PtdIns(3,4,5)P_3 *in vitro* (Woscholski and Parker, 1997).

Inositol Lipid 3-Phosphatases

Giloblastoma derived cell lines have been shown to have elevated levels of immunoprecipitatable PKB activity, PtdIns(3,4)P_2 and PtdIns(3,4,5)P_3 (Haas, *et al.*, 1998). These tumour cell lines contain a mutation in the PTEN tumour suppresser gene which has been identified as an inositol lipid phosphatase, negatively regulating the levels of 3-phosphorylated inositol lipids (Stambolic, *et al.*, 1998).

1.5 GTPases: Molecular Timer Switches.

Signalling events within the cell must be controlled beyond the mere presence of an environmental cue. Kinase cascades which relay these signals are regulated by molecular switches which are capable of controlling not only the presence of a signal but also its duration. In work originally carried out by Rodbell and co-workers, studies to define the regulatory inputs into adenylate cyclase identified Guanosine triphosphate (GTP) and its membrane associated hydrolysis to Guanosine diphosphate (GDP) as a key regulatory element (reviewed by (Rodbell, 1980)). G proteins also referred to as GTPases are the enzymes responsible for the nucleotide hydrolysis and it is their intrinsic or trans-regulated rate of action which is seen to be central to the regulation of many diverse signalling pathways. While the GTPases can be divided into two main groups (heterotrimeric and small) and the multiple members of each group are seen to be highly specific for many different signalling pathways, they all share a common enzymatic mechanism.

1.5.1 The GTPase Cycle.

GTPases cycle between GTP and GDP-bound states (figure 1.3A). It is this cycling that results in their behaviour as molecular switches: the GTP-bound form is associated with an active state which signals to downstream effector molecules, whereas the GDP-bound form is not active with respect to signalling. The various GTPases have a specific intrinsic GTPase activity which results in the hydrolysis of the GTP's γ-phosphate and so a return to the GDP, inactive state.

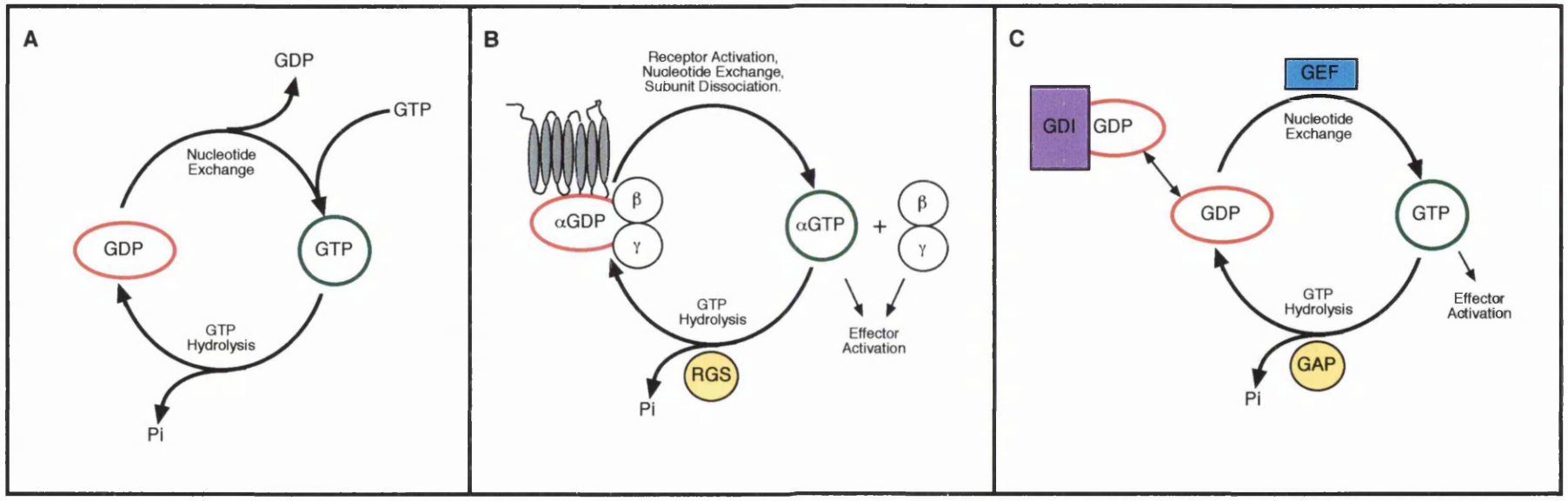

Fig. 1.3: The G Protein Cycle

A) The general GTPase cycle from an inactive, GDP-bound form, via nucleotide exchange to an active, GTP-bound form. The subsequent G protein activity hydrolyses the GTP to produce the inactive form and free inorganic phosphate. B) The Heterotrimeric G proteins are inactive in the complex of subunits and receptor when the Gα subunit is in a GDP-conformation. Ligand stimulation of the receptor results in nucleotide exchange on the Gα and subsequent dissociation from both the receptor and the Gβγ heterodimer. The subunits are active towards effectors until the RGS-enhanced hydrolysis of the GTP takes place. C) The small G proteins are inactive is a GDP-bound state and are bound to a GDI in the cytosol. The translocation to the membrane and action of a GEF results in the active, GTP-bound form which subsequently contributes to the activation of effectors. The GTPase activity is promoted by GAPs.

1.5.2 The Heterotrimeric G proteins

As suggested by the name these proteins are made up of three subunits (α,β and γ) which associate with the cytoplasmic domains of serpentine receptors. The cellular effects resulting from receptor stimulation are mediated through the G proteins. There are 5 classes of Gα subunit (i, s, q, 12 and 13) with a total of 20 gene products having been identified to date. They contain two domains; a GTPase domain that contains all of the features seen in the small G proteins and a second domain which is entirely α-helical in character and acts to bury the nucleotide deep within the subunit (reviewed by (Hamm and Gilchrist, 1996)). There are 6 β and 12 γ gene products known. G$\beta\gamma$ subunits are tightly complexed and can be thought of as a functional monomer. They interact with the Gα via an interface that covers the switch domains of the GTPase domain. On ligand binding structural rearrangements in the receptor act allosterically to promote the Gα to exchange of GDP for GTP (Bourne, 1997). The presence of the γ-phosphate produces gross morphological changes in the switch regions of the Gα subunit resulting in the loss of G$\beta\gamma$ binding potential (Hamm, 1998). The two functional subunits (Gα.GTP and G$\beta\gamma$) dissociate from the receptor and both activate specific downstream effector molecules.

The Gα subunits have been seen to transduce activity to a variety of effector molecules including: adenyl cyclase, photoreceptor cGMP phosphodiesterase, phospholipaseC-β and Bruton's tyrosine kinase (Btk) (Bence, *et al.*, 1997, Hamm, 1998). In an interesting link between the two groups of G proteins the $G\alpha_{13}$ subunit has been shown to bind to p115 RhoGEF and stimulate its ability to catalyse nucleotide exchange on Rho (Hart, *et al.*, 1998).

The Gβγ subunits also acts to regulate a plethora of downstream cellular pathways by activating PLC-β2 , adenylate cyclase, ion channels, kinases Raf1, Tsk and Btk and recruiting β-adrenergic receptor kinase to the membrane (Hamm, 1998, Jan and Jan, 1997, Langhans, *et al.*, 1995, Pumiglia, *et al.*, 1995). The increase in cellular levels of PtdIns(3,4,5)P_3 on stimulation of heterotrimeric G protein-linked receptors is explained by the presence of a PI3-kinase catalytic activity seen to be specifically activated by Gβγ. This lipid kinase is tightly bound to a novel p101 regulatory subunit (Stephens, *et al.*, 1997, Stoyanov, *et al.*, 1995).

The active state persists until the GTP bound to the Gα subunit is hydrolysed. The Gα has been seen to have approximately a 100-fold higher intrinsic GTPase activity than members of the small GTPase families. This is due to a presence of a catalytic arginine located on an extension of the switch one region (Markby, *et al.*, 1993). The GTPase activity of Gα can still be enhanced by Regulators of G-protein signalling (RGS). RGS proteins are thought to stabilise the transition state G protein and enhance the intrinsic GTPase activity by at least 40-fold (Koelle, 1997). Once the Gα is returned to a GDP-bound form the Gβγ dimer re-associates and an inactive complex is restored. This GTPase cycle is represented in figure 1.3B.

1.5.3 The Small GTPases

Like the Gα subunit of the heterotrimeric G proteins the small GTPases bind guanine nucleotides and hydrolyse the γ-phosphate of GTP. As their name suggests they are of low molecular weight (between 20 and 30 kDa) and are folded into a single GTPase domain. The first small GTPase to be identified was H-Ras which was seen to be the transforming gene of the Harvey, BALB and Rasheed sarcoma virus (reviewed by (Boguski and McCormick, 1993)). Thus the small GTPases are often referred to as the Ras superfamily. There are over 70 mammalian members of this superfamily now identified and they can be divided into subfamilies based on sequence similarities: Ras, Rho, Rab, Arf and Ran. Figure 1.4 displays an alignment of a single member of each subfamily with the exception of Rho where the three most well characterised members of the subfamily are present. Most members of the Ras superfamily contain a 'CAAX' motif at their carboxy-termini (where C, cysteine; A, aliphatic amino acid and X is any amino acid). This motif is a peptide signal for posttranslational modification: prenylation, proteolysis and methylation. Studies have shown the identity of the last amino acid of the motif to confer the specific modification. Proteins will be geranylgeranylated if X is leucine or phenyalanine, while a farnesyl group will be added if the X is methionine, serine, alanine cysteine or glutamine (Moores, *et al.*, 1991, Reiss, *et al.*, 1991). Thus Ras has a CAAX which specifies farnesylation whereas Rho subfamily members end in either leucine or phenylalanine and are geranylgeranylated.

1.5.3.1 The Small G Protein GTPase Cycle

As can be seen from the schematic in figure 1.3C, while the basic enzymatic properties of the small GTPases are the same as the Gα subunits of the heterotrimerics, the regulation of the process is different. Guanine nucleotide Exchange Factors (GEFs) catalyse the exchange of GDP for GTP resulting in

the conformation necessary for interaction with specific effectors (Boguski and McCormick, 1993). GTPase Activating Proteins (GAPs) promote the intrinsic activity of the GTPase. The importance of GTPase regulation is evident from the disease phenotypes resulting from mutations that disrupt the GAP tumour-suppressing function (Gutmann and Collins, 1993). The mechanism of GAP action on the GTPase has been elucidated with the use of structural studies and GDP-AlF_4 which was seen to mimic the transition state of the hydrolysis process (Scheffzek, *et al.*, 1998). Invariant arginine residues on the GAP have been shown to be present at the active site of small GTPases and their positive charges are able to neutralise negative charges on the leaving oxygen groups, thus stabilising the incurred transition state (Scheffzek, *et al.*, 1997). The GDI proteins act to sequester some inactive GTPases masking their lipid modifications and so allowing a soluble cytoplasmic complex to form (reviewed in (Sasaki and Takai, 1998)). Thus the regulated dissociation from GDIs and translocation to the membrane adds a regulated step to the small GTPase's cycle. Rho-specific GEF, GAP and GDI proteins will be discussed later in this Introduction.

1.5.3.2 Point Mutations that Effect the Small GTPase Cycle

Ras oncogenes isolated from human tumour cells often have single point mutations affecting residues 12, 13, 61 or 146 in the gene product (Bos, 1989). Structural studies on both Ras and Rho have now identified these residues to be within the nucleotide binding pocket of the GTPase, with residues 12, 13, 59 and 61 (Ras) involved in interactions with the phosphate groups of the nucleotide while the more C-terminal residues co-ordinate the base of the nucleotide (Ihara, *et al.*, 1998, Prive, *et al.*, 1992). Residues 12 or 61 are vital for the nucleophilic attack by water on the γ-phosphate of GTP hence their mutation results in a GTPase-deficient G protein that is also insensitive to GAP stimulation. Such a GTPase is seen to exist within the cell predominantly in the

GTP-bound form. The conserved serine or threonine at position 17 in Ras stabilises the interaction with the GTP. A mutation in this residue results in the GTPase being unable to exchange GDP for GTP and hence is always in the GDP-bound state when expressed in cells. Equivalent residues are found in all of the other subfamilies of small GTPases as can be seen from figure 1.4. Further, a mutation at the conserved phenylalanine 28 (Ras) to leucine results in a GTPase with transforming potential. This mutated GTPase hydrolyses GTP to GDP in a GAP sensitive manner but has a high dissociation rate for the nucleotides and hence is found predominantly in the GTP-bound form (Reinstein, *et al.*, 1991). The strong nucleotide binding by the GTPases is absolutely dependent on the presence of divalent cations; Mg^{2+} ions play a key role in bringing together the functional regions of the phosphate binding, switch I and switch II domains.

1.5.3.3 Small GTPase Effector Interactions

Other than the amino acid conservation in and around the regions involved in the catalytic activity or lipid modification, one other homologous region of the small GTPases is seen to have functional significance. The use of mutagenesis identified regions on Ras which are vital for biological activity in both yeast and mammalian systems (Sigal, *et al.*, 1986, Willumsen, *et al.*, 1986). The so-called effector binding loop (residues 30-40 in Ras) is a region involved in protein-protein interactions, it overlaps with the switch I domain (see figure 1.4) which undergoes gross conformational changes on nucleotide exchange and hydrolysis. The majority of downstream targets for GTPases only functionally interact with the GTP-bound form. Thus the movement of the effector binding loop results in a conformation capable of interacting with Ras effectors. Structural studies also showed the switch II region to undergo conformational change on GTP binding. Encompassing amino acids 59-76 in Ras this region contains residues directly involved in GTPase activity. The specific interaction of a monoclonal antibody with this region (Y13-259) results in a neutralisation of

Ras biological potential (Sigal, *et al.*, 1986). The relative effector binding regions of the various small GTPases is discussed at length in chapter 7.

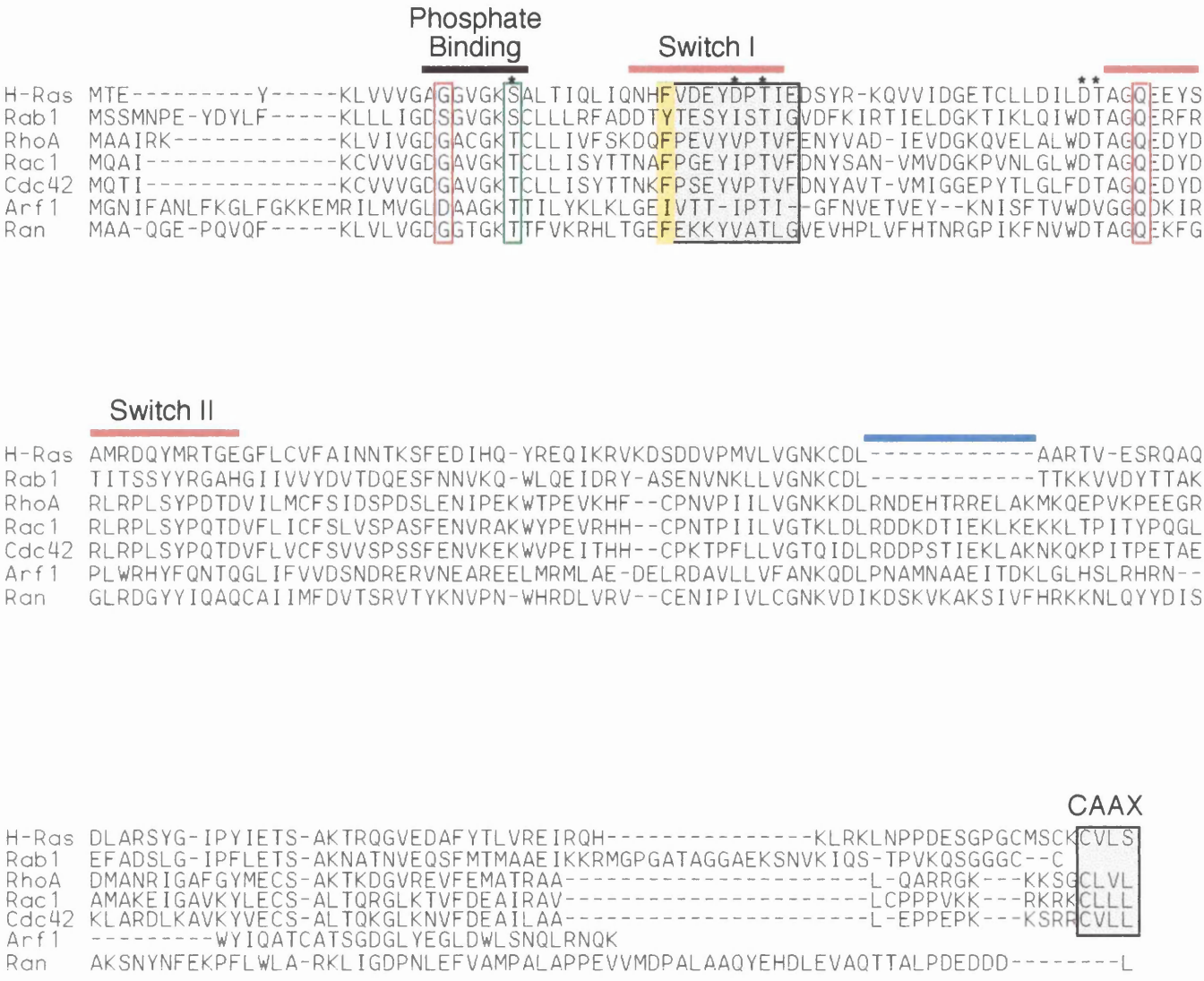

Fig.1.4: Alignment of Representative Members of the Ras Superfamily

DNAstar™ software was used to align members of each of the subfamilies of small GTPases by Clustal method. The common functional areas are displayed: The effector binding loop is boxed and in grey; the phosphate binding loop is marked with a black bar; the confomationally variant switch I and switch II regions are marked with a red bar; the insert loop, present in the Rho GTPases but not the Ras or Rabs is marked with a blue bar; the residues required for effective GTPase activity are boxed in red while the serine/threonine residue required for stable nucleotide binding is boxed in green; the Phe residue required for normal nucleotide cycling is boxed in dark yellow; residues involved in Mg^{2+} interactions are highlighted with an asterix and the isoprenylation signal sequence (CAAX) is boxed and in grey.

1.5.3.4 The Functions of Small GTPases

The Ras-related nuclear protein Ran is predominantly localised in the nucleus and it lacks the C-terminal isoprenylation signal sequences (see figure 1.2). Ran.GTP has been demonstrated to play a role in nuclear protein import in budding yeast (Rush, *et al.*, 1996). There are six mammalian ADP-ribosylation factor (Arf) proteins identified. They have been shown to regulate the formation of COP1 vesicles *in vitro* and clathrin coated vesicles at the trans-Golgi network and endosomes (reviewed in (Roth, 1999)). Arf proteins are also seen to work synergistically with PKC and Rho in the activation of phospholipase D (PLD). PLD has a demonstrated role in intracellular membrane transport (Ktistakis, 1998). There is therefore a functional link between GTPase and effector. Rabs constitute the largest of the Ras-related subfamilies with over 40 mammalian and 11 yeast proteins now identified (Novick and Zerial, 1997). The interaction of Rab.GTP with specific effector molecules at the destination membrane sites is thought to be the docking signal which is followed by vesicular fusion.

Ras GTPases are associated with growth and differentiation signals from receptor tyrosine kinases (RTKs), non-receptor tyrosine kinases and heterotrimeric G protein-coupled receptors (Marshall, 1996). The most well characterised Ras activation event is via the previously discussed receptor tyrosine kinase recruitment of Sos GEF. Class I PI3-kinase which is also recruited to the activated receptor through SH2 domain specificity is seen to directly bind Ras.GTP. The interaction is on the p110 catalytic subunit and results in kinase activation. The transfection of mammalian cells with the GTPase-deficient Ras.V12 resulted in an elevation of PI3-kinase products whereas the dominant negative N17 Ras inhibited growth factor induced PI3-kinase activity (Rodriguez-Viciana, *et al.*, 1994). Other Ras effectors include the atypical PKCζ and the MAPKKK which is upstream of SEK and ultimately the JNK/SAPK pathway (Campbell, *et al.*, 1998). Closely related to the three Ras

gene products (H, N and K-Ras) are the Rap proteins, found in granules in the Golgi and endoplasmic reticulum and the Ral proteins which appear to be involved in exocytic and endocytic processes (Denhardt, 1996a).

1.6 The Rho Subfamily of Small GTPases

The Ras-Homology (Rho) subfamily has become one of the most well characterised groups of human GTPases since its initial identification by P. Chardin and co-workers (Chardin, *et al.*, 1988, Yeramian, *et al.*, 1987). The Rho protein was identified as the p21 target of ADP-ribosylation by the *Clostridium botulinium* toxins C_1, C_3 and D (Aktories, *et al.*, 1989, Sekine, *et al.*, 1989). The toxins specifically ribosylate Asn 41 of Rho proteins resulting in a modification of the effector loop that renders the Rho biologically inactive without affecting its intrinsic biochemical properties. It was the observed disassembly of microfilaments on C_3 treatment of Vero cells that first suggested Rho GTPase involvement in cytoskeletal rearrangements (Chardin, *et al.*, 1989). Subsequently the microinjection of either GTPase deficient V14, wildtype or ADP-ribosylated Rho confirmed it's role in the formation of these cellular processes (Paterson, *et al.*, 1990). There are now 15 mammalian Rho GTPases identified: RhoA, B, C, D, Rnds 1, 2, 3 , 6, Rac1, 2, 3 TC10, TTF and Cdc42h. These gene products are seen to be highly homologous on amino acid sequence comparison and 30% homologous to Ras subfamily members. Structural studies have shown the Rhos to have the same overall pattern of motifs as Ras with the exception of an extra α-helices spanning residues 125-137 in RhoA (Ihara, *et al.*, 1998) (see figure 1.4). This so-called insert loop is implicated in the specificity of Rho GTPase signalling to downstream effectors (Freeman, *et al.*, 1996).

1.6.1 Rho GTPases in Yeast

Rho family GTPases are seen to regulate a variety of cellular functions in both budding and fission yeast. Extrapolation of the information gained in these lower organisms highlights the possible roles of Rho proteins in mammalian cells. In *S. cerevisiae* 5 Rho family proteins have been identified Rho1 and

Cdc42 being the most well characterised. Cdc42 was originally identified as a gene product required for polarised budding. It has been demonstrated to affect the actin cytoskeleton of *S. cerevisiae* during mating via a direct interaction with the FH1 and FH2 domain (formin homology) containing protein Bni1 (Evangelista, *et al.*, 1997). This effector may regulate the actin cytoskeleton through an interaction with profilin and Bud6p. The use of temperature-sensitive mutants of both Cdc42 and its dbl-homology GEF Cdc24 placed these gene products on a signalling pathway from the G protein coupled mating factor receptors to the kinase cascade resulting in the transcriptional activation of mating-specific genes (Simon, *et al.*, 1995, Zhao, *et al.*, 1995). The upstream regulation of the GTPase is via an interaction of the β subunit (Ste4) of the βγ heterodimer with the exchange factor Cdc24 which results in its and subsequently Cdc42 activation. The downstream target of Cdc42 is seen to be the $p65^{PAK}$ homologue Ste20 which is the initial kinase in a MEK/ERK-like cascade which involves Ste11, Ste7, Kss1 and Fus3 and is scaffolded by Ste5. This pathway has also been shown to be required for pseudohyphal development during periods of nutrient deprivation. It was the observation that one of the Ras homologues in *S. cerevisiae*, Ras2 stimulates filamentous growth that led to the demonstration of a Ras regulation of Cdc42 (Mosch, *et al.*, 1996). While the molecular mechanism of this event is unclear, it may be a parallel to the activation of Rac1 by Ras in mammalian cells (see later sections).

Rho1 is absolutely required for bud formation (Yamochi, *et al.*, 1994). It too is seen to interact with Bni1 which is required for cytokinesis (Kohno, *et al.*, 1996). Other downstream targets of Rho1 identified are the PKC homologue Pkc1; the interaction of the GTPase is at a pseudosubstrate site suggesting the interaction results in an active serine/threonine kinase (Nonaka, *et al.*, 1995). It is of interest to note that a similar Rho input is required for the activation of PRK as demonstrated in the present study. The active Pkc1 signals to another kinase cascade which includes the Bck1, Mkk1 and Mpk1 kinases and results in

transcriptional activation of genes involved in the response to environmental stresses, including glucan synthases (Irie, *et al.*, 1993). Rho1 also regulates cell wall biosynthesis via an interaction with β1-3 glucan synthase (Qadota, *et al.*, 1996). The upstream regulation of Rho1 is analogous to the mammalian system; with GEFs including Rom1 and Rom2 which contain PH domains and an upstream lipid kinase activator of these GEFs: Tor2 (Schmidt, *et al.*, 1997). A scheme of the pathways involving both Rho1 and Cdc42 in *S. cerevisiae* is shown in figure 1.5.

The molecular details of signalling events involving Rho GTPases in *S. pombe* are less clear. Rho1 but not Cdc42 is seen to be required for cell wall biogenesis through the activation of (1-3) β-D-glucan synthase (Arellano, *et al.*, 1996). Two PKC homologues Pck1/2 were identified and their disruption resulted in cell shape defects (Toda, *et al.*, 1993). Further, a direct and functional interaction between Rho1 and Pck has recently been demonstrated (Sayers, Nakano, Mabuchi, Katayama, Toda and Parker, unpublished results). In another recent study Mok1, a downstream target of Pck1/2 was shown to have glucan-synthase activity and was localised in close proximity to actin dependent structures (Katayama, *et al.*, 1999). While MAP kinase pathways have been identified in fission yeast, a regulation by Rho GTPases has not been directly demonstrated. A Mpk1 homologue, Pmk1 is seen to be required for cell wall integrity and acts either independently of Pck or via a bifurcated pathway (Toda, *et al.*, 1996).

It is of particular interest to the present study that the interaction of Rho1 from both *S. cerevisiae* and *S. pombe* with their respective PKC homologues is through a PRK Homology Region 1 (HR1) domain (see below). Thus this domain has been retained by a subset of serine/threonine kinases in higher organisms resulting in a specific upstream regulation that is not seen in the other mammalian PKC isoforms.

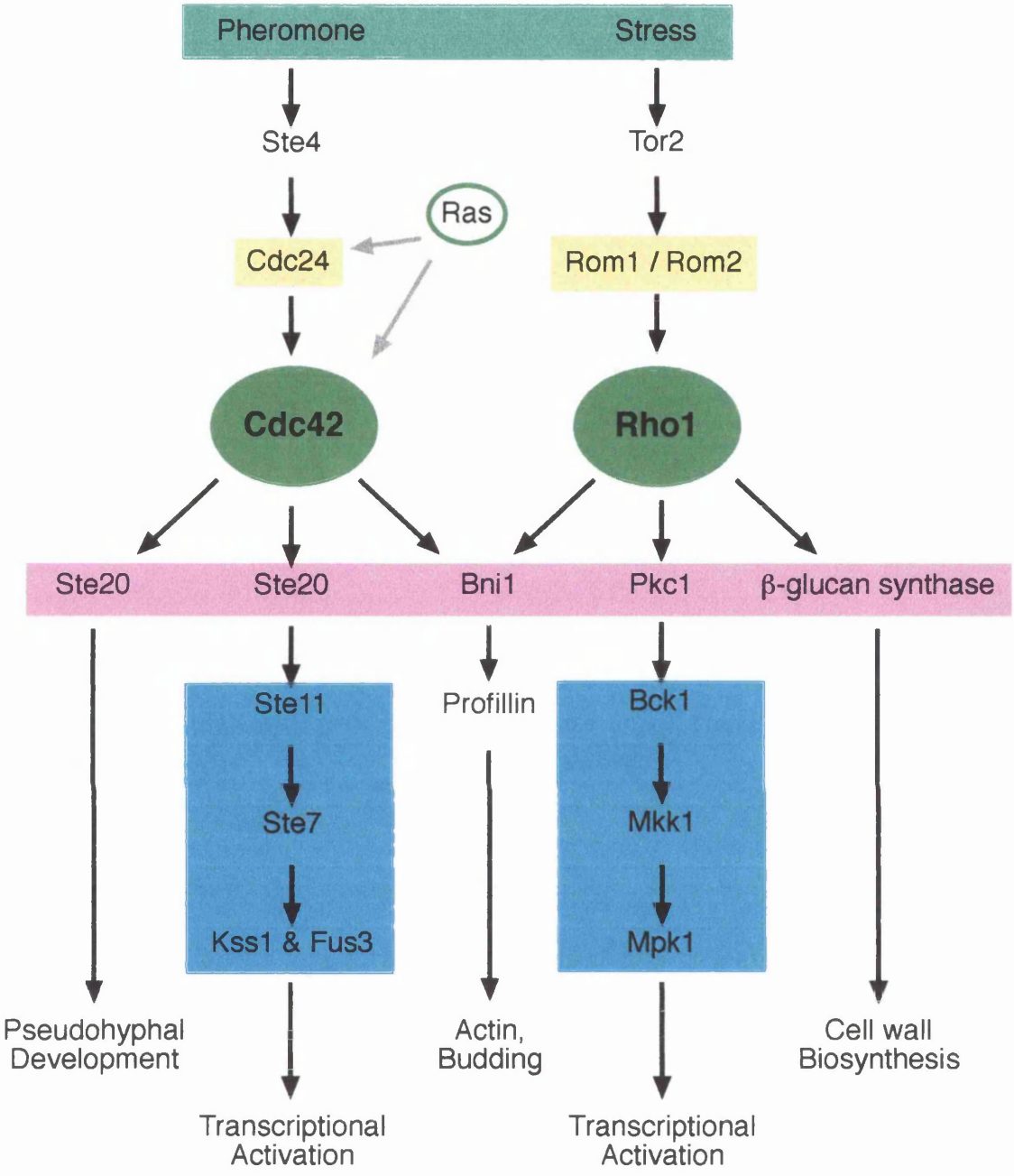

Fig. 1.5: The Roles of Cdc42 and Rho1 in *S. cerevisiae*

Scheme depicting the various roles of the most well characterised Rho subfamily GTPases in yeast. The basic elements of signalling processes are blocked in colour: The environmental factors are in light green and lead to the activation of the GTPases (dark green) via GEFs (yellow). The GTPases act on a variety of downstream effectors (pink) some of which are kinases that feed into MAP kinase cascades (blue) resulting in transcriptional activation. The cellular responses to the environmental stimuli are therefore regulated at multiple levels.

1.6.2 Rho Guanine nucleotide Exchange Factors (GEFs)

All the Rho subfamily GEFs contain a characteristic Dbl-homology (DH) domain which is responsible for exchange activity and a PH domain. The Dbl oncogene was originally demonstrated to induce foci formation when expressed in fibroblasts. Its function was subsequently identified through its sequence homology with the *S. cerevisiae* Cdc42 GEF, Cdc24. Numerous DH domain-containing GEFs have now been identified, some are specific for a particular GTPase; Lbc, Lfc and Lsc are specific for Rho, whereas some are active towards many; Vav, which was originally seen to activate Ras also exchanges nucleotide on Rac and Cdc42 (Crespo, *et al.*, 1997). Microinjection and overexpression studies of these GEFs have resulted in the phenotypes expected from the GTP loading of Rho GTPases: cytoskeletal rearrangements, SAPK/JNK activation etc. (reviewed in (Cerione and Zheng, 1996)). The PH domains of Dbl-GEFs have been demonstrated to be vital for the proteins transforming potential. A ΔPH Dbl was seen to be completely inactive in transformation assays while retaining nucleotide exchange activity. Further, the membrane targeting of the same ΔPH protein by fusion to the CAAX motif of Ras was insufficient to recover the transforming potential (Zheng, *et al.*, 1996). This suggests not only that phosphoinositides are required for the function of the GEFs but also that they impart a specific location signal. However, a subsequent study has shown the PH domain of the Rac GEF Tiam 1 can be functionally replaced by the myristolation signal of c-Src (Michiels, *et al.*, 1997). A further localisation signal may be through the SH2 and SH3 domains present on some members of the Dbl GEF family. Some of these GEFs also contain domains with exchange activity towards other GTPases: Ras GRF / mSOS contain both Ras and Rho GEF potential through different domains and in the case of Sos Rac activation is dependent upon the presence of an active Ras (Nimnual, *et al.*, 1998). Trio contains two functional GEF domains one for Rho

and one for Rac1, suggesting a possible co-ordination of signalling pathways (Bellanger, *et al.*, 1998).

1.6.3 Rho GTPase Activating Proteins (GAPs)

There are many potential RhoGAPs now identified, the most well characterised being p50 RhoGAP, p190GAP and Bcr. *In vitro* studies show these proteins to have preferences for members of the Rho subfamily. Further, the relative cellular responses to Rho GTPases could be selectively inhibited by the microinjection of the different GAP proteins: while Bcr inhibited Rac mediated lamellipodia formation but not stress fibres p190 RhoGAP and p50GAP both blocked LPA-stimulated stress fibre formation without any effect on lamellipodia formation (Ridley, *et al.*, 1993). A functional link between Rho and Ras GAPs was described by Settleman *et al* who demonstrated an interaction between RasGAP and p190 RhoGAP via the simultaneous binding of phosphorylated tyrosine residues on the latter to the tandem SH2 domains on the RasGAP (Hu and Settleman, 1997). A subsequent study has implicated c-src as the tyrosine kinase responsible for the p190 phosphorylation (Roof, *et al.*, 1998). The Rho GAPs have also been implicated in processes other than GTPase down-regulation: the RacGAP n-Chimaerin was seen to induce Rac associated effects when microinjected into cells (Kozma, *et al.*, 1996). Further this effect was seen irrespective of GTPase activity but did require a Rac binding potential. Thus a synergistic effect between the G protein and its regulators may exist.

1.6.4 Rho Guanine nucleotide Dissociation Inhibitors

Guanine nucleotide Dissociation inhibitors have only been identified for the Rho and Rab subfamilies of small GTPases. Rho.GTP is generally associated with a membrane compartment whereas Rho.GDP is cytoplasmic. GDIs bind to the GTPases, burying their lipid modifications within a hydrophobic pocket. The resulting heterodimer exists within the cytoplasm and has been shown to

interact with potential Rho effectors (Tolias, *et al.*, 1998). Upon mitogen activated or cell cycle dependent association of Rho with membrane compartments an interaction between the F-actin binding proteins ezrin, radixin and moesin (ERM) and the GDI results in the displacement of the GTPase (Takahashi, *et al.*, 1997). The action of GEFs produces a Rho.GTP which is able to activate effector molecules. The subsequent GAP-enhanced GTP hydrolysis results in a membrane bound Rho.GDP which is extracted into the cytoplasm by the GDI (Sasaki and Takai, 1998). Contrary to the observed membrane translocation of most of the GDIs, the RhoB/G specific GDI3 is associated with a Triton X100 insoluble membrane or cytoskeletal compartment on subcellular fractionation (Zalcman, *et al.*, 1996). This may reflect the fact that RhoB is only seen to be associated with membrane compartments and does not cycle to the cytoplasm.

1.6.5 Rac GTPase

Rac.GTP has been demonstrated to be the link between growth factors such as PDGF, insulin and bombesin and an observed polymerisation of actin at the cells plasma membrane (Ridley, *et al.*, 1992). The resulting lamellipodia may detach from the substratum and fold back to form characteristic ruffles. Rac has also been shown to induce the formation of focal complexes that are distinct from those formed by Rho (Nobes and Hall, 1995). PI3-kinase has been shown to be an upstream regulator of Rac: PDGF can increase the level of Rac.GTP within cells via a PI3-kinase dependent process and the Rho family GEF molecules such as Vav are positively regulated by the products of PI3-kinase activity (Han, *et al.*, 1998, Hawkins, *et al.*, 1995, Wennstrom, *et al.*, 1994). Thus this mammalian system mirrors that defined genetically in *S. cerevisiae*: a lipid kinase relative (Tor2/Mss4) acts upstream of a PH domain-containing GEF (Rom) resulting in a functionally active GTPase (Rho1). Ras has also been implicated as an upstream regulator of Rac. GTPase deficient Ras produces lamellipodia in fibroblasts, a process that is blocked with the use of a dominant

negative Rac (Ridley, *et al.*, 1992) and a dominant negative PI3-kinase was seen to completely block RasV12-induced ruffling (Rodriguez, *et al.*, 1997) suggesting Ras can function upstream of Rac via PI3-kinase. Rac is also required for Ras transformation and co-operates with Raf1 in a transformation process (Qiu, *et al.*, 1995a). As well as its effects on the cytoskeleton Rac also signals to a variety of transcription factors. GTPase deficient Rac can activate the SAPK/JNK MAP kinase pathway via SEK (Coso, *et al.*, 1995, Minden, *et al.*, 1995). This process may be mediated through the Rac / Cdc42 effector serine/threonine kinases PAK, MEKK4 or MLK3, although a Rac effector domain mutant that is unable to bind PAK is still able to activate this pathway (Westwick, *et al.*, 1997). Rac GTP can also activate the transcription factors SRF and NF-kβ (Hill, *et al.*, 1995, Perona, *et al.*, 1997). Further, a novel Rac effector, POSH, was recently identified and was shown to stimulate the JNK pathway and NF-kβ translocation to the nucleus (Tapon, *et al.*, 1998). In phagocytic cells Rac1 is required in addition to its two cytosolic effectors $p47^{phox}$ and $p67^{phox}$ for the activation of NADPH oxidase (Abo, *et al.*, 1992). Several Rac effectors have been implicated in the regulation of the cytoskeleton: POR1, PI5-kinase and IQGAP (Van and D'Souza, 1997). A feature of a number of Rac and Cdc42 effectors is a 18 amino acid Cdc42/ Rac interactive binding (CRIB) domain which as the name suggests is the conserved GTPase binding region. With particular interest to the present study is the observed GTP-dependent interaction of Rac with PRK2, an interaction which was seen to increase the autocatalytic activity of the effector kinase (Vincent and Settleman, 1997).

1.6.6 Cdc42 GTPase

Cdc42 is activated by bradykinin to produce filopodia and focal complexes when microinjected into fibroblasts (Nobes and Hall, 1995). These finger-like extensions most probably play a role in the phagocytic process in macrophages. Cdc42 interacts with many of the same cellular targets as Rac

and produces similar responses, including SAPK/JNK activation. One notable exclusive effector molecule is Wiskott-Aldrich syndrome protein (WASP) which has been implicated in the Cdc42-dependent cytoskeletal rearrangements (Van and D'Souza, 1997). More recently two novel Cdc42 effectors have been identified: the myotonic dystrophy kinase-related Cdc42-binding kinases (MRCKs) contain ROK-like kinase domains (see below) but CRIB domains for GTPase interaction and they are directly involved in cytoskeletal rearrangements (Leung, *et al.*, 1998). Both Cdc42 and Rac have been shown to associate with and activate the ribosomal subunit kinase $p70^{S6K}$. The activation was sensitive to both rapamycin and wortmannin and the association required the GTPases to be in a GTP-bound form (Chou and Blenis, 1996).

1.6.7 Signalling Between the Rho GTPases

As well as producing lamellipodia on microinjection into fibroblasts Rac was also seen to stimulate the formation of stress fibres (Ridley and Hall, 1992). This process was blocked with the use C3 toxin and N17 Rac blocked PDGF but not LPA stimulated stress fibre formation. Thus it was concluded that Rac in some way signals to Rho (Ridley, *et al.*, 1992). Further, Cdc42 microinjection also produces lamellipodia and stress fibres; a process that could be blocked by N17Rac (Nobes and Hall, 1995). A functional cascade between the GTPases from Cdc42 to Rac to Rho exists. The method of crosstalk remains unclear although possible mediators have been suggested. The mitogen-stimulated activation of Rac was seen to be required for the metabolism of arachidonic acid to produce leukotrienes which promote Rho-dependent stress fibre formation (Peppelenbosch, *et al.*, 1995). Thus a pathway from Rac to Rho may be via the production of Leukotrienes. A PAK associated GEF, PIX is seen to be active towards Rac. The interaction of Cdc42 with PAK may promote nucleotide exchange on Rac hence activating it (Manser, *et al.*, 1998). An outline of the various stimulatory inputs into Cdc42, Rac and Rho can be seen in figure 1.6.

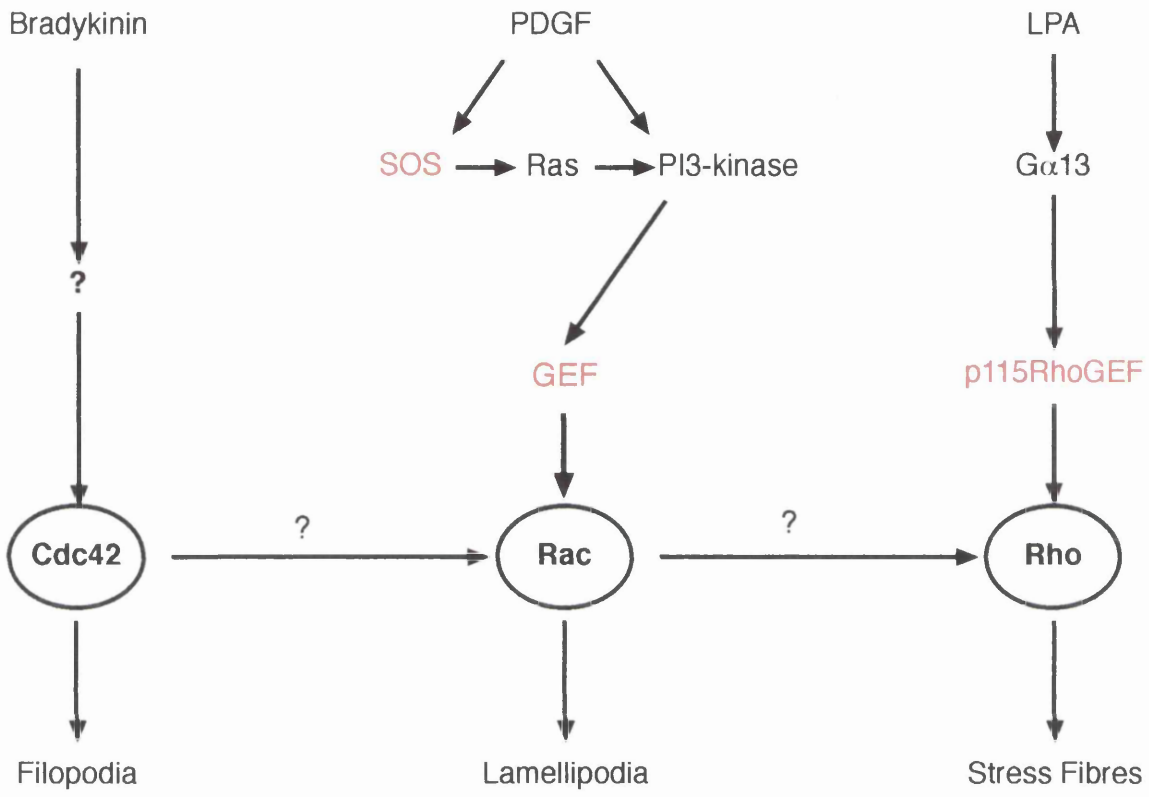

Fig. 1.6: The Regulatory Inputs and Crosstalk of Rho-family GTPases
While the connection between agonist and Cdc42 is unclear, many elements upstream of Rac and Rho GEFs (red) have been elucidated. Crosstalk between the GTPases is hierarchical, with Cdc42 activating Rac and Rac activating Rho. However, the mechanism of this relationship is still to be confirmed.

1.6.8 The Rho GTPases (RhoA, B, C and D)

RhoA is activated by the mitogens LPA and Bombesin via the activation of serpentine receptors and heterotrimeric G proteins (Van and D'Souza, 1997). PI3-kinase has been shown to be an upstream signalling component of RhoA associated effects such as stress fibre and focal adhesion formation but not Rho-stimulated transcriptional activation (Reif, *et al.*, 1996). An input which is assumed to be via PH domain-containing GEFs. The tyrosine phosphorylation of Rho GEFs has also been implicated in the activation of Rho (Nobes, *et al.*, 1995). The direct phosphorylation of RhoA at its C-terminus by PKA was seen to increase its affinity for GDI (Lang, *et al.*, 1996). RhoB is seen to differ from RhoA/C in that it's accumulation is cell cycle dependent: first detectable in G1/S phase transition it is maximal within S phase and declines over the S/G2-M transition (Zalcman, *et al.*, 1995). Primarily the study of RhoA has implicated these proteins in a variety of cellular functions.

Cell Proliferation / Transformation

C3 toxin treatment is able to inhibit serum stimulated G1-S progression of quiescent Swiss 3T3 cells into the cell cycle and a constitutively active RhoA induces entry in the absence of serum (Olson, *et al.*, 1995, Yamamoto, *et al.*, 1993). Like Rac RhoA is required for Ras induced transformation and co-operates with RafCAAX, while Rho.GTP alone does not cause transformation (Qiu, *et al.*, 1995b). This suggests that Rho functions downstream of Ras in mediating loss of growth control. The G1-S phase progression requires the elimination of the Cyclin-dependent kinase (Cdk) inhibitor $p27^{Kip1}$. A modified Rho was shown to promote the degradation of p27 in rat thyroid cells (Hirai, *et al.*, 1997). Conversely, Olson and co-workers have recently demonstrated the inhibition of Rho causes constitutively active Ras to induce the Cdk inhibitor $p21^{Wif1/Cip1}$ and entry into DNA synthesis is blocked. The active Rho is thought to antagonise the expression from the $p21^{Wif1/Cip1}$ promoter (Olson, *et al.*, 1998).

As well as cell cycle progression G1-S, Rho is also required for cytokinesis. The disruption of RhoA function prevents cytokinesis in *Xenopus* oocytes post fertilisation (Drechsel, *et al.*, 1997). This effect has subsequently been seen to be mediated through the Rho effectors Citron and members of the formin homology domain containing proteins homologous to the *Drosophila* diaphanous gene product. There are two splice variants of Citron, one with an N-terminal kinase domain which is 50% homologous to that of the ROCK family serine/threonine kinases (Citron-K), and one which is missing this domain (Citron-N). Both forms contain a Rho binding domain also homologous to that of ROCK. Citron-K is found predominantly in dividing tissues whereas Citron-N is found in neurons. Citron-K is localised within the cleavage furrow of dividing cells and a truncated form of the protein caused cytokinesis in Hela cells to fail (Madaule, *et al.*, 1998). While the diaphanous gene product is required for cytokinesis in *Drosophila* the S. cerevisiae homologue (Bni1) is required for budding (Castrillon and Wasserman, 1994, Evangelista, *et al.*, 1997).

Cytoskeletal Rearrangements

Rho.GTP is sufficient to cause the formation of F-actin stress fibres and its function is required for their Serum, LPA and bombesin-induced formation in fibroblasts (Ridley and Hall, 1992). Rho also causes the clustering of vinculin, talin and other cytoskeletal components at the sites of integrin contact with the extracellular matrix to form focal adhesions (Yamada and Geiger, 1997). Rho dependent tyrosine phosphorylation events are required for the formation of focal adhesion complexes and stress fibres (Ridley and Hall, 1994). It is now known that the Rho-dependent formation of stress fibres is mediated through the Rho-kinase/ROCK class of Rho effectors. The two members of this class are distantly related to myotonic dystrophy kinase. Several groups identified these gene products; p160ROCK, ROCKII and ROKβ are the same product as are Rho-kinase and ROKα (Ishizaki, *et al.*, 1996, Leung, *et al.*, 1995, Matsui, *et al.*,

1996, Nakagawa, *et al.*, 1996). Both ROCK and Rho-kinase bind to RhoA in a GTP-dependent manner through a conserved region also present in the Rho effectors Citron and kinectin. They are serine/threonine kinases and also contain a PH domain. The binding of Rho activates their kinase activity and the overexpression of either member of this class results in stress fibre and focal adhesion formation (Amano, *et al.*, 1997, Ishizaki, *et al.*, 1997, Leung, *et al.*, 1996). Rho-kinase phosphorylates the regulatory subunit of myosin light chain phosphatase (MBS), an event which results in a decrease in phosphatase activity (Kimura, *et al.*, 1996). Rho-kinase was also shown to directly phosphorylate the myosin light chain (MLC) (Amano, *et al.*, 1996a). The phosphorylation of MLC results in a conformational change which is required for binding to actin and thus the bundling of actin into stress fibres. The study of ROCK/Rho-kinases has been aided by the use of the specific inhibitor Y-27632 which has been shown to correct cardiac hypertension in animal models so confirming the role of Rho and Rho-kinase in smooth muscle contraction (Uehata, *et al.*, 1997). Recently this inhibitor has been used to demonstrate the requirement of ROCK in Rho/Ras-dependent cellular transformation (Sahai, *et al.*, 1999).

RhoA has been demonstrated to interact directly with type 1 Phosphatidylinositol 4-Phosphate 5-kinase activity and to stimulate it (Chong, *et al.*, 1994, Ren, *et al.*, 1996). The product of this activity PtdIns(4,5)P_2 has been implicated in the structural rearrangement of cytoskeletal proteins vinculin, gelsolin, capZ α-actinin and profilin adding to the mechanisms of Rho-dependent cytoskeletal changes (Tapon and Hall, 1997). Further, the formin homology domain containing proteins mDia and mDia2 co-localise with profilin and Rho.GTP and cause the formation of filametous actin (Watanabe, *et al.*, 1997).

Transcriptional Activation

Whereas Cdc42 and Rac activate the SAPK/JNK and p38 pathways in Hela, NIH3T3 and Cos cells, Rho has only been reported to activate JNK in HEK293T cells (Teramoto, *et al.*, 1996). RhoA is required for the activation of the Serum Response Factor (SRF) in response to serum, LPA and AlF_4 (Hill, *et al.*, 1995). The SRF stimulates transcription of genes with Serum Response Elements (SREs) including those encoding several cytoskeletal components such as vinculin and β-actin (Treisman, 1995). Thus Rho may confer cytoskeletal control at the level of transcription. Rac and Cdc42 can also activate the SRF in a Rho-independent manner but are not required for the serum response. RhoA mutants that have differential binding for known effectors were used to demonstrate that either a novel protein or co-operation between effectors is required for Rho-dependent signalling to the SRF (Sahai, *et al.*, 1998). It is of interest to note that a partial effect on signalling to the SRF by a ROCK mutant negative for Rho binding was still sensitive to C3 toxin (see discussion). Rho, like Rac and Cdc42 was seen to induce the transcriptional activity of NF-κB via a mechanism that leads to the phosphorylation of I-κB (Perona, *et al.*, 1997).

Rho and Endocytosis

Rho GTPases have been implicated in various different stages of the endocytic process. The expression of GTPase-deficient forms of either Rac or RhoA in Hela cells caused an inhibition of receptor mediated endocytosis. Further, endocytosis was promoted in the presence of a RhoGDI, suggesting Rho negatively regulates the process (Lamaze, *et al.*, 1996). Both PLD and PI5-kinase have been proposed to have an effect on coated pit assembly and are activated by Rho proteins. Unlike RhoA and C which are localised to the plasma membrane RhoB is only ever visualised on early endosomes and a pre-lysosomal compartment (Adamson, *et al.*, 1992). RhoD is also localised to early

endosomes and the use of an active mutant of this GTPase results in a decrease in the motility of the endosomes (Murphy, *et al.*, 1996). The process of endosomal movement along microtubules is mediated by a dynein motor fused to a dynactin receptor and requires ATP and GTP, the only connection between the motor complex and GTP is through the binding of Rho to kinectin (the positive-directed equivalent of dynactin) (Sheetz, 1999). Kinectin has a ROCK-like Rho binding motif and interacts preferentially with Rho.GTP (Alberts, *et al.*, 1998).

1.7 Protein Kinases

The regulated phosphorylation and dephosphorylation of proteins is probably the most well characterised event in signal transduction. The cascades of protein kinases seen to operate within the cell function to amplify signals from surface receptors in a controlled manner. Since the identification of phosphorylase kinase over 40 years ago a plethora of serine/threonine and tyrosine kinases have been demonstrated to play key roles in cellular events. However, the elucidation of how these gene products are regulated and dysregulated by mutation is an on going process. Examples of serine/threonine kinases and the regulation of their activity by the previously mentioned signalling intermediates and GTPases are given below.

1.7.1 Protein Kinase C

Originally identified in 1977 as a kinase activity against histone that could be activated by proteolysis, PKC was subsequently seen to be activated by phosphatidylserine (PS) and diacylglycerol (DAG) in a Ca^{2+}-dependent manner. Further the tumour promoting agent phorbol myristate acetate (PMA) was shown to activate PKC both *in vitro* and *in vivo* by mimicking DAG's promotion of Ca^{2+} binding (Nishizuka, 1984). The molecular cloning of three gene products from bovine brain responsible for the observed kinase activity (Coussens, *et al.*, 1986, Parker, *et al.*, 1986) led to the subsequent use of degenerate probes for the identification of other members of this kinase family. There are now 12 mammalian PKC isotypes characterised (including the PRKs (see below)). These have been subdivided into groups on the basis of regulation and enzymatic properties.

Classical PKCs (cPKCs)

This group comprises the α, βI, βII and γ isotypes. The β gene is alternatively spliced and produces two gene products that differ at their C-termini. As can be seen from figure 1.7 these proteins contain C1 domains which bind DAG or phorbol ester and classic C2 domains which bind PS in a Ca^{2+}-dependent manner. Thus they are activated by PS in the presence of Ca^{2+} and the interaction with DAG both increases the kinases specificity for the phospholipid and increases its affinity for Ca^{2+} (Nishizuka, 1984). The PMA activation of the classical PKCs operates by reducing the concentration of Ca^{2+} required for activation to that present in the cell prior to IP_3-induced mobilisation.

Novel PKCs (nPKCs)

This group consists of the δ, θ and slightly larger ε and η isotypes. Like the classical enzymes they contain a C1 domain for DAG / PMA binding. However, they do not bind Ca^{2+} and are seen to contain a C2-like domain that is missing Asp residues required for the cation co-ordination. They are activated by the DAG in the presence of PS (Ono, *et al.*, 1988). There is also some evidence of nPKC activation by phosphoinositides *in vitro* (Palmer, *et al.*, 1995a).

Atypical PKCs (aPKCs)

The two members of this group ζ and ι both contain a reduced C1 domain (a single rather than double zinc-finger) and do not bind DAG or PMA. They too have a C2-like domain and do not co-ordinate Ca^{2+}. However, ζ activity was shown to be dependent on the presence of phospholipids (Ono, *et al.*, 1989).

The observed proteolytic activation of PKC would suggest an autoinhibitory effect regulates its activity. Indeed all of the isotypes contain a pseudosubstrate site N-terminal to the C1 domain. While the sequence at this site is seen to be slightly different for the various isotypes, perhaps a function of their substrate

specificities, the residue equivalent to the serine or threonine in the substrate is replaced by an alanine (House and Kemp, 1987).

PKCs have been implicated in many cellular processes including proliferation and differentiation. PKC isotypes are seen to be activated as a result of RTK, G protein coupled and cytokine receptor activation. Members of all three classes of PKC have been demonstrated to activate the MEK-MAPK pathway, although only c/nPKCs were seen to operate through the upstream kinase Raf1 (Schonwasser, *et al.*, 1998). However, PKC also displays a negative role in this pathway by specifically phosphorylating the EGF receptor resulting in a reduced tyrosine kinase activity (Murray, *et al.*, 1997). PKCα acts synergistically with Arf and Rho GTPases in the activation of PLD. PLD activity results in the production of DAG at a sustained rate. Thus PKC may effect the production of its own activator. Many other PKC-dependent events have been elucidated through the use of phorbol ester activation, however the identification of non-PKC PMA-responsive proteins would suggest that the use of these activators alone is not an absolute proof of PKC involvement (see (Mellor and Parker, 1998)).

1.7.2 The Role of Phosphorylation in the Regulation of AGC family Kinases

The AGC-family of protein kinases include the cAMP activated kinase PKA the cGMP activated kinase PKG and the Ca^{2+}, DAG activated PKC. Other members based on sequence homology within their serine/threonine kinase domains are the phosphoinositide activated PKB/Akt and the ribosomal subunit kinases $p70^{S6K}$ and $p90^{RSK}$ (Hanks and Hunter, 1995). The kinase domains of these family members are made up of 12 conserved subdomains and catalyse the phosphorylation of serine or threonine residues on target substrates utilising the γ-phosphate group of ATP. This involves the binding of both ATP and the specific substrate in the correct orientation to allow transfer of the phosphate to

the accepting hydroxyl group, a process that is dependent upon the presence of divalent cations (Mg^{2+}, Mn^{2+}) which bridge the β and γ phosphates of the ATP. Based on the structure of PKA the kinase domain's general structure is organised into two lobes separated by a cleft which is the active site (Knighton, *et al.*, 1991). The smaller N-terminal lobe is responsible for ATP binding whereas the C-terminal lobe interacts with the substrate and catalyses phosphate transfer. Catalytic activity against target substrates follows both ATP binding and certain key phosphorylation events within the kinase which contribute to the 'priming' of the enzymes of this family.

For PKC the phosphorylation of a conserved threonine residue on the 'activation loop' between catalytic subdomains VII and VIII was shown to be an absolute requirement for kinase activity (Cazaubon, *et al.*, 1994). The mimicking of a phosphorylation event by the mutation of this threonine to a negatively charged Glutamate results in an active kinase (Orr and Newton, 1994). This activation loop was originally identified in PKA and it was proposed that the negative charge at this site is required for the stabilization of the conformation required for catalysis (Taylor and Radzio-Andzelm, 1994). Later biochemical data suggested that the phosphorylation of PKC at this site was mediated *in trans* by another kinase rather than being an autophosphorylation site (Keranen, *et al.*, 1995). As described for PKB (see below) and demonstrated for PRK in chapter 6 of this thesis, the class of kinases responsible for this event have now been identified.

A further area of sequence homology within this family of kinases is the very C-terminal region which contains two conserved phosphorylation sites (named the V_5 region in PKC isotypes). A serine residue within a highly conserved FSY motif (this site will be termed 'FSY' throughout this thesis) was originally thought to be autophosphorylated (Keranen, *et al.*, 1995). However, more recent studies on PKB have shown it to be the target of a transphosphorylation event (Alessi,

et al., 1996) and in chapter 7 the identification of a potential kinase of this site is discussed. The phosphorylation of this site is required for the full activation of the kinase. Interestingly the threonine residue is replaced by a negatively charged Glu or Asp in the PRKs and atypical PKCs. A second residue which undergoes phosphorylation is that equivalent to T638 in PKCα (see figure 6.1). This has been shown to be an autophosphorylation site (Keranen, *et al.*, 1995) and its occupation while not required for catalytic activity does affect the conformation and hence the rate of dephosphorylation and inactivation of the kinase (Bornancin and Parker, 1996).

1.7.3 Protein Kinase B

This 58 kDa serine/threonine kinase was identified through molecular cloning by three independent groups and was named PKB (due to homology to PKA and PKC kinase domains), c-Akt and RAC (for Related to A and C kinase) (Bellacosa, *et al.*, 1991, Coffer and Woodgett, 1991, Jones, *et al.*, 1991). It is the cellular homologue v-Akt, the product of the AKT-8 transforming retrovirus. Two other isoforms have now been identified and named PKBβ (also called RAC-PKβ or Akt2) and PKBγ. PKB contains an N-terminal PH domain followed by a kinase domain and V_5 region. It is activated in response to many cellular stimuli including insulin, PDGF and EGF. The use of receptor mutants negative for PI3-kinase binding, specific inhibitors wortmannin or LY294002 and dominant negative Ras demonstrated PKB to be a target of PI3-kinase products and associated its activation with a serine phosphorylation event (Burgering and Coffer, 1995, Cross, *et al.*, 1995, Franke, *et al.*, 1995). PI3-kinase activity was also shown to be sufficient for PKB activation through the expression of constitutively active forms of the lipid kinase (Klippel, *et al.*, 1996, Didichenko, *et al.*,1996).

PKB has been implicated in a variety of cellular functions by its kinase activity towards downstream targets. PKB phosphorylation of Glycogen synthase kinase 3 (GSK3) results in the substrates inactivation and subsequent activation of glycogen synthesis (Cross, *et al.*, 1995). Another target of PI3-kinase activity, $p70^{S6K}$ has been shown to be activated by the overexpression of a Gag-PKB fusion protein in Rat-1 cells (Burgering and Coffer, 1995), however whether this is a consequence of the direct action of PKB is unclear. PKB activity has been demonstrated to protect cell from apoptosis induced by the withdrawal of survival factors. One mechanism for this action is the observed phosphorylation of the proapoptotic protein BAD which in the unphosphorylated form heterodimerises with survival factors Bcl-2 or Bcl-Xl preventing their action. The PKB phosphorylation results in the formation of a binding site for the 14-3-3 protein and hence titration of BAD (reviewed by (Downward, 1998)). This protection from apoptosis may account for PKB's transforming potential.

The recent studies of PI3-kinase dependent activation of PKB has resulted in the elucidation of a mechanism which is common for many members of the AGC-family of kinases. The activity of the kinase is dependent upon an intact PH domain which specifically binds both PtdIns(3,4,5)P_3 and PtdIns(3,4)P_2. However, PKB activity *in vitro* is not seen to be extensively enhanced in the presence of these lipids. Residues on the kinase were identified that become phosphorylated in response to insulin (Alessi, *et al.*, 1996) and a plasma membrane translocation event on growth factor stimulation was observed that resulted in these phosphorylations (Andjelkovic, *et al.*, 1997). Together these events suggested that the intact PH domain was required for activity as a targeting signal: bringing PKB to the membrane through its interaction with newly synthesised PI3-kinase products and localising it with activating kinases. This model is established further by the observed phosphorylation of a PKB chimera that contains a PKC CI domain and so is localised to the membrane via interaction with PKC activating phorbol esters but not PI3-kinase generated lipids (Andjelkovic, *et al.*, 1999). However, as described below the interaction of

the PKB PH domain with lipid would also seem to disrupt a inhibitory intramolecular interaction within the kinase.

The residues phosphorylated on agonist stimulation were mapped to threonine 308 within the activation loop of the kinase domain and serine 473 in the 'FSY' site of the V_5 region. The phosphorylation of both of these residues is required for full activation of the kinase and each event was seen to be independent of the other. Further, both sites were phosphorylated *in vivo* on a kinase dead PKB (Alessi, *et al.*, 1996). These results suggested that these events were not a result of autokinase activity and were thus mediated by an upstream kinase. The kinase responsible for the PI3-kinase-dependent phosphorylation of threonine 308 on PKB was subsequently identified and named 3-Phosphoinositide Dependent Kinase (PDK1). The kinase responsible for the 473 site phosphorylation remains to be identified.

1.7.4 3-Phosphoinositide Dependent Kinase (PDK1)

3-Phosphoinositide-dependent protein kinase (PDK1) was originally purified as an activity responsible for the activation loop phosphorylation of PKBα (Alessi, *et al.*, 1997b, Stephens, *et al.*, 1998). This 67kDa serine/threonine kinase has an N-terminal kinase domain and a C-terminal PH domain. It was found to phosphorylate PKB at threonine 308 in a PtdIns(3,4,5)P_3 dependent manner resulting in an activation of the substrate. Subsequently it has been demonstrated to phosphorylate equivalent residues in other members of the AGC kinase family, specifically $p70^{S6K}$, PKC and PKA (Alessi, *et al.*, 1998, Cheng, *et al.*, 1998, Chou, *et al.*, 1998, Dutil, *et al.*, 1998, Le, *et al.*, 1998, Pullen, *et al.*, 1998). The *in vitro* lipid dependence of the activation loop threonine phosphorylation seems to be mainly substrate specific: the PKB phosphorylation and activation by PDK1 shows a much greater lipid

dependence when the PKB PH domain is intact, suggesting the lipid interaction with the substrate causes the removal of an intramolecular interaction masking the activation loop from PDK1. The removal of this domain results in a more lipid independent phosphorylation event (Alessi, *et al.*, 1997a, Stokoe, *et al.*, 1997). The equivalent phosphorylation event on a truncated $p70^{S6K}$ is also independent of lipid (Alessi, *et al.*, 1998).

The *in vivo* mechanism for PDK1 dependence on the action of PI3-kinase activity is less clear. The observation that PDK1 activity immunopurified from cultured cells is seen to be independent of mitogenic stimulation (Alessi, *et al.*, 1997a, Pullen, *et al.*, 1998) and that PI3-kinase-dependent translocation of PDK1 to the membrane is associated with its ability to activate PKB (Anderson, *et al.*, 1998) would suggest PDK1 to be constitutively active, only specifically phosphorylating substrates when co-localised at the same cellular site. However, PDK1 is seen to have some *in vivo* dependence for PtdIns(3,4,5)P_3 even when the substrate lacks a lipid binding site suggesting that lipid regulation operates at both the level of kinase and substrate (Le Good, *et al.*, 1998, Stokoe, *et al.*, 1997).

1.7.5 Protein Kinase C Related Kinase (PRK)

The PRKs were independently identified by molecular cloning, protein purification and PCR screening of cDNA libraries with degenerate oligonocleotides covering highly conserved motifs present in PKC isoforms (Morrice, *et al.*, 1994b, Mukai and Ono, 1994, Palmer, *et al.*, 1994). The PCR based approach resulted in three novel PKC related gene products one of which was identical to that purified and cloned by other workers. This protein was independently named PRK1, PAK1 and PKN; PRK will be the terminology used in this thesis. Two human isoforms PRK1 and PRK2 were fully cloned and expressed in cultured cells. PRK1 (942 amino acids) and PRK2 (984 amino acids) have predicted molecular masses of 103 and 118 kDa respectively but migrate on SDS-PAGE at 120 and 140 kDa as judged by comparison with molecular markers. Both kinases were shown to be present in a wide variety of tissues (Mukai and Ono, 1994, Vincent and Settleman, 1997). Alignment of the amino acid sequences of the two isoforms with each other and regions of PKC isoforms has identified conserved regions (Palmer, *et al.*, 1995b) as can be seen in figure 1.7. Both PRKs contain a C-terminal kinase domain that shares 50-58% identity with the PKCs, V_5 region at the very C-terminus and a central conserved domain, named the Homology Region 2 (HR2) that bears significant similarity to the C2-like (also named V_0) domains of PKCε and PKCη. Unlike the other human PKC isoforms the PRKs contain a novel amino-terminal region which was termed the Homology Region 1 (HR1) and contains three homologous repeats a, b and c. Sequence data-base searches identifies similar motifs in a variety of gene products, most notably the yeast PKC isoforms and the Rho-binding proteins Rhophilin and Rhotekin (see below and figure 1.7). This domain will be described in detail in chapters 3 and 4. It is of interest to note that the yeast PKC enzymes contain all of the domains which are seen on specific kinase isoforms in higher organisms.

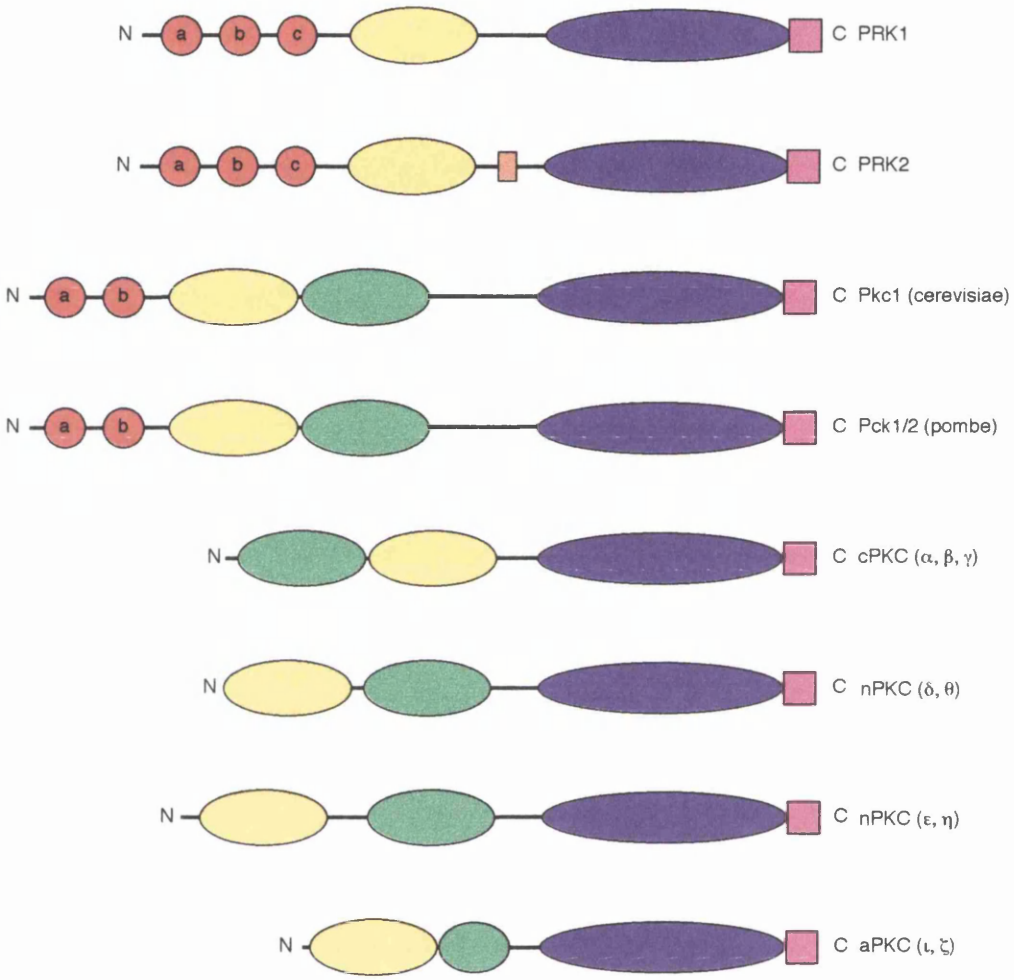

Fig. 1.7: Domain structures of the PKC Subfamilies

A schematic representation of the domain architecture of the various subgroups of PKC kinases. The various domains are: HR1 domains (red); C1 domains (green); C2 and C2-like domains (yellow); serine/threonine kinase domains (blue); the V5-region is shown in pink and a proline rich region in PRK2 is orange. It can be seen that the yeast PKC homologues contain all the relative domains suggesting an archetypal enzyme.

Initial characterisation of the PRKs demonstrated a serine/threonine kinase activity that is optimal in the presence of 100μM ATP and 10mM Mg^{2+}. Proteolysis by trypsin results in catalytic fragments of 50-60 kDa that have increased kinase activity against exogenous substrate MBP (Mukai, *et al.*, 1994, Palmer and Parker, 1995). As expected from its domain structure, PRK is not activated by diacylglycerol Ca^{2+} or phorbol esters. However, several studies demonstrated a potent activation and increased autophosphorylation of purified PRK1 with unsaturated fatty acids and acidic phospholipids *in vitro* (Morrice, *et al.*, 1994b, Mukai, *et al.*, 1994). On further investigation the polyphosphoinositides PtdIns(4,5)P_2 and PtdIns(3,4,5)P_3 were also seen to activate purified PRK when presented either as pure sonicated lipids or in non-ionic detergent mixed micelles (Palmer, *et al.*, 1995a) whereas PtdIns and PtdSer were only effective activators in their pure form. The non-specific effect of these lipids and fatty acids *in vitro* suggests a co-activator delivering specificity exists *in vivo.* Several phosphorylation events on rat PRK1 were associated with its activation *in vitro*. A threonine at position 778 was seen to be phosphorylated *in vivo* and therefore distinct from subsequent *in vitro* phosphorylations (Peng, *et al.*, 1996).

At the outset of the present study PRK was identified as a potential Rho GTPase effector: one group purified PRK1 by affinity chromatography using a Rho.GTP column (Amano, *et al.*, 1996b), while another study identified a novel gene product in a 2-hybrid screen using Rho as bait (Watanabe, *et al.*, 1996). This novel protein was named Rhophilin and was seen to be homologous to PRK within the HR1 domain. Further experiments demonstrated PRK to interact with RhoA in a GTP-dependent manner. As described in chapters 3 and 4 of this thesis, the HR1 domain was subsequently identified as the Rho interaction domain (Flynn, *et al.*, 1998). A similar situation has been described for PRK2, although a high affinity interaction is also demonstrated with Rac1 (Vincent and Settleman, 1997). The potential role of the GTPase interaction in the regulation of the PRK kinases activity is the basis for this thesis.

Immunofluorescence studies has shown both PRKs to be localised within the cytoplasm of fibroblasts, however after a period of expression time a more punctate staining pattern is seen. While RhoA is cytoplasmic with a small amount of protein found on the plasma membrane, RhoB is found exclusively on early endosomes. Studies completed in parallel with this thesis demonstrated PRK translocation to endosomes to be dependent upon its interaction with RhoB, an event which is associated with the accumulation of a hyperphosphorylated form of the kinase (Mellor, *et al.*, 1998). Consistent with these observations the majority of PRK2 is found within the soluble fraction of mouse liver whereas a greater amount is within the detergent soluble fraction of cultured cells suggesting a localisation event during cell growth (Vincent and Settleman, 1997).

Other proteins are seen to interact with the PRKs. The Nck adaptor protein contains three consecutive SH3 domains and a C-terminal SH2 domain, while the SH2 domain is seen to bind to activated RTKs the SH3 domains interact with effector molecules containing proline rich motifs. PRK2 interacts with the second SH3 domain of NCK but not with the SH3 domains of various other adapter molecules, kinases or cytoskeletal proteins (Quilliam, *et al.*, 1996). The interaction site for NCK is predicted to be the proline-rich region present within the hinge region N-terminal of the kinase domain. This region is unique to PRK2 and is predicted to be a receptor localisation motif.

A possible role for the PRKs in cytoskeletal organisation is suggested by the observations of a number of studies. The microinjection of a kinase-deficient PRK2 into fibroblasts caused a complete loss of actin stress fibres (Vincent and Settleman, 1997). It was demonstrated that the use of the minimal Rho-binding domain did not have the same effect, suggesting the lack of stress fibres was not due to a simple competition of active Rho. Intermediate filaments are 10nm cytoskeletal elements made up of subunits which form coiled-coil dimers. The

subunits are classified into 5 distinct types based on sequence homologies within a central α-helical head-rod domain. PRK has been demonstrated to bind the rod domain of both the neuron-specific neurofilament protein and vimentin. The subsequent phosphorylation of the subunits by PRK prevents the assembly of filaments *in vitro* (Matsuzawa, *et al.*, 1997, Mukai, *et al.*, 1996). In a further link between PRK and the cytoskeleton, the kinase was shown to bind α-actinin both *in vitro* and *in vivo* (Mukai, *et al.*, 1997). This interaction was PtdIns(4,5)P_2 dependent and the site on contact was mapped to residues 136-139 of PRK1 which corresponds to the second HR1 repeat (HR1b). PRK was seen to phosphorylate α-actinin but the stoichiometries were low and the functional significance of this remains unclear. The interaction of PtdIns(4,5)P_2 with α-actinin has previously been shown to increase its F-actin gelating activity (Fukami, *et al.*, 1992). Recently the characterisation of a loss-of-function mutant in the *Drosophila* PRK1 homologue, Pkn revealed the kinase to be involved in the dorsal closure of the developing embryo (Lu and Settleman, 1999). Its activity is required for the stretching of leading edge cells and the phenotype resulting from loss of kinase activity is consistent with that seen for Rho1 mutant embryos. The same lack of dorsal closure is seen with a mutant Rac-dependent JNK pathway and while this is independent of the Pkn, some cross talk between pathways has been genetically identified.

PRK has also been implicated in transcriptional activation events. PRK2 was demonstrated to induce transcriptional activation from an SRF-luciferase reporter construct and co-operate with Rho and Cdc42 as well as the GEF Dbl (Quilliam, *et al.*, 1996). However, a later study showed Rho mutants negative for PRK1 interaction to still activate SRF reporter genes and the PRK1 kinase domain alone to be ineffectual at SRF activation (Sahai, *et al.*, 1998). This may suggest a differential downstream target for the two PRK isoforms.

Caspases are cysteine proteases with aspartate specificity that are demonstrated to induce apoptosis when ectopically expressed in cultured cells. Normally present as catalytically inactive proenzymes their proteolytic activation during the onset of apoptosis results in the subsequent cleavage of specific cellular targets. The cleavage of certain protein kinases such as MEKK-1 and PKCδ results in an induction of their kinase activity. Both PRK1 and PRK2 are seen to be proteolytically cleaved by caspase-3 *in vitro* and *in vivo* on Fas or staurosporine-induced apoptosis in Jurkat or U937 cells (Cryns, *et al.*, 1997, Takahashi, *et al.*, 1998). The cleavage produces similar fragments for both kinases: a minimal, catalytically active kinase domain; a short N-terminal fragment including the HR1a and pseudosubstrate site (see section 5.1) and a central fragment containing the rest of the HR1 domain the HR2 and hinge region. Thus the kinase activity of the PRKs may well be deregulated during the onset to apoptosis.

It has been suggested that PRK1 is directly involved in the regulation of glucose uptake of 3T3 L1 adipocytes via a PRK-provoked increase in GLUT4 translocation to the plasma membrane (Standaert, *et al.*, 1998). This study demonstrated that insulin and GTPγS-stimulated glucose transport was blocked by C3 toxin, LY294002, wortmannin and the broad specificity PKC inhibitor RO 31-8220 suggesting the involvement of Rho PI3-kinase and a protein kinase. Further, dominant negative forms of Rho and PRK1 inhibited glucose transport whereas wildtype PRK1 activated this process.

Thesis Aim

PRK has been implicated in many cellular processes associated with both Rho and lipid kinase activity. Its kinase activity can be stimulated *in vitro* by non specific fatty acids and polyphosphorylated inositides but its true *in vivo* regulators remain undefined. The initial aim of this thesis is to study the role of a potential Rho GTPase-PRK interaction in the regulation of the kinase. By gaining an insight into the activation process it is anticipated that a greater knowledge of PRK-dependent events will be gained.

Chapter 2 - Materials and Methods

2.1 Materials

All chemicals and biochemicals were obtained from Sigma Chemical company, apart from the exceptions listed below. Ethandiol, methanol, ethanol Tween 20, Triton X100 and NNN'N Tetramethylethylenediamide were obtained from BDH. Glutathione Sepharose, Nick desalting columns and ultra pure dNTPs were obtained from Pharmacia Biotech. Radioisotopes, protein standard markers, Hyperfilm MP, ECL western blotting kit and anti-mouse / anti-rabbit IgG (from donkey) coupled to horseradish peroxidase were all from Amersham Lifescience. The inhibitors: microcystin-LR, calyculin A, okadaic acid, LY294004, aprotinin and leupeptin were from Calbiochem. Both restriction enzymes and Vent™ polymerase along with the relevant buffers were from New England Biolabs whereas T4 ligase was obtained from Boehringer. GTP, GDP and thrombin was also from Boeringer. Nitro-cellulose membrane was from Schleicher and Schull and skimmed milk powder was obtained from Boots company Ltd. Ultra pure agarose and DNA marker standards were both obtained from Gibco as was foetal calf serum. Sterile plastic-ware for cell culture was obtained from Falcon. Molecular biology kits used: Qiagen mini/maxi prep kit; ABI prism™ Dye terminator cycle sequencing kit (with Amplitag polymerase) and the Quickchange™ Site Directed Mutagenesis kit from Stratagene. The D-enantiomer of sn-1-stearoyl, 2-arachidonyl PtdIns $(3,4,5)P_3$ was a gift from Dr P. Gaffney.

2.1.2 Vectors Used

Mammalian

Vector	Origin	Use
pCDNA3	Invitrogen	High level expression
pRC/RSV	Invitrogen	High level expression
pCMV5	D. Alessi (Dundee)	High level expression

Bacterial

Vector	Origin	Use
pGEX 4T1	Pharmacia Biotech	GST-fusion expression
pRSET	Invitrogen	His-tag expression
pBluescript SKII	Stratagene	General cloning and blue/white selection

2.1.3 Cell Types Used

Mammalian

Cell Type	Origin	Brief Description
293	ICRF Cell Services	Adenovirus transformed human embryonic kidney cells with fibroblast morphology.
Cos-7	ICRF Cell Services	Derived from African Green Monkey kidney; transformed by SV40; fibroblast morphology.
NIH 3T3	ICRF Cell Services	Derived from swiss mouse embryos; contact inhibited and with fibroblast mophology.

Bacterial

Cell Type	Origin	Brief Description
DH5α	Gibco	E.coli providing α-complementation of the β–galactosidase gene for blue/white selection screening.
BL21 pLysS	Novagen	Chemically competent E.coli carrying T7 lysozyme-encoding plasmid to suppress basal T7 RNA polymerase prior to induction. For protein expression.
BL21 GroES/EL	Du Pont	Chemically competent E.coli carrying chaperone plasmid to aid folding and hence solublization of expessed proteins.

2.1.4 Primary Antibodies Used

Name	Origin	Description	Use
9E10	ICRF Monoclonal	Mouse monoclonal specific for Myc-tag	W, IP, IF
EE	ICRF Monoclonal	Mouse monoclonal specific for Glu-Glu tag	W, IP
12CA5	ICRF Monoclonal	Mouse monoclonal specific for HA-tag	W, IP
GST (Z-5)	Santa Cruz	Rabbit polyclonal	W
RhoA (26C4)	Santa Cruz	Rabbit polyclonal	W
RhoA (119)	Santa Cruz	Rabbit polyclonal	W
RhoB (119)	Santa Cruz	Rabbit polyclonal	W
HA (Y-11)	Santa Cruz	Rabbit polyclonal	W, IP
PRK1 COOH	ICRF Polyclonal	Rabbit polyclonal purfied by affinity chromatography	W
PRK2 COOH	ICRF Polyclonal	Rabbit polyclonal purfied by affinity chromatography	W

PRK1 mab	Trasduction labs.	Mouse monoclonal	W
PRK2 mab	Trasduction labs.	Mouse monoclonal	W, IP
Phos. PRK Activation Loop	ICRF Polyclonal	Rabbit polyclonal purfied by affinity chromatography (see 2.3.6)	W
Phos. PRK Auto site	ICRF Polyclonal	Rabbit polyclonal purfied by affinity chromatography	W

(W - Western blotting, IP - Immunoprecipitation, IF Immunofluorescence)

2.1.5 Commonly used Buffers

Luria-Bertani (LB) medium, SOC medium, PBS, trypsin-versine and Dulbeccos MEM (DMEM) were obtained from ICRF central services.

TAE 50X: 2.0M Tris-acetate
0.05M EDTA (pH 8.0)

TE (pH 8.0): 10mM Tris-HCl (pH 8.0)
1mM EDTA (pH 8.0)

Alkaline Lysis Buffers: Sol. 1. 50mM Glucose
25mM Tris-HCl (pH8.0)
10mM EDTA (pH8.0)

	Sol. 2.	0.2M NaOH 1% (w/v) SDS
	Sol. 3.	5M potassium acetate 11.5% (v/v) glacial acetic acid
SDS Running Buffer:		0.025M Tris-HCl 0.192M Glycine 0.1% (w/v) SDS
SDS Sample Buffer (4X):		1M Tris-HCl pH 6.8 20% (w/v) SDS 10% (v/v) Glycerol 0.1M DTT 0.01% (w/v) Bromophenol Blue
Semi-dry transfer buffers:	Anode I:	0.3M Tris -HCl (pH 8.0) 20% (v/v) Methanol
	Anode II:	25mM Tris-HCl (pH 8.0) 20% (v/v) Methanol
	Cathode I:	25mM Tris-HCl (pH 8.0) 40mM Amino Caproic acid 20% (v/v) Methanol

Wet transfer buffers:

26mM Tris-HCl
192mM Glycine
20% Methanol (omitted as indicated)

Calcium Phosphate

Transfection buffer:

25mM $CaCl_2$

2X BBS:

50mM BES (pH 6.95)
280mM NaCl
1.5mM Na_2HPO_4

GST Purification - Buffer A:

50mM Tris (pH 7.5)
50mM NaCl
5mM $MgCl_2$ (GTPases Only)
5% (v/v) Glycerol
1% (v/v) Triton X100
10μg/ml Leupeptin
1mM PMSF
1mM DTT
10mM Benzamidine

Nucleotide loading

Buffer B:

50mM Tris (pH 7.5)
5mM EDTA
1mM DTT
1mg/ml BSA
1μM GTP

Buffer C: 50mM Tris (pH 7.5)
20mM $MgCl_2$
0.1mM DTT

Overlay Renaturation - Buffer D: PBS
0.1% BSA
0.5mM $MgCl_2$
50μM $ZnCl_2$
0.1% (v/v) Triton X100
5mM DTT

Mammalian Cell Harvest - Buffer E: 50mM Hepes (pH 7.5)
100mM NaCl
5mM EDTA
20mM NaF
1% (v/v) Triton X100
1mM DTT
10μM Leupeptin
10μM Aprotinin
0.1mM PMSF
5mM Pyrophosphate
1μM Microcystin-LR

Kinase Assay - Buffer F: 20mM Hepes (pH 7.5)
50mM NaCl
0.1mM EGTA

0.1% (v/v) β-mercaptoethanol

1μM Microcystin-LR

100 μM ATP

2.5mM $MgCl_2$

Chromatography Buffer G: 20mM Hepes (pH 7.5)

0.5M NaCl (omitted where indicated)

2mM EDTA

0.3% (v/v) β-mercaptoethanol

0.05% (v/v) Triton X100

10mM Benzamidine

2.2 General Experimental Methods

2.2.1 Standard Molecular Biology procedures

Restriction digests were carried out in accordance with the manufacturer's instructions, using the buffers provided. Standard procedures such as ethanol precipitation and agarose gel electrophoresis were performed as described in (Maniatis, *et al.*, 1989).

2.2.2 DNA Purification

Small scale DNA purifications (mini-preps.) from colonies of transformed *E. coli* were carried out using the Qiagen QIAprep™ kits, in accordance with the manufacturer's instructions. Large scale purification was completed by alkaline Lysis of transformed bacteria followed by double banding on a CsCl gradient, as described in Maniatis. Fragments of DNA purified by gel electrophoresis were extracted from the gel using a Qiagen gel extraction kit.

2.2.3 Polymerase Chain Reaction (PCR)

Either Vent™ or Taq polymerase were used in combination with the buffers provided by the manufacturer to perform PCR reactions. A 10mM stock of ultrapure dNTPs; with respect to each deoxynucleoside triphosphate (dTTP, dCTP, dATP and dGTP) was diluted to 200μM final for each reaction. A general reaction would contain 1μM of purified sense and antisense primers, a double stranded template (amount depending upon reaction) and 1 unit of polymerase in a final volume of 50μl. A basic program would be a 5 minute, 95°C 'Hot Start',

followed by 30 cycles of a 95°C denaturation step, a 45-65°C annealing step and an extension step at 72-74°C. The times and temperatures of both the annealing and extension steps varied relative to the primers and the templates used.

2.2.4 Ligations

Generally digested inserts and vectors for ligation were purified by gel electrophoresis using low melting point agarose. The relative bands were excised from the gel and either extracted using the Qiagen gel extraction kit or the agarose was melted at 65°C. A 2:1 ratio of insert to vector was mixed with 1 unit of T4 DNA ligase and buffer to 1X, typically in a 20µl reaction. The reactions were incubated at either room temperature for 1 hour or 15°C over night for sticky and blunt ended fragments respectively. Successful ligations were generally screened using blue/white selection (see 2.2.6).

2.2.5 Transformation of *E. coli*

E.coli for use either in blue/white selection or protein expression (see 2.1.3) were made chemically competent as out lined in Maniatis. An aliquot of cells was incubated with typically between 0.05µg-1.0µg of plasmid DNA for 30 minutes on ice, heat shocked for 45 seconds at 45°C and returned to ice for 2 minutes. The *E. coli* were then incubated for 1 hour at 37°C with agitation in 800µl antibiotic-free SOC medium. This was to allow the transformed bacteria time to recover antibiotic resistance. 100-500µl of the culture was then plated on antibiotic LB plates (typically 50mg/ml ampicillin and/or 20mg/ml chloramphenicol).

2.2.6 Blue / white selection of positive clones

Sub-cloning of inserts into the multiple cloning site of vectors containing the β-Galactosidase (lacZ) gene was assessed using blue/white colony selection. Transformed bacteria were plated on LB / ampicillin which had been spread with 40µl of inducer; 100mM isopropyl-β-D-thiogalactopyranoside (IPTG) and 100µl of substrate; 2% 5-bromo-4-chloro-3-indolyl-β-D-galactoside (X-Gal) (in sterile dimethylformamide). After incubation for 16 hours at 37°C colonies positive for inserts i.e. those with disrupted LacZ genes were white whereas colonies containing vectors re-ligated to themselves were blue in colour.

2.2.7 Double stranded DNA sequencing

All sequencing reactions were carried out according to the ABI prism™ Dye terminator cycle sequencing kit. The data generated from the ABI cycle sequencer was analysed using the soft-ware provided (Perkin Elmer) and DNA Star™ sequence manipulation program.

2.2.8 Mutagenesis

In vitro site directed mutagenesis was carried out using the Quickchange™ mutagenesis kit (Stratagene) according to the manufacturer's instructions. This method utilised mutant oligonucleotide primers complementary to opposite strands of the vector and *Pfu* DNA polymerase which replicated both strands without displacing the primers. The mixture of parental plasmid template and the newly synthesised, mutant DNA was then subjected to Dpn1 endonuclease digestion. Dpn1 is specific for methylated DNA and so preferentially digested the parental template, leaving the mutant plasmid to be transformed into

competent *E.coli*. The resulting mutants were checked by cycle sequencing for both the successful incorporation of point mutants and for lack of unwanted random mutations.

2.2.9 Protein expression in Bacteria

Colonies of a BL21 strain of bacteria were transformed as described (2.2.5) with a pGEX or pRSET recombinant vector. Generally a single colony, grown on an antibiotic selection plate (ampicillin and/or chloramphenicol), was used to inoculate a 10ml LB culture, again containing the relavant antibiotics. This culture was incubated in a 37°C shaking incubator for 16 hours. After dilution of this mini-culture 50-fold in LB it was returned to 37°C until it had reached mid-logarithmic growth (A_{600}nm~0.6). Protein expression was induced by the addition of 0.3mM IPTG and the culture was incubated at 25-37°C for 3-6 hours depending upon the proteins to be expressed. The bacteria were pelleted by a 10 minute centrifugation at 4000rpm and proteins were purified as described (2.2.10/11).

2.2.10 Purification of His6-tag proteins from Bacteria

Protein expression was carried out as described (2.2.9). Purification procedures were generally as described in the QIAexpressionist hand book: cells were resuspended at 5ml/g bacteria in 50mM $Na_2H_2PO_4$, 300mM NaCl, 1mM PMSF, 3mM β-mercaptoethanol and 10mM benzamidine. Cells were lysed by the addition of 1mg/ml lysozyme and incubation on ice for 30 minutes, followed by three 30 seconds probe-sonications (200-300W). Lysates were cleared by centrifugation (10,000rpm for 20 minutes at 4°C). Between 250µl and 1ml of a 50% slurry of Ni-NTA agarose was added to the lysates which were then

tumbled at 4°C for 30 minutes - 1 hour. Three wash steps were carried out as outlined in the handbook. Two rounds of elution were performed by tumbling the agarose with 0.4M imidazole for 30 minutes at 4°C. The concentration of the purified proteins was calculated by Bradford assay (2.2.12) and concentrated with the use of a centricon (Amicon) if necessary. Proteins were stored at -20°C in either 50% (v/v) glycerol or ethandiol.

2.2.11 Purification of Glutathione-S-transferase fusion proteins from Bacteria

Bacterial pellets were resuspended at 5ml/g of pellet in buffer A (2.1.5) and lysed by three 30 second rounds of probe-sonication (200-300W).The nucleotide binding capacity and hence stability of the GTPases was ensured by the addition of Mg^{2+} to the extraction buffer. Lysates were cleared by centrifugation at 14,000rpm for 20 minutes at 4°C. Cleared lysates were then tumbled for up to 1 hour at 4°C with 250µl-1ml of pre-equilibrated glutathione Sepharose 4B (50% slurry). Three large volume washes of the Sepharose with buffer A, including one with 0.5M NaCl was followed either by elution of the fusion proteins or thrombin / Factor XA cleavage. Elution was carried out by a double incubation of the Sepharose with buffer A or the relevant storage buffer (as described in the results) containing 50mM reduced glutathione (pH 8.0).

Proteolytic cleavage of the fusion protein away from GST was performed using either thrombin or Factor XA proteases. Sepharose 4B loaded with fusion protein was resuspended as a 30% slurry in Buffer A or relevant storage buffer containing 2.5mM $CaCl_2$ and 3.0 units protease/ml Sepharose. Cleavage took place at 4°C for between 30 minutes and 16 hours, depending on the fusion protein. The resulting eluent was incubated with 5% (v/v) of p-aminobenzamidine agarose to remove the thrombin. Purified protein

concentration was calculated using Bradford reagent (2.2.12) and stored as described in text.

2.2.12 Determination of Protein Concentration

Concentrations of purified proteins were assessed using the method of (Bradford, 1976). A volume of 1-20µl of sample, or BSA standard, made up to 20µl with H_2O was added to 700µl of Bradford reagent (5 fold dilution from Bio Rad stock). After a five minute incubation at room temperature the sample's A_{595}nm was read. Protein concentration was calculated from the BSA standard curve.

2.2.13 Polyacrylamide Gel Electrophoresis

Sodium dodecyl sulphate - polyacrylamide gel electrophoresis (SDS-PAGE) was performed according to (Laemmli, 1970). Gel apparatus from Hoefer Scientific Instruments were used for the pouring and running of gels. Running buffer and 4X sample buffer were made as described (2.2.5). In general a 6% stacking gel was used throughout in combination with running gels from 8%, for full length PRK proteins, to 15% for Rho GTPases, HR1 domains and Myelin Basic Protein (MBP) from kinase assays. Rainbow marker standards were run alongside the samples for assessment of apparent molecular weight. Proteins were visualised by either Coomassie blue staining or transfer to nitrocellulose for western blotting (see 2.2.15). Gels for storage or autoradiography were sandwiched and stretched between porous cellophane (Pharmacia Biotech) and left to dry; typically for 16 hours.

2.2.14 Western Blotting

Proteins separated by SDS-PAGE as outlined (2.2.14) were transferred to nitrocellulose using either the Hoefer Semiphor™ semi-dry blotting apparatus at room temperature for 1 hour (180mA, constant voltage) or the Bio Rad wet transfer tanks for 90 minutes at 4°C (constant current). The full length PRK proteins were transferred in methanol-free buffer, whereas for smaller proteins, such as the GTPases, 20% methanol was added. The effectiveness of the transfer was assessed by ponceau staining of the nitrocellulose membrane (Salinovich and Montelaro, 1986). The membranes were blocked by incubation in either PBS or TBS 0.1% (v/v) Tween-20 with 5% (w/v) skimmed milk powder for 1 hour at room temperature. After a brief wash in PBS/TBS 0.1% Tween-20 the primary antisera were applied, diluted in PBS/TBS 0.1% Tween-20 with 0.5% milk powder at concentrations stated in the text. Incubations with the primary antibodies were either 1 hour at room temperature or 16 hours at 4°C. Several washing steps were followed by a 1 hour incubation with either anti-rabbit or anti-mouse IgG coupled to horseradish peroxidase. Extensive washes were carried out prior to developing the blot using ECL reagents according to the manufacturer's instructions.

2.2.15 Mammalian Cell Growth and Maintenance

HEK293, COS-7 and NIH 3T3 cells were all routinely grown in Dulbecco's modified Eagle's medium supplemented with penicillin and streptomycin (50μg/ml) and 10% (v/v) foetal calf serum (FCS). Normal maintenance was at 37°C in a humidified atmosphere of 10% CO_2. Generally cells were passaged when they reached 80-100% confluence by removal of old medium and treatment with 0.25% (v/v) trypsin-versene for 3-8 minutes, depending upon cell type. Suspended cells were centrifuged at 250rpm and washed in PBS before

resuspension in fresh DMEM / 10% (v/v) FCS. Cells were then seeded at 20-30% confluence.

2.2.16 Calcium Phosphate Transfection of Mammalian Cells

This highly efficient method for transfection of adhered cells is discussed by (Chen and Okayama, 1988). In an adapted four day procedure, cells were passaged on the evening of day 1 and seeded at $1x10^5$ / ml in DMEM 10%FCS. The following day the filter sterilised transfection mix was applied (see 2.1.5); typically for a 15cm plate 10-20µg of plasmid DNA was added to 1.25ml $CaCl_2$ which was then mixed with 1.25ml of 2xBBS. After a 15 minute incubation at room temperature this was applied to the cells in a drop-wise fashion. The plates were then placed in a 37°C humidified atmosphere which had been adjusted to 3% CO_2 (this was for the maintenance of the optimum pH for transfection). After a 14-16 hour incubation, the medium was removed and the cells were washed twice in PBS. Fresh medium (10%FCS) was applied and the cells were returned to 37°C and 10% CO_2 for a further 24 hours prior to harvesting. This time period was seen to be optimum for the expression of the full length PRK proteins. For experiments requiring the withdrawal of growth factors cells were generally maintained in media supplemented with 0.25% FCS / 0.5% (w/v) BSA (fatty acid free) for 16-24 hours (depending on cell type) followed by 1 hour in 0% FCS just prior to harvest. Any application of inhibitors or stimuli are outlined in the results chapters.

2.2.17 Preparation of Cell Extracts

Whole cell extracts for analysis by western blot were prepared by washing the adhered cells in ice cold PBS, prior to lysis and collection in 4X Laemmli

sample buffer. Samples were heated to 95°C for 5 minutes prior to loading on SDS-PAGE.

The preparation of cell extracts for immunoprecipitation routinely required the cells to be washed in ice cold PBS, drained and lysed in 800µl (15cm plate) of mammalian cell harvest buffer E.

2.2.18 Purification of PRK1 from HEK 293 Cells

This procedure has been previously published (Palmer and Parker, 1995). Untagged PRK1 was transiently transfected into HEK 293 cells using the calcium phosphate technique. 8-10 15cm plates of cells were washed twice in ice cold PBS prior to cell lysis in buffer E (except with the use of 0.3% (v/v) β-mercaptoethanol rather than DTT). Lysates were clarified by centrifugation at 70,000g for 10 minutes at 4°C. All subsequent steps were carried out at 4°C. The supernatant was loaded onto a 200ml Sephacryl S-300 column (Pharmacia), equilibrated and developed in buffer G. Eluted fractions (2ml) were then assayed for PRK1 activity (see below) and peak fractions were pooled. Pooled fractions were diluted to less than 0.1M NaCl in buffer G (minus NaCl) and chromatographed on a 5ml HiTrap SP column (Pharmacia). Proteins were eluted in a linear salt gradient from 0 to 1M NaCl. Fractions (1ml) were again assayed for kinase activity, peak fractions pooled and diluted to less than 0.1M NaCl. This procedure was repeated for the subsequent steps of HiTrap Heparin (5ml) and HiTrap Q (1ml) columns. The final peak activity fractions (0.5ml) were pooled and stored at -20°C in 50% (v/v) ethandiol.

2.2.19 Immunoprecipitation from Mammalian Cells

Transiently overexpressed or endogenous proteins were routinely immunoprecipitated from 293 cells. Cell extracts were prepared as described (2.2.18) and kept on ice or at 4°C throughout the procedure. Extracts were clarified by centrifugation for 15 minutes at 12,000rpm and pre-cleared by tumbling with 100µl of 10% (w/v) insoluble protein A for 20 minutes. The supernatant resulting from a second centrifugation was incubated an appropriate amount of antibody (as indicated) for 20 minutes e.g. for a 15 cm plate of 293 cells; 10µg 9E10 for an overexpressed PRKmyc protein or 2µg of Transduction Labs PRK2 antibody for immunoprecipitation of endogenous PRK2. Addition of 100µl (50% slurry) Protein G Sepharose was followed by a 1 hour incubation with tumbling. The resulting Sepharose was washed three times in buffer E (middle wash at 0.5M NaCl), followed by kinase buffer F or relevent storage buffer. Immunoprecipitated proteins were eluted either by heating to 95°C in 4X sample buffer or by incubation with an excess of a competing peptide antigen.

2.2.20 *In vivo* Labelling in 293 Cells

293 cells were transfected with PRK2myc, in combination with RhoA (Q61L) or *Clostridium* C3 toxin constructs, as outlined in the results chapters. Cells were washed into phosphate free DMEM (10%FCS) 40 minutes prior to the labelling with 3.3mCi Orthophosphate per plate (15cm). After a 6 hour incubation at 37°C in a humidified 10% CO_2 atmosphere, the cells were washed twice in ice-cold TBS prior to a typical immunoprecipitation procedure (2.2.19). The protein G Sepharose was heated to 95°C in 4X sample buffer to elute the PRK. The samples were run on a 10% SDS-PAGE which was fixed in 50% methanol / 10% acetic acid, dried and used to produce an autoradiograph.

2.2.21 Tryptic Digestion and Two-Dimensional Electrophoresis

The acrylamide gel segment containing the radiolabelled PRK protein from the *in vivo* labelling was desiccated with acetone prior to tryptic digest with 20µg trypsin/ml in ammonium bicarbonate. The resulting tryptic phospho-peptides were dried under vacum and resuspended in 40µl electrophoresis buffer (pH2.2 water:formic acid:acetic acid (90:2:8)). The samples, containing 1-5X10^3 cpm, were loaded onto Thin Layer Chromotography (TLC) plates and were electrophoresed for 30 minutes at 50mA. The TLC plates were dried before the second dimension chromatography (buffer; n-butanol: pyridine:acetic acid:water (75:50:15:60)). The plates were dried once again and the phospho-peptides were visualised by autoradiography.

2.2.22 Lipid Presentation for *in vitro* Kinase Assays

PRK proteins are activated *in vitro* by phosphorylated inositol lipids PtdIns(4,5)P_2 and PtdIns(3,4,5)P_3 (Palmer, *et al.*, 1995a). During kinase assays these lipids were generally displayed to the immunoprecipitated PRKs with a background of a Triton X100 micelle. The mol% of the inositol lipid within a given micelle was calculated as outlined by (Hannun, *et al.*, 1985). The relative amount of lipids were aliquoted from stock and dried under N_2 or vacuum followed by resuspension in kinase buffer containing 1% (v/v) Triton X100. Ten minutes bath sonication with intermittent vortexing was required for the formation of the micelles.

For the work involving the lipid dependence of PDK1 10µM PtdIns(3,4,5)P_3 was displayed in a background vesicle of 100µM Phosphatidylserine and 100µM Phosphatidlycholine. These were mixed from stock, dried under N_2 and resuspended in Kinase buffer F free of detergent. Again bath sonication and vortexing was required for the formation of mixed lipid vesicles.

2.2.23 *In vitro* Assays to Determine PRK Kinase Activity

The kinase activities associated with the column fractions generated by procedure 2.2.18 were assayed *in vitro* against protamine sulphate (10μg/assay). The kinase activity of either immunoprecipitated or GST-fusion PRK proteins was routinely assessed by *in vitro* kinase assay using Mylein Basic Protein (MBP) as substrate. A typical 40μl reaction would contain 100ng PRK, 5μg MBP, 5μCi [γ^{32} P] ATP and be made up to kinase buffer F (2.1.5), unless otherwise stated. Lipids were prepared as described in 2.2.22 as 4X stocks and diluted into the reaction volume. Reactions were carried out for 20 minutes at 30°C and were stopped either by spotting onto Whatman P81 paper and immersion in 30% (v/v) acetic acid, or addition of sample buffer to 1X. The p81 papers were washed three times in excess 30% acetic acid followed by Cerenkov counting to determine MBP phosphorylation. Alternatively, samples were run on a 15% SDS-PAGE which was Coomassie stained, dried and used in autoradiography. This gel could then be cut and counted to accurately determine specific activity.

As described in more detail in the results chapters, the *in vitro* PDK1 activation of PRK was established using a two-stage reaction based on that described by others (Alessi, *et al.*, 1997b). Briefly, stage 1: GST-PDK1 was used to phosphorylate GST-PRK1kin in a 40 minute reaction at 30°C in the presence of ATP but absence of [γ^{32} P] ATP. Stage 2: 5μCi [γ^{32} P] ATP and 5μg MBP were added to the reaction followed by a further 10 minute incubation at 30°C.

Reactions were placed in a water bath for the incubation periods, except when the PRK proteins were immobilised on Protein G Sepharose, where reactions were agitated in a shaking incubator (Microtherm™ by Camlab).

2.3 Specialised Methods

2.3.1 Guanine Nucleotide Loading Efficiency Assay

Rho-family GTPases were routinely expressed as GST-fusions, purified and thrombin cleaved (see 2.2.9/10). The relative nucleotide loading capacities of these proteins were determined using a guanine nucleotide nitrocellulose binding assay (Self and Hall, 1995b). GTPases were incubated with 10μCi [α^{32} P] GTP / assay made up to 32.5μl with buffer B for 10 minutes at 30°C. This Mg^{2+}-free incubation allowed the GTPase to exchange nucleotides freely. The exchange was stopped by dilution in 0.5ml of buffer C (20mM $MgCl_2$) and by placing the tubes on ice. The assays were then filtered through pre-wetted nitrocellulose using a Millipore device. The filters were washed three times in ice cold buffer C and allowed to dry in air. The radiolabel attached to the filters was detected by Cerenkov counting.

The relationship between the mol of nucleotide retained on the filter and the mol of GTPase added to the assay was then used to calculate the percentage loading capacity of the purified protein (see Appendix I). Typically, 15-30% of the Rho-GTPase purified was capable of nucleotide exchange.

2.3.2 Ligand Overlay Assay

Potential Rho family binding proteins and relative controls were run on SDS-PAGE and transferred to nitrocellulose membrane. This was then incubated in renaturation buffer D at 4°C for 15 hours, followed by a 1 hour blocking step in buffer D containing 1% (w/v) BSA. The recombinant Rho-family proteins were assessed for nucleotide loading capacity (see 2.3.1). Protein concentrations

were adjusted so that typically 0.5μg of Rho was GTP loaded by incubation in buffer B plus 20μCi [α^{32} P] GTP at 30°C for 20 minutes, followed by 1/10 dilution in buffer C and placed on ice. The membrane was immediately incubated in PBS, 5mM $MgCl_2$ with 0.1μg/ml GTP loaded Rho for 1 hour at 4°C. Three wash steps in excess PBS, 5mM $MgCl_2$ were carried out at 4°C and Rho proteins were visualised by autoradiography.

2.3.3 BIAcore Analysis

BIAcore methodologies employed were as previously published (Jonsson, *et al.*, 1991) and were carried out on a BIAcore 2000 (Pharmacia Biosensor). All experiments were performed at 25°C and at a constant flow of 5ml/min in running buffer: phosphate buffered saline, 10mM $MgCl_2$. For immobilisation of proteins, a carboxymethylated dextran layer on a CM5 sensor chip (Pharmacia) was activated by a 40ml injection of a 1:1 mixture of 11.5mg/ml N-hydroxysuccinimide (NHS) and 75mg/ml N-Ethyl-N'-(3-dimethylaminopropyl)-carbodiimide (ECD). Proteins were diluted in coupling buffer (10mM acetate buffer, pH4.5) and injected over the activated surface. Excess, uncoupled sites were blocked by an injection of 1M ethanolamine. Rho proteins were nucleotide loaded and passed through small desalting columns (NICK columns, Pharmacia) in order to exchange them into running buffer (as above). They were then injected over the immobilised proteins at a concentration of between 10 and 20μg/ml. The response was recorded in arbitrary Resonance Units (RU) and the resulting RU vs time plots were analysed with the evaluation software supplied with the instrument.

2.3.4 Solution Binding Assays

Equimolar amounts of the PRK1 GST fusion proteins; HR1abc^{PRK1}, HR1a^{PRK1}, HR1b^{PRK1}, HR1c^{PRK1} and GST control were bound to glutathione Sepharose which was packed into Clontech mini-columns (50µl bed volume). Any non-specific sites on either the column or the Sepharose were then blocked by washing the columns with PBS containing 10mM $MgCl_2$, 1mg/ml bovine serum albumin (BSA) and 0.1mM GTP or GDP.

The recombinant wild type RhoA (10µg) was loaded with either GTP or GDP. The reaction was stopped by the addition of 10mM $MgCl_2$. The nucleotide-loaded RhoA was applied to the Sepharose columns and the flow through the columns blocked for an incubation period of 1 hour. The columns were then washed with between 0 and 80X Sepharose bed volumes of PBS, 10mM $MgCl_2$. Proteins were then eluted using 20mM glutathione. Both the application of the RhoA and the subsequent washes were carried out at 4˚C, whereas the glutathione-dependent elution was performed at room temperature.

Samples of the eluates were run on 15% SDS-PAGE, transferred to nitrocellulose and western blotted for RhoA. Westerns were scanned and NIH Image™ software was used to integrate pixel intensity.

2.3.5 Active Rho Pull-Down Assays

HR1a^{PRK1} or HR1abc^{PRK1} GST-fusion proteins were purified as described (2.2.10) and stored on Glutathione Sepharose in buffer A, 5mM $MgCl_2$ at 4°C.

293 cells were transfected and either starved or stimulated as described in the results chapters. The cells were washed once in ice cold PBS, drained and lysed in 0.6ml PBS, 100mM NaCl, 5mM $MgCl_2$, 1% Triton X100, 1mM DTT, 10μg/ml leupeptin, 0.1mM PMSF and 1μM microcystin. Lysates were clarified by centrifugation (14,000rpm for 15min) and an aliquot of total cell extract was taken. The remaining extract was incubated for 20 minutes with 100μl of HR1-bound Sepharose (50% slurry). The Sepharose was washed three times in extraction buffer followed by heating to 95°C in 4X sample buffer. Samples were run on a 15% SDS-PAGE and western blotting for Rho proteins allowed the comparison between total cellular Rho and that pulled down. The procedure, up until elution in sample buffer, was completed at 4°C and as quickly as possible to preclude the action of GTPase Activating Proteins (GAPs).

2.3.6 Phospho-Specific Antibody Generation and Purification.

Peptides corresponding to the activation-loop (DRTSTFCG) and potential autophosphorylation site (PLTSPPR) of the PRKs were made both as standard C-terminal amides and with a phosphate group on the 5th and 4th residues (T778 and S916 in PRK1) respectively. These peptides were coupled to Keyhole limpet hemocyanin with 25% glutaraldehyde and used in the immunisation of rabbits. The resulting immune-serum was checked by western blot for specificity to the phosphorylated form of PRK, prior to purification by competition affinity chromatography.

For the purification of phospho-specific IgG molecules 2mg of phosphorylated peptide was coupled to 2.5ml (bed volume) of sterogene Actigel ALD according to the manufacturer's instructions. After several washing steps the peptide-coupled actigel was stored in the wash solution: PBS, 0.1% (v/v) Tween 20, 0.02% (w/v) sodium azide at 4°C. The immune-serum (20ml) was made up to 40ml with PBS, 0.1%Tween 20, 0.02% sodium azide, 20mM NaF, 10mM β-glycerophosphate, 1mM EDTA, 100μg/ml unphosphorylated peptide and incubated at room temperature for 1 hour. After clearing by centrifugation (10,000rpm for 10min) the serum was applied to a column which had been pre-packed with the phospho-peptide coupled Actigel. With a flow rate of 1ml/min the column was washed with 40ml wash solution, 15ml wash solution plus 0.5M NaCl and then back into low salt. Elution was in 100mM Glycine pH2.0 which was collected in 0.5ml fractions and immediately neutralised with 50μl 1M Tris-HCl (pH8.8). The elution profile was analysed using Bradford reagent and peak fractions were pooled, treated with a protease inhibitor cocktail mix (Boeringer) and stored at 4°C or -70°C. An outline of the purification procedure can be seen in figure 2.3.1.

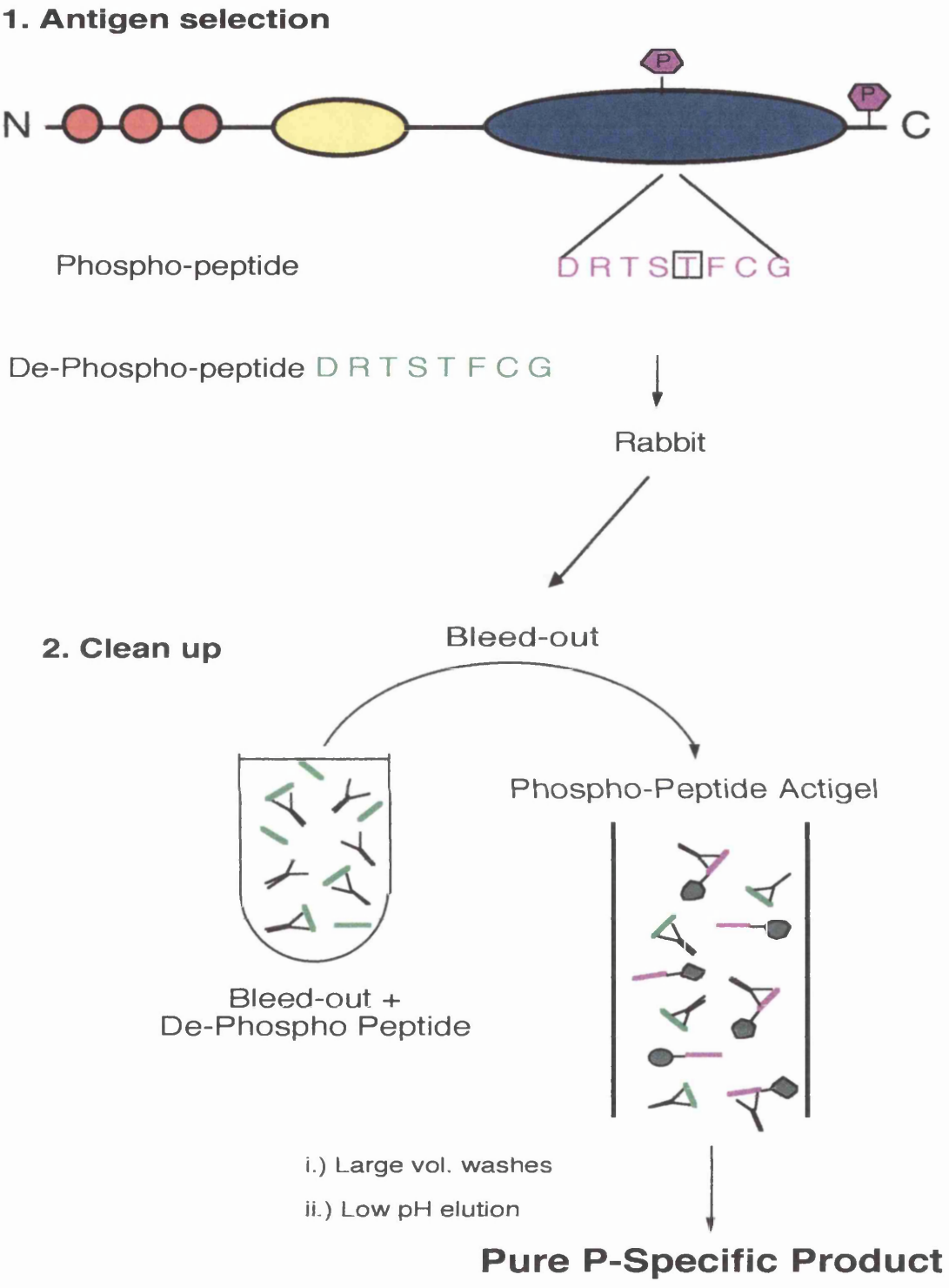

Fig. 2.3.1: Phospho-Specific Antibody Generation and Purification

Schematic of the antigen selection (activation-loop) and subsequent clean-up of the immune-serum by affinity chromatography, using de-phospho peptide competition.

Chapter 3 - Establishing the Sites of Contact Between PRK and RhoA.

3.1 Introduction

At the outset of this project several groups were embarking on searches for potential Rho effectors. Through the use of both conventional affinity purification and yeast 2-hybrid studies numerous Rho targets were identified. One study identified a cDNA clone positive for RhoA interaction that encoded a 643 amino acid protein with homology to PRK's novel N-terminal domain (Homology Region 1), this protein was named Rhophillin (Watanabe, *et al.*, 1996). In another study a 128KDa protein was enriched, along with others, on a RhoA-GST affinity column. This was later identified as PRK1 (PKN) (Amano, *et al.*, 1996b). An initial goal was to explore the potential role of a Rho-family GTPase interaction with PRK.

This chapter describes the use of a ligand overlay assay to define the sites of interaction between the PRK and Rho proteins. The assay was developed from a method used to identify GTPase activating Proteins (Manser, *et al.*, 1995b). Recombinant Rho proteins loaded with GTP by pre-incubation in a low Mg^{2+} buffer were used to overlay target proteins fractionated on SDS-PAGE. The rate-limiting step for the nucleotide exchange reaction is the nucleotide off rate. For RhoA the off rate of GDP can be increased to a half-life of less than a minute by dropping the Mg^{2+} concentration to 0.5μM compared to a GTP off rate in high Mg^{2+} (10mM) of approximately 50 minutes (Self and Hall, 1995a). A second consideration is the intrinsic GTPase activity of the recombinant proteins; for Rho A this has been measured at a half-life of 18 minutes. It could therefore be predicted that the [α^{32}P] GTP-loaded Rho would be stable for the time period required for the binding assays.

3.2 Results: Mapping the Rho Binding Site on PRK.

3.2.1 Expression and Purification of Rho Proteins

All the Rho proteins were in pGEX vectors (Pharmacia) and were transformed into the BL21 plysS strain of *E.coli* as described in 2.2.5. The expression protocols were as described in the methods chapter with induction times optimised to 3 hour at 37°C for all the GTPases. On purification 5 mM $MgCl_2$ was added to the usual buffer A, this stabilised the nucleotide binding and therefore the stability of the GTPases (Self and Hall, 1995b). With the exception of some RhoA/Rac1 chimeras (see section 3.3) all the small GTPases expressed to a high level and were soluble with yields of 0.25-4.0mg/litre bacterial culture. Samples were taken throughout the procedure for analysis on coomassie stained SDS-PAGE (15%). Figure 3.2.1 displays the purification profile of wild type RhoA. Thrombin cleavage was for 1 hour at 4°C and produced a single band of product of between 21 and 25 kDa (depending on GTPase). Purified proteins were dialysed for over 3 hours at 4°C in 1000X volumes of 50 mM Tris (pH7.5), 50 mM NaCl, 5 mM $MgCl_2$ and 1 mM DTT followed by a 16 hour dialysis in the same buffer but with 50% (v/v) glycerol. Proteins were then stored at -20°C.

Figure 3.2.2 shows 4μl of the dialysed wild type RhoA, Rac1 and Cdc42 on a coomassie stained SDS-PAGE. The protein concentration assessed by Bradford gave values of 1.5 and 1.9 mg/ml (RhoA), 2.4 and 9.5 mg/ml (Rac) and 0.35 and 6.1 mg/ml (CDC42) for the thrombin digested and GST-fusions respectively. The samples were estimated to be 90% pure. The RhoA used in pGEX vectors had a stabilising mutation of F25N which produced a sharper, slower migrating band on SDS-PAGE; throughout this thesis it will be termed wtRhoA to avoid confusion with the activating mutations.

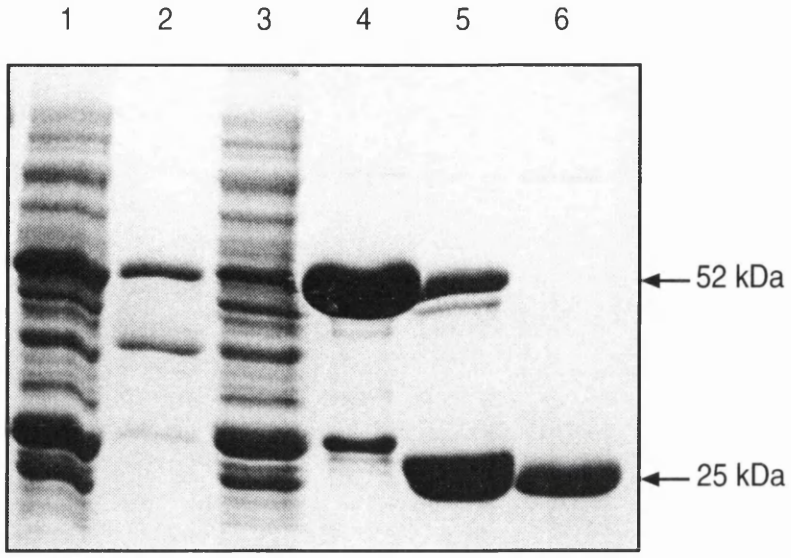

Fig. 3.2.1: Coomassie Stain of Small GTPase Purification from *E. coli.* wtRhoA purified as a GST-fusion from BL21 pLysS *E. coli*: 1). Total cell lysate; 2). Triton X100 insoluble fraction; 3). Soluble fraction after incubation with Glutathione sepharose; 4). Sepharose after wash steps; 5). Sehparose after thrombin digestion (3units/ml, 16hrs); 6). Final eluted Rho. Run on a 15% SDS-PAGE.

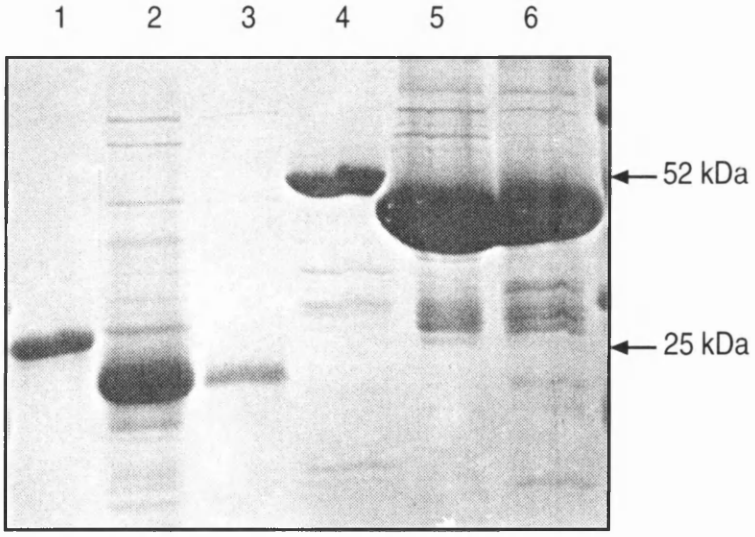

Fig. 3.2.2: Coomassie Stain of final Preparations of Rho, Rac and Cdc42. From BL21 pLysS, of thrombin cleaved 1, 2, 3 and GST-fusions 4, 5, 6 of wtRhoA, wtRac 1, and wtCDC42 respectively. Samples were run on a 15% SDS-PAGE.

3.2.2 Determining the Nucleotide Loading Efficiency of the Recombinant Rho Proteins.

The protein concentration of the purified recombinant Rho proteins could be determined with the use of Bradford reagent and a BSA standard curve. However, before any comparative binding assays were carried out the nucleotide loading efficiency of each GTPase was calculated. This allowed equimolar amounts of nucleotide-loaded Rho to be used in each assay. The relative efficiencies were determined using the filter binding assay described in 2.3.1 and the calculation seen in appendix I. Panel A. of the example (figure 3.2.3) shows that if 100% of the purified wtRhoA were capable of nucleotide loading a linear increase in dpm from the [α^{32}P] GTP would be seen with increasing pmol Rho, i.e. 1 pmol Rho would bind 1 pmol GTP. The actual dpm reading is seen to be only a fraction of this; over the first four readings (0.585-4.68 pmol Rho) the pmol GTP : pmol Rho ratio was 25.9% (panel B.), a value which was typical for all of the GTPases purified. The fifth reading (9.36 pmol Rho) was not included in the calculation of loading efficiency due to it not being saturated with respect to GTP over the 10 minute assay time.

Once similar calculations had been completed for the other recombinant GTPases the relative concentrations to be used in comparative binding assays could be assigned.

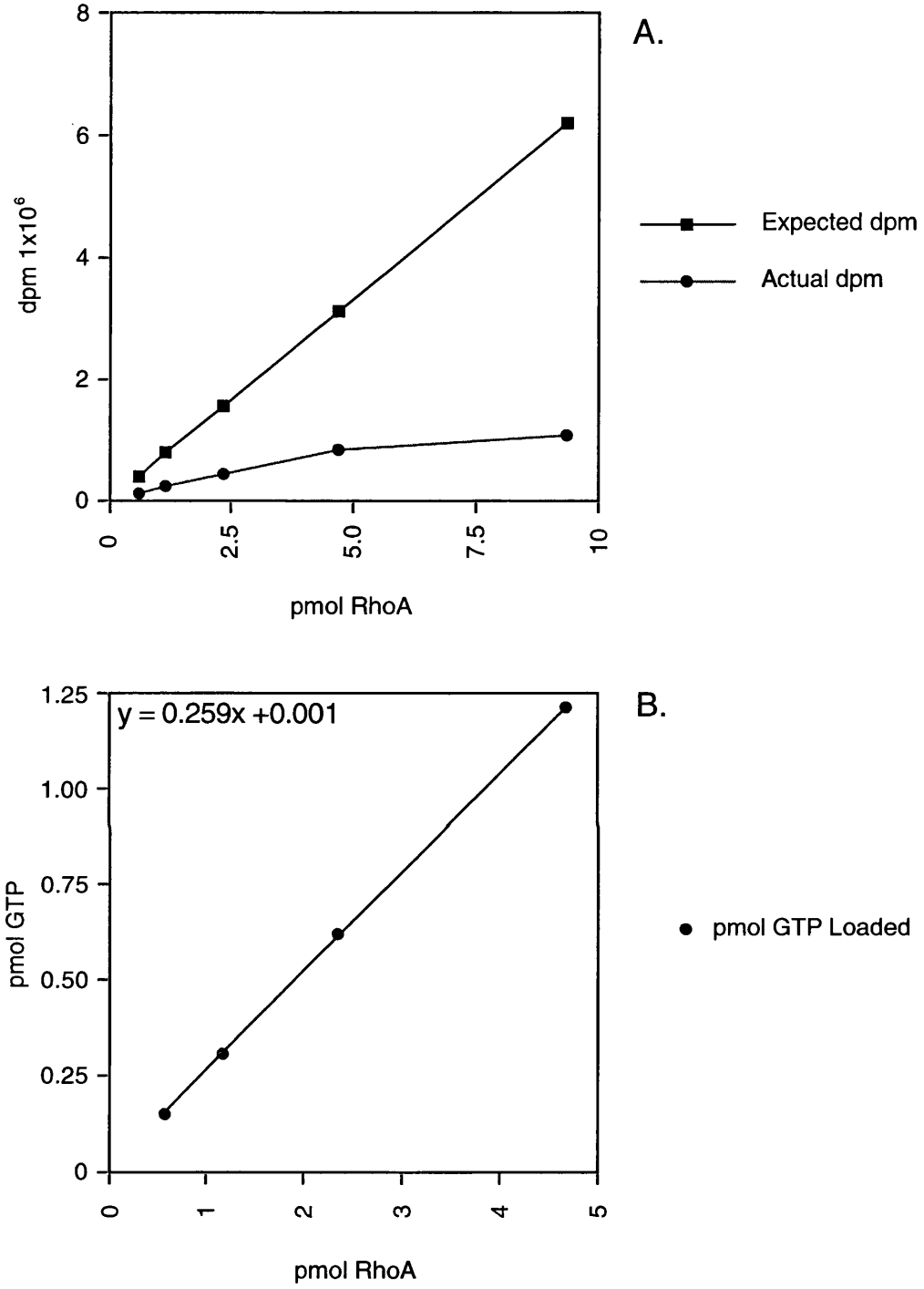

Fig. 3.2.3: GTP Loading Assay of Rho GTPases Purified from *E. coli.*

wtRhoA loading with [α^{32}P] GTP measured by filter binding assay and conversion calculated to dpm and nMol GTP (see Appendix 1). A) The expected increase in dpm seen to be linear (1mol GTP:1mol Rho) whereas the actual dpm is a percentage of expected and biphasic. B) The pmol GTP incorporated with increasing [Rho] (0.585-4.68pmol) displays a linear fit where y=.259x+0.001 i.e. 25.9% of the purified Rho exchanges nucleotide.

3.2.3 PRK Constructs used to Identify Rho Binding Region

The screens for novel Rho binding proteins had implicated PRK's novel N-terminal region in as the GTPase interaction domain (Watanabe, *et al.*, 1996). A selection of constructs covering the various domains and subdomains identified by sequence alignment of the two isoforms were therefore used to try and identify the areas key for Rho family binding. A scheme of the polypeptides used in the ligand overlay assays can be seen in figure 3.2.4. The full length PRK1 was overexpressed in Cos-7 cells to levels outlined in later chapters. The cells were lysed directly into Lammli 4X sample buffer and fractionated on SDS-PAGE prior to the overlay assays. The rest of the constructs, covering the individual domains outside of the catalytic region were purified to various degrees from *E.coli* prior to use.

As can be seen from figure 3.2.5 the GST-HR1abc^{PRK1} amino acids (aa) 1-106 was expressed in a BL21 Gro ES/EL strain of *E.coli* (this strain produced the greatest amount of soluble product) with an induction time optimised to 5 hours at 25°C, typically producing 0.7-1.0mg/litre of *E.coli* culture. The purification was as outlined in the methods chapter and samples were taken for analysis on coomassie stained SDS-PAGE. The final eluted product was left as a GST-fusion and stored at 1mg/ml in 50 mM Tris (pH7.5), 100 mM NaCl, 1 mM DTT at -70°C. Both the GST-HR1abc^{PRK2} amino acids 1-380 and the His6-HR2^{PRK1} amino acids303-508 were expressed in BL21 cells, but were always seen in the Triton X100 insoluble fraction irrespective of induction conditions. They were therefore used in a semi-purified form for the overlay assays i.e. the bacteria were lysed in buffer A, centrifuged to pellet the insoluble fraction which was then directly boiled in sample buffer. Protein levels were assessed by comparison with a BSA standard coomassie stain. GST-HR1abc^{PRK2} was seen to migrate approximately 20-30 KDa lower than expected on SDS-PAGE, this was assumed to be due to degradation, but as can be seen (3.2.7) this did not

affect its Rho binding potential. The individual subdomains of PRK1: HR1a, HR1b and HR1c were all expressed as GST-fusions to very high levels in BL21 Gro ES/EL (4-8mg/litre of E. coli culture) and were completely soluble. They were purified and stored as described for GST-HR1abc^{PRK1}. They were estimated to be over 90% pure, as can be seen from the ponceau stain in figure 3.2.9. For a possible explanation of the HR1 subdomain's solubility and how this may be related to their structure see the discussion chapter (7.2).

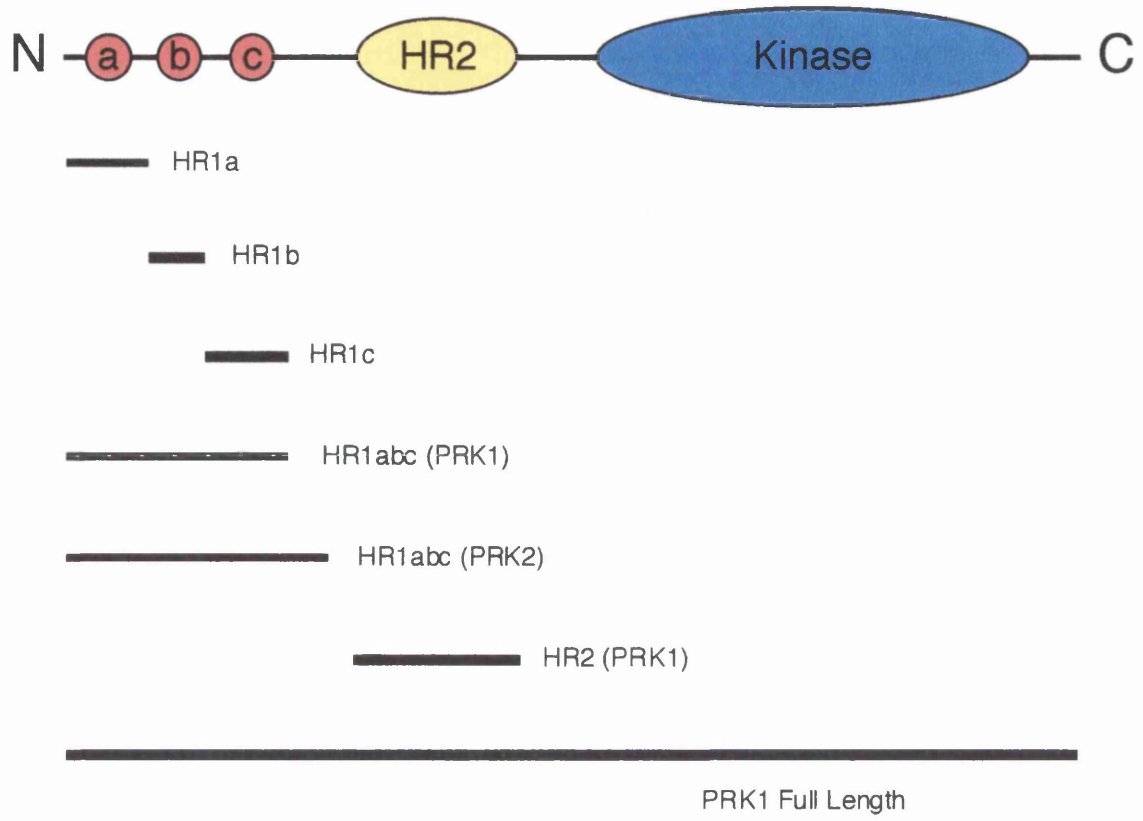

Fig. 3.2.4: PRK Constructs used to Define the Rho Binding Region.

Schematic depicting the regions tested in assays for Rho binding potential. From the top: $HR1a^{PRK1}$ amino acids (aa) 1-106, $HR1b^{PRK1}$ aa 122-199, $HR1c^{PRK1}$ aa 200-293, $HRIabc^{PRK1}$ aa 1-293 and $HR1abc^{PRK2}$ aa 1-380 were all in pGEX vectors and expressed as GST-fusions in *E. coli*. $HR2^{PRK1}$ aa 393-508 was in pRSET and expressed in *E. coli* with a N-terminal His6 tag. The full-length PRK1 was in pCDNA3 and expressed in Cos-7 cells.

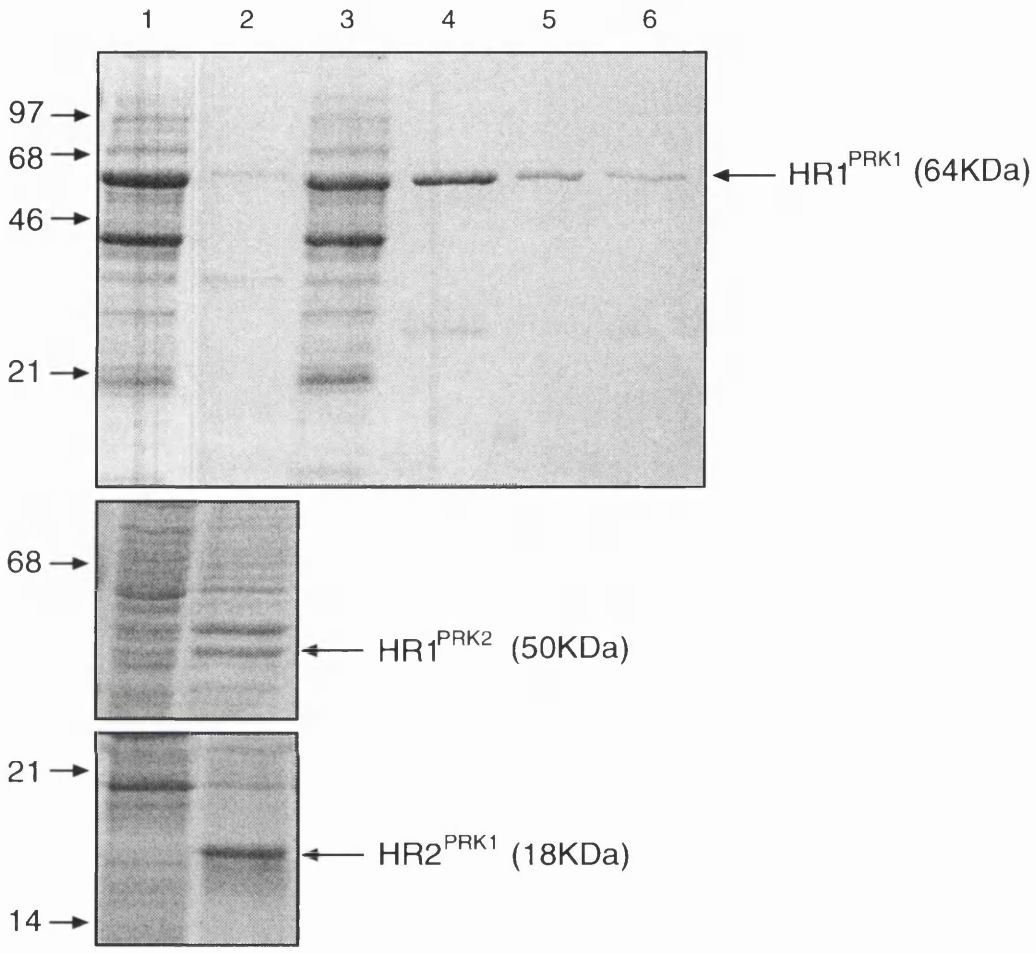

Fig. 3.2.5: Coomassie Stained SDS-PAGE of the Expression of HR1PRK1, HR1PRK2 and HR2 PRK1 from *E.coli.*

All three constructs were expressed in BL21 GroES/EL cells and purified as described (2.2.11). Lanes: 1). Total cell lysate; 2). Triton X100 insoluble fraction 3). Soluble fraction after incubation with gluathione sepharose; 4). Sepharose after wash steps; 5). Sepharose after glutathione elution; 6) Final eluted protein. HR1PRK1 was seen to soluble and was purified to homogeneity whereas both the HR1PRK2 and HR2PRK1 domains were completely insoluble.

3.2.4 Full length PRK1 Binds wtRhoA by Ligand Overlay Assay.

PRK1 (942 amino acids) was transiently overexpressed in Cos-7 cells (15cm plate) which were then lysed directly into 1 ml Laemmli 4X sample buffer. The whole cell lysate was briefly sonicated to reduce viscosity and 25µl was fractionated on a 10% SDS-PAGE. The proteins were transferred to nitro-cellulose which was then incubated in the renaturation solution, as described in the methods chapter. Purified wtRhoA was loaded with [α^{32}P] GTP and incubated with the renatured membrane at a final concentration of 0.1µg/ml. After washing and autoradiography it could be seen that while a strong signal for the RhoA [α^{32}P] GTP was seen at the position characteristic of PRK1 migration, no equivalent Rho binding activity was detected in the Cos7 cell extracts from vector-transfected cells (see figure 3.2.6).

3.2.5 The HR1 but not the HR2 Domain Interacts with RhoA.

Amino acid sequence alignment of the two members of the PRK family identifies several conserved regions: the C-terminal kinase domain ,which is highly homologous to those present in the rest of PKC family; the HR2 domain which is homologous to the V_0 domain of PKC-ε and PKC-η and the HR1 domain which isn't seen in any of the other PKC family members and has only recently been identified in gene products other than the PRKs. While the kinase domain was almost certainly responsible for the proteins catalytic activity, the HR1 and HR2 regions were thought to be involved in the regulation of that activity. These two domains were therefore tested for Rho binding potential (figure 3.2.7). 2.5 µg of purified GST-HR1abc^{PRK1} and GST control or semi-purified GST-HR1abc^{PRK2} and His6-HR2^{PRK1} were overlaid with RhoA [α^{32}P] GTP. Strong signals for Rho binding were seen for both the HR1 domains of PRK1 and PRK2 whereas no

signal was observed for either the His6-HR2^{PRK1} or the GST control. The HR1 domain was therefore the region responsible for Rho binding.

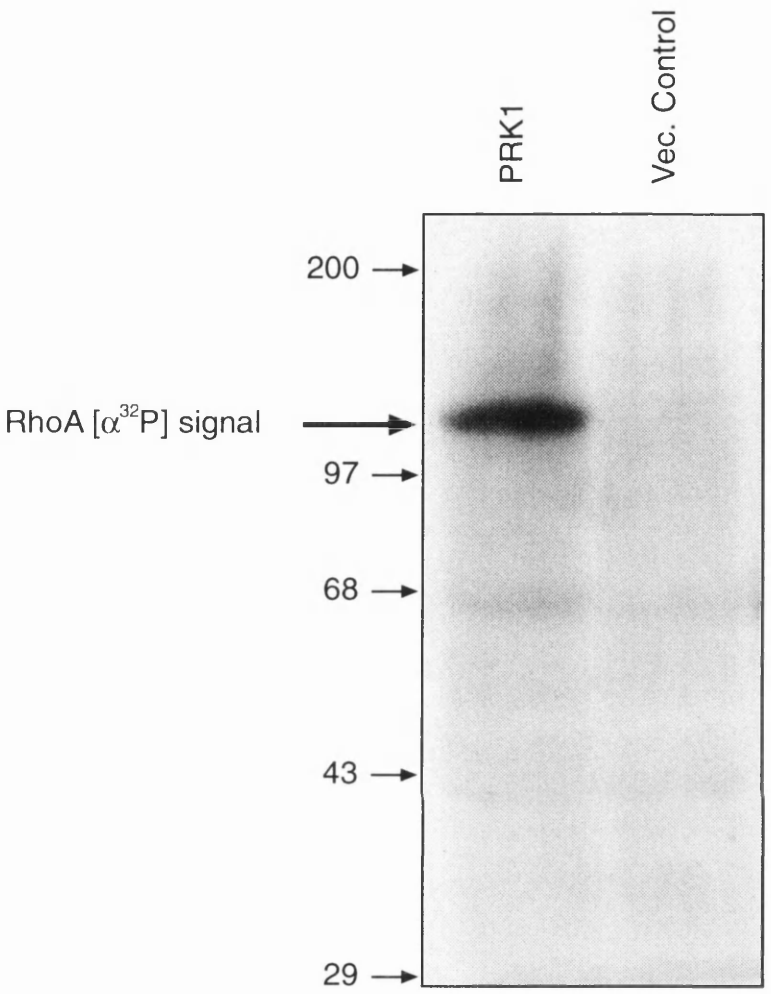

Fig. 3.2.6: Autoradiograph showing RhoA Binding to PRK1 Transiently Expressed in Cos-7 Cells.

PRK1 in pCDNA3 or the vector alone control were transiently transfected into Cos-7 cells and expressed for 48hrs. Whole cell lysates were fractionated on 10% SDS-PAGE and transferred to nitrocellulose for the wtRhoA overlay assay. By autoradiography PRK1 (942 amino acids) which runs at 120KDa, was seen to bind the RhoA [α^{32}P] GTP, whereas no equivalent band was seen in the control lane. Molecular weight markers are shown in kDa.

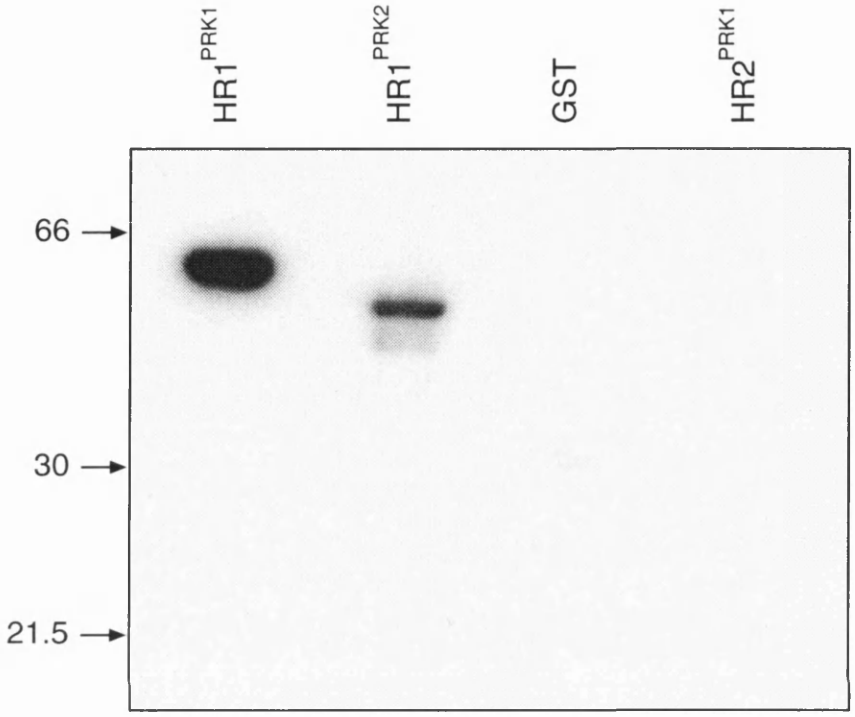

Fig. 3.2.7: Autoradiograph showing RhoA Interaction with the HR1 Domains of both PRK1 and PRK2.

GST-HR1$_{PRK1}$ (2.5µg purified from *E. coli*), GST-HR1$_{PRK2}$, HR2$_{PRK1}$ His6 (2.5µg as assessed in comparison with BSA standards) and GST control (2.5µg purified) were tested by Ligand overlay assay for a potential interaction with RhoA [α^{32}P] GTP. While both HR1 domains displayed very strong signals for radiolabelled GTPase no signal was seen for either the semi-purified HR2 domain or the GST control.

3.2.6 HR1 Region Contains Three Homologous Repeated Subdomains.

Having identified the HR1 region as that which binds RhoA attention was focused on its amino acid sequence. As can be seen from figure 3.2.8 the domain is made up of three contiguous repeats of approximately 80 amino acids (denoted a, b and c) with a central core of homology within the 50 residues highlighted. While the repeats are very similar to each other, any differences between a, b and c are conserved both across isoforms and species: aligned are the repeats of both PRK1 and 2 with those present in *C. elegans* PRK-A. A mammalian HR1 repeat can be characterised as having a central GAXN motif (where X is a charged residue) preceded by a very basic region, with lysine and arginine residues at conserved spacing, and followed by leucine repeats suggestive of a leucine zipper-like motif. It can be seen from the alignment that while the first two repeats (a and b) are extremely similar to each other the third (c) has some charge differences both within the central GAXN and the preceding basic region.

Terming these repeats 'subdomains' suggests a degree of discrete modular character produced by secondary structure. No structural data is yet available but the solubility of the repeats and a predicted structure point to the formation of three independent structural units which fold together to form a full domain (see discussion 7.2).

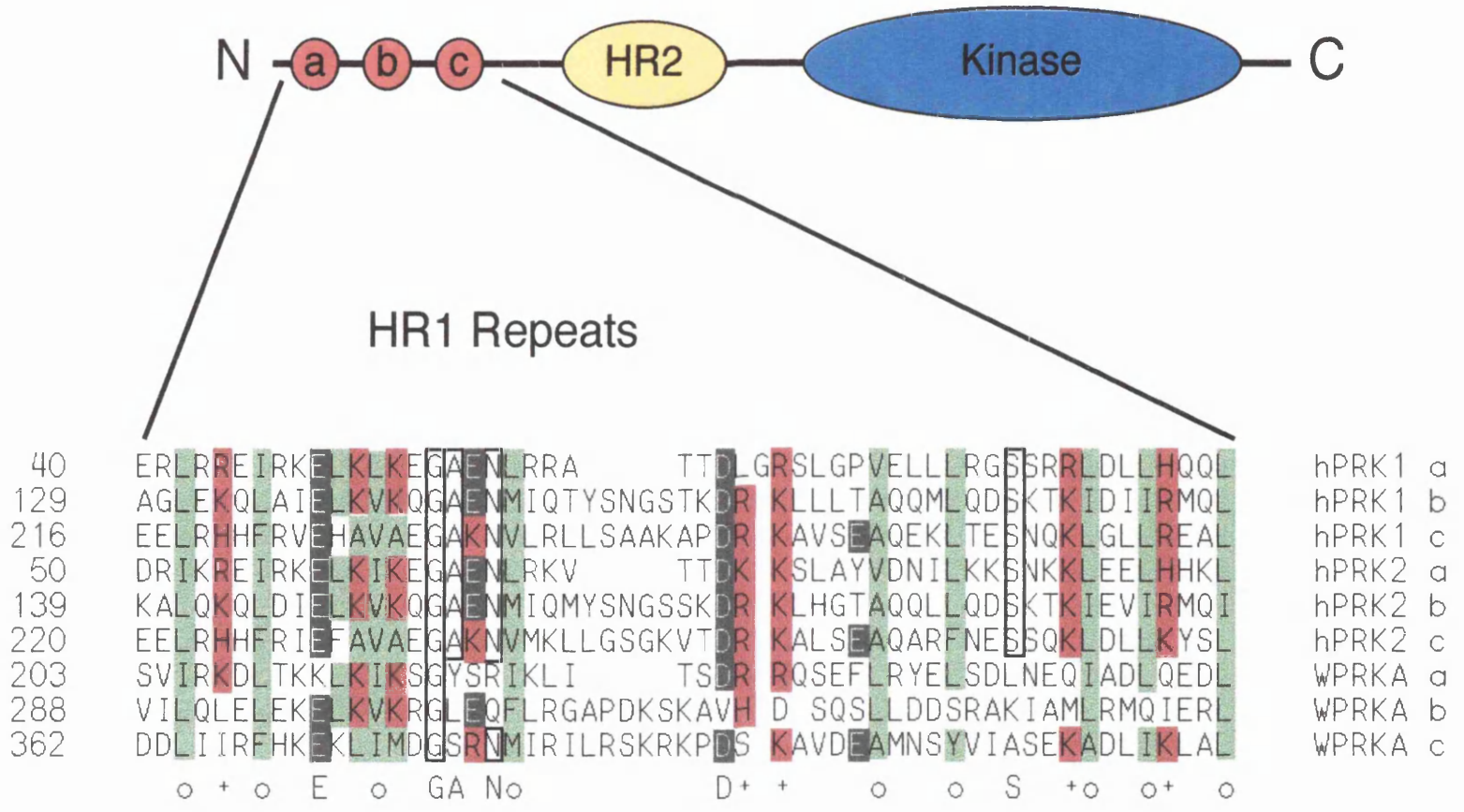

Fig. 3.2.8: Amino Acid Sequence Alignment of the HR1 Subdomains of PRK.

The HR1 domains of the PRK family are made up of repeated subdomains of approximately 100 residues which are conserved across both human isoforms and species. A core region for the three repeated domains a, b and c of human PRK1 and 2 along with those from a *C. elegans* isoform (denoted WPRKA) are shown. Conserved hydrophobic sequences (O) are highlighted in green, conserved acidic residues (E/D) are shown in dark grey and basic residues (+) are shaded in red. Any other regions of complete conservation are boxed.

3.2.7 The HR1a^{PRK1} and HR1b^{PRK1} Subdomains Interact with RhoA.

To further define the site of Rho binding on the PRK the individual HR1 subdomains were overlaid with RhoA. The domains were expressed and purified as discussed (3.2.3) and were judged to be over 90% pure. 4μg of each subdomain along with a GST control were fractionated on a 15% SDS-PAGE, transferred to nitro-cellulose and overlaid with 0.1μg/ml RhoA [α^{32}P] GTP. As can be seen from panel A in figure 3.2.9 HR1a and b of PRK1 displayed a Rho binding potential, whereas HR1c showed absolutely no binding activity above the GST control. The ability of an individual subdomain to bind Rho (rather than a requirement for the full domain) was substanciated by using the equivalent HR1a from *C. elegans* PRK-A as a target in RhoA [α^{32}P] GTP overlay. Once again a strong signal was seen over a very low background (panel B figure 3.2.9).

3.2.8 Comparative binding of wtRhoA wtRac1 and wtCdc42 to the HR1 Subdomains.

The inability of the HR1c^{PRK1} to bind RhoA irrespective of its obvious sequence similarity to both HR1a and HR1b provoked the question of whether it was actually specific for another member of the Rho family. In order to address this all three subdomains were overlaid with equimolar amounts of wtRhoA, wtRac1 and wtCdc42 (as assessed by GTP loading efficiency). Figure 3.2.10 displays the resulting autoradiographs: RhoA [α^{32}P] GTP displayed the same binding pattern as before i.e. signals for both HR1a and HR1b; Rac1 [α^{32}P] GTP while showing a much reduced signal on comparison to RhoA did consistently produce a signal for binding to HR1a that was above background; whereas wtCdc42 [α^{32}P] GTP produced no signal reflecting no specific binding.

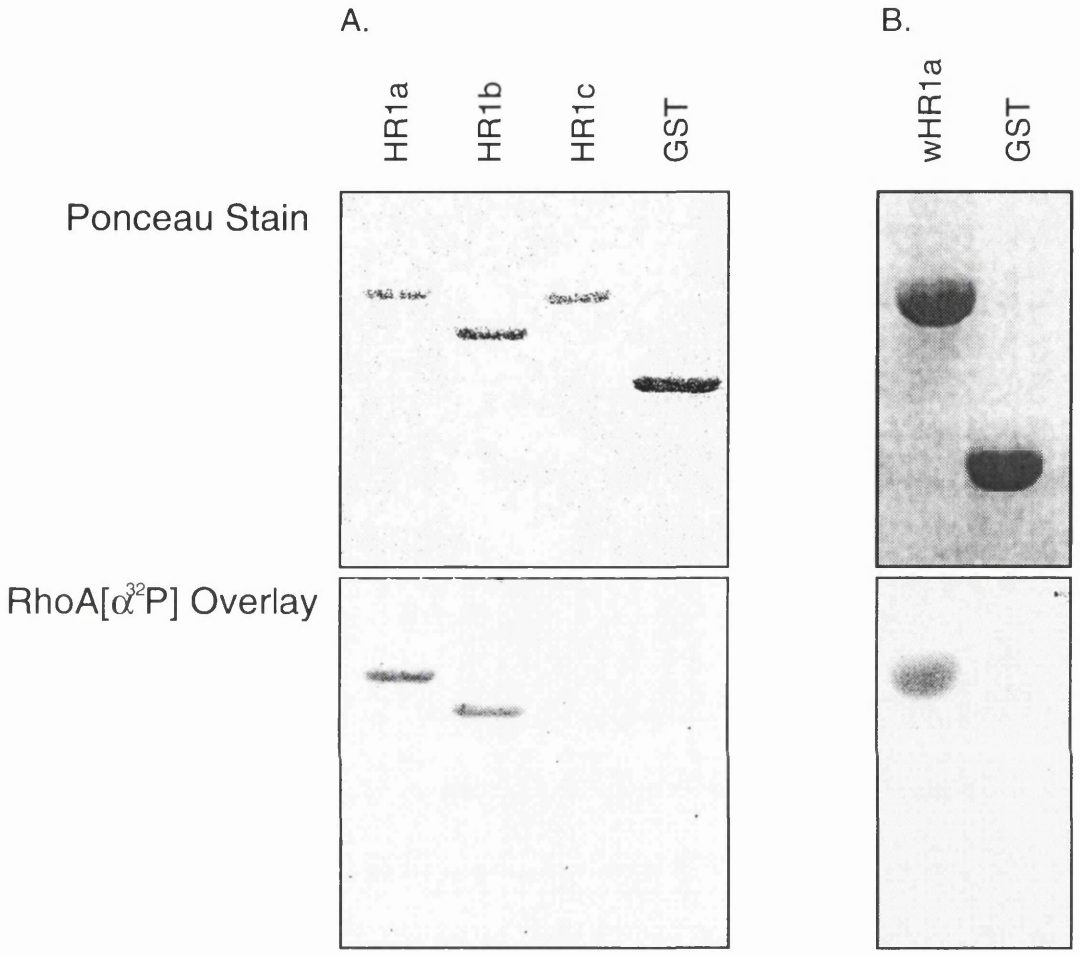

Fig. 3.2.9: Ligand Overlay Assay of the HR1 Subdomains and the *C. elegan* PRK-A HR1a with RhoA [α^{32}P]GTP.

A).The individual HR1 subdomains (a, b and c) of PRK1 were expressed and purified as GST-fusion proteins. 4μg of each domain along with a GST control were run on a 15% SDS-PAGE, transferred to nitrocellulose and overlayed with RhoA [α^{32}P]GTP. B). The *C. elegans* PRK-A HR1a (wHR1a) was also expressed as a GST-fusion and 4μg was subjected to human RhoA [α^{32}P]GTP overlay.

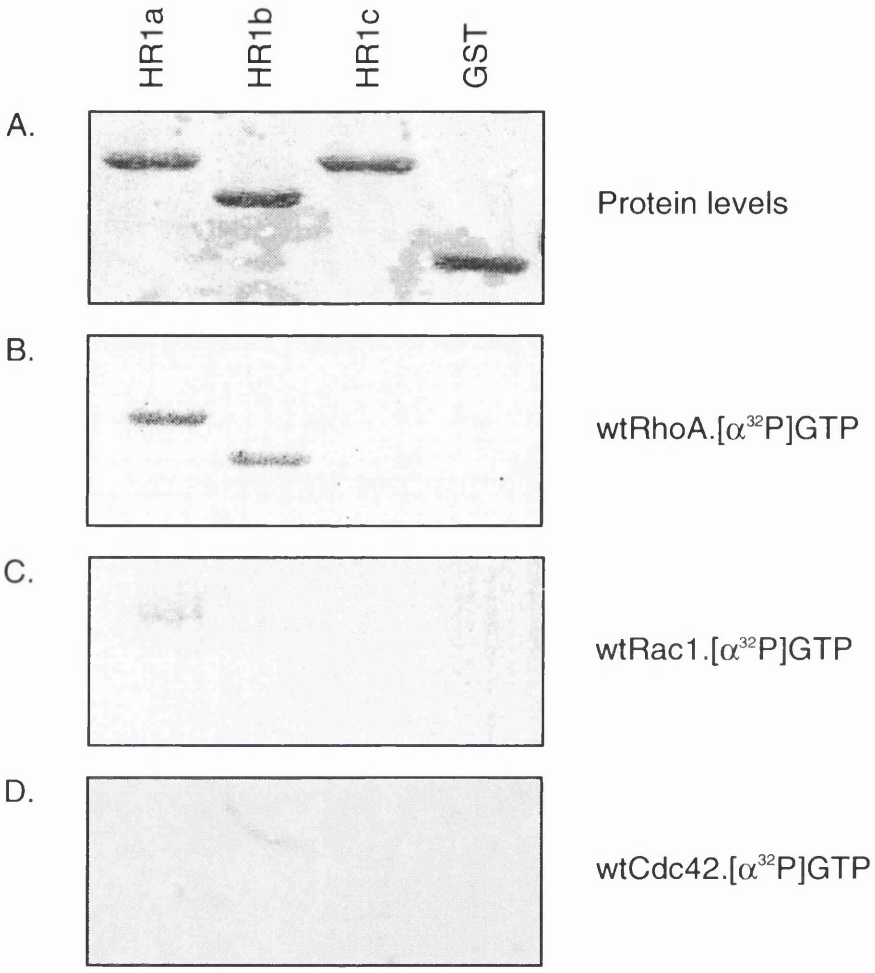

Fig. 3.2.10: Ligand Overlay Assay of the HR1 Subdomains with RhoA [α^{32}P]GTP, Rac-1 [α^{32}P]GTP and Cdc42 [α^{32}P]GTP.

The three Rho-family GTPases RhoA, Rac-1 and Cdc42 were all purified from *E.coli* and assessed for nucleotide loading. The HR1 subdomains of PRK1 (4µg/lane) were then overlayed with 0.1µg/ml of the radiolabelled GTPases. A). shows the protein load of the HR1 subdomains, B.C.D). Displays the relative binding of the three GTPases by overlay.

3.3 Results: Mapping the PRK Binding Sites on Rho

Having demonstrated that wtRhoA could bind independently to two sites in the PRK1 N-terminus it was of interest to establish both where on the Rho molecule a contact was made and whether two contacts were made at distinct sites. An alignment of members of the Rho family can be seen in figure 3.3.1. The functional areas highlighted include the switch I and II (see chapter 4). Other regions of interest when determining binding sites for potential effectors are the residues 32-42 (Rho) which were identified in Ras by mutational analysis as being essential for effector activation and residues 14 and 63 (Rho) which are involved in the regulation of GTPase activity (see Introduction 1.5.3.2).

In order to define the areas of HR1a and HR1b contact on the Rho, chimeric Rac/Rho GTPases were utilised. Such constructs had been used previously and were seen to be active for effector binding and cytoskeletal rearrangements in fibroblasts (Diekmann, *et al.*, 1995). A variety of chimeras were therefore assessed for expression and nucleotide loading prior to use in ligand overlay assays.

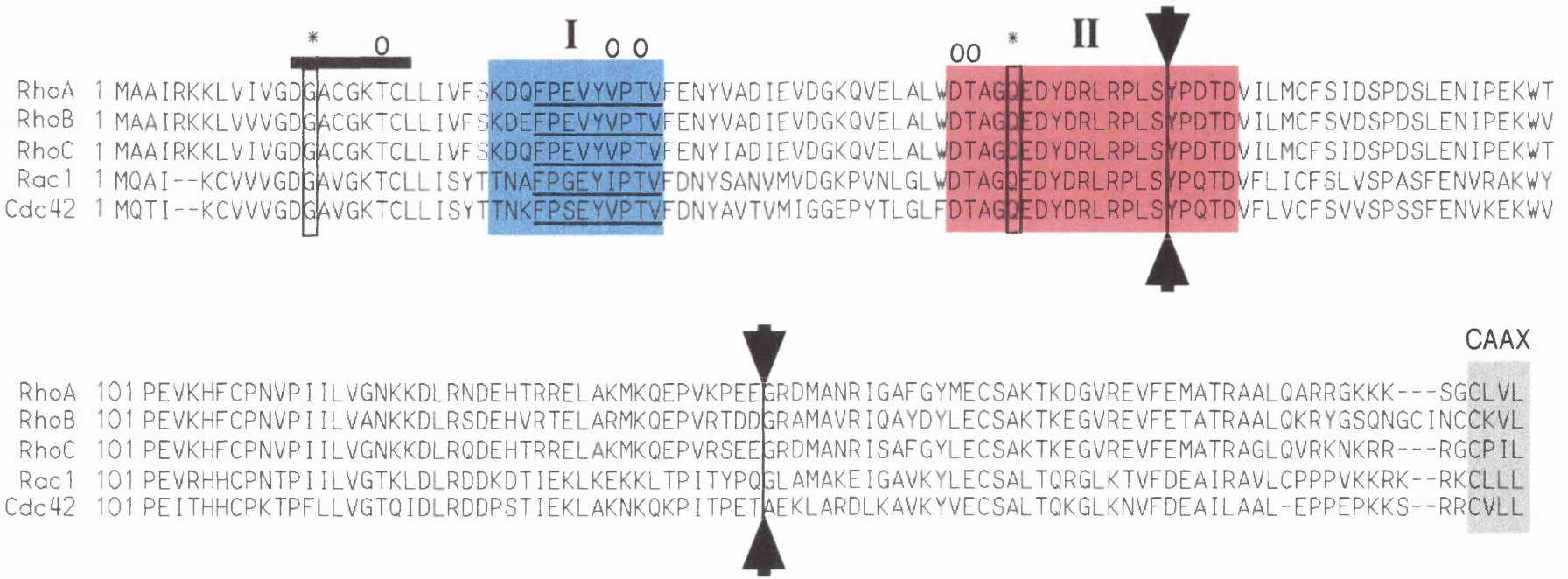

Fig.3.3.1: Amino Acid sequence Alignment of Rho Family Members.

Alignment of human Rho proteins with functional regions highlighted: the switch I (in blue) and switch II (in red) are based on those described by (Ihara, 1998). Residues 14 and 63 (RhoA) which are essential for GTPase activity are boxed; the modification target sequence (CAAX) box is shaded in grey; the region regarded as the phosphate binding loop is marked with a thick black line; residues involved in Mg^{2+} co-ordination are marked (o); residues equivalent to those important for effector binding in Ras are underlined and the break points for the Rho/Rac chimeras (see 3.3.2) are denoted by the large arrows.

3.3.1 Expression and Purification of Rac/Rho Chimeras

All the GTPases were expressed as GST-fusions in BL21 pLysS *E.coli* as previously described. Figure 3.3.2 shows coomassie stained SDS-PAGE of the purification steps for the V14RhoA and three Chimeras. All of the proteins expressed to high levels and with the exception of the V14 mutant were seen to be completely soluble. The chimeras Rac73Rho and Rac143Rho along with the V14 mutant were all thrombin cleaved and purified from their GST tag to give homogeneous products. As indicated by Panel B of fig. 3.3.2 the Rho73Rac chimera was purified as a GST- fusion, allbeit with a relatively high level of degradation. However, thrombin cleavage resulted in a completely unstable product which was never produced at a level to allow further use. Several attempts to purify other Chimeras with an N-terminal Rho portion were also ineffective.

The nucleotide loading efficiencies of the chimeras were assessed and used to ensure equimolar quantities of the [α^{32}P] GTP-loaded GTPases were used in all the subsequent overlay assays. It is of interest to note the fractionation of the wild type Rho or Rac, by chimera formation does not affect its ability to exchange nucleotide; the two chimeras shown in figure 3.3.3 were actually purified from *E.coli* with a higher percentage loading capacity than the wild type or mutant forms.

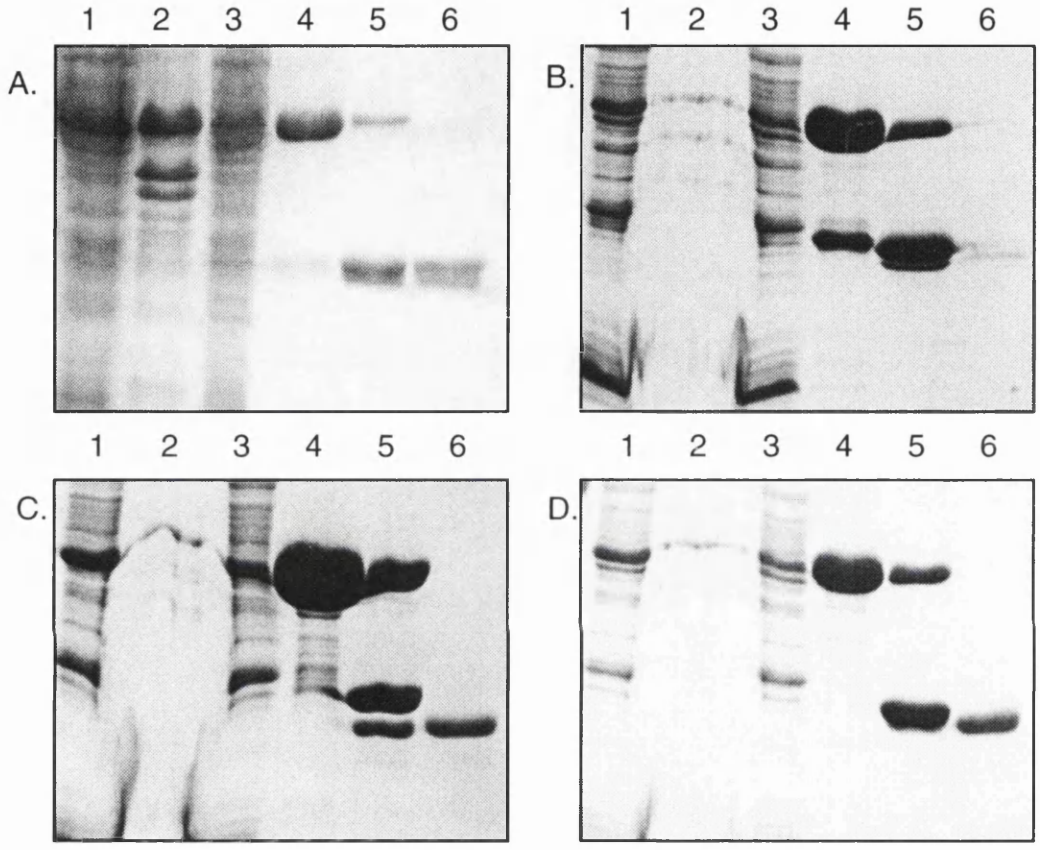

Fig. 3.3.2: Expression and Purification of Rac/Rho Chimeras

Coomassie stained 15% SDS-PAGE of the expression and purification profiles of: A. V14 RhoA, B. Rho73Rac, C. Rac73Rho and D. Rac143Rho from Bl21 pLysS *E.coli.* The lanes correspond to: 1). Total cell lysate; 2). Triton X100 insoluble fraction; 3). Soluble fraction after incubation with Glutathione sepharose; 4). Sepharose after wash steps; 5). Sehparose after thrombin digestion (3units/ml, 16hrs); 6). Final eluted GTPase.

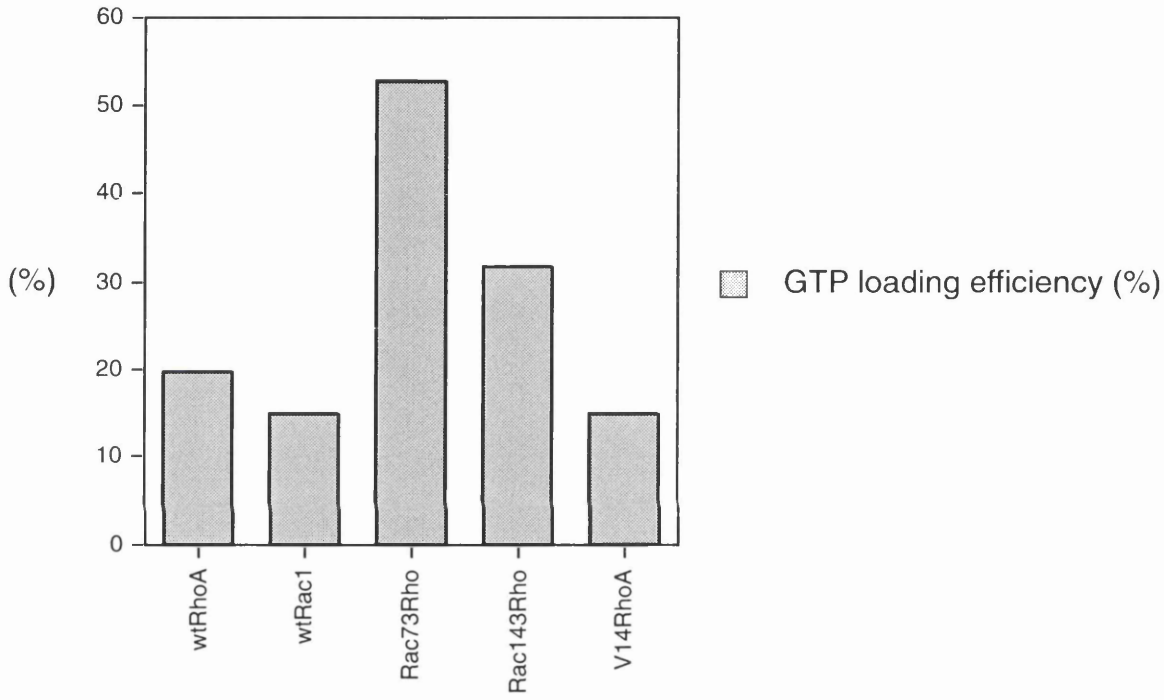

Fig. 3.3.3: Nucleotide Loading Efficiency of GTPases used in Chimeric Overlay Assays.

The nucleotide loading efficiency of the various Rho family proteins and chimeras were calculated as described in 3.2.2. Protein concentration (µg/ml) in the subsequent overlay assays was therefore adjusted so equimolar [α^{32}P]GTP-labelled GTPases were used.

3.3.2 HR1a and HR1b bind to Distinct Regions on RhoA

Ligand overlay assay was implemented once more to test wild type RhoA, Rac1, mutant V14 RhoA and Chimeras Rac73Rho and Rac143Rho for binding potential to the individual HR1 subdomains. 4μg of the subdomains overlaid with 0.1mg/ml [α^{32}P]GTP-labelled GTPase produced the binding patterns seen in figure 3.3.4.

The wtRhoA protein exhibited binding to the HR1a and b subdomains as expected. A low-level of wtRac1 association with HR1a was again seen and was maintained by the Rac143Rho chimera. This suggested the region(s) responsible for the increased signal associated with RhoA binding and the low-level Rac1 interaction are not in the C-terminal 50 amino acids of the GTPase. The Rac73Rho chimera bound the HR1a subdomain with equal intensity as wtRhoA while no significant binding over background was seen for HR1b, clearly distinguishing the sites of HR1a and HR1b binding on the Rho. The instability of the Rho73Rac chimera prevented the obvious inverse experiment. However, the observation that the mutant V14Rho, which lacks both intrinsic and GAP-stimulated GTPase activity, only bound the HR1a suggests that the amino terminal third of the Rho is required for binding to the HR1b. It was also seen consistently that the HR1a interacts with the V14 mutant with a much greater affinity than the wild type and Rac73Rho GTPases. While overlay assays can't be used to determine true affinity constants comparative affinities can be attributed. Further, the fact that HR1b binds GTP-Rho implies that the lack of binding to the V14 mutant is not due to the conformational changes induced by the triphosphate nucleotide but rather by a hindrance directly resulting from the change of residue (see the discussion chapter).

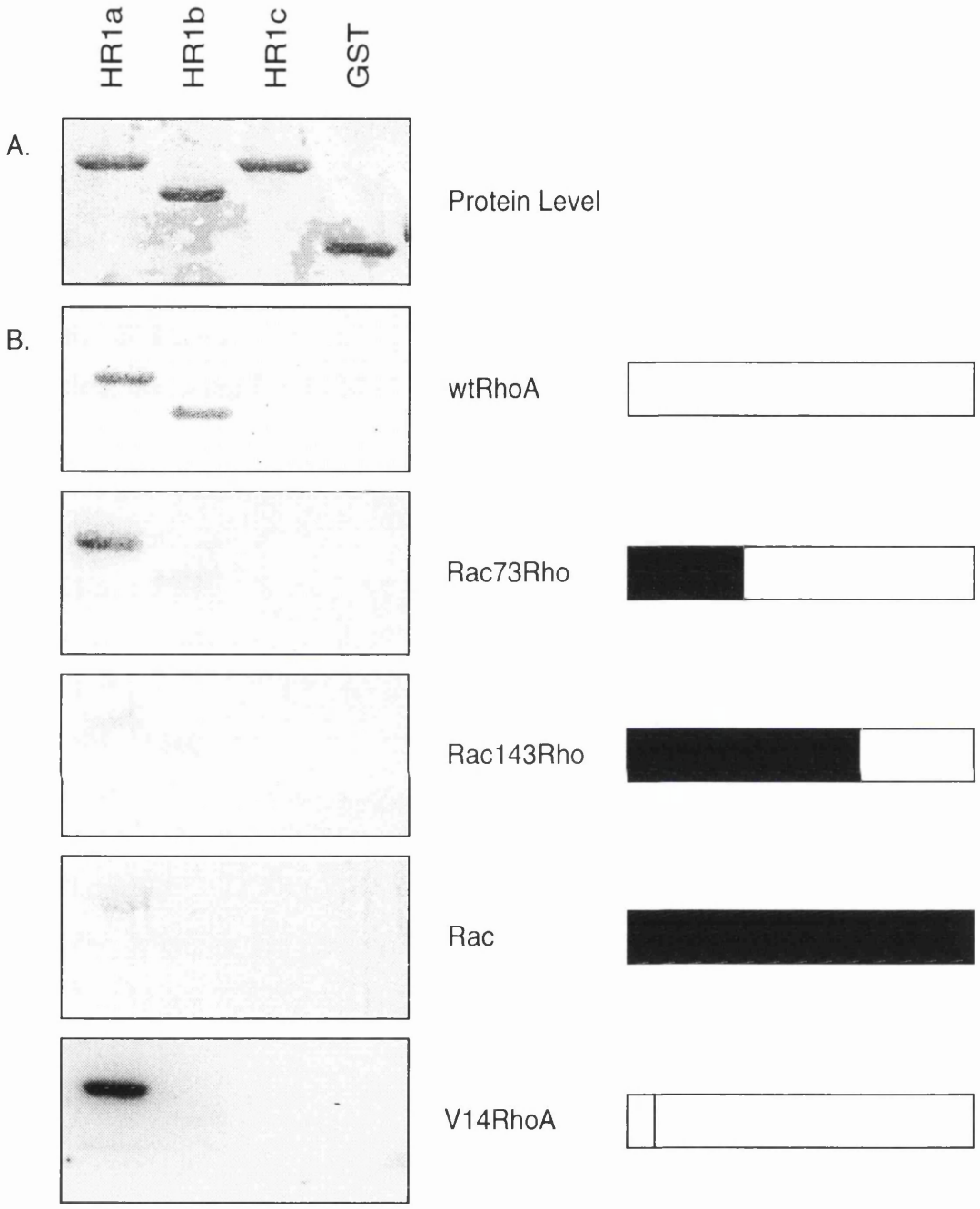

Fig. 3.3.4: Ligand Overlay Assay of the HR1 Subdomains with Rho/Rac Chimeras and V14RhoA

The various Rho proteins were purified from *E. coli,* assessed for nucleotide loading efficiency and radiolabelled so that 0.1μg/ml of each was used to overlay the HR1 subdomains of PRK1 (4μg of each). A). The equal protein loading of the HR1 motifs; B). The autoradiographs corresponding to the overlays with Rho proteins as indicated.

3.4 Chapter Discussion

Small GTPases co-ordinate signalling pathways through a nucleotide dependent regulation of downstream effectors. PRK1 has been identified as a potential effector of RhoA (Amano, *et al.*, 1996b, Watanabe, *et al.*, 1996). An initial step in establishing the role of a Rho interaction in the control of PRK's activity was to determine the sites of contact between the proteins. Recombinant Rho family GTPases were used in ligand overlay assay with an array of polypeptides, covering the identified domains of PRK as targets.

The full length PRK1 was clearly seen to interact with wtRhoA over a background of whole cell lysate. On further investigation the HR1 domains of both PRK1 and PRK2 were sufficient to produce a Rho binding activity whereas the conserved HR2 domain was not involved. While the *in vitro* data was convincing, it was confirmed *in vivo* by work completed in collaboration (Mellor, *et al.*, 1998). Having established that intact PRK1 would translocate from the cytoplasm of HEK 293 cells to an endosomal compartment in a RhoB dependent manner; this translocation event was seen to be dependent upon an intact HR1 domain. In panel A, of figure 3.4.1 the overexpressed HR1 domain is seen to have a broad cytoplasmic staining pattern and produces multinucleated cells. Given the recently described role of Rho in cytokinesis this is suggestive of a dominant negative effect on Rho function (Madaule, *et al.*, 1998). The HR1 is shown to translocate and co-localise with the overexpressed RhoB in the characterised endosomal compartment. The inverse experiment (panels D-F) shows the inability of a PRK1ΔHR1 to translocate from the cytoplasm in a Rho-dependent fashion.

Sequentially the HR1 domain is three contiguous repeats. On alignment of these it can be seen that while all three share between 28-32% absolute identity within the central core 50 amino acids (higher when conservative

replacement is taken into account) several charge differences can be seen in HR1c. The ligand overlay of these individual subdomains with wtRhoA mirrored the observed sequential difference: while both HR1a and HR1b were sufficient for Rho binding, no signal was seen over HR1c. It had been established previously that PRK1 did not interact with Rac (Amano, *et al.*, 1996b). On testing the three subdomains for binding potential to other members of the Rho family a low-level, but reproducible, interaction between Rac1 and HR1a was seen. As discussed in chapter 7, this observation is relevant with respect to the work of others (Vincent and Settleman, 1997).

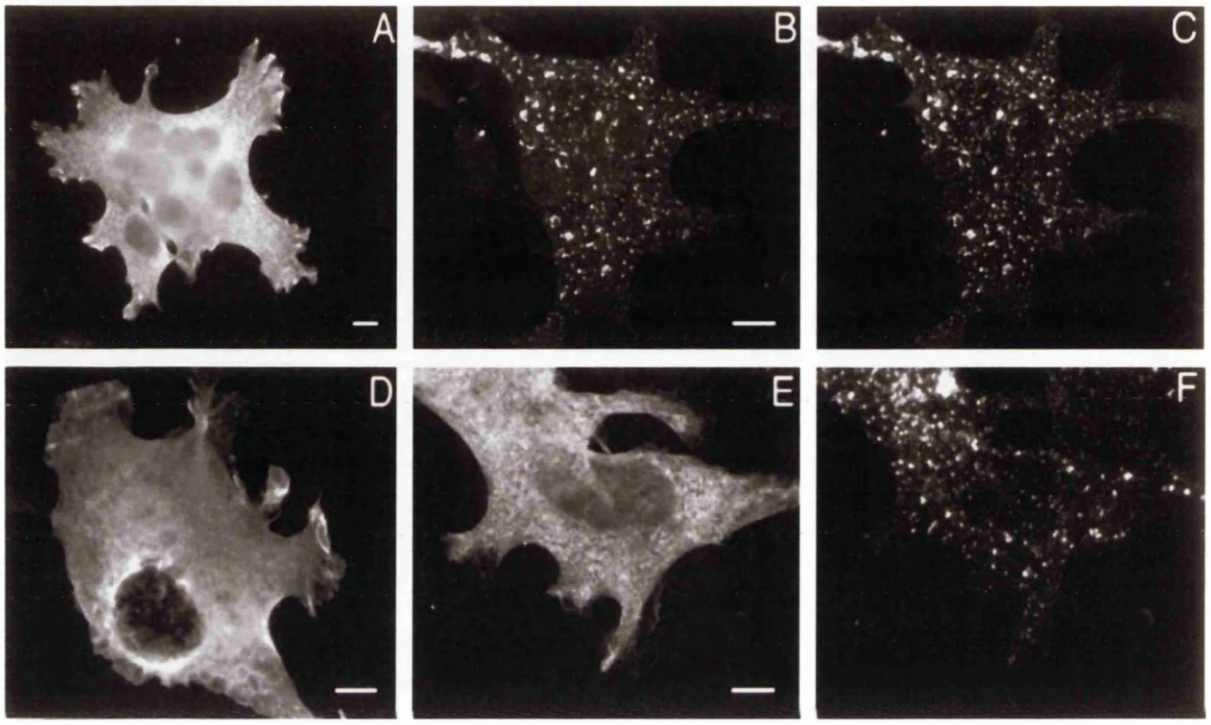

Fig. 3.4.1: The HR1 Domain Targets PRK1 to an Endosomal Compartment in a RhoB Dependent Manner.

PRK1 truncation mutants and RhoB were expressed in 293 cells. Panels A-C, cells were transfected with the HR1 domain; panels D-F, cells were transfected with the HR1-deleted PRK1 construct. Cells in panels B,C,E and F were also expressing RhoB. Rho was detected by immunofluorecence using and anti-myc monoclonal and the staining pattern is seen in C and F. PRK1 constructs were detected using an anti-HA polyclonal antibody and their staining pattern is seen in panels A, B, D and E.

Having established two distinct sites on PRK1 that could interact with RhoA, Rac/Rho chimeras were employed to determine whether the two points of contact shared a common binding region on the GTPase. As can be seen from the schematic in figure 3.4.2 the HR1a interaction was mapped between amino acids 73-143 on the Rho, a region which partially overlaps the switch II domain. While the chimera studies inferred a HR1b contact with residues 1-73 of Rho, further assessment using the V14 mutant confirmed a requirement for a wild type amino terminus.

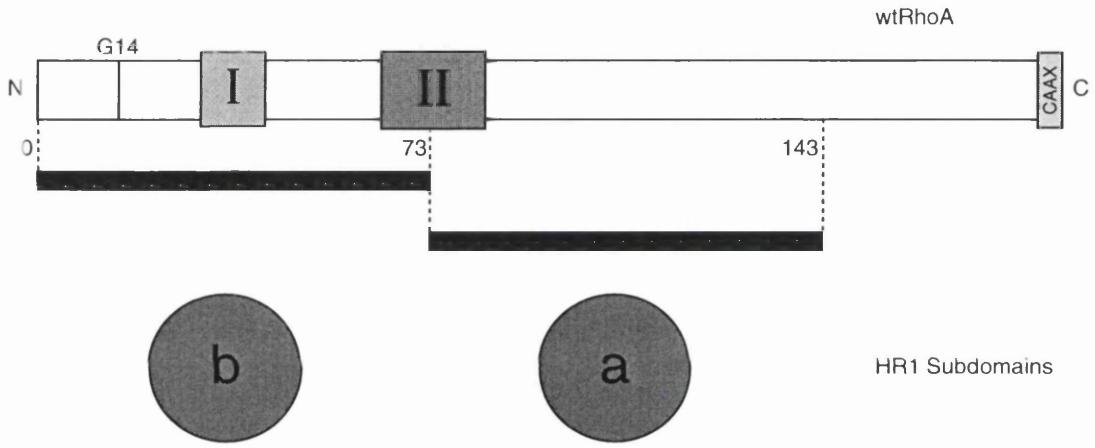

Fg. 3.4.2: The Individual HR1 Subdomains Bind to Different Regions of the wRhoA Protein.

A schematic picture of the regions of RhoA that interact with the $HR1a^{PRK1}$ and $HR1b^{PRK1}$ subdomains. It can be seen that while the HR1a binds the region between residues 73 and 143, HR1b only binds when the first 73 amino acids of wRhoA are present and not when the G14V mutation is introduced.

It had been established that the cycling of GTPases from the inactive GDP-bound state to the active GTP-bound form allows them to act as molecular switches in signalling pathways. There is a precedent for the interaction between a GTPase and its direct downstream effector to be dependent upon the

structural arrangements exhibited by the GTP bound state, for review see (Denhardt, 1996b). PRK1 can be seen to interact with GTP-RhoA and to a degree with GTP-Rac1 and the areas of contact overlap with those associated with conformational changes due to nucleotide specificity (Ihara, *et al.*, 1998). Chapter 4 describes the techniques used to determine the nucleotide specificity of the PRK-Rho interaction.

Chapter 4 - The Nucleotide Specificity of the Rho Interaction with PRK.

4.1 Introduction

The introductory chapter describes that while protein interactions can be made with the GDP-bound form of small GTPases; such as the Guanine Dissociation Inhibitors, practically all the effector protein interactions are dependent on the GTPase being GTP loaded. This is the case for the recently identified Rho effectors such as Rho-kinase, mDia, $p160^{ROCK}$ and Rhophillin (Ishizaki, *et al.*, 1996, Matsui, *et al.*, 1996, Watanabe, *et al.*, 1996, Watanabe, *et al.*, 1997). It was established that the PRK-Rho interaction is mediated through two distinct sites on both the PRK and the Rho molecule. The overlay assays using Rac/Rho chimeras displayed these sites to overlap with the switch II domain, in the case of HR1a and the N-terminal third of the Rho molecule in the case of HR1b. As has been previously discussed the two switch domains and flanking regions undergo conformational change depending upon which nucleotide is bound. These changes can be seen in figure 4.1 where the Cα–carbon tracings of V14Rho bound to GTPγS and wtRhoA bound to GDP are aligned. It is assumed that the structural arrangement of the GTP-bound form is necessary for effector binding. The nucleotide and hence structural dependence of the PRK interaction was assessed using the recombinant Rho and HR1 proteins for *in vitro* solution binding studies.

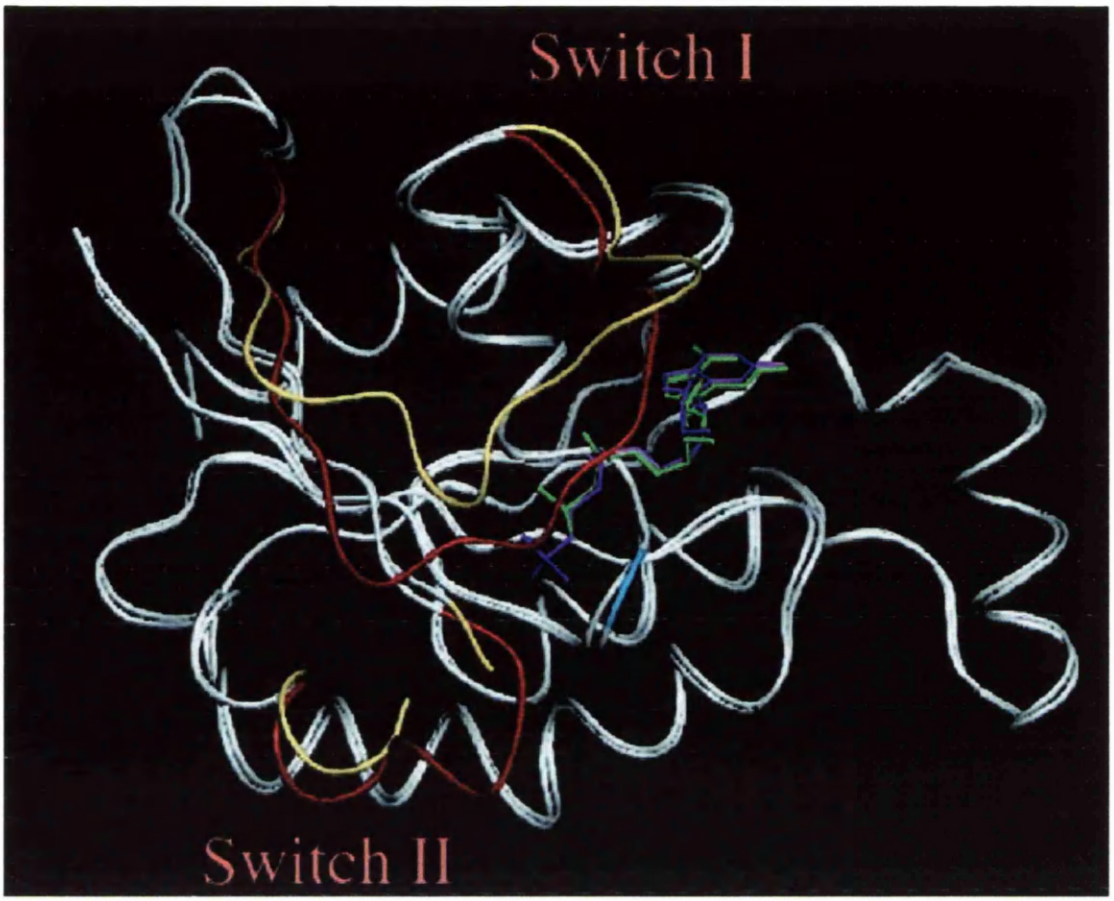

Fig. 4.1: Structural Comparison of V14 RhoA-GTPγS and wtRhoA-GDP.

Superposition of Cα-carbon atom tracings of V14 RhoA-GTPγS (*magenta*) and wtRhoA bound to GDP (*green*) with segments displaying large displacements in *red* and *yellow* , respectively. These include switch I and the C-terminal flanking region (residues 28-44) and the N-terminal region of switch II (residues 62-69). Val14 of V14RhoA is highlighted in *blue*. Figure from [Ihara, 1998].

4.2 Results.

4.2.1 BIAcore Analysis Background

In order to evaluate the nucleotide specificity of the interaction of Rho with the HR1 domains real time Biospecific interaction analysis measurements were employed using a BIAcore™. The BIAcore 2000 (Pharmacia Biotech) employs surface plasmon resonance (SPR) to assess the interaction between two unlabelled molecules to give rate measurements for association and dissociation in real time. The technique utilises the fact that an incident light interacting with a thin metal film (usually gold) produces an evanesent electric field i.e. one which extends into a region where the boundary conditions prevent it from propagating, on the other side of the film. SPR detects the optical properties to a distance of about 1μm out into the medium on the non-illuminated side of the film. SPR is observed as a dip in reflectance intensity at a specific angle of reflection (the resonance angle). Thus as the optical properties of the medium interfacing the non-illuminated side of the film change so the resonance angle changes. The resonance angle is then followed as a function of time.

As can be seen from figure 4.2.1 one member of the potential heterooligomer is immobilised by coupling to the activated hydrophilic polymer (either directly or via a specific antibody) which is on the non-illuminated side of the gold film. A constant buffer flow over the immobilised target is set. The potential binding partner is injected over the target, maintained in constant buffer flow and the change in the resonance angle, expressed as arbitrary units (RU), produces an association curve. The dynamic measurement range is 30,000 RU where an increment of 1 RU corresponds to a shift in the resonance angle of 10^{-4}degrees. The shift in resonance angle correlates with the refractive index of the medium close to the metal film, and this in turn is a linear function of the concentration of macromolecules on the surface. It has been seen that a SPR response of 1RU

corresponds to an increase in the protein concentration at the surface of a CM5 sensor chip (Pharmacia Biotech) of 1pg/mm^2 and that the response is linear over the entire dynamic range (0-30kRU). After injection has been stopped a real time curve of dissociation can be obtained. The comparison of the curves with defined kinetic models allows constants for association (ka), dissociation (kd) and the stoichiometry of complex formation to be assigned. For reference see (Jonsson, *et al.*, 1991).

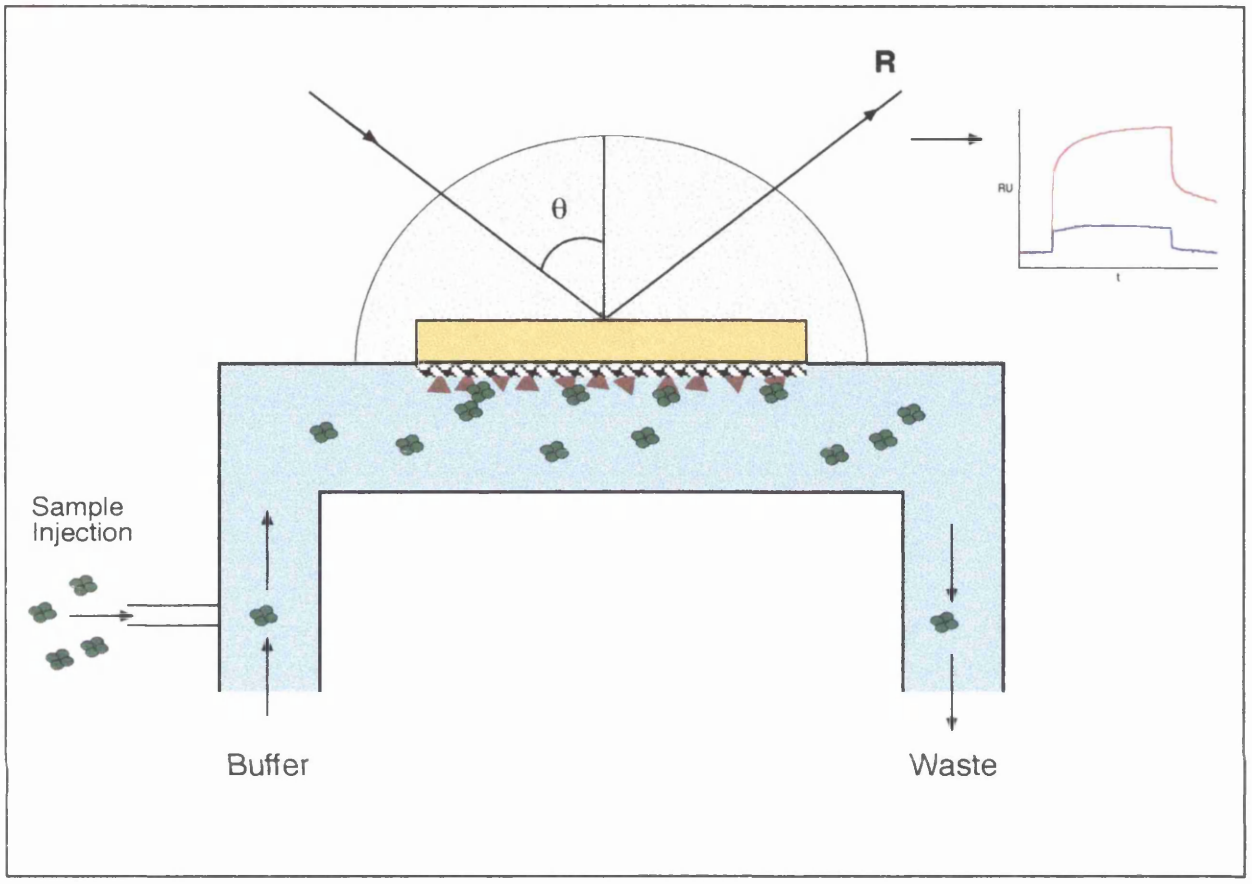

Fig. 4.2.1: Schematic Representation of the BIAcore™ Interaction Surface.
A representation of the various elements involved in the obtaining of binding data from biospecific interaction analysis using surface plasmon resonance. The incident light hits the thin metal film (gold), which is on a glass support, at angle θ producing an evanescent electric field on the side of the medium. The immobilised binding partner is seen as red triangles imbedded in the hydrophilic polymer. The injection and subsequent binding of the second molecule (shown in green) results in a change in the refractive index on the medium surface, which is then translated as a change in the resonance angle (R). This change in R is expressed as resonance units (RU) and plotted to give association and dissociation constants.

4.2.2 The RhoA Interaction with the $HR1^{PRK1}$ is GTP-dependent.

The HR1 domain or a GST control purified from *E. coli* were injected over the activated surface of a CM5 sensor chip as described in 2.3.3. After uncoupled sites on the surface had been blocked a constant buffer flow (PBS, 10mM $MgCl_2$) of 5ml/min was set. wtRhoA protein, again purified from bacteria was then loaded with either GDP or GTP using the method outlined in 2.3.1, after which it was passed through a NICK desalting column (Pharmacia) to exchange it into running buffer. The Rho proteins (400nM) were then injected over the immobilised HR1 and GST for the time periods indicated. As can be seen from the resulting BIAcore™ plot (figure 4.2.2), while the GTP-loaded RhoA produced a curve of association rising to 220 RU over the 500 second injection time, the GDP-loaded RhoA exhibited no binding. The GST control did not produce a curve consistent with RhoA association.

4.2.3 The Recombinant RhoA Binds the HR1 Subdomains with Different Affinities and Nucleotide Specificities

The BIAcore™ was used again in order to assess the nucleotide specificities of the interactions between the individual HR1 subdomains and RhoA. The subdomains were purified from bacteria as GST-fusions and immobilised on the activated surface of the CM5 chip. As with the full HR1 domain, a 400nM solution of either GTP or GDP-loaded RhoA was injected over the surface and changes in the resonance units were plotted. As can be seen from figure 4.2.3 the HR1a displayed complete GTP dependence for the Rho interaction. Consistent with the overlay data RhoA did not display a binding potential for HR1c in either of the nucleotide-loaded forms. The HR1b subdomain was seen to bind the RhoA.GTP preferentially but with a signal that was consistently lower than both the full HR1 and the HR1a. Interestingly, a reproducible interaction was seen between the RhoA.GDP and the HR1b.

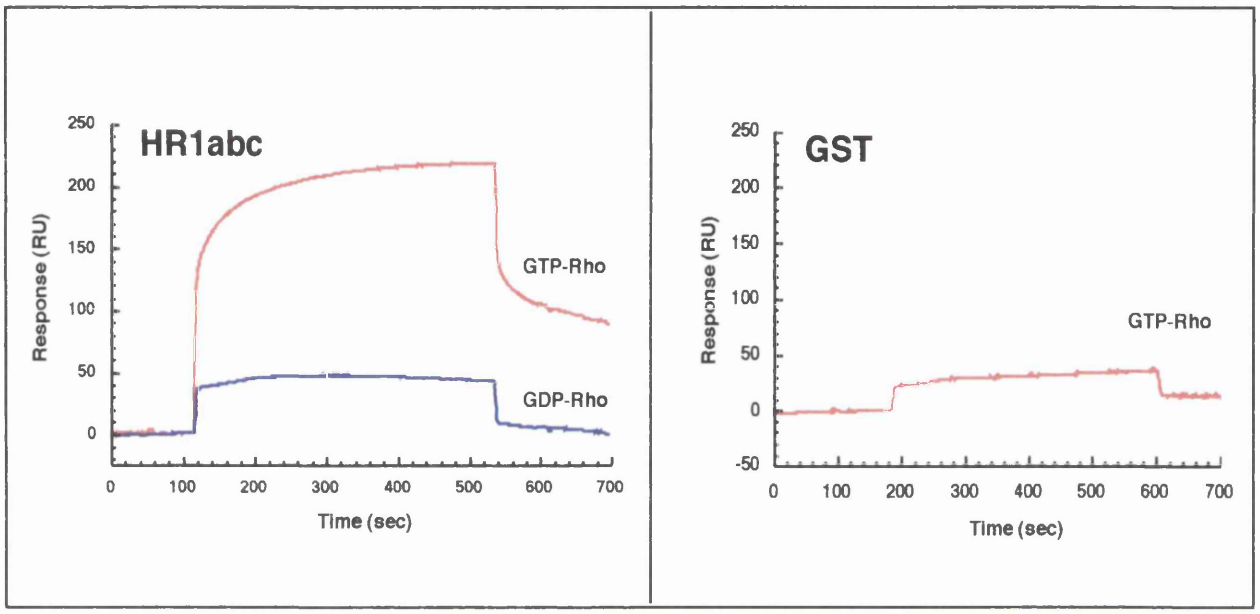

Fig. 4.2.2: HR1$_{PRK1}$ Binds Recombinant RhoA in a Nucleotide Dependent Manner.
Two panels indicating BIAcore™ (Pharmacia Biosensor) measurements of change in Resonance Units (RU) over real time for binding of bacterially expressed RhoA (preloaded with either GTP or GDP) to immobilised GST-HR1$_{PRK1}$ or as a control to GST-alone.

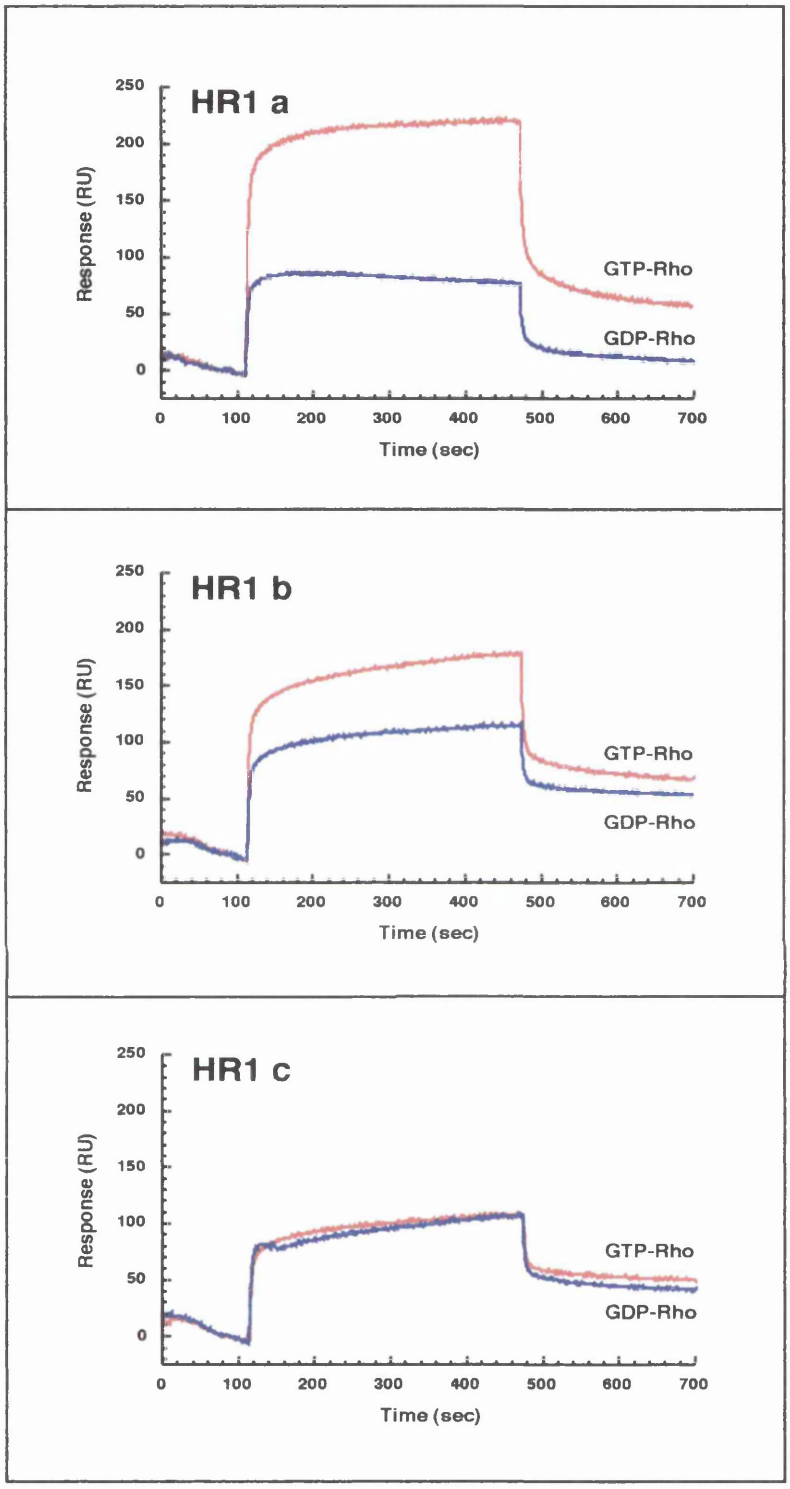

Fig. 4.2.3: Recombinant RhoA Binds the HR1 Subdomains with Different Affinities and Nucleotide Specificities.

BIAcore™ measurements for the binding of wtRhoA preloaded with either GTP or GDP to immobilised HR1 subdomains. Comparisons are semi-quantitative; the higher the response in RU the higher the affinity for the immobilised ligand is presumed to be.

While it is possible to obtain kinetic parameters such as association and dissociation rates from BIAcore analysis, a simple correlation between the data obtained here and defined kinetic models was not seen. Having already established that two sites of contact on both binding partners existed, it was presumed that the stoichiometry of the interaction was affected by dimerization of the GST tags on the immobilised proteins. The observed homooligomerization of the individual subdomains after cleavage from the GST tag (see discussion chapter) precluded their use to gain a clearer result. The chimeric overlay studies showed that the HR1b was unable to bind the HR1a site of interaction on the Rho, but the reverse situation was unclear i.e. in a situation where two HR1a GST fusions had dimerised on the active surface, could one HR1a mimic the HR1b and bind in the amino terminal site on the Rho? Thus the comparisons between the binding properties are semi-quantitative; the proteins that give the highest response in RU are presumed to have the highest affinity for the immobilised ligand.

In order to gain some insight into the properties of the interaction the equilibrium of binding was assessed over a range of RhoA-GTP concentrations. This was completed by injecting Rho at the lower concentration, and allowing the dissociation to take place over time. High salt washes were seen to be ineffective at clearing the HR1s of the bound Rho, and a 0.1M NaOH wash denatures the immobilised proteins. Once the base level signal had been reached the Rho was reinjected at an increased concentation. An example of this can be seen in figure 4.2.4. Increasing the Rho.GDP concentration from 100-200nm makes no difference to the lack of binding potential observed. A concentration of 100nM RhoA.GTP was seen to be the minimum required to gain a signal of binding. While an increase in Rho concentration to 150nM produced an Increase in RU of 45% suggesting a relationship of (y=0.8x-30). However, on injection of 200nM Rho.GTP a subsequent increase of ~80% of expected was seen. This pattern of decreasing signal compared to expected continued with subsequent injections. Having established that the HR1a was

not saturated with respect to Rho at the concentrations tested, it was concluded that the immobilised proteins were unstable in the constant buffer flow over time.

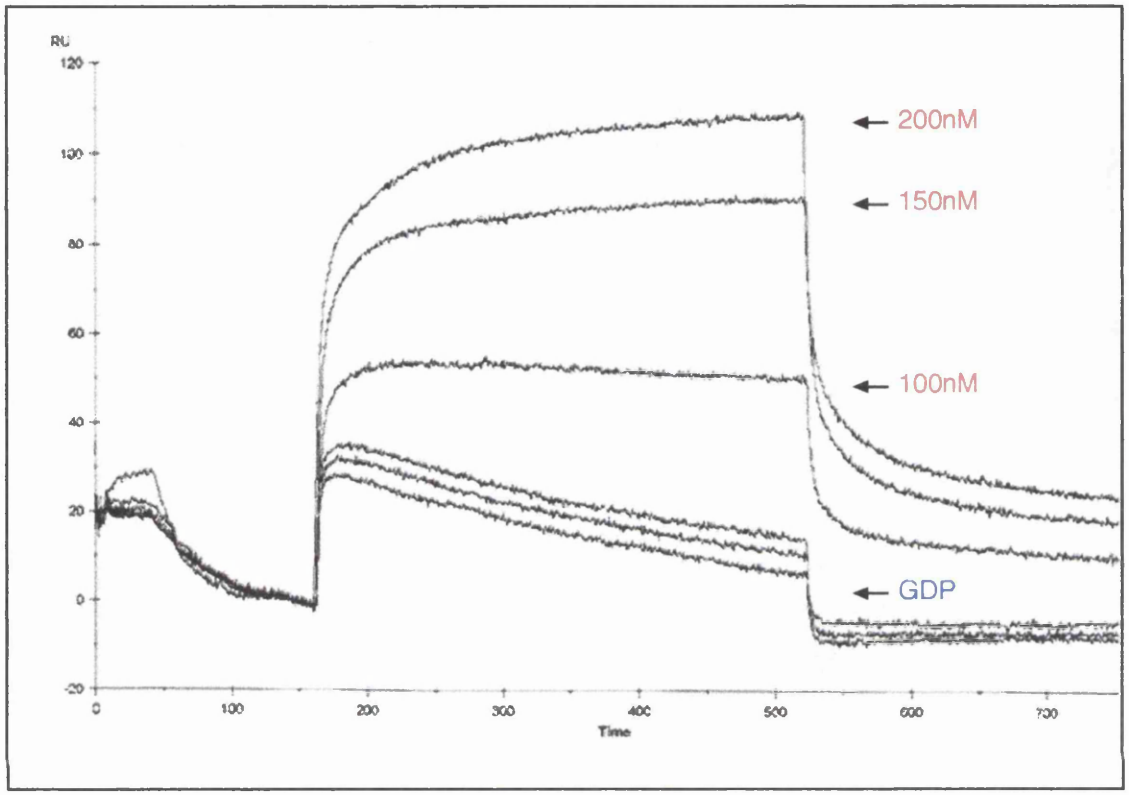

Fig. 4.2.4: The Immobilised HR1 motifs are Unstable in the Constant Buffer Flow Over Time.

The binding potential of the HR1 subdomains with repect to the Rho concentration was assessed. The concentrations of GTP-loaded Rho are indicated in *red* ; the signal RU was seen to increase with respect to increasing Rho concentration, but not at the increments expected. It was concluded that the relative binding site concentration was decreasing over time in the constant buffer flow. The same concentration increases of GDP-loaded Rho didn't produce an increase the signal indicating binding.

4.2.4 RhoA Exhibits a Distinct Nucleotide Dependence for Binding to the HR1 Subdomains.

The data obtained from the BIAcore™ had indicated that while the full HR1 domain only interacted efficiently with the GTP-bound form of RhoA, the individual subdomains, which presumably combine to form the contact, display different degrees of dependence for the nucleotide bound to Rho. To further investigate this a solution affinity assay was developed which used a sequential washing procedure to assess the pattern of dissociation of the Rho from GST-HR1 proteins immobilised on glutathione Sepharose. Experimental procedures were carried out as described in 2.3.4.

Figure 4.2.5 shows an example of the initial solution binding experiments; the GST-HR1 domains were bound to the Sepharose columns and blocked with BSA prior to the addition of the pre-loaded Rho proteins (10μg). After an incubation period of 1 hour in which the flow through the columns was blocked, each column was washed with 20X bed volume (1ml) of PBS, 10mM $MgCl_2$. Proteins which were retained on the Sepharose were eluted, resolved on a 15% SDS-PAGE and western blotted for RhoA. The signals obtained from the westerns were analysed using NIH Image™ software. It was seen that while no RhoA.GDP is retained on the HR1a column almost equivalent amounts of GTP and GDP-loaded RhoA were seen to be retained on the HR1b column. The full HR1 domain was able to bind the RhoA.GTP with greater affinity than both the individual domains and retained 30% as much Rho.GDP.

This distinct binding pattern of the domains was more apparent when the dissociation was assessed over increasing wash volumes. Figure 4.2.6 displays this dissociation pattern for all the domains tested, and figure 4.2.7 overlays the curves, comparing the dissociation of GTP and GDP-bound Rho. While the RhoA.GTP dissociates from HR1c after the first wash step and from the HR1a and b with a similar pattern, the full HR1 domain retains the active Rho for

longer so that even after an 80X bed volume wash Rho protein can still be seen by western. Perhaps more interestingly, the pattern of dissociation of RhoA.GDP from the full HR1 is seen to be very similar to that of the HR1b whereas the RhoA.GDP dissociates from the HR1a on the first wash. The complete GTP dependence for HR1a binding was succesfully predicted to be the case for the homologous motif in *C. elegans* : an identical solution affinity assay carried out for $HR1a^{PRKA}$ produced the result seen in figure 4.2.8. After a 20X bed volume wash only the GTP-bound form of the RhoA was retained in the PRK-A fragment.

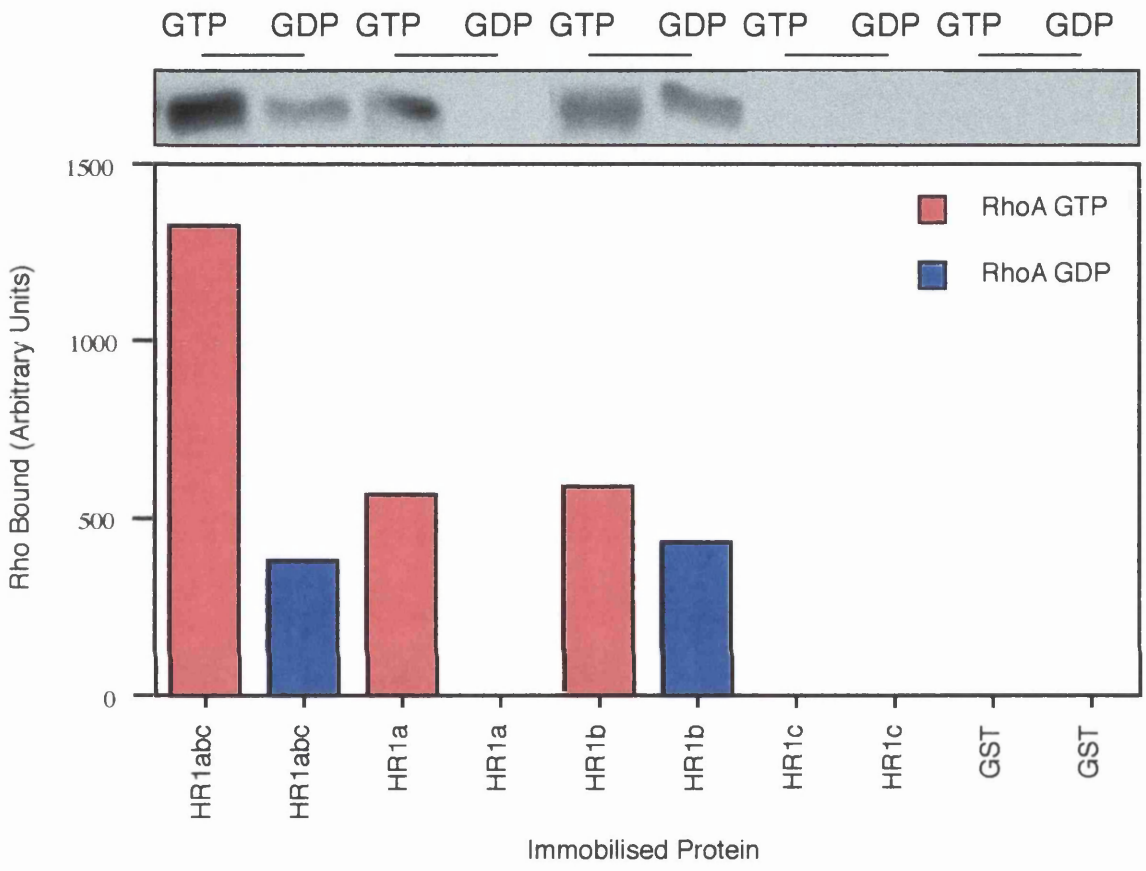

Fig. 4.2.5: Solution Affinity Assays Indicate a Distinct Nucleotide Dependence for the RhoA Interaction with the HR1 Subdomains.

Solution affinity assays were carried out as described (2.3.4) with column washes of 20X bed volumes. The RhoA remaining bound to the HR1 subdomains can be seen by western in the top panel and by graphical representation in the bottom panel where arbitrary units were generated by Western analysis using NIH Image software.

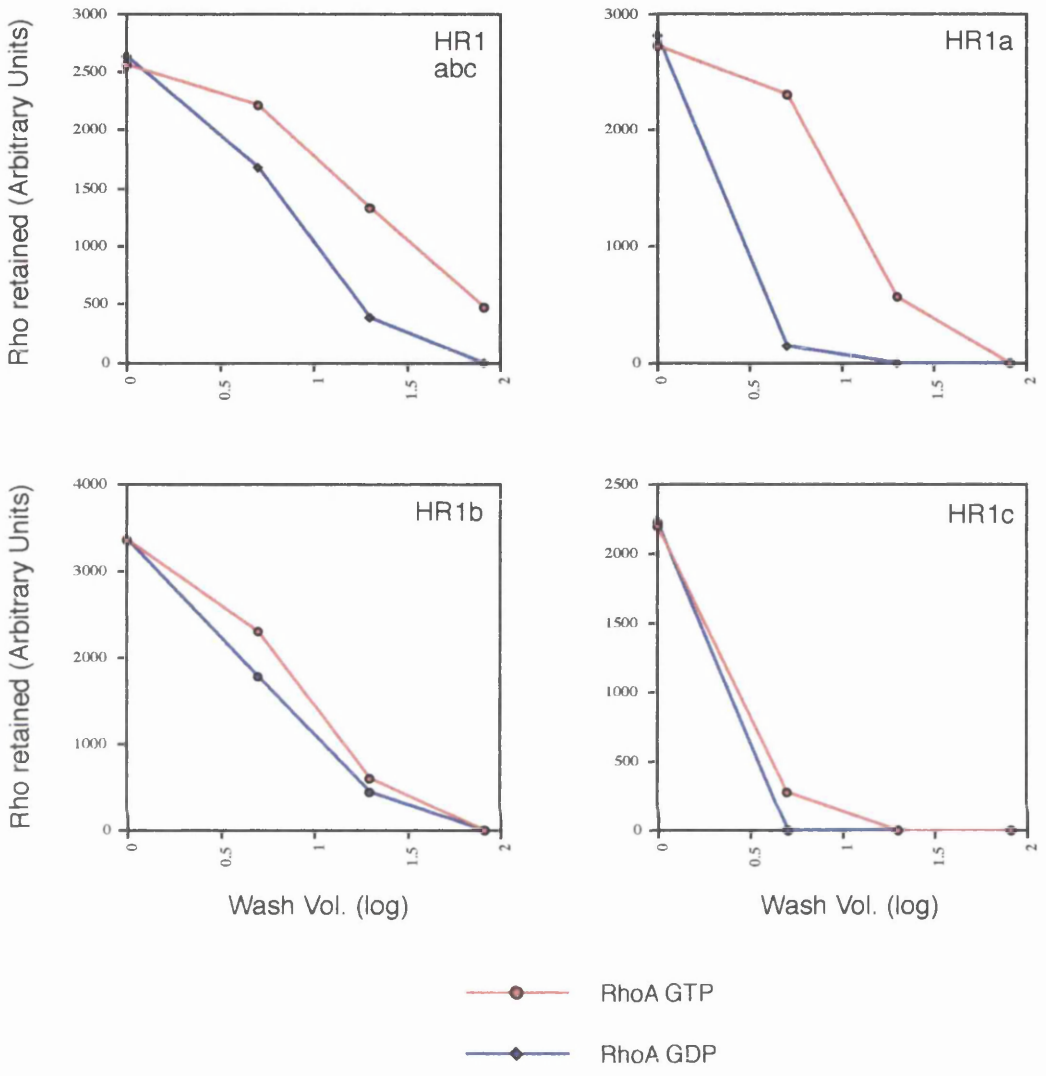

Fig. 4.2.6: Sequential Washing Procedure Defines the Dissociation of RhoA from the HR1 Subdomains with Respect to their Nucleotide-loading. Parallel columns of 10μg RhoA on the various HR1 subdomains were washed with 0-80X bed-volumes as described (2.3.4). Rho proteins retained on the columns were eluted and visualised by western blots which were subsequently analysed for signal intensity. The relative patterns of dissociation are seen as *red* for RhoA.GTP and *blue* for RhoA.GDP.

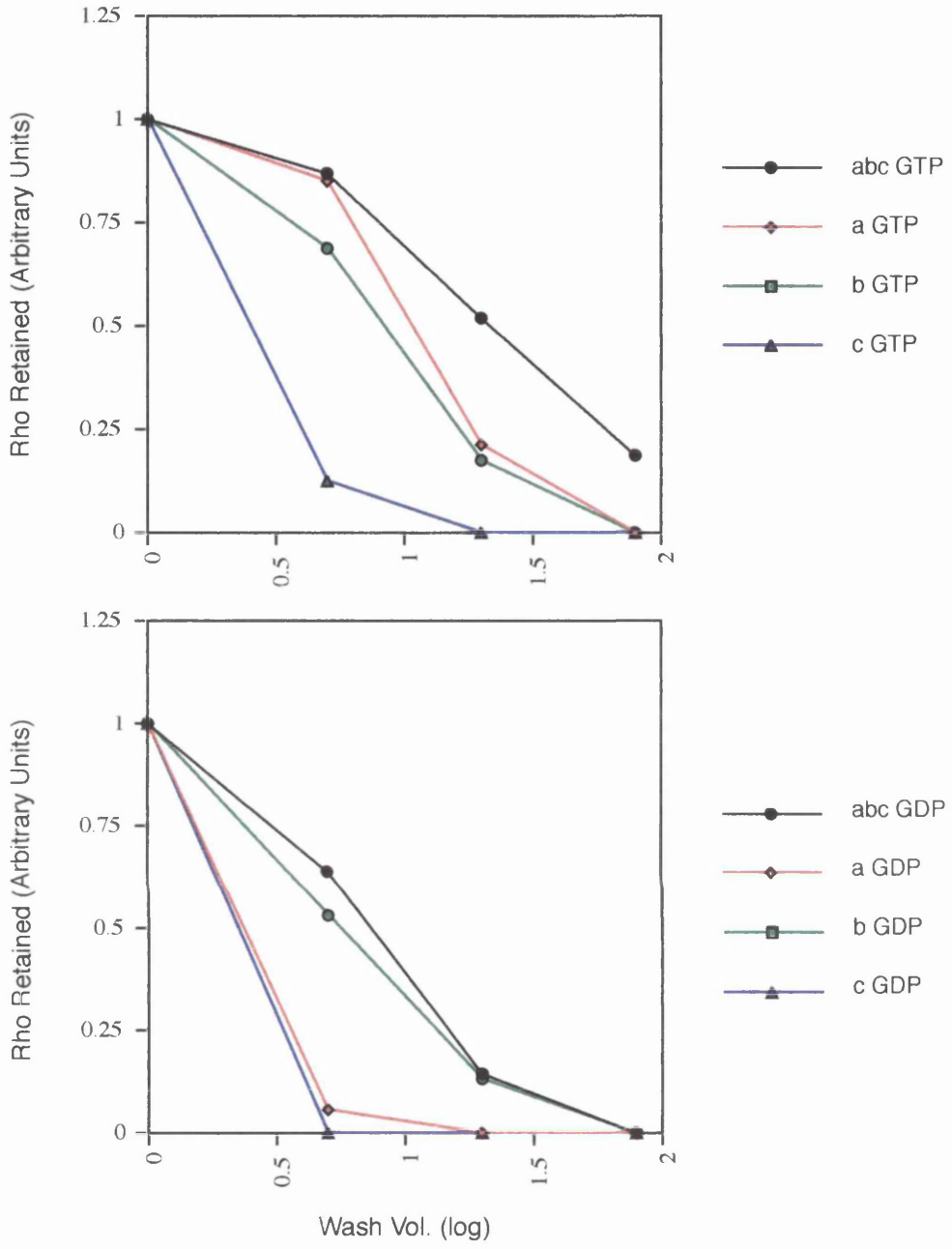

Fig. 4.2.7: Direct Comparison of the Dissociation Patterns of GTP and GDP-Loaded RhoA from the HR1 Subdomains.

The data from figure 4.2.5 normalised to unwashed column and overlaid for direct comparison reveals the distinct nucleotide dependencies of the HR1 subdomains: while the HR1a was seen to form a stable complex exclusively with the GTP-bound RhoA, the HR1b displayed an ability to bind to both nucleotide-loaded forms. The full length HR1 domain exhibited the binding characteristics of both its constituent Rho binding motifs and was seen to bind with a greater affinity than the subdomains to RhoA.GTP.

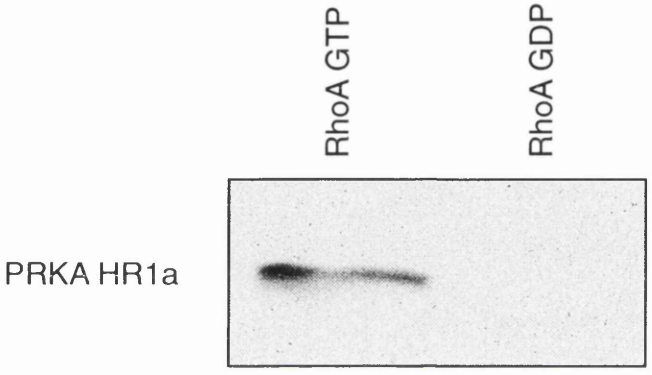

Fig. 4.2.8: The Nucleotide Dependence of Rho Binding to the HR1 Subdomains can be Predicted.

Having established the pattern of nucleotide-dependent binding for Rho to the HR1 subdomains, it was predicted that the *C. elegans* HR1a$_{PRKA}$ would only bind effectively to the GTP-loaded RhoA. A solution affinity assay showed this to be the case: by western analysis a HR1a$_{PRKA}$ column was seen to only retain RhoA.GTP after a 20X bed-volume wash, exactly mimicking its human homologue.

4.2.5 The HR1 domain is a Specific Probe for Active Rho.

In order to test the ability of the HR1 domain to act as a specific probe for the active form of Rho HEK 293 cells were transfected with mutant forms of RhoB +/- *Clostridium* C3 toxin. The wild type, Q63L active and T19N inactive mutants were used and the transfection procedure was according to 2.2.17. The cells were serum starved by incubation DMEM, 0.5% FCS, 0.5% fatty acid-free BSA for 16 hours followed by 1 hour in 0% FCS prior to harvest. The intact HR1 domain was used in the pull down procedure outlined in 2.3.5. The total amounts of RhoB compared to that pulled out were analysed by western blot using a polyclonal antibody (Santa Cruz). As can be seen in figure 4.2.9 the RhoB proteins all expressed to a high level although there was 1.5 and 2.5-fold more wild type than the QL mutant and TN mutant respectively. The blots for total Rho used 2.0% of the cell lysate, whereas 10% of the material pulled down was analysed. The lower western panels show that while a comparatively small amount of the wild type Rho was pulled down a much greater percentage of the QL mutant was seen (approx. 2.5% compared to 25%). No TN mutant was seen to be pulled down. As expected, when the C3 toxin was co-expressed with the Rho proteins no wild type was active whereas the QL was still seen to be pulled out. This could either be due to the C3 toxin's action of specifically ADP-ribosylating asparagine-41 doesn't affect the active mutant or that there is simply more QL expressed in these cells than C3 toxin.

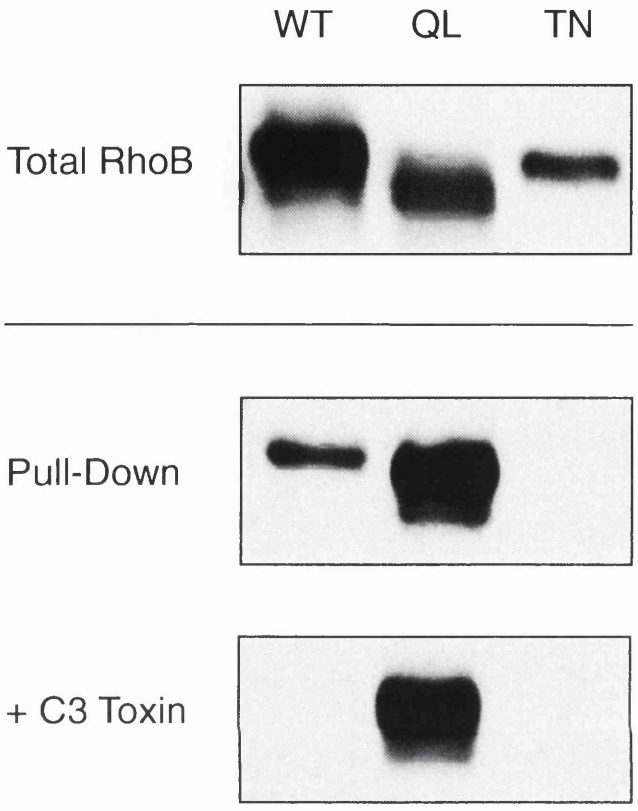

Fig. 4.2.9: The HR1 Domain can be used as an Activation-Specific Probe for Overexpressed RhoB in Mammalian Cells.

To assess whether the HR1$_{PRK1}$ can be used as an effective tool to pull Activated Rho from mammalian cells relevant activation mutants were overexpressed in HEK293 cells. Either the wild type, Q61L active mutant or the T19N inactive mutant were expressed to the comparative level seen in the RhoB-specific western blot (top panel). The Rho pull-down assay was completed as described (2.3.5) and the relative yields can be seen in the middle panel i.e while the active mutant is efficiently pulled out and the wild type is to a degree the inactive mutant is undetectable by western. Consistent with the Rho proteins being pulled down as a function of their activation state, when they are co-expressed with the *Clostridium* C3 toxin the wilt type RhoB is no longer seen to be pulled down with the HR1 domain whereas the active mutant is at a very slightly reduced level.

4.3 Chapter Discussion

The work completed in this chapter assessed whether the interactions described in chapter 3 required the RhoA GTPase to be in the conformation associated with the active state; the GTP-bound form. The use of BIAcore™ technology in combination with solution affinity assays established that while the HR1a binds exclusively to RhoA.GTP, the HR1b is able to make stable contacts with both the GTP and GDP forms. Consistent with these findings the full HR1 domain binds preferentially but non-exclusively to RhoA.GTP. Although kinetic data for the Biacore interactions did not fit the defined models, it can be concluded from the pattern of dissociation of Rho from the HR1 fragments that the full domain binds with higher affinity than the individual subdomains. This would suggest that in the intact PRK the Rho interacts via combined contacts with both subdomains.

Combining the data from chapters 3 and 4 it can be seen that while the HR1b is able to interact with Rho irrespective of conformational changes induced by nucleotide, it cannot interact with the V14 mutant suggesting that this affect on binding is due to the sequence change. HR1a binds to the Rho molecule in an area which overlaps the switch II domain. Its absolute dependence on the GTP-form for interaction suggests that it will only recognise the conformational change induced by the tri-phosphate form of the nucleotide. The relevance of these interactions with respect to the findings of other groups will be discussed at greater length in the chapter 7. The *in vitro* and possible *in vivo* contacts elucidated are outlined in figure 4.3.1.

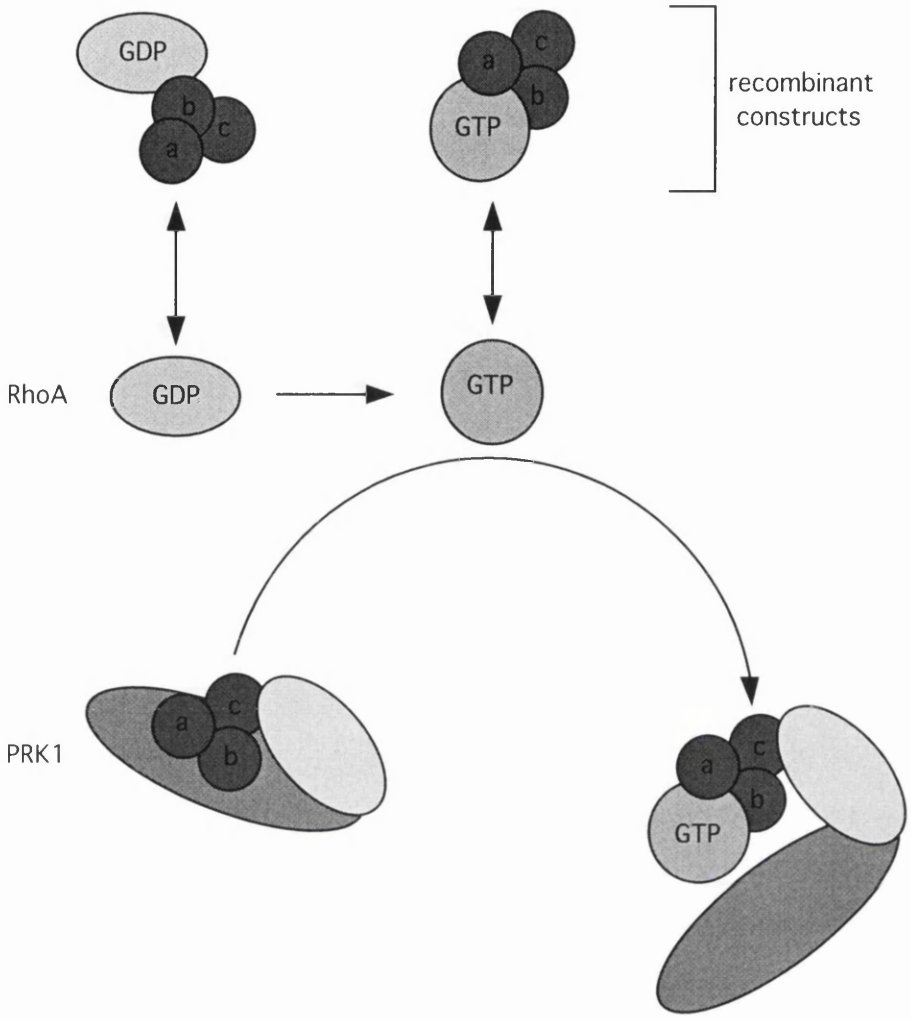

Fig. 4.3.1: A Summary of the Interaction of RhoA and PRK1.

In the upper section of the figure, the binding behavior of the recombinant HR1 domain is illustrated. RhoA.GDP is shown to interact at the single HR1b subdomain within the recombinant protein. In the GTP-bound state, RhoA contacts both the HR1a and HR1b motifs. For the intact PRK1, binding through the HR1 domain may contribute to the activation process by relieving the pseudo-substrate site from the catalytic domain (discussed in the next chapter).

4.3.2 Developing a Quantifiable Assay for Rho Activity

The activity of Rho family GTPases on mitogen stimulation has traditionally been assessed through the visualisation of the classically associated cytoskeletal rearrangements (Ridley and Hall, 1992). Additionally, the use of the inactivating *Clostridium botulium* C3 exoenzyme and a range of constitutively active or inactive mutants has been pivotal in our understanding of Rho dependent signalling events (Kumagai, *et al.*, 1993). However, a quantifiable assay for analysing the levels of active Rho in mammalian cells on mitogen stimulation, stress or at the defined checkpoints of the cell cycle has yet to be produced.

The most well characterised small GTPases are those of the Ras sub-family. Original methods for assessing the modulation of active Ras in a mammalian cell system required [^{32}P] orthophosphate labelling of the cells. The ratio of GTP to GTP + GDP bound to immunopreciitated Ras was analysed by chromatography to give a relative percentage of active Ras (Gibbs, *et al.*, 1990). However, the ability of even low levels of radioisotopes to cause cell cycle arrest or apoptosis due to elevated levels of p53, precluded their use in measuring Ras activity over the cell cycle (Yeargin and Haas, 1995). Later studies utilised the minimal Ras binding domain (RBD) of Raf1 (residues 51-131) to specifically "pull-down" the active form of Ras from cell lysates (Taylor and Shalloway, 1996), (De Cammili and Bos, 1997). The RBD had been shown to bind tightly (kd 20nM) to the GTP-bound form of Ras and to the GDP-form with a kd three orders of magnitued lower (Herrmann, *et al.*, 1995). Such a system was used to show that the activation of Ras and ERK (one member of a characterised Ras signalling pathway) were temporally dissociated during G1 phase of the cell cycle (Taylor and Shalloway, 1996).

As described in later chapters the interaction between an active Rho molecule and PRK is implicated in both the subcellular localisation and activation of the

kinase. Chapters 3 and 4 have characterised a homology region within the PRKs as a binding domain for Rho family GTPases. The intact HR1 domain preferentially binds RhoA in the GTP-bound form, as does the HR1a subdomain. The HR1 domain was therefore assessed as a probe for active Rho in mammalian cells. The N-terminal region of PRK1 was shown to inhibit both the intrinsic and GAP stimulated GTPase activity of RhoA in a concentration dependent manner (Shibata, *et al.*, 1996). This effect would be advantageous: protecting the level of GTP-loaded Rho during the extraction from whole cell lysate.

Chapter 5 - The Effect of the Rho Interaction on PRK Phosphorylation.

5.1 Introduction

The precedent for small G-proteins acting as binary switches; relaying extracellular ligand-stimulated signals to downstream kinases is typified by the Ras-Raf1 interaction. The active Ras.GTP recruits Raf1 to the plasma membrane resulting in the kinase's activation (Leevers, *et al.*, 1994, Stokoe and McCormick, 1997). Although the exact mechanism of Raf1 activation remains unclear it is thought that elements other than Ras alone are required. This is demonstrated by the lack of Raf1 activation on incubation with Ras *in vitro* and the ability of a membrane targeted c-Raf1 (Raf-caax) to be activated *in vivo* in the absence of Ras (Leevers, *et al.*, 1994, Stokoe and McCormick, 1997, Traverse, *et al.*, 1993, Zhang, *et al.*, 1993). Other small GTPase kinase effectors are seen to be directly activated by the interactions *in vitro*: the autophosphorylation of $p65^{PAK}$ serine/threonine kinase and related isoforms is seen to be stimulated on incubation with Rac1.GTP and Cdc42.GTP (Bagrodia, *et al.*, 1995, Manser, *et al.*, 1995a, Manser, *et al.*, 1994, Martin, *et al.*, 1995). This p21-mediated autophosphorylation leads to an increased activity against exogenous substrates. A similar situation pertains for the Rho-associated kinases p160 and Rho-kinase, which have increased auto and trans catalytic activity when incubated with Rho.GTP *in vitro* (Ishizaki, *et al.*, 1996, Matsui, *et al.*, 1996). Once again the mechanism for these events is unclear.

It seems likely that the observed interaction between Rho-family GTPases and the PRKs would result in kinase activation. Indeed an increase in phosphate incorporation into PRK has been shown on *in vitro* incubation with RhoA.GTP (Amano, *et al.*, 1996b, Watanabe, *et al.*, 1996) and interestingly a similar situation is seen for PRK2 irrespective of the nucleotide loading of Rho (Vincent and Settleman, 1997). Associated with this phosphorylation event is an

increased activity against exogenous substrate, while PRK immunoprecipitated from Cos-7 cells is seen to have approximately a two-fold activation when co-expressed with V14RhoA (Amano, *et al.*, 1996b). Unlike the previously described GTPase-mediated kinase activation events the situation for PRK-Rho may be explained by an allosteric mechanism: a potential pseudosubstrate site has been identified within the amino-terminal regulatory region (HR1 domain) of the PRKs (Kitagawa, *et al.*, 1996). The site can be seen aligned with a consensus PKC phosphorylation site in figure 5.1. The peptide corresponding to residues 39-53 of PRK1 except with a I46S substitution was an efficient substrate for PRK and the wildtype peptide inhibited kinase activity *in vitro* in a dose-dependent manner (Kitagawa, *et al.*, 1996). Thus it may be the case that a Rho interaction acts to disrupt the inhibitory intramolecular interaction resulting in an activated kinase. However, an increase in the rate of autophosphorylation of the rat PRK1 on incubation with fatty acids is also observed (Peng, *et al.*, 1996) and PRKs are known to be activated *in vitro* on incubation with fatty acids and phospholipids (Morrice, *et al.*, 1994a, Palmer, *et al.*, 1995a).

Taken together these observations suggests that phosphorylation events are required for kinase activation, but that either multiple independent inputs can lead to this phosphorylation or that Rho and lipids can perform the same or a cooperative function. In this chapter the role of the Rho interaction in PRK phosphorylation is assessed both *in vitro* and *in vivo*.

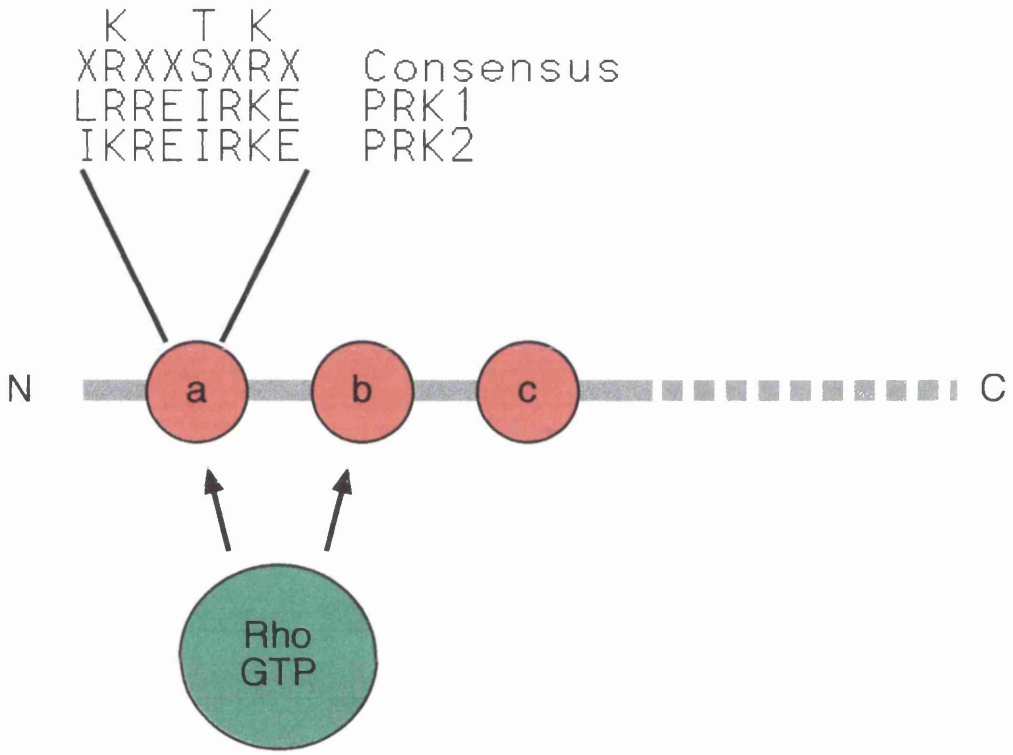

Fig. 5.1: Position and Sequence of the Proposed PRK Pseudosubstrate Site.
Schematic representation of the position of the proposed pseudosubstrate region of PRK (Kitagawa, 1996) in relation to the defined Rho binding site. The alignment shows the consensus PKC substrate sequence and the relative sequences from human PRK1 and PRK2.

5.2 Results

5.2.1 PRK1 Purification from HEK 293 Cells

In order to obtain pure PRK1 for subsequent *in vitro* activity assays a previously published purification procedure was employed (Palmer and Parker, 1995). PRK1 was expressed and purified from 293 cells as described in section 2.2.18. 5µl of the fractions generated from the various column steps were assayed for kinase activity against protamine sulphate to give the elution profiles displayed in figure 5.2.1. PRK1 activity was seen to elute from the HiTrap SP, Heparin and Q columns at 0.65, 0.7 and 0.6M Nacl respectively. The purification procedure was routinely completed in less than 36 hours with every step carried out at 4°C. The peak fractions pooled from each step were analysed on a coomassie stained SDS-PAGE as can be seen in figure 5.2.2. The purified PRK1 was stored in 50% (v/v) ethandiol at -20°C and was used in subsequent assays.

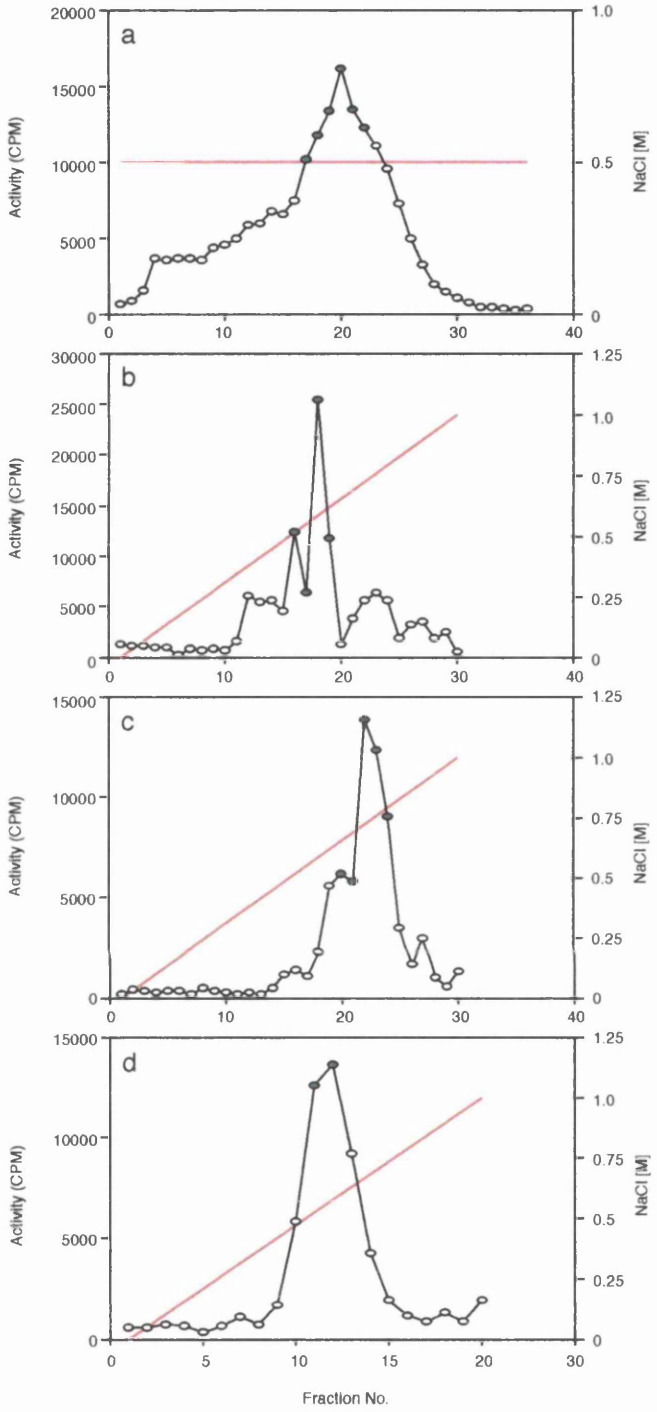

Fig. 5.2.1: Sequential Chromatography steps in the Purification of PRK1 from HEK293 Cells.

The activity profiles for the four chromatography steps employed for the purification of overexpressed PRK1 from HEK 293 cells: a) Sephacryl S-300 column; b) HiTrapSP column; c) HiTrap Heparin column; d) HiTrapQ column. PRK1 activity was assayed against protamine sulphate. The NaCl concentration gradients are shown in red and the fractions pooled for application to the following column are marked in green.

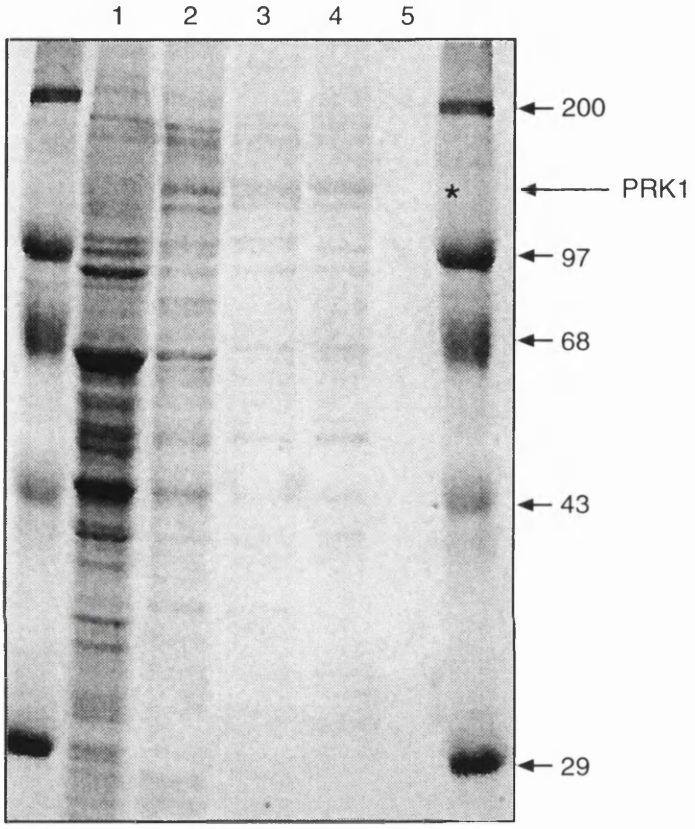

Fig. 5.2.2: Coomassie-Stained SDS-PAGE of the Pooled Fractions from the PRK1 Purification.

25µl of the pooled fractions (see figure 5.2.1) from the PRK1 purification profiles analysed on 10% SDS-PAGE; lane 1) Triton X100 soluble lysate, 2) Sephacryl S-300 pool, 3) HiTrapSP pool, 4) HiTrap Heparin pool, 5) HiTrap Q pool. The PRK1 is marked (*) and the molecular weight standards are indicated in kDa.

5.2.2 The Activity of Purified PRK1 is Enhanced by Lipid but not Rho

PRK1 generated as described (5.2.1) was assayed for kinase activity against exogenous substrate Myelin Basic Protein in the presence of phospholipids and Rho.GTP. Purified PRK1 (5µl) was added to a 40µl reaction of buffer F containing 100µM ATP + 10µCi [γ^{32}P]ATP, 5µg MBP and either PtdIns(4,5)P_2 or phosphatidic acid (PA), both of which were displayed at 10 mol% in a Triton X100 micelle (see section 2.2.22). Assays were carried out for 15 minutes at 30°C and were terminated by spotting onto P81 papers (Whatman) and 3X washes in excess 30% (v/v) acetic acid. The PRK activity was measured as ^{32}P incorporated into MBP in counts per minute (cpm) by Cerenkov counting. Consistent with previous findings (Palmer, *et al.*, 1995a) the PRK1 activity against MBP was enhanced in the presence of PtdIns(4,5)P_2 (figure 5.2.3 panel A). An equivalent 2.5-fold activation was seen in the presence of phosphatidic acid which is again consistent with previous findings (Morrice, *et al.*, 1994a).

Assays were carried out to the same protocol but in the presence of wildtype RhoA. The Rho was expressed as a GST-fusion protein in *E. coli*, purified and cleaved from its tag as described in section 3.2.1. It was loaded with the non-hydrolysable GTP analogue GTPγS and passed through a NICK-desalting column (Pharmacia) in order to exchange it into kinase buffer F. The RhoA.GTPγS was added to the kinase reactions to a final concentration of 10nM (approximately equimolar for PRK1) and the PRK1 activity against MBP was assessed as above. It can be seen from panel B of figure 5.2.3 that while the PtdIns(4,5)P_2 produced a characteristic enhancement of the kinase activity, the presence of Rho did not alter either the basal or stimulated PRK1 activity significantly. This was surprising given the findings of other studies (Amano, *et al.*, 1996b, Watanabe, *et al.*, 1996).

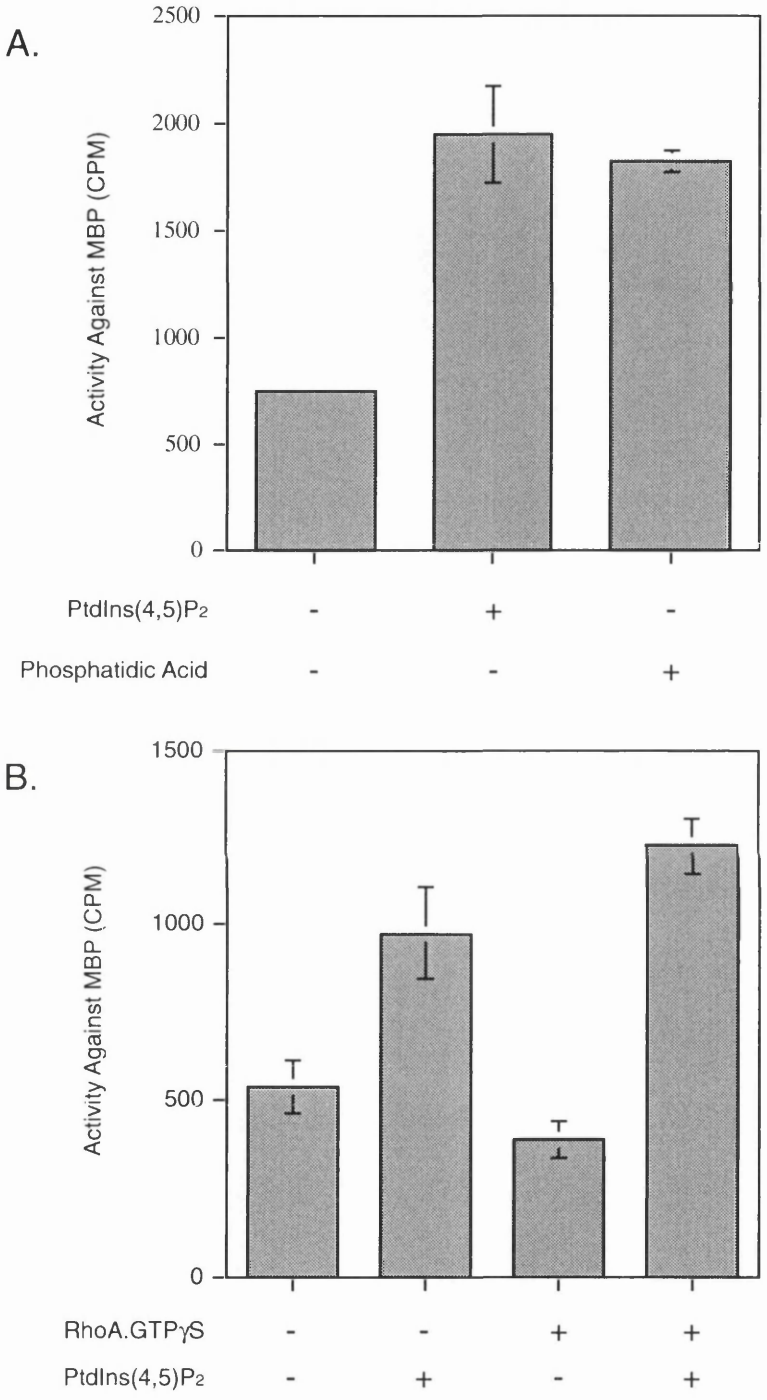

Fig. 5.2.3: Lipid and Rho Dependence of Purified PRK1 Activity *in vitro*. PRK1 (5µl) purified from 293 cells was assessed for kinase activity against Myelin Basic Protein (MBP) in the presence of; A) PtdIns(4,5)P_2 or phosphatidic acid (both at 10 mol% in Triton X100 micelles), B) bacterially expressed RhoA loaded with GTPγS and/or PtdIns(4,5)P_2 as indicated. Duplicate activities in the two independent experiments were measured as ^{32}P incorporated into MBP (CPM) by cerenkov counting.

5.2.3 The *in vitro* Phosphatase Treatment of Purified PRK1 Inhibits Kinase Activity.

The Rho-dependent PRK1 activation is associated with a PRK phosphorylation event. Having been unable to establish a Rho stimulation of kinase activity, *in vitro* protein phosphatase treatment was used to test whether the purified PRK1 could be inactivated. Purified PRK1 (5µl) was treated for 15 minutes at 30°C with 2.0ng of a PP1, PP2A mix (1:1 by activity) prior to a typical kinase assay. As can be seen from the resulting activities (figure 5.2.4) both the basal and PtdIns(4,5)P_2 (10 mol%) stimulated activities were significantly reduced with phosphatase pre-treatment. However, the relative lipid stimulation, albeit minor in this assay, remains intact. These data suggest that any Rho-dependent phosphorylation events may have taken place prior to the onset of the *in vitro* assay. Indeed, the tracking of PRK1 activity in order to purify the kinase by definition may result in only the active form being present. However this does not immediately explain the observed lipid-stimulated activity.

5.2.4 PRK and Rho Proteins were Immunoprecipitated from HEK 293 Cells.

For ease of preparation and to circumvent the possible shortcomings of using purified PRK proteins for *in vitro* kinase assays, immunopurified proteins were prepared by transient overexpression and immunoprecipitation from cultured cells. 293 cells were transiently transfected with either Myc-tagged PRK1, PRK2 or RhoA (Q63L) as described in the materials and methods section. Cells containing the PRK proteins were serum starved for 18 hours prior to harvest into buffer E. Cells containing overexpressed RhoA were starved followed by a 30 minute stimulation with 10% FCS prior to harvest in buffer E containing 5mM $MgCl_2$ and without EDTA present; so as to maintain Rho GTP loading. Immunoprecipitations using the 9E10 monoclonal were as described in section

2.2.18. The purified proteins on protein G-Sepharose were washed into kinase buffer: 20mM Hepes pH 7.5, 50mM NaCl, 1mM EGTA, 1mM DTT, 1μM Microcystin, 0.25% (v/v) Triton X100 and 5mM $MgCl_2$. Proteins were then eluted from the Sepharose by incubation in kinase buffer in the presence of 1mg/ml 9E10 antigen. As can be seen in figure 5.2.5, the elutions were at best 50% complete but yielded enough protein for subsequent kinase assays.

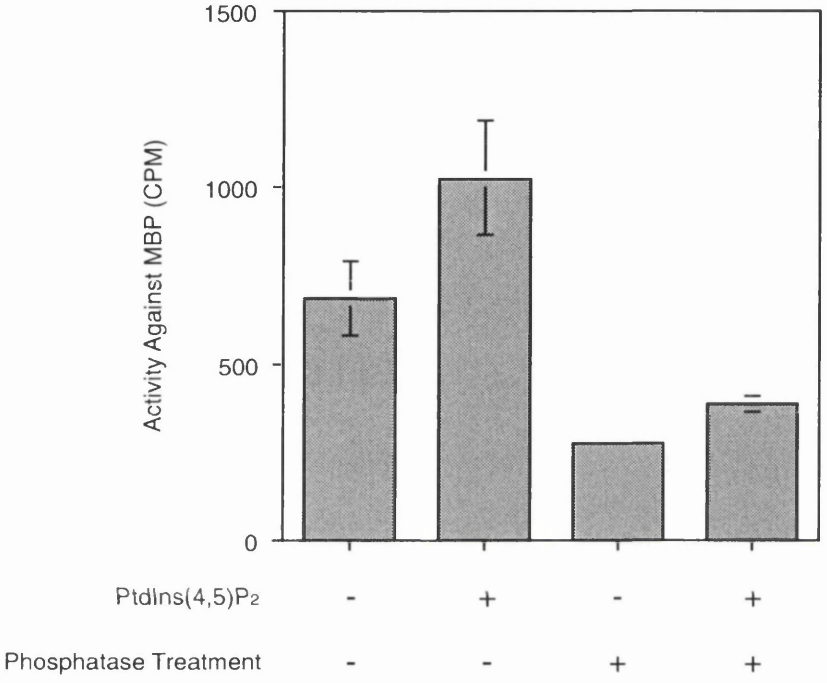

Fig. 5.2.4: Effect of Phosphatase (PP1A, PP2A) Treatment on PRK1 *in vitro* Kinase Activity.

In order to assess the effect of phosphorylation on PRK kinase activity 5µl of purified PRK1 was treated with 2.0ng of a PP1A, PP2A mix (1:1 by activity) for 15 minutes at 30°C prior to a kinase assay. The phosphatase activity was inhibited with exess okadaic acid. The kinase activity was assessed by phosphate (^{32}P) incorporation into MBP.

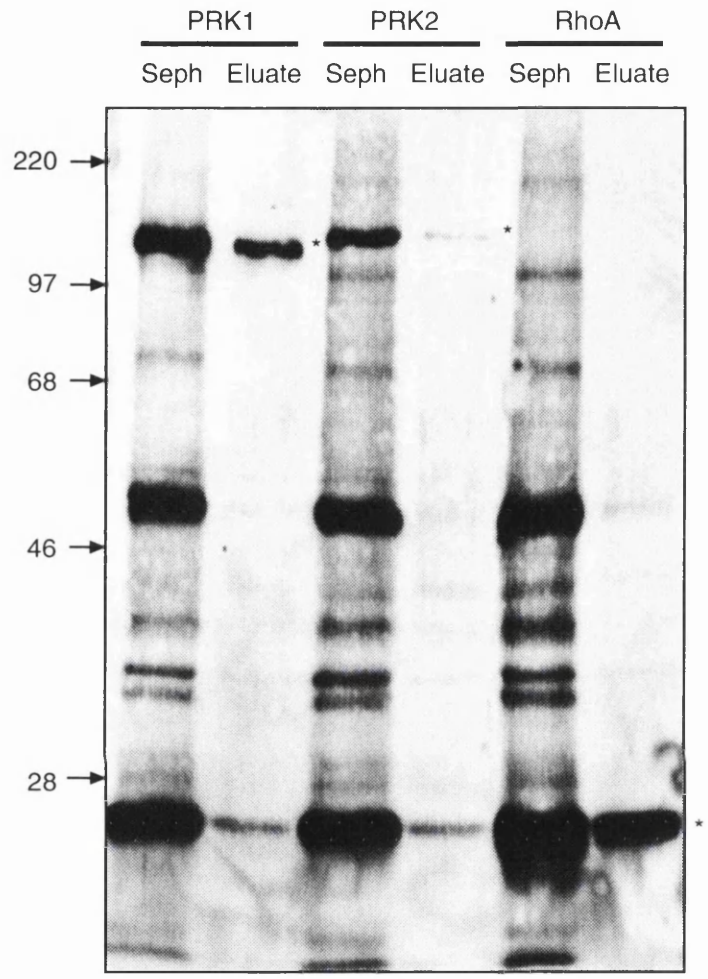

Fig. 5.2.5: Western Blot of Immunoprecipitated PRK and Rho Proteins

Myc-tagged PRK1, PRK2 and RhoA (Q63L) were transiently expressed in HEK 293 cells as described in the methods section. Proteins were immunopurified on protein-G Sepharose using the 9E10 monoclonal antibody and eluted from the washed Sepharose using the 9E10 epitope peptide. 15µl samples of both the washed Sepharose and the eluted proteins were run on a 12.5% SDS-PAGE and analysed by western blot, again using the 9E10 monoclonal. Purified proteins are marked (*).

5.2.5 The Phosphorylation of PRK *in vitro* is Unaffected by PtdIns(4,5)P_2 or RhoA (Q63L).

Assessment of the effect of lipids on PRK's potential autophosphorylation activity was carried out by incubation of the immunopurified PRK with PtdIns(4,5)P_2 in the presence or absence of the immunopurified RhoA(Q63L). Reactions were in 40µl and contained 10µl of the PRK proteins with 100µM ATP + 10µCi [γ^{32}P]ATP and 10 mol% PtdIns(4,5)P_2 in Triton X100 micelles. Rho(Q63L) (10µl) (in excess with respect to PRK) was added as indicated. Reactions took place for 15 minutes at 30°C and were terminated by the addition of 20µl Laemmli 4X sample buffer. Samples were fractionated on a 10% SDS-PAGE which was subsequently coomassie stained dried and assessed by autoradigraphy. The signals produced were used to orientate the position of the PRK bands which were cut out and analysed by Cerenkov counting. The resulting ^{32}P incorporation into PRK (cpm) can be seen in figure 5.2.6 where the values are representative of three independent experiments. Surprisingly no significant changes in the phosphorylation of PRK1 or PRK2 were observed either in the presence of PtdIns(4,5)P_2 or RhoA(Q63L) or both. This further suggested that these activators had no effect on the intrinsic autokinase activity of the PRKs *in vitro*. While the immunopurified RhoA(Q63L) was not GTP-loaded *in vitro* the maintenance in high Mg^{2+} and immediate use should have resulted in a proportion of the protein being positive for PRK binding. Indeed the interaction between this mutant and PRK1 has been shown to withstand immunoprecipitation (Mellor, *et al.*, 1998). Further, PRK2 autokinase activity has been shown to be stimulated by both GTP and GDP loaded Rho (Vincent and Settleman, 1997).

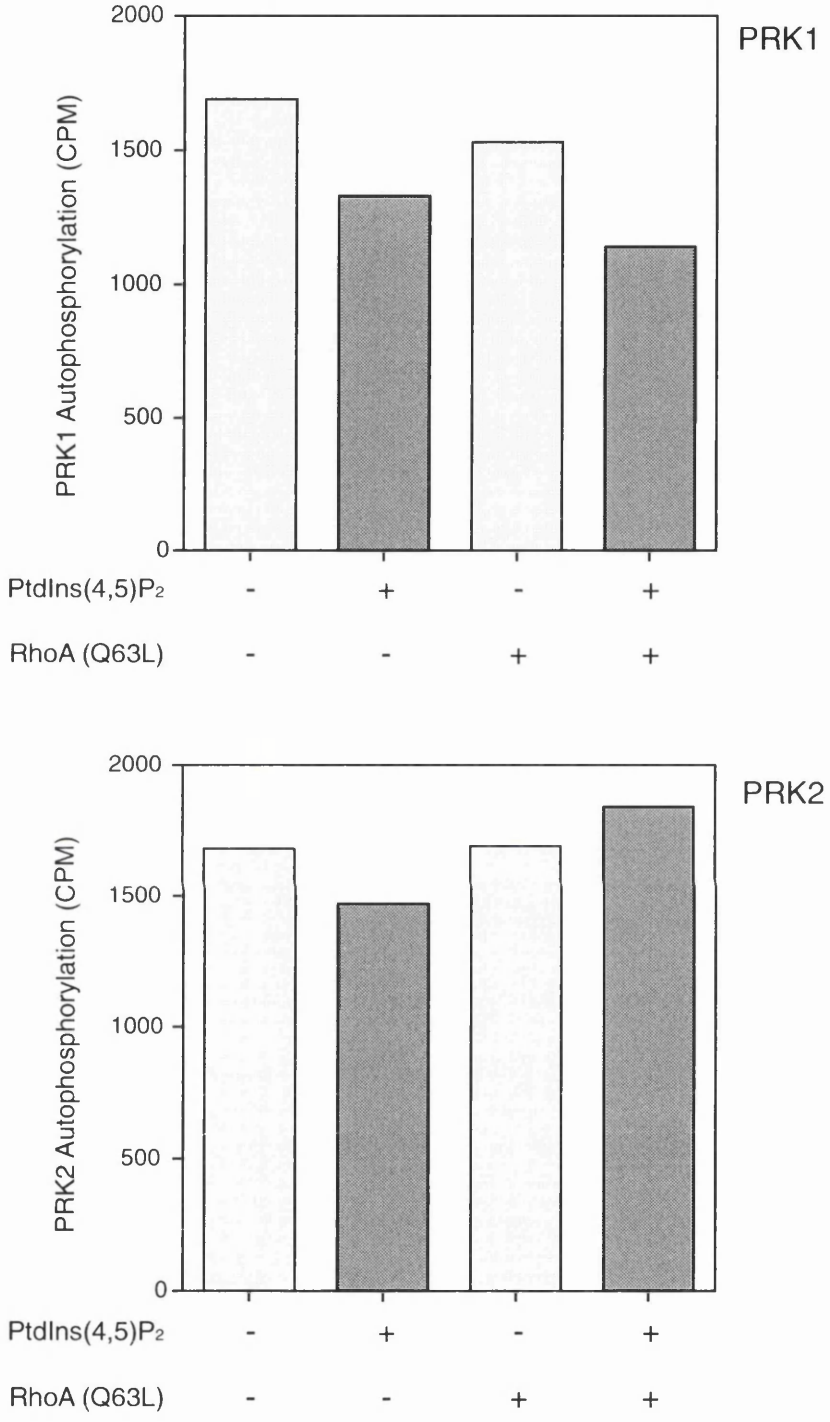

Fig. 5.2.6: Effect of PtdIns(4,5)P_2 and RhoA(Q63L) on PRK Autokinase Activity *in vitro.*

Immunopurified PRK1 (upper panel) and PRK2 (lower panel) was assessed for autokinase activity by incubation with Mg^{2+}/ATP in the presence of PtdIns(4,5)P_2 or immunopurified RhoA (Q63L) as indicated. The lipid was displayed in a Triton X100 micelle at 10 mol%, 10µl Rho was used in each assay and reactions were for 20 minutes at 30° C. Phosphate incorporation was assessed by Cerenkov counting of the SDS-PAGE purified PRK.

5.2.6 PtdIns(4,5)P_2 but not RhoA(Q63L) Induces Increased Catalytic Activity in Immunopurified PRK against Myelin Basic Protein (MBP).

The surprising lack of effect of lipid and Rho on the autokinase activity of PRK provoked the assessment of the immunopurified kinase activity against exogenous substrate MBP. Kinase reactions were carried out exactly as described in 5.2.5 but in the presence of 5μg MBP. Reactions were terminated by spotting on P81 paper (Whatman) and immersion and three washes in excess 30% (v/v) acetic acid. The papers were then counted to produce the levels displayed in figure 5.2.7. The values are representative of three independent experiments. Consistent with previous results the PtdIns(4,5)P_2 produces an increase in PRK catalytic activity against MBP of approximately 2-fold for PRK1 and 10-fold for PRK2. However, the presence of RhoA(Q63L) in the assay had no effect on the basal activity of PRK. Further, the effect of the lipid on PRK activity was entirely inhibited by the presence of Rho. A putative lipid binding site has been suggested within the HR1a region of PRK1 (Peng, *et al.*, 1996). Should this region be the site of lipid interaction *in vitro* the observed Rho inhibition may be explained by steric hinderence. The saturating concentration of modified Rho may inhibit all PRK-PtdIns(4,5)P_2 interactions. For this to be inhibitory would require the Rho to dislocate the kinase from its substrate. This will be discussed further in section 7.3.

Taken together the data presented above suggests that Rho is unable to stimulate either the phosphorylation or kinase activity of PRK *in vitro*. And, while PtdIns(4,5)P_2 is able to enhance PRK phosphorylation of exogenous substrate it does not alter the phosphorylation state of the kinase as evidenced by autophosphorylation. It may either be the case that the majority of the kinase is already in a fully active form or that the purification of PRK away from another species necessary for phosphorylation and activation results in the observed lack of response. MBP has been shown to bind to detergents and phopholipid micelles through hydrophobic and electrostatic interactions (Boggs, *et al.*, 1981,

Burns, *et al.*, 1981, Palmer and Dawson, 1969). The lipid may therefore merely act as a localisation signal; increasing the relative concentration of kinase and substrate on the two-dimensional surface of the mixed micelle so causing the observed increased in activity. In order to address these points the effect of Rho on PRK phosphorylation *in vivo* was investigated.

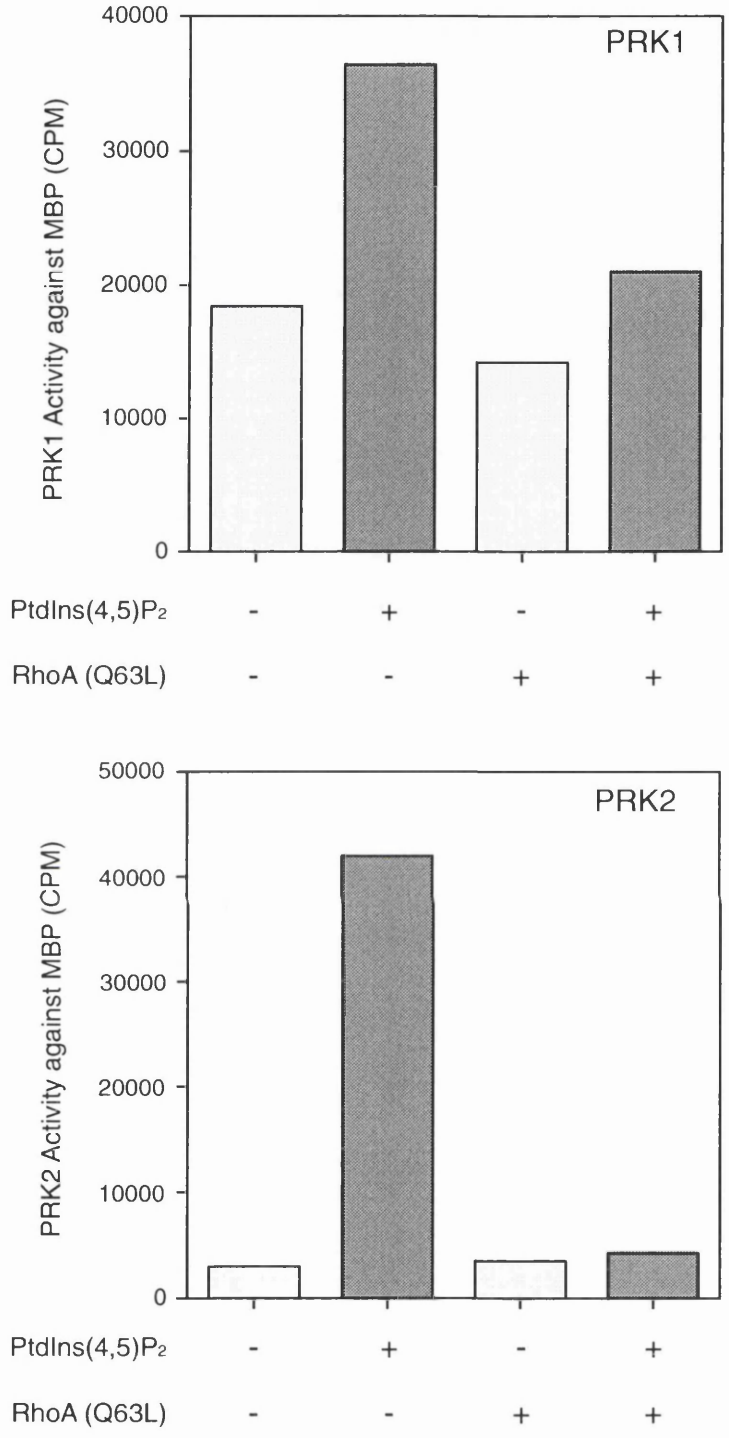

Fig. 5.2.7: Effect of PtdIns(4,5)P_2 and RhoA(Q63L) on PRK kinase activity against Exogenous Substrate Myelin Basic Protein (MBP) *in vitro*.

Kinase assays were carried out as described (5.2.7) in the presence of 10 mol% PtdIns(4,5)P_2 and/or RhoA(Q63L) as indicated. Reactions were terminated by spotting on P81 paper (Whatman) and washing in 30% acetic acid. MBP phosphorylation was detected by Cerenkov counting and values are corrected for MBP-alone control.

5.2.7 Co-expression of GTPase-Deficient Rho Proteins with PRK results in an Increased Autophosphorylation *in vitro.*

In order to assess whether other cellular elements are required to synergise with Rho and possibly lipids in the activation of PRK, co-expression experiments were carried out. Once again the Calcium phosphate precipitation method was used to transiently transfect 293 cells with HA-tagged PRK2 and either the GTPase deficent mutants RhoA(Q63L) and RhoB(Q63L) alone or a three-way transfection with the *Clostridium* toxin C3. Protein expression was as described in 2.2.16 and PRK proteins were immunoprecipitated as previously described (2.2.19) using the anti-HA polyclonal antibody (Santa Cruz). The immunopurified proteins on protein-G Sepharose were washed into kinase buffer F and 10µl of each was incubated in a 40µl reaction with 100µM ATP + 10µCi [γ^{32}P]ATP for 20 minutes at 30°C. The reactions were terminated by the addition of 20µl Laemmli 4X sample buffer and heating to 95°C. Samples were fractionated on a 10% SDS-PAGE and the ^{32}P incorporation into the PRK was assessed by autoradiography. The signals produced were analysed using NIH Image™ software to give the histogram displayed in figure 5.2.8. It can be seen that while the PRK protein yields from the various plates are equivalent, the autokinase activities differ substantially: both RhoA(Q63L) and RhoB(Q63L) coexpression results in a 9 and 4-fold increase in activity respectively and the expression of C3 toxin results in a partial inhibition of the RhoA-dependent response. The observed differences in activation with the different Rho proteins may be due to dosage, but the lack of effect of C3 on the RhoB-dependent increase is unclear. The rate of expression of the various constructs may afford an explaination. It would therefore seem that Rho is able to produce a significant activation of PRK autokinase activity when present as a pre-treatment within the cellular environment but is unable to support a similar response when presented *in vitro*.

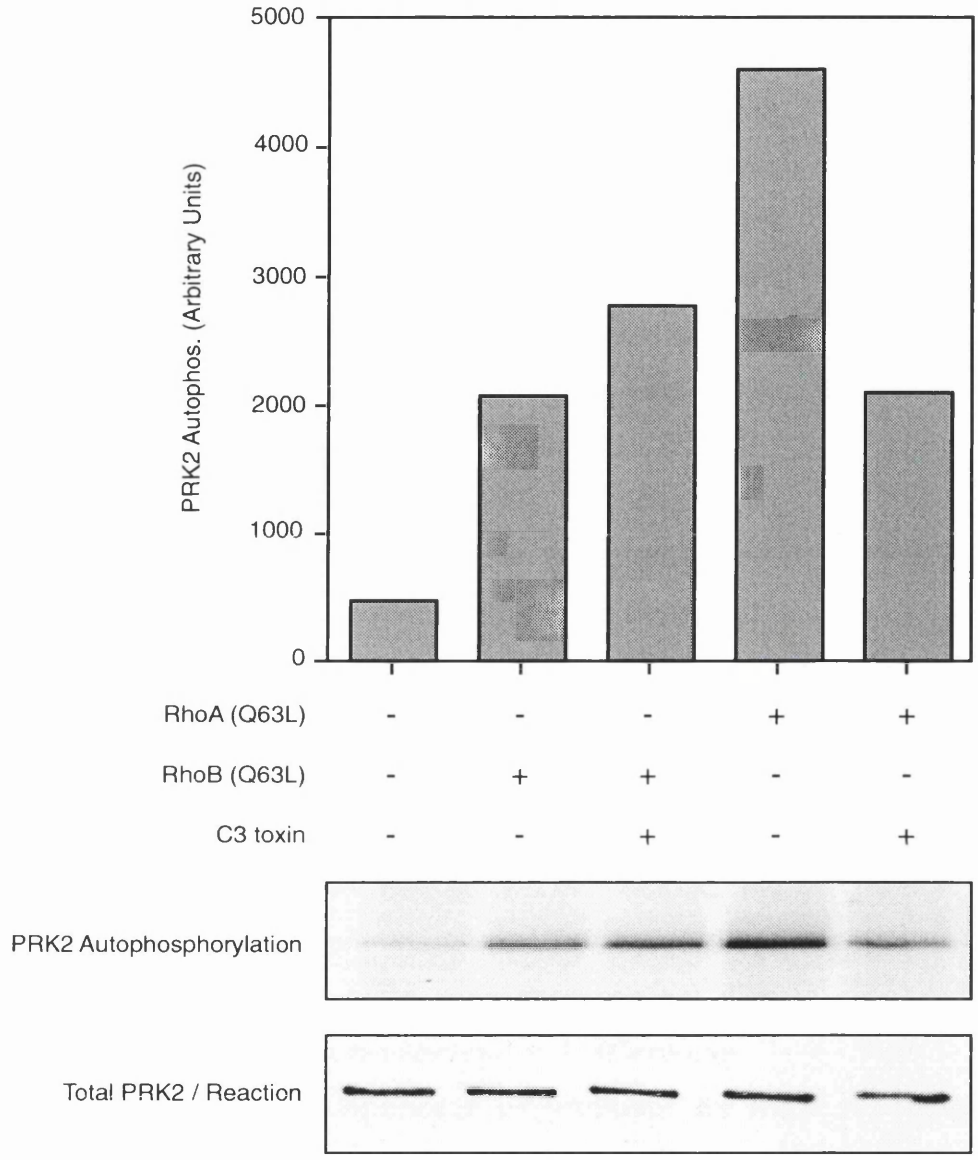

Fig. 5.2.8: The Effect of GTPase-deficient Rho or *Clostridium* C3 Toxin Co-expression on PRK Autokinase Activity *in vitro*.

293 cells were transfected with HA-tagged PRK2 and either a vector control (pcDNA3), GTPase-deficient Rho mutants or the Rho-inactivating C3 toxin as indicated. Immunopurified PRK proteins were then assessed for autokinase activity by incubation with Mg^{2+}/ATP. Reactions were terminated by addition of Laemmeli 4X sample buffer and samples were fractionated on SDS-PAGE. Phosphate incorporation into PRK was assessed by autoradiography as shown in the lower panels and NIH Image™ was used to generate the histogram display.

5.2.8 Rho Co-expression with PRK Results in *in vivo* Phosphorylation Changes.

The RhoB interaction with PRK has been shown to cause translocation of the kinase to a membrane compartment an event which is associated with the accumulation of a slower migrating form of the kinase on SDS-PAGE (Mellor, *et al.*, 1998). It was of interest, therefore, to find out whether the observed Rho-dependent increase in autokinase activity was associated with an *in vivo* phosphorylation change. ^{32}P orthophosphate was used to *in vivo* label plates of 293 cells transfected with PRK2 and either RhoA(Q63L) or C3 toxin. The procedure was carried out as described in 2.2.20 and the PRK was immunoprecipitated as for 5.2.7. The phosphate incorporation into the immunopurified PRK2 can be seen as an autoradiograph in figure 5.2.9, where the signal follows the same pattern as the yield of protein; there was less PRK2 recovered from cells co-expressing RhoA(Q63L) which was due to some cell loss. The acrylamide gel segments containing the radiolabelled PRK2 were cut from the SDS-PAGE and subjected to tryptic digest as outlined in 2.2.21. $1x10^3$ cpm of the resulting phospho-peptides were spotted onto thin-layer chromatography plates, separated by two dimensional electrophoresis and the resulting peptide spots were visualised by autoradiography. Figure 5.2.10 displays the distributions of the phosphopeptides along with a schematic representation dipicting the similarities and differences between the samples. Over the course of three independent experiments the PRK2-alone and PRK2 with C3 toxin samples produced an almost identical pattern whereas the PRK which had been co-expressed with RhoA(Q63L) produced a consistently different staining pattern: the spot marked (1) in the schematic is approximately 50% less intense in the RhoA sample as in the other two and the two spots marked (2) appear only to be present in the case of PRK2 co-expressed with RhoA.

The identification of the relative tryptic peptides by analysis on a LaserMat™ (Finnigan) were persistently hampered by technical problems with a reverse-

phase HPLC step. However, the two dimensional plots alone demonstrated that Rho is able to produce phosphorylation changes in PRK *in vivo* . This posed the question of whether such a phosphorylation event was responsible for activating the PRK, resulting in the observed increase in autokinase activity in vitro? Another question was whether the phosphorylation event was a result of autokinase activity or the action of a PRK-kinase?

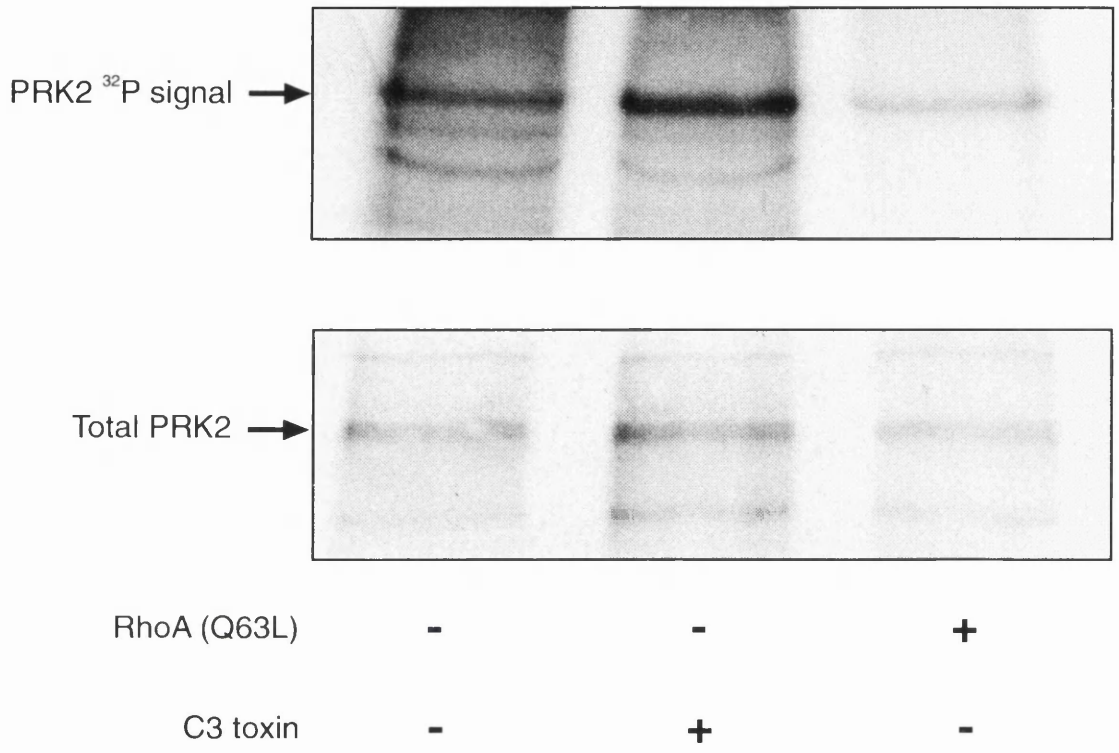

Fig. 5.2.9: ^{32}P Orthophosphate Incorporation into PRK2 after *in vivo* Labelling
293 cells transiently transfected with HA-tagged PRK2 and either RhoA (Q63L) or C3 toxin were incubated in phosphate-free medium for 20 minutes prior to the addition of 3.3µci ^{32}P orthophosphate per plate. After a 6 hour incubation PRK proteins were immunopurified, fractionated on SDS-PAGE and phosphate incorporation was assessed by autoradiography (upper panel). The relative PRK2 yield from the three plates was assessed by western blot using the HA-polyclonal (Santa Cruz Biotech.) (lower panel).

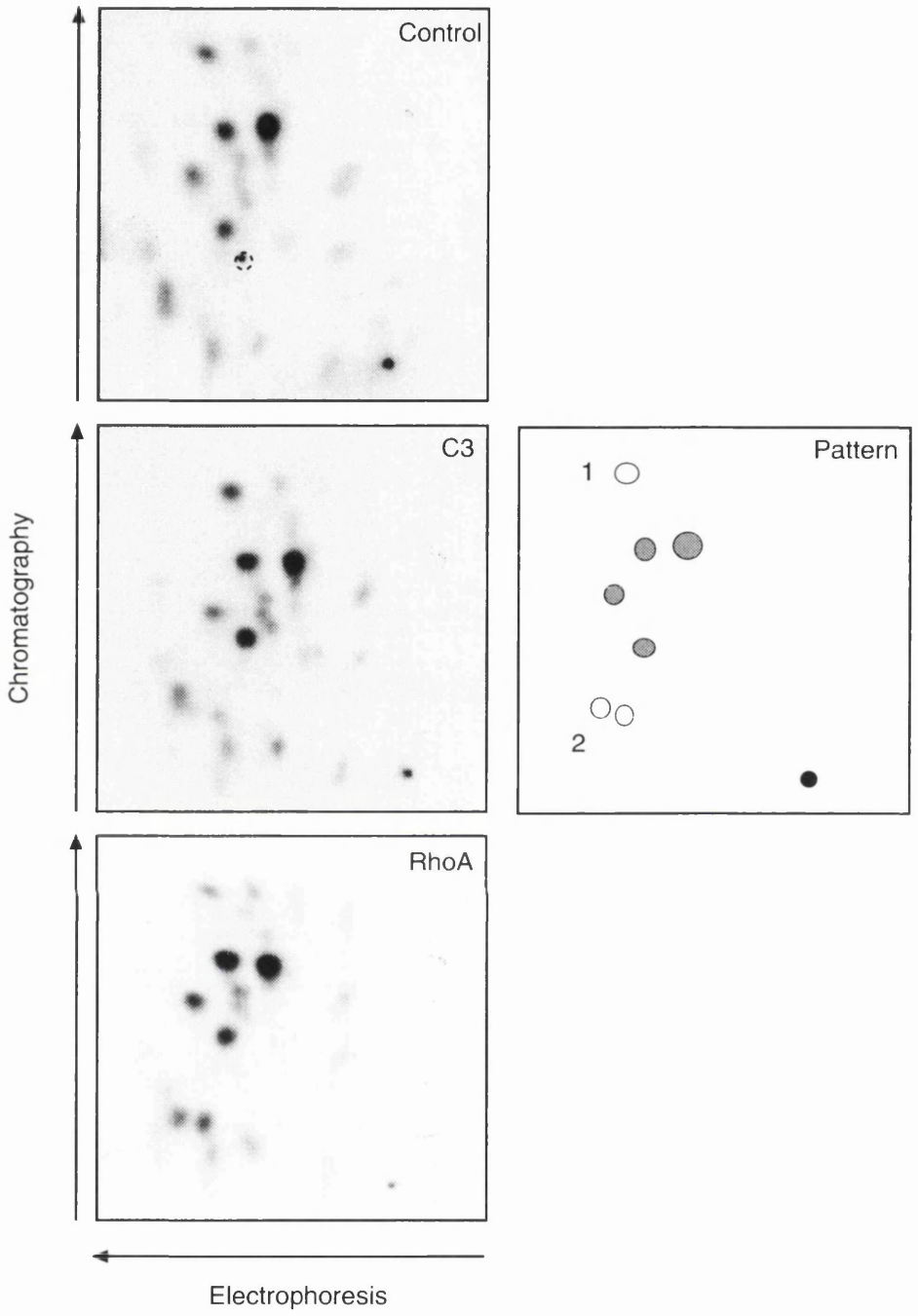

Fig. 5.2.10: Two-Dimensional Electrophoresis analysis of *in vivo* labelled PRK2

Digestion of the PRK2 with trypsin and subsequent two-dimensional electrophoresis was completed as described (2.2.20) with 1000 cpm per map. Maps for PRK2 co-transfected with either vector control, C3 toxin or RhoA are shown with a schematic representation where black filled circle denotes the origin; grey filled circles denote unchanging phospho-peptides and the open circles 1 (single) and 2 (double) denote phospho-peptides that change on RhoA (Q63L) co-expression. Note the relative decrease in signal 1 and the appearance of signals at 2. Broken circle in control panel marks a background spot from the autoradiography cassette.

5.2.9 PDK1 Co-Expression Results in an Increase of the Autokinase Activity of PRK.

As described in greater detail in the next chapter, the 3-Phosphoinositide-Dependent Kinase (PDK1) was purified as an activity against PKB and is seen to specifically phosphorylate and activate this kinase in a PtdIns(3,4,5)P_3 dependent manner (Alessi, *et al.*, 1997b). It was therefore of interest to investigate whether the *in vivo* PRK2 phosphorylation event seen to be Rho-dependent was also dependent on a known AGC-family kinase. The experiment described in 5.2.7 was repeated: HA-tagged PRK2 was co-expressed with either RhoA(Q63L) or Myc-PDK1. The PRK2 was immunoprecipitated and incubated with Mg^{2+}/ATP as previously described. The resulting *in vitro* autokinase activity was assessed by autoradiography as shown in figure 5.2.11. The co-expression of PRK2 with a GTPase-deficient Rho resulted in an increased autokinase activity as expected. Interestingly, the co-expression of the wildtype PDK1 also led to an increased PRK autokinase activity (two fold increase).

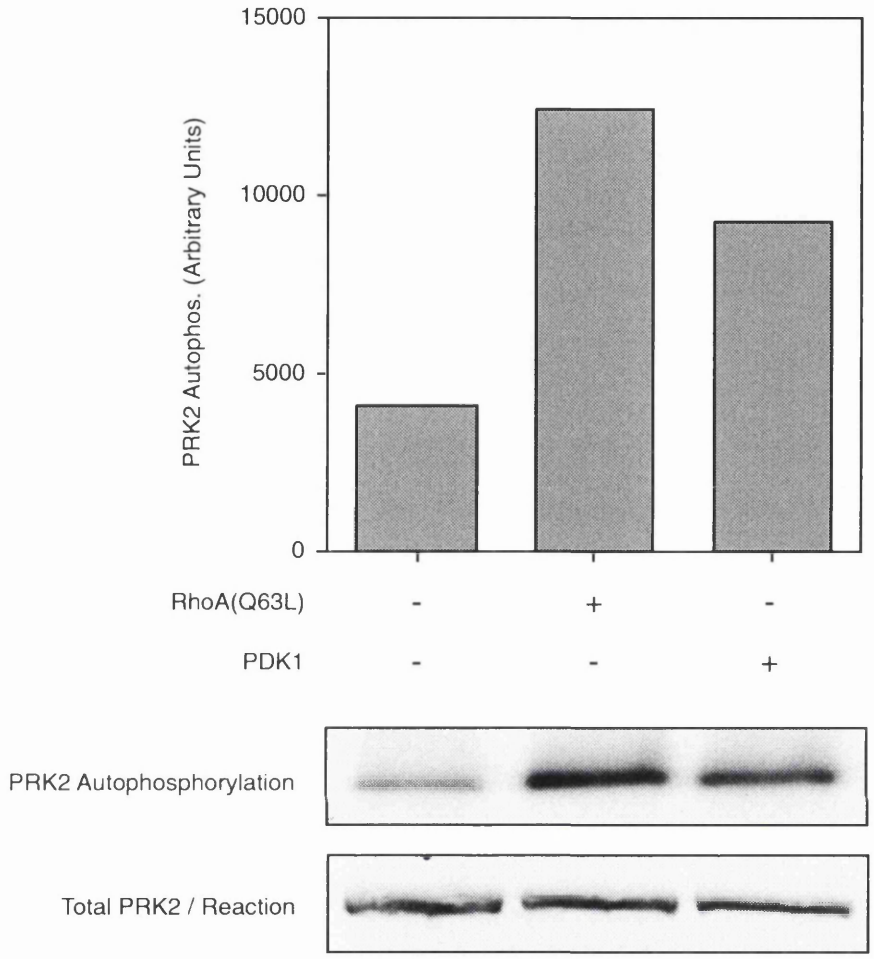

Fig. 5.2.11: Effect of PDK1 Co-expression on PRK2 Autokinase Activity *in vitro.*
PDK1 (Glu-Glu tagged) or RhoA (Q63L) were co-expressed with HA-tagged PRK2 in 293 cells. Immunopurified PRK2 was assessed for autokinase activity by incubation with Mg^{2+}/ATP for 20 minutes at 30°C. Phosphate incorporation was observed by autoradiography (lower panel) followed by analysis using NIH Image™.

5.3 Chapter Discussion

Within this chapter both purified and immunoprecipitated PRK have been shown to have an *in vitro* kinase activity against exogenous substrate MBP. This activity was enhanced by phospholipids displayed in Triton X100 micelles but was unaffected by the addition of either bacterially or mammalian expressed Rho.GTP. Further, the presence of modified Rho inhibited the lipid-dependent activation. The inhibition of PRK kinase activity on phosphatase treatment suggests that phosphorylation events can be activating, but neither the lipids or Rho are able to alter the phosphorylation state of PRK *in vitro*. However, the *in vitro* autokinase activity was significantly enhanced when PRK was immunoprecipitated from cells overexpressing GTPase deficient RhoA or RhoB, suggesting an *in vivo* Rho-dependent process was activating the kinase. Further, Rho overexpression was shown to produce specific phosphorylation events on the kinase. Although these *in vivo* events have not been directly associated with the *in vitro* autokinase activity it would seem likely that cellular elements other than Rho and lipid are responsible for the activation of PRK. To this end it was shown that the AGC-specific kinase PDK1 was able produce a PRK protein with increased autokinase activity when the two kinases were co-expressed.

These observations are different from those seen in previous studies (Amano, *et al.*, 1996b, Vincent and Settleman, 1997, Watanabe, *et al.*, 1996). The reasons for these potential differences will be discussed at length in chapter 7. The observed effect of Rho on the phosphorylation state of PRK does fit with the proposed model of an amino terminal pseudosubstrate inhibition (Kitagawa, *et al.*, 1996). However, it would seem that the simple release of this autoinhibition by a Rho interaction is not the only process required for kinase activation. Some form of priming event may be required before both auto and trans-phosphorylation can take place. PRK's *in vitro* activation by phospholipid shows no particular specificity suggesting that this may not be the *in vivo* priming event

required. A specific phosphorylation event by an activating kinase would however follow with the observations of this chapter. This possibility is looked at in greater detail in chapter 6. Figure 5.3. dipicts a potential model for Rho involvement in PRK phosphorylation and activation.

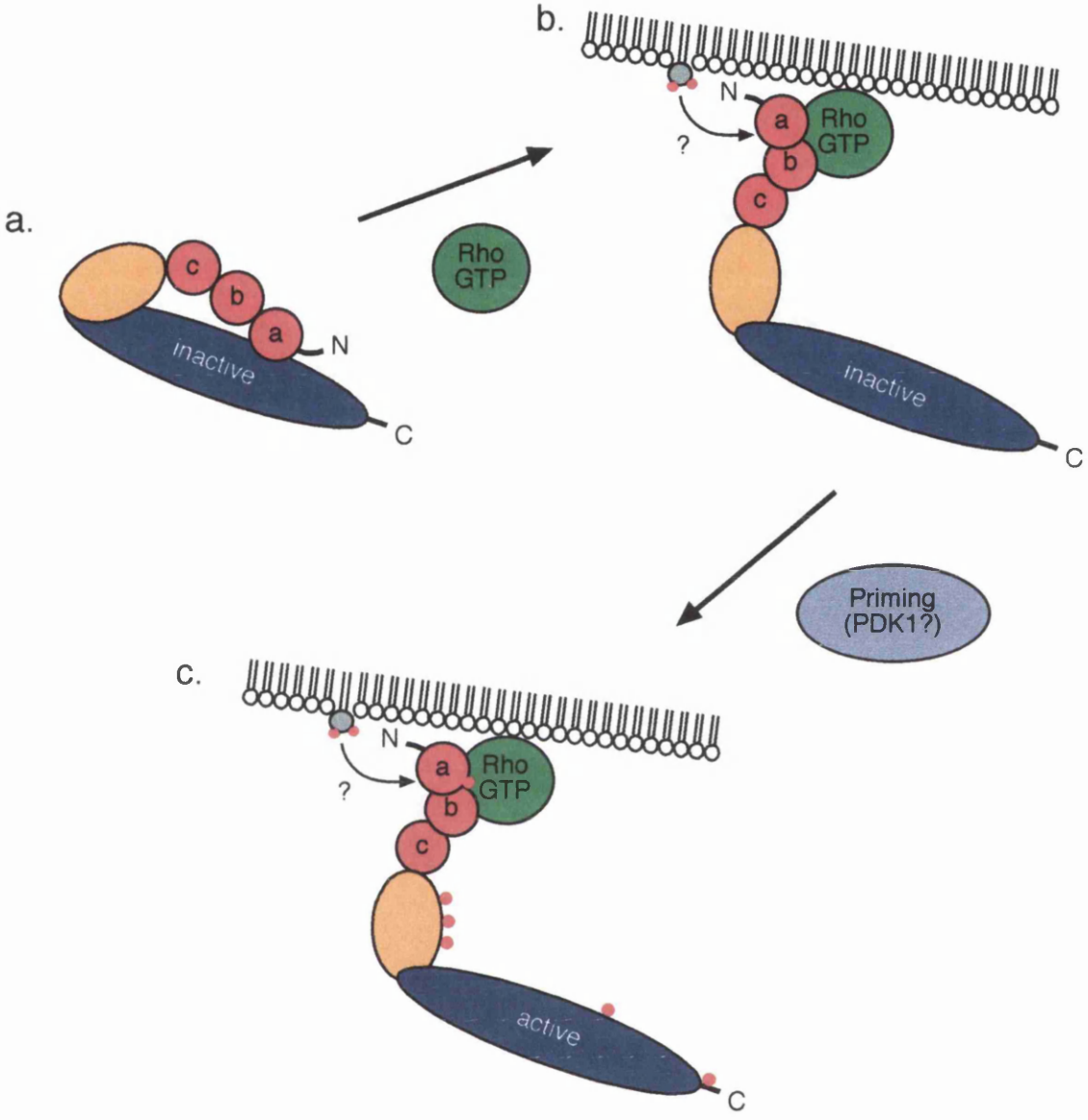

Fig. 5.3: Model Depicting the Proposed Role of Rho in PRK Phosphorylation and Activation.

a.) the cytoplasmic inactive form of PRK with the pseudosubstrate site within the HR1a region (red) buried in the activation loop of the kinase domain (blue). b.) the interaction with the Rho.GTP (green) results in both the kinase translocating to a membrane compartment and the disruption of the inhibitory intramolecular interaction. There may be an *in vivo* input from phospholipids as denoted by the question mark. The kinase is however still inactive. c.) a priming event which may be phosphorylation by a kinase such as PDK1 results in a PRK capable of autophosphorylation leading to full activation. Phosphate groups are shown as small red circles.

Chapter 6 - 3-Phosphoinositide Dependent Kinase (PDK1) Phosphorylates and Activates PRK.

6.1 Introduction

As described in chapter 1, the AGC kinase family members contain conserved serine and threonine residues which undergo either trans or auto-phosphorylation. The high level of homology between these kinases, including the PRKs (see figure 6.1) signifies that common regulatory mechanisms may exist. The activation loop threonine, which is located between subdomains VII and VIII of the kinase domain, is known to be transphosphorylated by another kinase for PKC (Cazaubon and Parker, 1993, Keranen, *et al.*, 1995) and this phosphorylation event is critical for the full activation of the kinase (Cazaubon and Parker, 1993). Other key phosphorylation events include the C-terminal 'FSY' site (S473 in PKBα and S657 in PKCα) which again is required for full activation of the respective kinases. Until recently the question of whether this site is trans or auto-phosphorylated for PKC has been a subject of debate. Interestingly the equivalent residue is acidic (Glu or Asp) in both the atypical PKCs and the PRKs. A third residue in this C-terminal region which is thought to be an autophosphorylation site (T638 in PKCα) (Keranen, *et al.*, 1995) may serve to control the kinase activity by regulating its inactivation (Bornancin and Parker, 1996).

The purification and characterisation of PDK1 as the PKB activation loop (threonine 308) kinase was described during the course of this thesis (Alessi, *et al.*, 1997b, Stephens, *et al.*, 1998). While providing an obvious incite into PKB activation in response to growth factor and insulin stimulation it also offered a common regulatory mechanism for other AGC-family kinases. In chapter 5 it was observed that the co-expression of PDK1 with PRK2 resulted in the latter

having an increased autokinase activity *in vitro* after immunoprecipitation. In this chapter the role of PDK1 as a potential activating kinase of the PRKs is investigated both *in vitro* and *in vivo*. The association between PDK1 and Rho-dependent events is also established.

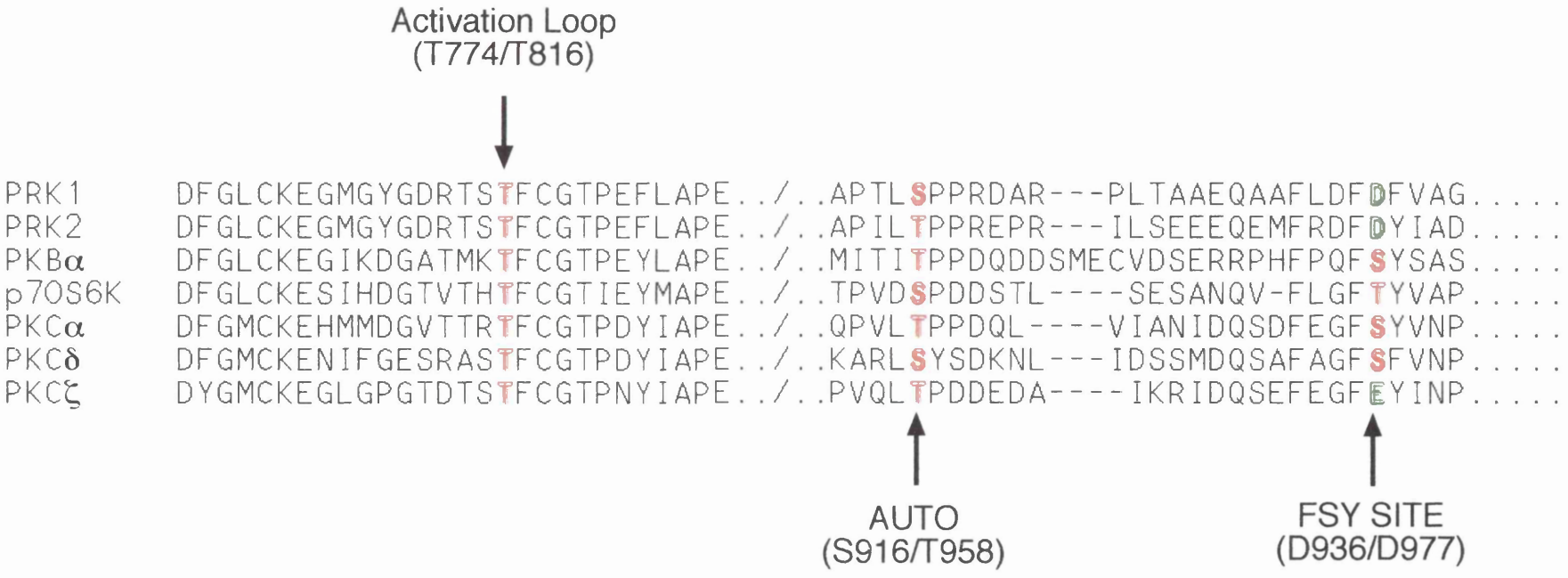

Fig. 6.1: Amino Acid Sequence Alignment of the Activation Loop and C-Terminus of AGC Kinase Family Members.

Alignment of regions from PRK1, PRK2, PKBα, p70S6kinase and the PKCs α, δ and ζ. The three serine and threonine residues, phosphorylation of which is thought to play a key role in the regulation of catalytic activity, are shown as coloured. The three residues are termed *Activation Loop* for the threonine between subdomains VII and VIII, *Auto* for the proposed autophosphorylation site and *FSY* for the C-terminal residue. The positions of the residues for PRK1 and PRK2 are shown in brackets.

6.2 Results

6.2.1 Subcloning of GST-PRK1kin

In order to preclude any dependence on a Rho GTPase or the prephosphorylation of PRK for the PDK1 phosphorylation of PRK *in vitro,* the PRK1 kinase domain was initially expressed in *E.coli* as a GST-fusion protein, GST-PRK1kin. The PRK1 kinase domain (amino acids 602-942) was amplified using the polymerase chain reaction (PCR) with the primers listed in the appendix. This produced a blunt-ended fragment with 5' BamH1 and 3' Not1 sites which was subsequently ligated into pBluescript SKII (Stratagene) that had been predigested with EcoRV. Ligations were used to transform DH5α E.coli (Gibco) and blue/white colony selection was used to identify positive clones. The kinase domain fragment was then digested out of the pBluescript with BamH1 and Not1 and religated into the GST-fusion expression plasmid pGEX4T1 (Pharmacia) which had been predigested with the same enzymes. Ligations were once again used to transform DH5α E.coli and positive colonies were detected by growth on antibiotics. The construct was sequenced and subsequently used for the expression of the PRK1 kinase domain with an amino-terminal GST-fusion tag.

6.2.2 Expression and Purification of GST-PRK1kin

The GST-PRK1kin was expressed in a BL21 GroES/EL strain of E.coli as described in 2.2.9. The induction time was 3 hours at 30°C with 0.3mM IPTG. The purification procedure was as described in 2.2.11 and as can be seen from figure 6.2.1 while a large percentage of the expressed protein was in an insoluble fraction enough was purified for subsequent studies. The final pure

GST-PRK1kin was seen to be homogeneous by coomassie stain, however on western analysis using both amino and carboxy-terminal specific antibodies (anti-GST (Santa Cruz) and Anti-PRK1$_{COOH}$ (ICRF)) a degree of degradation of the protein from the C-terminus was seen. This degradation was not continued during storage of the pure protein as judged by re-western. The purified protein was kept at a concentration of 0.1mg/ml in buffer A, snap frozen in liquid nitrogen and stored at -70°C.

6.2.3 Purification of PRK1/PRK2 Phospho-Specific Activation Loop Threonine Polyclonal Antibody.

The PRK specificity of an immune-serum generated from the immunisation of rabbits with a phosphorylated 7 amino acid peptide covering the PRK activation loop was tested for by western blot. As can be seen from the first panel in section B of figure 6.2.2, while the whole serum used at a concentration of 1/1000 in TBS 0.1% (v/v) Tween 20 0.5% (w/v) milk produce signals for both endogenous PRK1 and PRK2, many other non-specific bands were also detected. The aim was to use this tool to specifically look at the phosphorylation state of endogenous PRK, therefore a purification protocol was refined to that presented in figure 2.3.1. The purified phospho-specific antibody was step eluted from the acti-gel column with low pH to give the protein elution profile seen in panel A of figure 6.2.2. The peak fractions (~0.1 mg/ml) were pooled and used in the western analysis of whole 293 cell lysates. On comparison with the previous westerns it could be seen that the purified antibody was absolutely specific for PRK1 and PRK2 and later experiments showed it to be specific for the phosphorylated form of the enzymes (phosphate groups on T774 and T816 of PRK1 and PRK2 respectively).

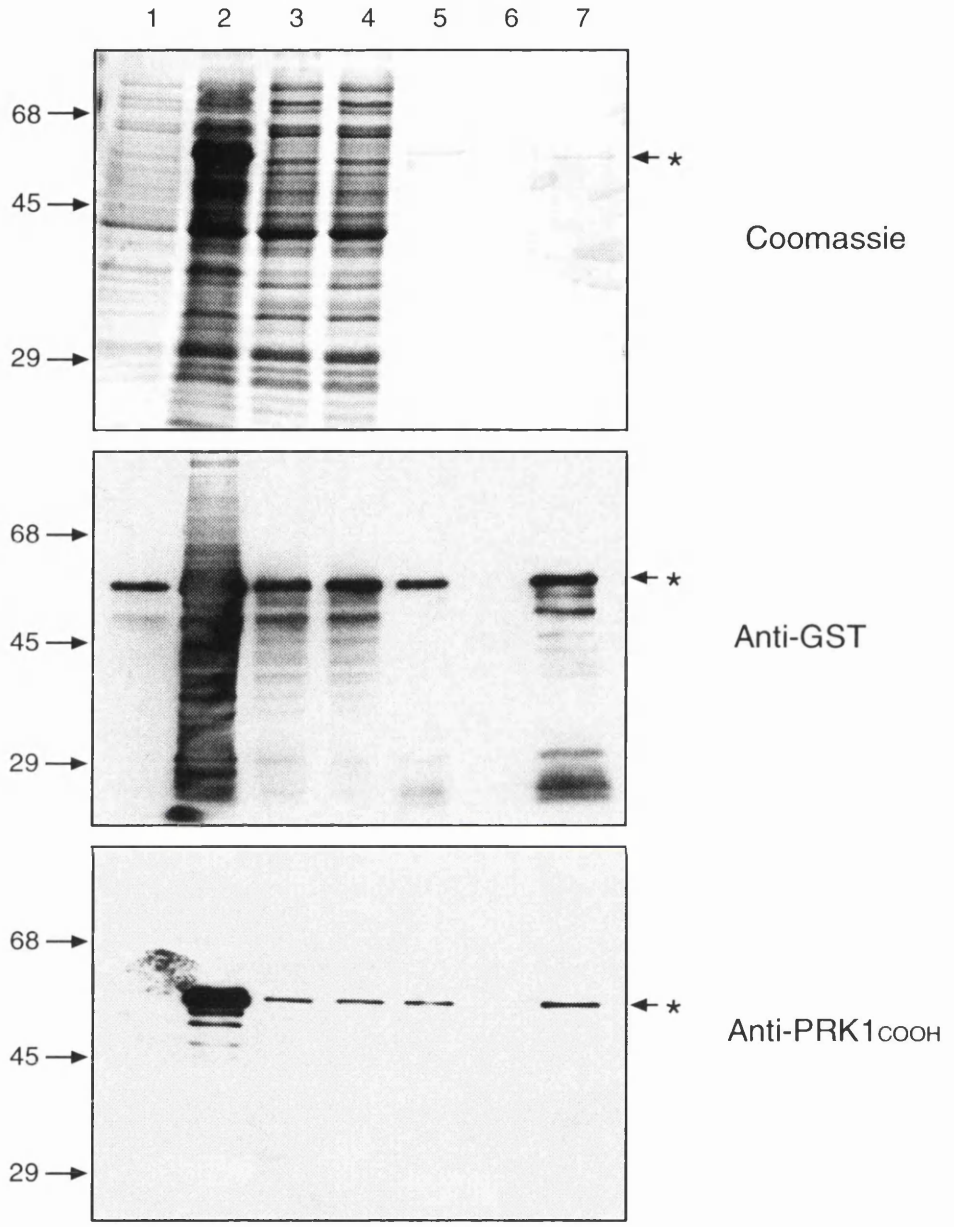

Fig. 6.2.1: Coomassie and Western Analysis of the Purification of GST-PRK1kin from *E. coli.*

A fragment of the PRK1 protein (amino acids 602-942) was expressed as a GST-fusion in *E. coli*, GST-PRK1kin. The purification profile displays: 1) Whole cell lysate prior to IPTG induction; 2) Whole cell lysate after 3 hour induction; 3) soluble fraction of lysate; 4) soluble fraction after incubation with glutathione Sepharose; 5) washed Sepharose (20µl 40% slurry); 6) washed Sepharose after 50mM glutathione elution; 7) final eluted GST-PRK1kin. The three panels indicate 10% SDS-PAGE either coomassie stained or western blots using the anti-GST polyclonal (Santa Cruz Biotech.) or the anti PRK1 carboxy-terminal polyclonal (anti-PRK1$_{COOH}$) as indicated.

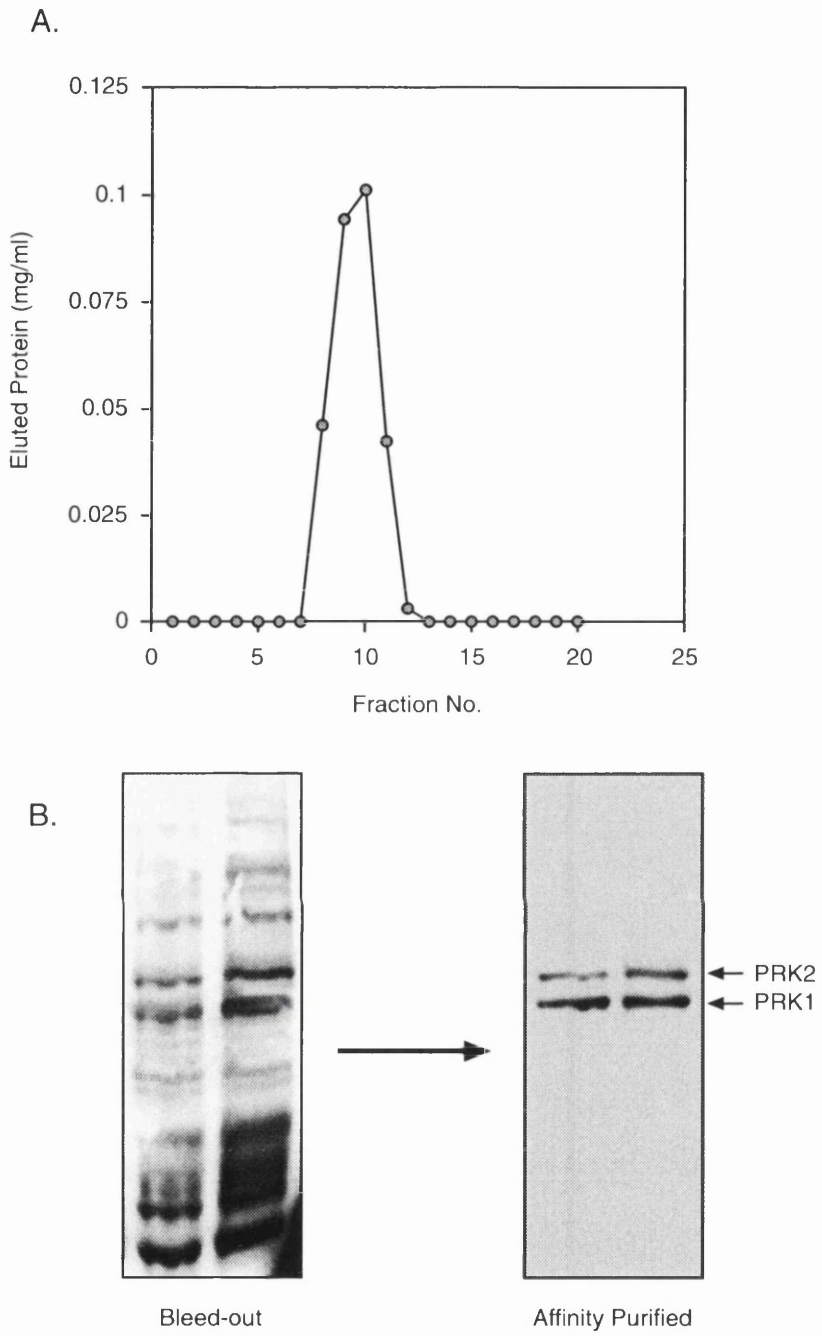

Fig. 6.2.2: Purification of the PRK1 / PRK2 Phospho-specific Activation Loop Threonine Polyclonal Immune-Serum.

The immune-serum generated from rabbits immunised with a phosphorylated peptide was tested for specificity in western blot against endogenous PRK1 and PRK2 in whole cell lysates from 293 cells. The resulting ECL signal (marked Bleed-out) was then compared with that produced in the same conditions but using affinity purified polyclonal (see section 2.3.6). A) the profile from a step elution of the purified polyclonal from a phospho-specific peptide acti-gel column in 100mM glycine pH2.0; B) western analysis of endogenous PRK1 and PRK2 using the immune-serum before and after the purification procedure.

6.2.4 PDK1 Phosphorylates GST-PRK1kin *in vitro* at T774.

The purified GST-PRK1kin was incubated in a 40µl reaction at a concentration of 35nM with 10mM $MgCl_2$, 100µM ATP and in the presence or absence of 12nM GST-PDK1 (provided by D. Alessi). The reactions took place at 30°C and were terminated at 0, 1, 5, 10, 20, 40 minute time points by the addition of 20µl Laemmli 4X sample buffer. The samples were fractionated on a 10% SDS-PAGE, transferred to nitrocellulose and blotted with the purified phospho-specific activation loop antibody at a concentration of 0.1µg/ml. The resulting western blot can be seen in figure 6.2.3. along with a graphical representation of the T774 site phosphorylation (NIH Image™). While the PRK incubated alone in the kinase reaction buffer gives no signal for T774 phosphorylation, in the presence of 12nM PDK1 a time dependent phosphorylation of T774 was seen. Thus PDK1 is capable of specifically phosphorylating PRK1 within its activation loop.

6.2.5 The Lipid Dependent Activity of GST-PDK1 Against MBP *in vitro* is Inhibited by Triton X100.

The possible role of lipids in the direct regulation of PDK1 activity *in vitro* and the effect of Triton X100 was assessed. In a 40µl kinase reaction 12nM GST-PDK1 was incubated with 5µg MBP with no lipids or in the presence of either mixed vesicles of phosphatidylserine (PS) and phosphatidylcholine (PC) with or without PtdIns(3,4,5)P_3. The mixed lipid vesicles were made up as described in 2.2.22 with 100µM PS and PC and 10µM PtdIns(3,4,5)P_3. Reactions were for 20 minutes at 30°C and $\gamma^{32}P$ incorporation into the MBP was assessed by Cerenkov counting of samples spotted onto P81 (Whatman) paper. As can be seen from figure 6.2.4 (0% Triton X100) the PDK1 activity against MBP was enhanced 3 fold in the presence of PS/PC vesicles and 6 fold when the same

vesicles contained 10μM PtdIns(3,4,5)P_3. Thus it would seem that the *in vitro* activity of PDK1 is stimulated by lipid although whether this is due to a disruption of and inhibitory intramolecular PDK1 interaction or the increased concentration of PDK1 and MBP on the surface of the lipid vesicle is uncertain. When the same reactions were completed in the presence of various concentrations of the non-ionic detergent Triton X100 the lipid stimulated activity of PDK1 was completely inhibited at concentrations as low as 0.2% (figure 6.2.4). A similar inhibition has been seen for PDK1's *in vitro* activity against PKB (Alessi, *et al.*, 1997b).

6.2.6 The *in vitro* Phosphorylation of PRK1 T774 by GST-PDK1 is PtdIns(3,4,5)P_3 Independent.

In order to assess any potentiation of the PDK1 phosphorylation of PRK in the presence of lipids an *in vitro* kinase assay was completed exactly as described in 6.2.4 with a reaction time of 20 minutes. As can be seen from figure 6.2.5 no significant increase in the overall phosphorylation of PRK was seen in the presence of either the PS/PC or PS/PC/PtdIns(3,4,5)P_3. As stated in chapter 5 a potential lipid binding site has been suggested in the amino-terminal region of PRK (Peng, *et al.*, 1996). It can therefore be concluded that the use of the truncated form of PRK1 precludes its vesicular localisation and direct input of lipids to its phosphorylation. Thus any increase in phosphorylation would be due to a lipid effect on the PDK1. The lack of any lipid dependent PDK1 activity suggests that the observed enhancement in the activity against MBP in the presence of PS/PC/PtdIns(3,4,5)P_3 is a result of both kinase and substrate being co-localised at the vesicle surface.

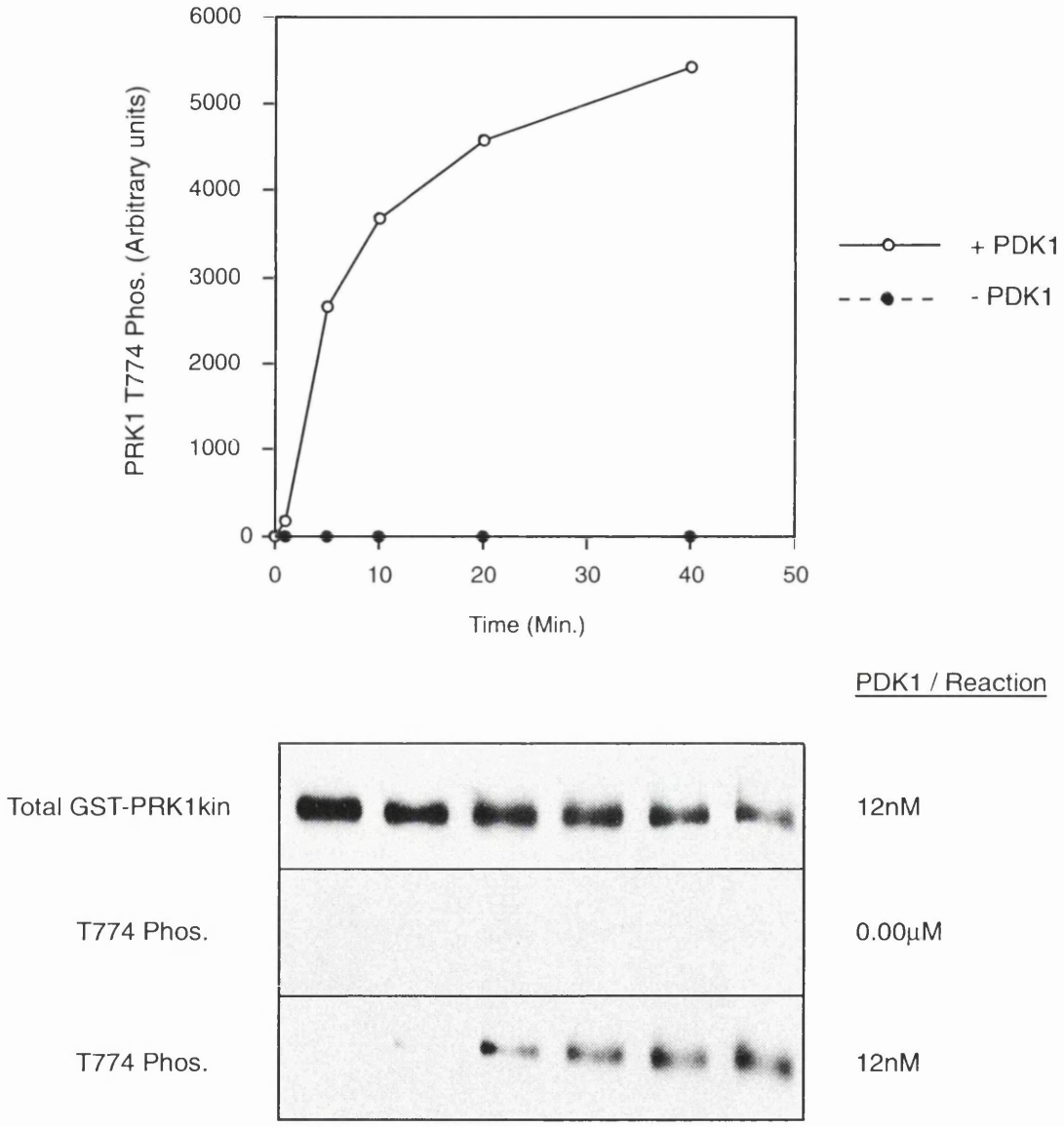

Fig. 6.2.3: GST-PRK1kin is specifically Phosphorylated by GST-PDK1 *in vitro.* Bacterially purified GST-PRK1kin (residues 602-942) incubated with 10mM Mg^{2+} and 100μM ATP for 0,1,5,10,20,40 minute time points at 30°C. The total GST-PRK1kin in each reaction assessed by western blot with anti-GST polyclonal (Santa Cruz Biotech.) is marked *total GST-PRK1kin.* The phosphate incorporation into T774 of GST-PRK1kin in the presence or absence of 12nM GST-PDK1 was assessed using a phospho-specific polyclonal; resulting signals seen as the panels marked *T774 phos.* and graphically in upper panel (westerns analysed using NIH Image™).

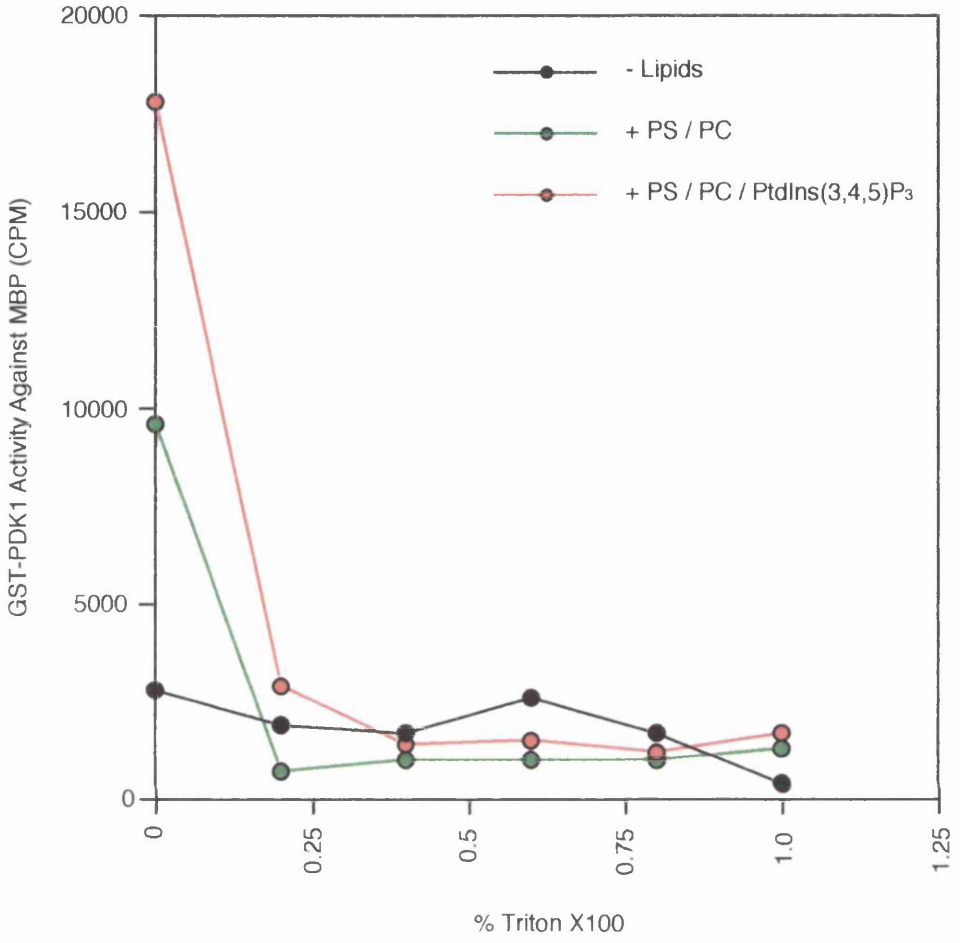

Fig. 6.2.4: GST-PDK1 *in vitro* Kinase Activity is Inhibited by Triton X100. The *in vitro* kinase activity of GST-PDK1 was assessed against MBP in the presence of 10mM Mg^{2+} and 100μM ATP and either with or without mixed lipid vesicles containing 100 μM PS, 100 μM PC +/- 10μM PtdIns(3,4,5)P_3 as indicated. The effect of increasing concentrations of the non-ionic detergent Triton X100 are shown. Values are the mean of duplicate assays.

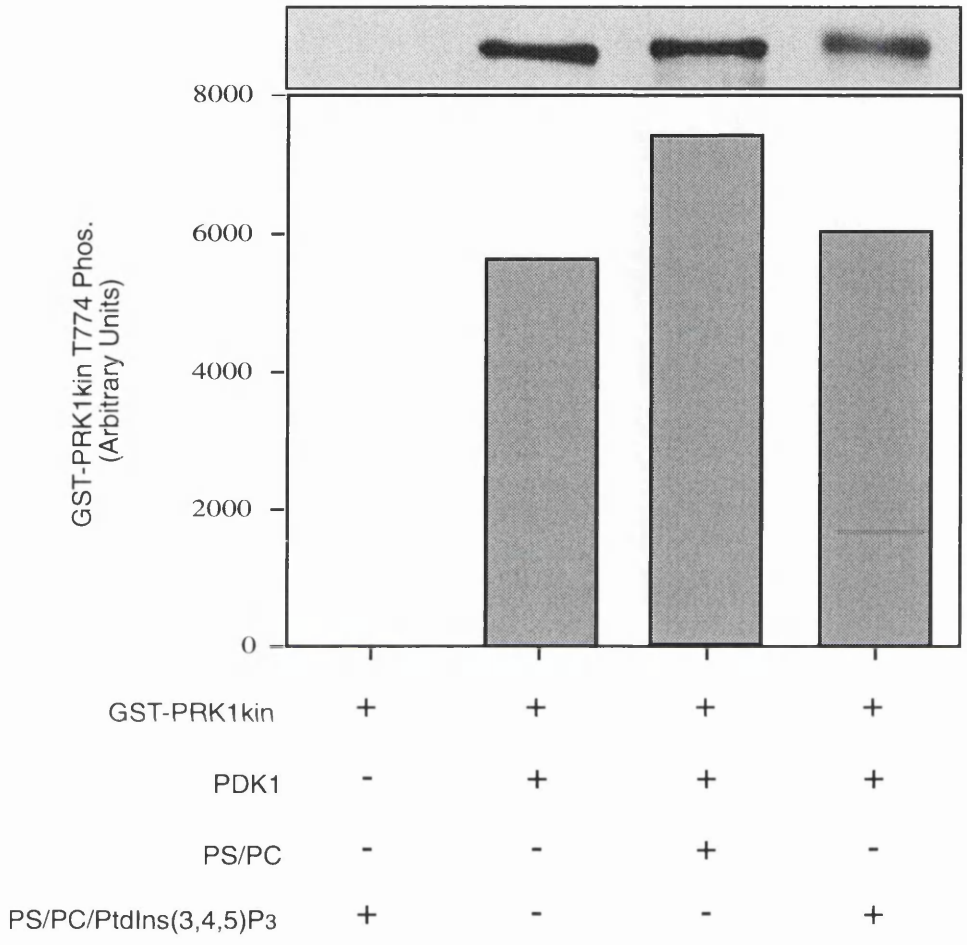

Fig. 6.2.5: The *in vitro* Phosphorylation of PRK1 T774 by GST-PDK1 is PtdIns(3,4,5)P_3 Independent.

Phosphorylation of GST-PRK1kin T774 assessed in the presence or absence of GST-PDK1 and mixed lipid vesicles containing PS/PC +/- PtdIns(3,4,5)P_3 (as indicated). Reactions were for 20 minutes and the resulting phosphorylation was determined using the phospho-specific polyclonal as for 6.2.4, with westerns analysed by NIH Image™.

6.2.7 T774 Phosphorylation is Associated with an Increased GST-PRK1kin activity.

Previous studies have indicated the activation loop threonine phosphorylation of AGC-family kinases to be an absolute requirement for activation (Cazaubon, *et al.*, 1994). The effect of the observed T774 phosphorylation of GST-PRK1kin by GST-PDK1 on the kinase activity against MBP was therefore assessed. A two step kinase assay was developed: stage 1 was the GST-PRK1kin phosphorylation by GST-PDK1 as described above (40 minutes at 30°C). Stage 2: 20µl buffer F containing 4% Triton X100, 0.5mg/ml MBP, 100µM ATP and 5µci [γ^{32}P]ATP / reaction was added to the reactions from stage 1 followed by a further 15 minute incubation at 30°C. Reactions were terminated by the addition of 20µl sample buffer and heating to 95°C prior to fractionation on 15% SDS-PAGE. The acrylamide gel was Coomassie stained, dried and the incorporation of ^{32}P into MBP was assessed by Cerenkov counting. As can be seen from figure 6.2.6 the T774 phosphorylation by GST-PDK1 for 40 minutes is associated with a >60-fold activation of GST-PRK1kin from a specific activity of <0.2 units/mg to >12.5 units/mg (where the specific activity is taken as nMol ^{32}P incorporated into MBP / minute / mg GST-PRK1kin). As expected the presence of PS/PC/PtdIns(3,4,5)P_3 mixed lipid vesicles throughout the two stages of the reaction had no effect on the kinase activity of the truncated PRK.

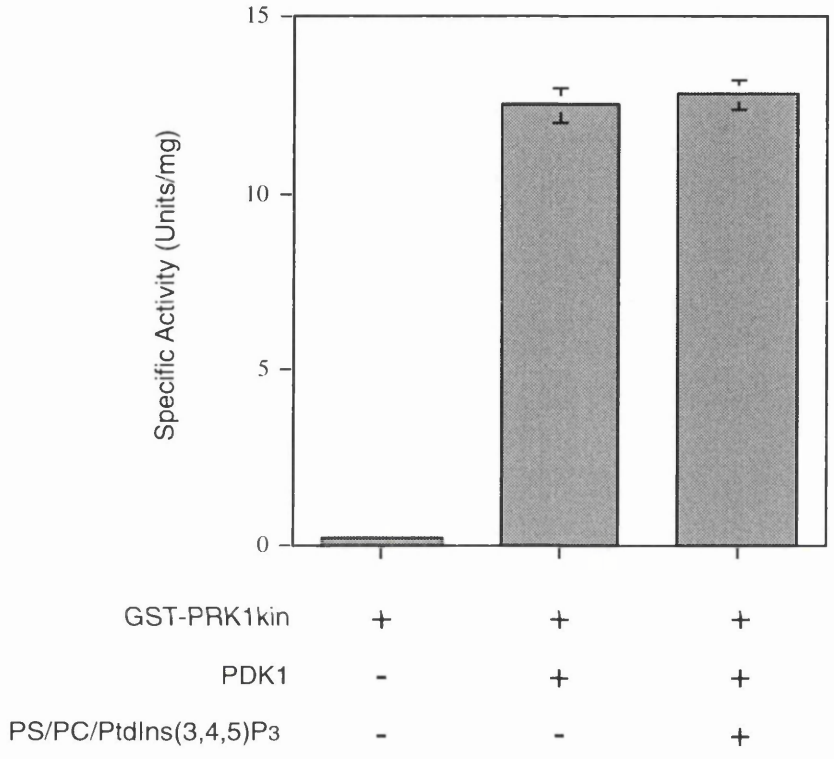

Fig. 6.2.6: GST-PRK1kin T774 Phosphorylation Results in an Increase of *in vitro* Kinase Activity Against MBP.

The affect of GST-PDK1-dependent phosphorylation of T774 on the specific activity (Units/mg) of GST-PRK1kin was assessed with a 2-stage reaction (see Materials and Methods) in the presence or absence of mixed lipid vesicles as indicated. Values are corrected for MBP phosphorylation by GST-PDK1 in the presence of PtdIns(3,4,5)P_3 (<0.7Units/mg). All values are representative of duplicate determinations from two independent experiments.

6.2.8 Phosphorylation of PRK1 at S916 is Independent of PDK1 Activity.

As shown on figure 6.1 the AGC kinase family have a serine or threonine residue in a conserved region near their carboxy-terminus which undergoes phosphorylation. This has been proposed as an autophosphorylation site for PKC family members (Flint, *et al.*, 1990, Keranen, *et al.*, 1995). Using an immune serum specific for the phophorylated form of PRK1 S916, the effect of PDK1 activity on the phosphorylation at this site was assessed by western blot. Kinase reactions identical to those described in 6.2.4 were carried out with a reaction time of 20 minutes and the relative phosphorylation of both the T774 and S916 was as shown in figure 6.2.7(A.). The T774 phosphoylation pattern was as expected for the various samples: no phosphorylation was seen in the absence of PDK1 and the phosphorylation in the presence of PDK1 was unaffected by PS/PC/PtdIns(3,4,5)P_3. However, the pattern of phosphorylation at S916 was suprising: the residue was phosphorylated in the absence of PDK1 and the signal did not increase with the addition of either PDK1 and lipids. Therefore the putative autophosphorylation event at S916 does not require the PRK1 to be pre-phosphorylated at T774.

On further investigation GST-PRK1kin gave a signal by western blot for S916 phosphorylation at time point '0' (figure 6.2.7(B.)) signifying possible autocatalytic activity when this construct is expressed in *E.coli*. Perhaps more intriguing is the observation of a mobility shift of the GST-PRK1kin on SDS-PAGE when a kinase assay is completed in the presence of 10-fold more GST-PDK1 (120nM). While a strong signal signifying T774 phosphorylation is seen immediately (note that time point '0' is likely to be 1-2 seconds) the shift consistently occurred between 5 and 10 minutes and the majority of the GST-PRK1kin was shifted (as judged by both T774 and total PRK signals) at 20 minutes. However, analysis of the S916 phosphorylation signal over the same assay, by stripping the blot of the previous antibody in 5% acetic acid and re-probing with the S916-specific immune serum, it was seen that the signal did

not shift and could be aligned with the faster migrating form of GST-PRK1kin. Therefore, while the T774 phosphorylation event does not result in a mobility shift of the truncated PRK1 the undefined events that do cause the shift may be dependent upon this phosphorylation. Further, the phosphorylation at S916 would seem to confer a non-shifting phenotype.

A.

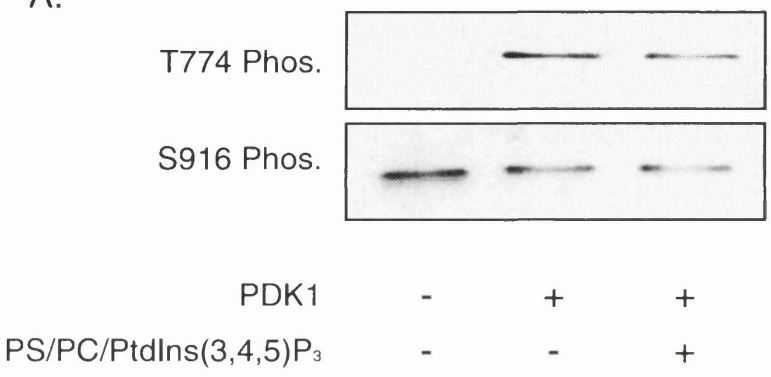

Fig. 6.2.7: The Phosphorylation Site S916 (PRK1) is Independent of PDK1 Activity.

A) The phosphorylation of S916 is independent of PDK1 activity: T774 and S916 phosphorylation was assessed by western analysis using phospho-specific polyclonal antibodies after 20 minutes incubation of GST-PRK1kin Mg^{2+}/ATP in the presence or absence of 12nM GST-PDK1 and PS/PC/PtdIns(3,4,5)P_3. B) See overleaf.

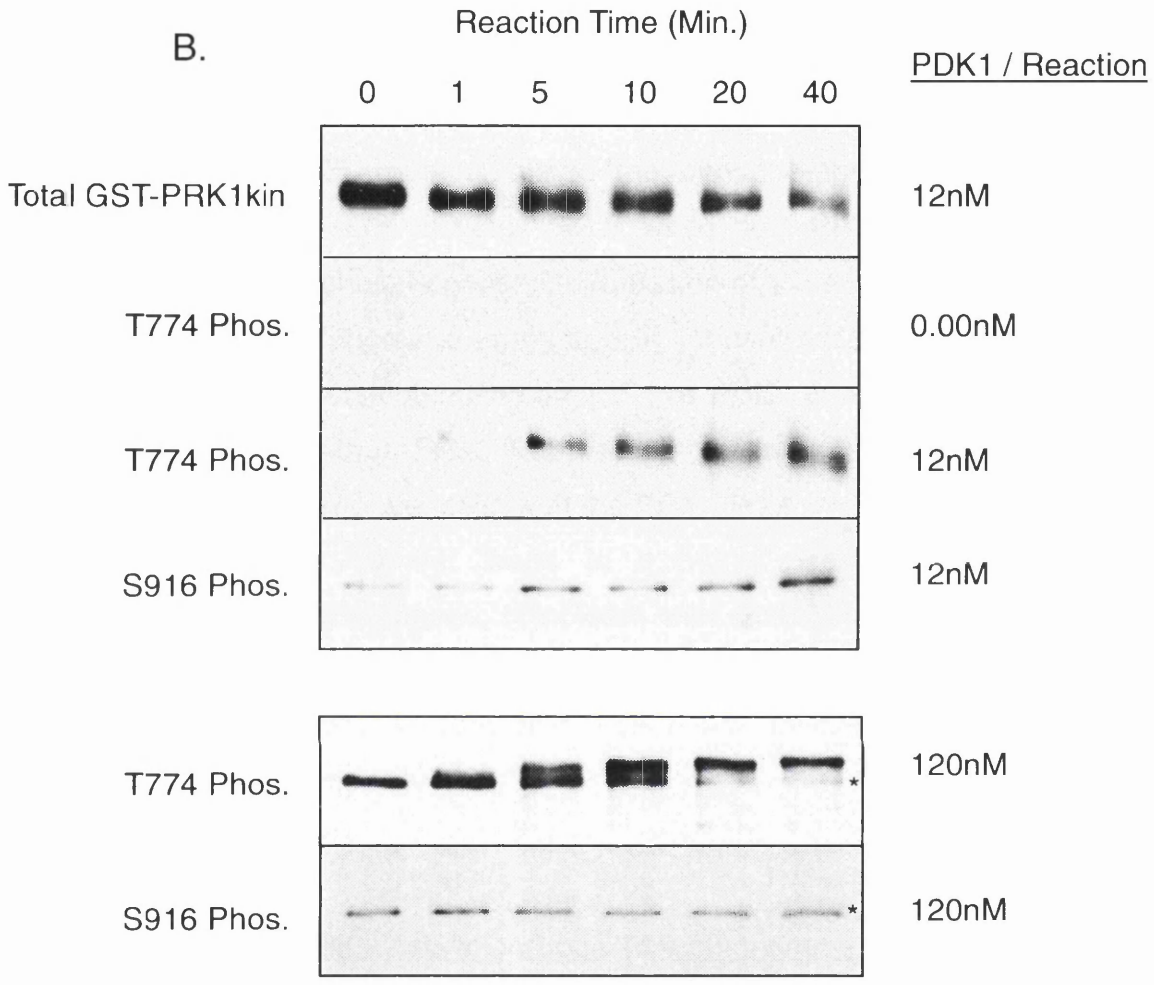

B) The phosphorylation states of both the T774 and S916 sites of GST-PRK1kin in the presence of two concentrations of GST-PDK1 (12 or 120nM) were assessed over time. The total GST-PRK1kin in each reaction was observed using a anti-GST polyclonal. Note that the time course using 120nM PDK1 is an independent experiment and cannot be compared directly with the 12nM time-course. The phosphorylated S916 signal in the 120nM PDK1 time-course does not shift on SDS-PAGE and aligns with the lower band in the T774 signal as denoted (*).

6.2.9 The PRK Activation Loop phosphorylation is Affected by PDK1 and Rho *in vivo.*

To assess the physiological potential of PDK1 as a PRK activation loop kinase, we monitored the phosphorylation state of endogenous PRK1 and PRK2 in HEK293 cells transfected with PDK1 or with the GTPases RhoA and RhoB (as GTPase-deficient Q63L mutants) using the phospho-specific activation loop antibody. As can be seen in figure 6.2.8, while both PRK isoforms show low basal activation loop phosphorylation, expression of either Rho mutant or PDK1 leads to a substantial increase in the specific phosphorylation of both kinases. The combination of transfected Rho protein plus PDK1 does not further increase phosphorylation of either PRK. This is not due to a high stoichiometry of phosphorylation: treatment of cells with the PP1, PP2A inhibitor okadaic acid for 40 minutes prior to harvest leads to a more extensive activation loop phosphorylation of both kinases, coincident with other undefined modifications which cause a shift in SDS-PAGE mobility (see upper panels). This implies that requirements additional to Rho and PDK1 are involved in the observed phosphorylation and mobility shift.

6.2.10 The *in vivo* PRK1 Activation Loop Phosphorylation Requires PI3-kinase Activity.

The products of PI3-kinase have been shown to play a key role in the phosphorylation of PKB and other AGC kinases by PDK1 (Stokoe, *et al.*, 1997). We therefore assessed the effect of the PI3-kinase inhibitor LY294002 on PRK activation loop phosphorylation. 293 cells were transiently transfected with the Myc-tagged constructs indicated in figure 6.2.9 and were treated with 20μM LY294002 for 20 minutes prior to harvest. While the basal T774 occupation of endogenous PRK1 is only slightly altered by the inhibitor treatment, the increased signal associated with the transient transfection of either GTPase

deficient Rho or PDK1 constructs are reduced to almost basal by a block of PI3-kinase activity. This is consistent with a PtdIns(3,4,5)P_3-dependent PDK1 localisation event being necessary for kinase-substrate association. Suprisingly, the PRK activation loop phosphorylation by ΔPH-PDK1 (residues 51-404) was also seen to be dependent upon PI3-kinase products by it inhibition with LY294002. This suggests that a separate pathway exists between PI3-kinase and PRK other than through PDK1. It is possible that the ΔPH-PDK1 localisation with PRK at a membrane surface is independent of PtdIns(3,4,5)P_3 (see below).

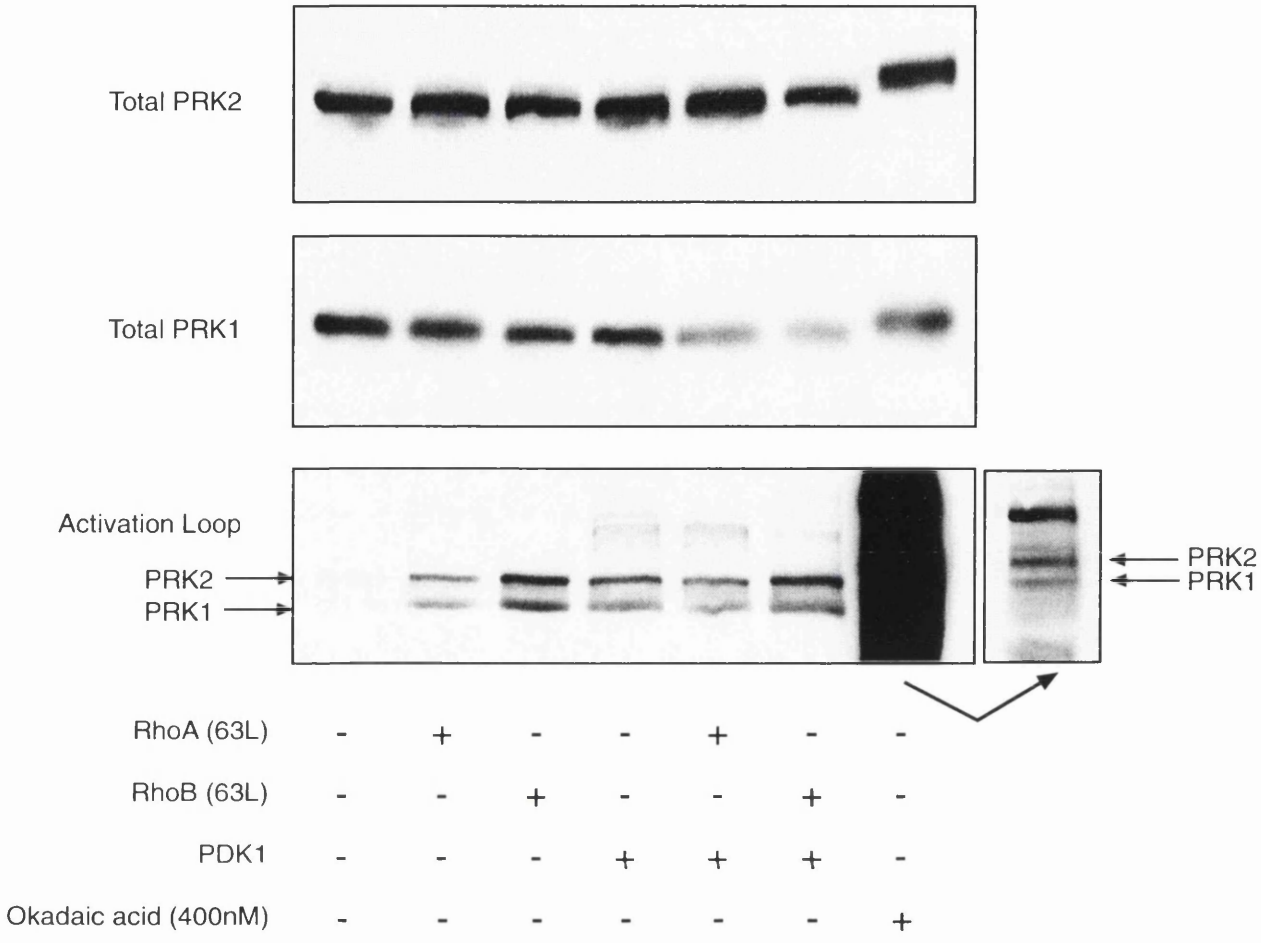

Fig. 6.2.8: *In vivo* Activation Loop Phosphorylation of Endogenous PRK1 and PRK2.

293 cells were transiently transfected with GTPase-deficient Rho constructs or mycPDK1, as indicated. Cells were treated with 400nM okadaic acid (as indicated) 40 minutes prior to lysis direct into Laemmli 4x SDS sample buffer. Samples were fractionated on SDS-PAGE (8%) and assessed by western blot. The upper and central panels indicate the total PRK2 and PRK1 levels in the samples (PRK1 and PRK2 monoclonals Transduction Labs). The lower panel indicates the T774 (PRK1) and T816 (PRK2) phosphorylation state as assessed with the ploYclonal antibody which is specific for the phosphorylated form of both isoforms. Note that PRK2 is the upper band and PRK1 the lower band of the apparent doublet. The extra insert in the lower panel displays a shorter exposure of the okadaic acid treated sample.

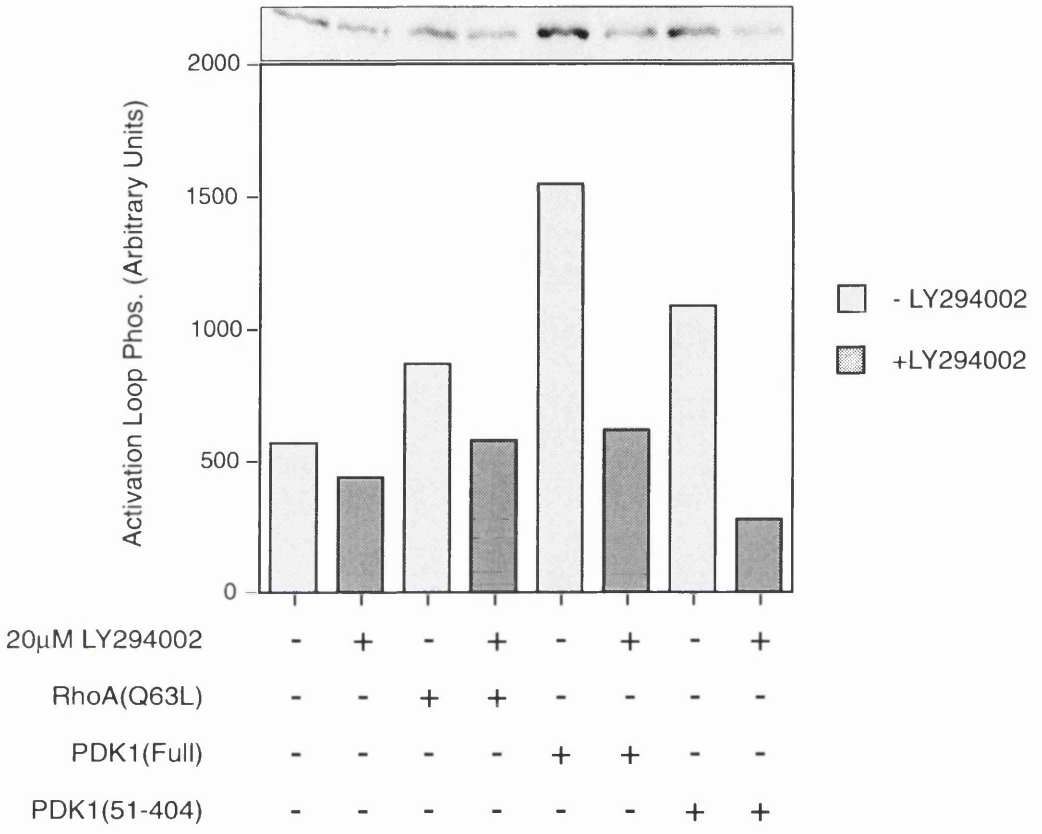

Fig. 6.2.9: LY294002 Inhibition of the Activation Loop T774 Phosphorylation.
In order to determine the effect of PI3-kinase activity on PRK activation loop phosphorylation *in vivo* the specific inhibitor LY294002 was utilised. Duplicate plates of 293 cells were transiently transfected with Rho or mycPDK1 constructs as indicated. 20 minutes prior to lysis in Laemmli SDS-sample buffer one set of duplicate plates was treated with 20μM LY294002. Samples were fractionated on SDS-PAGE (8%) and T774 phosphorylation of endogenous PRK1 was assessed by western with Phospho-specific polyclonal antibodies. The top panel exhibits the western signals attributed to the graphical display generated by NIH Image™.

6.2.11 An Increased Activation Loop phosphorylation *in vivo* is Associated with Increased Immunopurified Activity.

In order to assess the association between the activation loop phosphorylation seen *in vivo* and the activity of the PRK, 293 cells were transiently transfected with either a vector control (pCDNA3) or PDK1 (full length EE-tagged) in duplicate and one of each pair was treated with 100nM Calyculin 40 minutes prior to harvest. The endogenous PRK2 protein was immunoprecipitated using a PRK2-specific monoclonal (Transduction Labs) and 10% of the resulting protein-G Sepharose was used in duplicate kinase reactions. Reactions (40µl) of buffer F containing 0.25% (v/v) Triton X100, 5µg MBP and 5µCi [γ^{32}P]ATP were carried out at 30°C for 15 minutes in a shaking incubator (Microtherm™ by Camlab). Reactions were terminated by the addition of Laemmli 4X sample buffer followed by fractionation on SDS-PAGE. ^{32}P incorporation into MBP was determined by Cerenkov counting. As can be seen from figure 6.2.10 while equal amounts of PRK2 were present in each reaction, the comparatively modest effect of PDK1 expression on phoshorylation was insufficient to elicit a significant change in catalytic activity. However, the much greater activation loop phosphorylation coupled with the modification resulting in the shift on SDS-PAGE, associated with phosphatase inhibition, produced a >3 fold increase in activity against MBP.

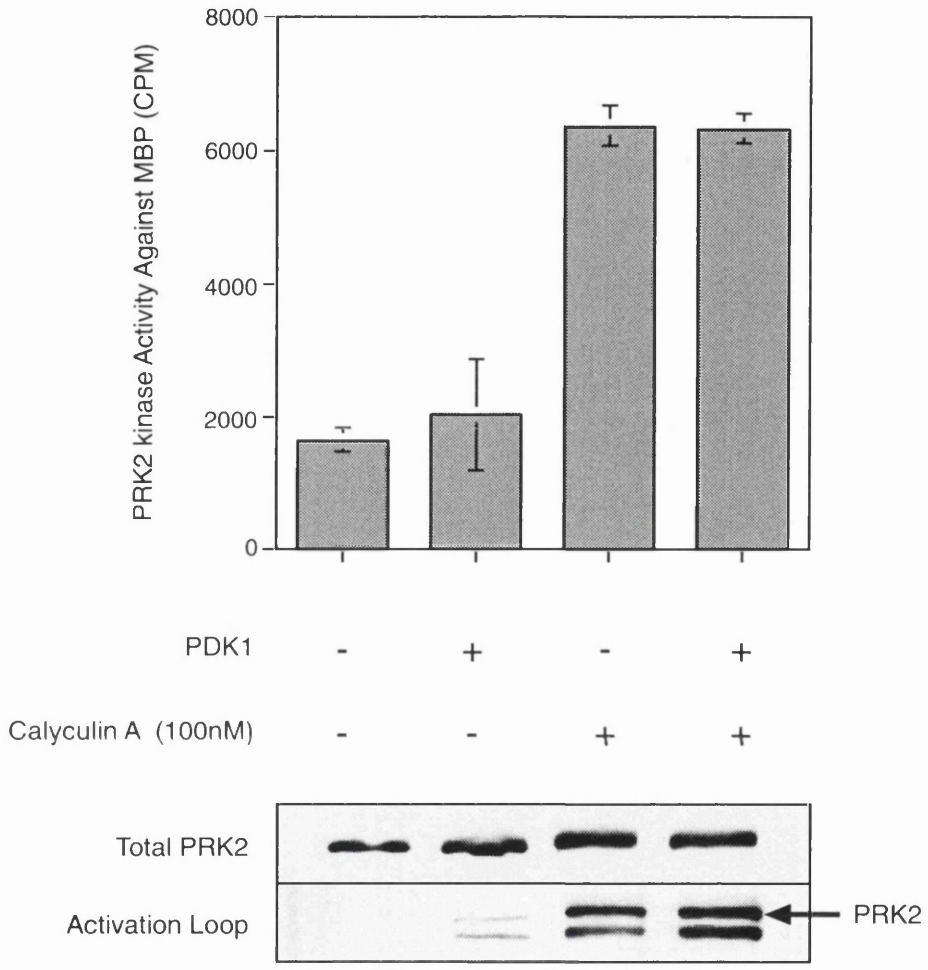

Fig. 6.2.10: The Effect of Activation Loop Phosphorylation on Immunopurified Activity.

293 cells transiently transfected with PDK1 and/or treated with 100nM Calyculin A for 40 minutes were lysed in buffer B and endogenous PRK2 immunopurified. Kinase activities associated with the immunoprecipitates were assessed in vitro against MBP resulting in the levels displayed graphically (CPM). Kinase assays were performed in the presence of 0.25% Triton X100 for 15 minutes at 30°C. Western blot analysis of the immunoprecipitates display equal PRK2 loads in each assay, while the phospho-specific polyclonal displays the relative phosphate occupation of the PRK activation loops in the whole cell lysates of the relative samples.

6.2.12 Generation of PRK2 Activation Loop Mutants.

While the *in vitro* data generated with GST-PRK1kin suggested an absolute requirement for the activation loop phosphorylation, the endogenous PRK proteins seemed to require additional modifications. To assess the direct influence of the activation loop phosphorylation on *in vivo* activity mutagenesis was employed. The *in vitro* site directed mutagenesis was carried out using the Quickchange™ mutagenesis kit (Stratagene) according to the manufacture's instructions and with the primers listed in appendix (III) (also see 2.2.8). This method successfully produced PRK2 point-mutants T816E and T816A, as judged by sequence analysis.

6.2.13 Activation loop Phosphorylation is Required for Catalytic Activity *in vivo.*

293 cells were transiently transfected with either wildtype PRK2 or the T816A or T816E mutants. Immunoprecipitation was carried out using a PRK2 monoclonal antibody which resulted in endogenous as well as exogenous protein being purified. The *in vitro* activity of immunoprecipitates was assessed using the same kinase assay and detection method as described in 6.2.11 and values were corrected to immunoprecipitates from untransfected cells. As can be seen from figure 6.2.11, the T816A mutant had an activity below basal level and the T816E mutant produced only 7% of wildtype activity. This indicates both that an intact threonine is required for activity and that the acidic mutation is an insufficient surrogate for phosphorylation. To determine whether T816 phosphorylation was required for the increased activity in response to phosphatase inhibition, we compared the two mutants with wildtype PRK2 on okadaic acid treatment of cells (400nM for 40 minutes). As seen previously for the endogenous PRK2, exogenous wildtype showed a marked activation due to phosphatase inhibitor treatment. Neither mutant displayed any significant activity increase over endogenous cellular activity. This demonstrates that

activation of PRK under these conditions has an absolute requirement for phosphorylation of the activation loop threonine.

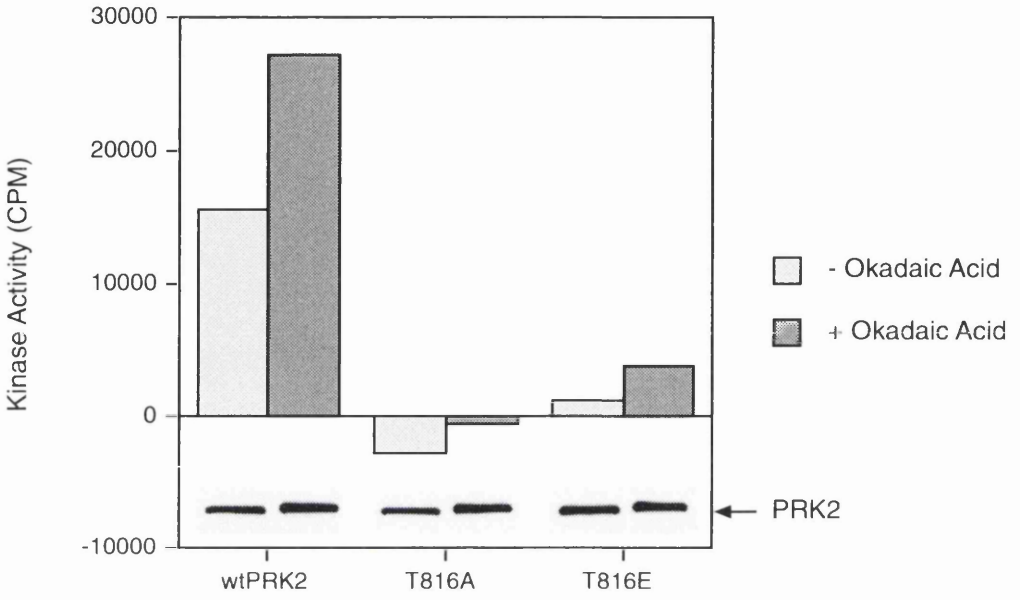

Fig. 6.2.11: The Activation Loop Phosphorylation of PRK is Required for Catalytic Activity *in vivo.*

Site directed mutagenesis of PRK2 T816 to either Ala or Glu allowed the determination of the catalytic requirement for phosphorylation at this site. 293 cells transiently expressing either the wildtype PRK2 or the mutants were treated with 400nM okadaic acid for 40 minutes as indicated. The subsequent immunopurification yielded equal amounts of the PRK2 proteins, as can be seen from the insert panels (westerns completed with Transduction Labs monoclonals). Kinase activity associated with the immunoprecipitates was determined *in vitro* as previously described (6.2.10) and the values displayed are corrected for immunoprecipitates from untransfected cells. Values are representative of three independent experiments.

6.2.14 PRK and PDK1 Co-immunoprecipitate in a Rho-Dependent Manner.

The presence of an *in vivo* complex formation between PDK1 and PRK was investigated. Co-expression of EE-tagged PDK1 and Myc-tagged PRK2 in 293 cells followed by immunoprecipitation of PDK1 (using a EE-specific monoclonal) led to the co-immunoprecipitation of PRK2 (figure 6.2.12.A). No PRK was present in immunoprecipitates from cells not expressing the tagged PDK1. Interestingly the complex formation was enhanced with the co-expression of RhoA (Q63L mutant). Evidence for a requirement for endogenous Rho; the expression of *Clostridium* toxin C3 transferase blocked the constitutive kinase-kinase interaction. It can therefore be concluded that PRK2 binds PDK1 in a Rho dependent manner. A similar situation was seen for a PRK1-PDK1 co-immunoprecipitation: the presence of an activated Rho greatly increased the extent of complex formation. However, unlike PRK2, the constitutive low level interaction seen in the absence of exogenous Rho was not eliminated by C3 transferase (figure 6.2.12.B). This implies that while a similar potential for Rho dependence exists for the PRK1-PDK1 interaction an alternative input to PRK1 must exist (see discussion).

6.2.15 PRK, PDK1 and Rho co-localise *in vivo.*

Previous studies on the RhoB-dependent recruitment of PRK1 to endosomes (Mellor, *et al.*, 1998) allowed the assessment of the assembly of a putative RhoB-PRK-PDK1 complex in intact cells. In work completed by Dr H. Mellor, NIH 3T3 cells transfected with wildtype RhoB displayed a characteristic punctate staining of the protein (figure 6.2.13.A) that has been shown to reflect early endosomal compartments (Adamson, *et al.*, 1992). The staining of PDK1 co-expressed with RhoB was diffuse cytoplasmic and non-nuclear (B) this was also the case when PDK1 was co-expressed with PRK1 in the absence of Rho. However, when PDK was expressed with RhoB in the presence of PRK1, it is

found to display a punctate distribution coincident with RhoB (D). Hence the Rho-dependence of PRK-PDK1 complex formation in the co-immunoprecipitation is recapitulated by the ternary complex formation of Rho-PRK-PDK1 in intact cells.

PDK1 has previously been shown to translocate from the cytoplasm of serum starved PAE cells to the plasma membrane on stimulation with PDGF-BB (Anderson, *et al.*, 1998). This PDK1 translocation event was seen to be dependent upon both an intact PH domain and the products of PI 3-kinase. Whether the observed ternary complex formation was also dependent upon PtdIns(3,4,5)P_3 or PtdIns(3,4)P_2 was therefore assessed. Treatment of the cells with 100nM wortmannin for 20 minutes was seen to disrupt the morphology of the endosomal compartment but did not disrupt PDK1 co-localisation with PRK1 and RhoB (F). Such a wortmannin treatment has been shown to cause rapid displacement of PtdIns(3,4,5)P_3 specific binding proteins from the plasma membrane (Venkateswarlu, *et al.*, 1998). It can therefore be concluded that both the translocation to and maintenance of PDK1 in the endosomal compartment is due to a protein-protein interaction with PRK rather than a lipid specific event. The full protocol for the immunofluorecense experiments are listed in appendix (IV).

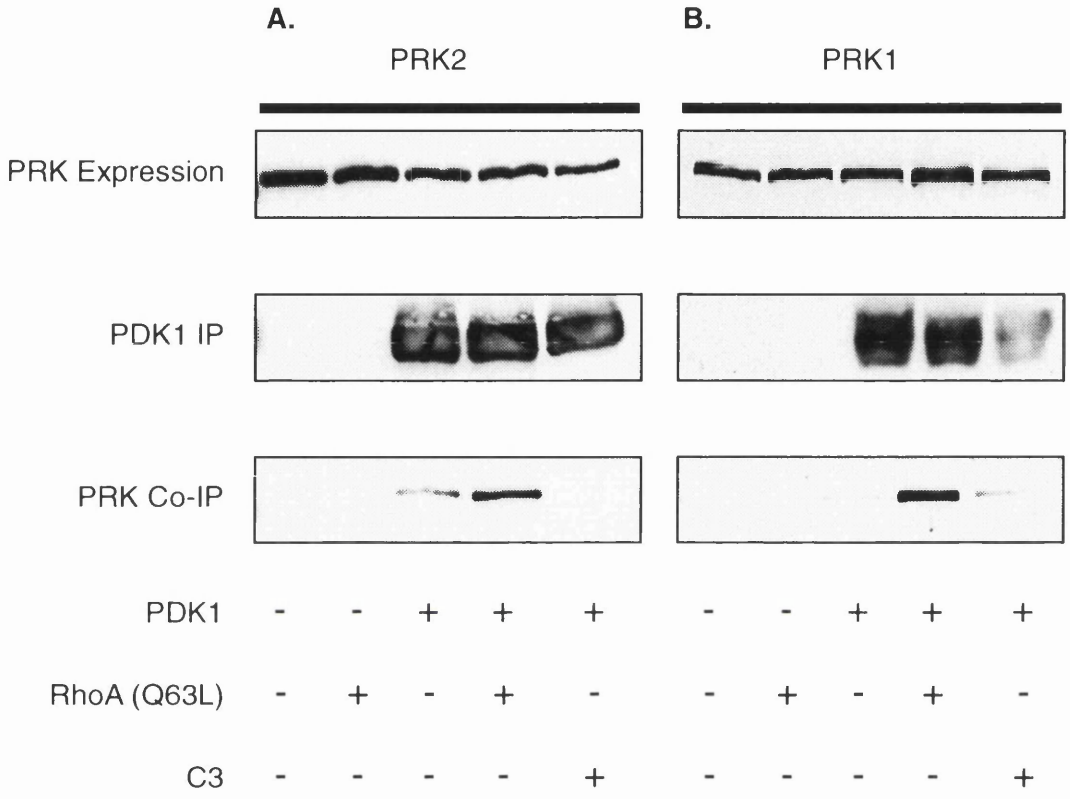

Fig. 6.2.12: Rho Dependent Co-Immunoprecipitation of PRK and PDK1.
293 cells were transfected with mycPRK1 (B) or mycPRK2 (A) alone or co-transfected with EE-tagged PDK1, RhoA(Q63L) or Clostridium C3 toxin as indicated. The subsequent immunoprecipitation of PDK1 allowed the determination of PRK-PDK1 complex formation *in vivo*. Immunoprecipitates were washed three times in buffer B prior to elution in Laemmli sample buffer. Western analysis exhibits the total PRK1 and PRK2 expression in the cells (upper panel); the PDK1 immunprecipitates (central panel) and the co-immunoprecipitated PRK (lower panel).

Fig. 6.2.13: PRK1, PDK1 and Rho Co-localise *in vivo.*

NIH 3T3 cells were co-transfected with RhoB (A-F), and either PDK1 alone (A, B) or PDK1 with PRK1 (C, D and E, F). Cells in E, F were treated for 20min with 100nM wortmannin prior to fixation. Fixed cells were stained with rabbit polyclonal anti-RhoB antibody (red) and mouse monoclonal anti-EE antibody (green, to detect PDK1). Figure 6.2.13 shows a projection of confocal images taken through the body of the cells. Bar represents 10μm. For full method see appendix (IV).

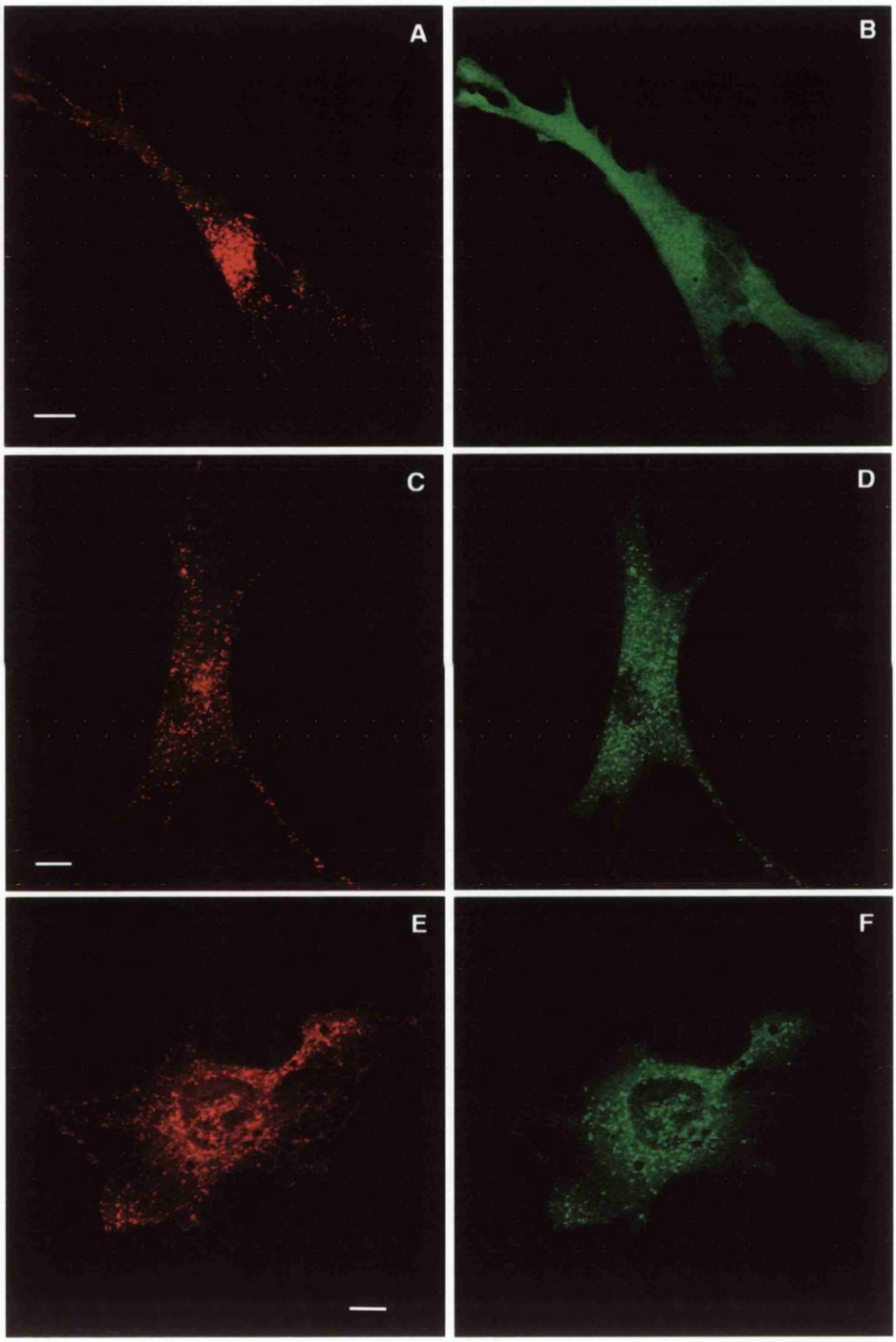
A
B
C
D
E
F

6.3 Chapter Discussion

This chapter has characterised PDK1 as a kinase which specifically phosphorylates threonine residues within the activation loops of both PRK1 and PRK2; residues 774 and 816 respectively. PDK1 phosphorylated GST-PRK1kin *in vitro* in a lipid independent manner reflecting the lack of a membrane localisation domain in the truncated PRK. The equivalent event *in vivo* for endogenous PRK1 and PRK2 could be produced by the overexpression of either Rho or PDK1 proteins and was dependent on PI3-kinase activity as judged by the use of the inhibitor LY294002. Interestingly the lipid products of PI3-kinase activity were seen to act at the level of PRK rather than PDK1 alone, for the ΔPH-PDK1 dependent phosphorylation of PRK1 was also blocked by this inhibitor. The ability of Rho alone to cause an increase in activation loop phosphorylation but not synergise with the effect of exogenous PDK1 expression raised the possibility of a third factor being limiting. Alternatively, the phosphorylation state of the PRKs may be acutely regulated by phosphatases. Indeed the use of phosphatase inhibitors resulted in a significant increase in both activation loop phosphorylation and other modifications resulting in mobility shift on SDS-PAGE. The GST-PRK1kin was activated *in vitro* as a direct result of T774 phosphorylation, equivalent phosphorylations in other AGC-kinase family members had previously been shown to be necessay for activity (Alessi, *et al.*, 1996, Cazaubon, *et al.*, 1994). While other events seem to be required for activation of the endogenous PRK *in vivo*, the use of mutagenesis displayed activaton loop phosphorylation to be vital for activity at any level.

The PDK1 phosphorylation of T774 on GST-PRK1kin was independent of the putative autophosphorylation event at S916. Further, phosphorylation at this site would seem to confer a resistence to mobility shift on SDS-PAGE. As descibed in greater detail in chapter 7, this may be due to a specific hinderence in the PDK1 - PRK interaction.

Co-immunoprecipitation experiments exhibited the formation of a Rho-dependent PRK and PDK1 complex *in vivo* . Further, a ternary complex between RhoB, PRK1 and PDK1 was observed by immunofluorescence. The insensitiveity of this complex to wortmannin suggests its maintainence is independent of PI3-kinase products and is more likely to be due to protein-protein contacts. As described in the next chapter the involvement of PDK1 in the activation of PRK and the Rho-dependence of the PRK-PDK1 interaction offers a mechanism for the observations presented in chapter 5.

7.1 PRK Interacts with Rho Family GTPases

PRK had been identified as a potential Rho GTPase effector in both yeast 2-hybrid screens and affinity chromatography (Amano, *et al.*, 1996b, Watanabe, *et al.*, 1996). Given the precedent for small GTPases acting as molecular switches; regulating signalling processes through the activation of kinase effectors, an aim of the project was to determine the role of Rho in the regulation of the PRK family. The first two results chapters describe the characterisation of the Rho-PRK interaction. Sequence alignment had established the presence of discrete homology regions within the PRKs. Polypeptides covering these domains were expressed and used as targets for Rho in a variety of *in vitro* binding assays. The intact PRK1 was seen to interact with RhoA as were the HR1 domains of both PRK1 and PRK2. The $HR2^{PRK1}$ domain did not display a Rho binding potential.

It had originally been proposed that the HR2 domain may function either as a pseudosubstrate inhibitor of the kinase or as a phospholipid binding site. These suggestions were based on the observed sequence similarity between the HR2 domains of PRK1 and PRK2 and the amino-terminal regions of PKC-ε and PKC-η (Palmer, *et al.*, 1995b). This region of the PKCs encompasses their V_0 domain and pseudosubstrate sites. However, no potential pseudosubstrate sequence is seen in the PRK HR2. The PRKs had been shown to be activated by the phosphoinositides PtdIns-(4,5)P_2 and PtdIns-(3,4,5)P_3, to similar extents as PKC β, ε, ζ and η, (Palmer, *et al.*, 1995a). The observation that a ΔV_0PKCη displayed the same phosphoinositide response as a wild type enzyme discounted both this domain and, by inference, the HR2 domain from a lipid binding potential

(Palmer, *et al.*, 1995a). The present study also discounts any direct input of the HR2 domain in a Rho-dependent regulation.

The HR1 domains were shown to be the Rho binding region of the human PRKs. Further analysis of the region highlighted three homologous repeats which were termed HR1a, b and c. Figure 7.1 shows a phylogenetic representation of the HR1 domains present in proteins (both kinases and non-kinases) from various species. While the mammalian kinases have three subdomains as does one of the *C. elegans* kinases (PRKA), the small non-kinase proteins Rhophilin and Rhotekin as well as the other *C. elegans* kinase (PRKB) only has a single motif. The yeast kinases (PCK1, 2 and PKC1) all have two subdomains. The multiple alignment exhibits two main blocks of similarity across species; a HR1a-like block which is present in all the proteins characterised as Rho binding to date and a block of HR1b and c like subdomains. This second block of homologous repeats can be further subdivided into the b and c subdomains of multicellular organisms and the second subdomain of the yeast kinases, which although by the alignment method utilised here seem to be most closely related to HR1c, actually have similar charge distributions to the mammalian HR1b repeats.

This sequence grouping bears functional significance, at least for the mammalian proteins, for it was shown that while HR1a and b have a Rho GTPase binding potential HR1c does not. No function for the HR1c motif has been proposed to date. The yeast proteins have a HR1a and a second motif that lies somewhere between the b and c by homology. Whether the HR1b has been evolved to add a degree of specificity to the GTPase interaction in higher eukaryotes is questionable considering its site of contact with the Rho (see later).

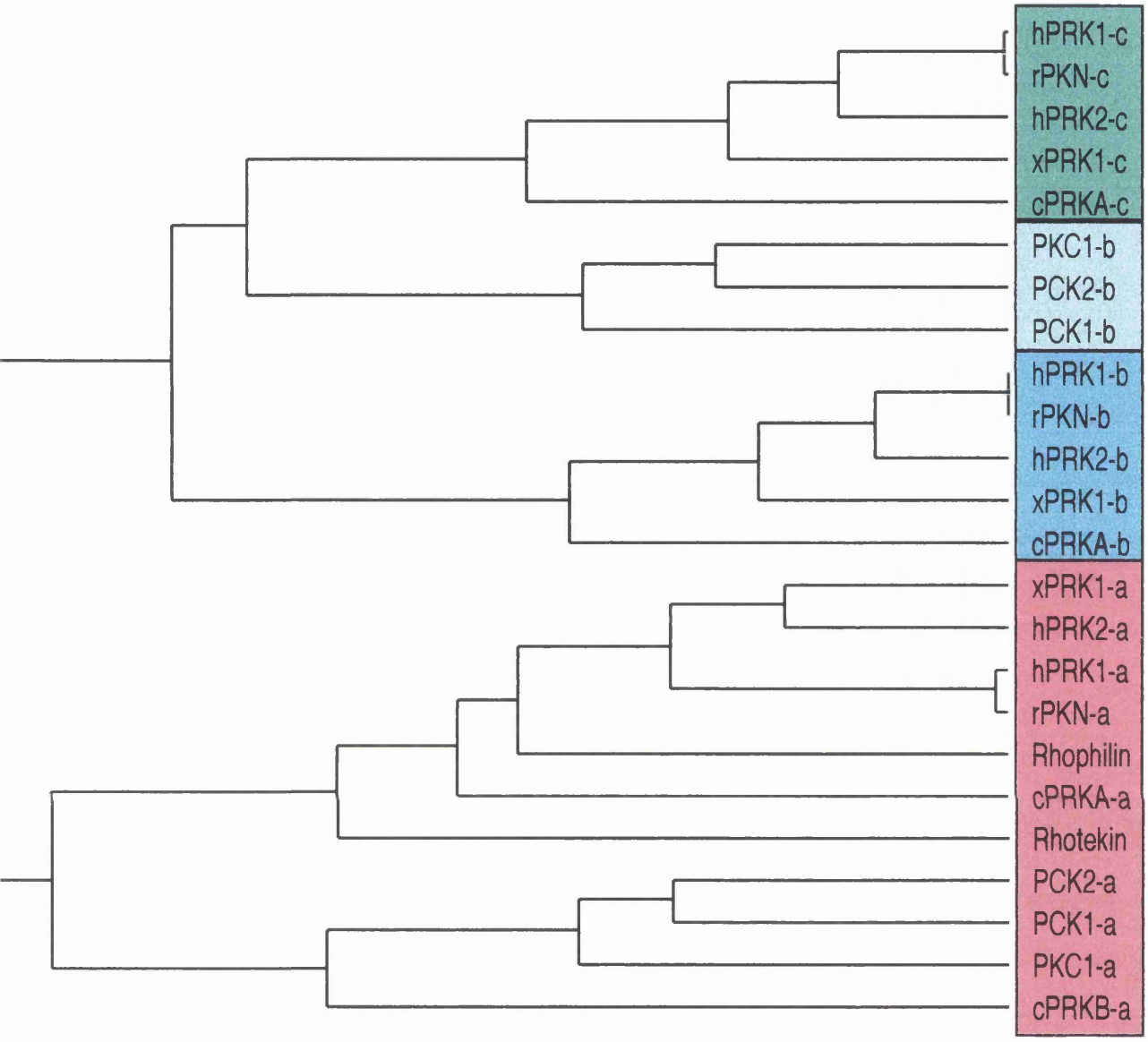

Fig. 7.1: A Phylogenetic Tree resulting from a Multiple Alignment of HR1 Subdomains both across Isoform and Species.

A multiple alignment of the central core of the HR1 subdomains (approx. 50 amino acids) of gene products from various species. DNAStar™ software was used to align sequences according to the Jotun Hein Method using PAM 250 residue tables. The species are denoted by the first letter in the abbreviation: (h) human; (r) rat; (x) *xenopus*; (c) *C. elegans*, Rhophilin and Rhotekin are both human and PCK and PKC1 are from *S. pombe* and *S. Cerevisiae* respectively. The subdomains are grouped according to their sequence similarity and their charge distribution about the core GAEN sequence: magenta for HR1a, blue for multicellular HR1b, green for multicellular HR1c and light blue for the yeast HR1b-like repeats.

The interaction between the HR1 domain and RhoA is in complete agreement with the original screens for Rho effectors which used both the yeast two hybrid and affinity chromatography to establish the amino terminal region of PRK1 as the Rho binding domain (Amano, *et al.*, 1996b, Watanabe, *et al.*, 1996). A subsequent study by (Shibata, *et al.*, 1996) looked in greater detail at the interaction. They mapped the Rho binding region to HR1a but excluded HR1b, however this study used the GTPase deficient mutant V14 which the present study shows not to bind HR1b. Further, in agreement with the work presented in this thesis a more recent study has shown the HR1 subdomains of PRK2 to interact with RhoA with a similar pattern as PRK1 i.e with relative affinities HR1a>HR1b>>>HR1c (Zong, *et al.*, 1999). The interaction analysis also suggested a consistent but low affinity interaction of the HR1a subdomain with Rac1. This was not seen in any of the studies referenced above but (Vincent and Settleman, 1997) showed endogenous PRK2 and to a much lesser extent PRK1 to be purified from liver extracts specifically on a GST-Rac.GTP column. The same study also showed that both Rho and Rac stimulate the autokinase activity of the purified PRK2 *in vitro*, implicating either GTPase in the activation of the PRKs.

It is implicit from the data on the dissociation of Rho from the various motifs that the HR1a and HR1b contacts combine to produce the relatively tighter interaction seen for the full HR1 domain. The interaction between the full domain and RhoA was GTP dependent. This dependence was most likely contributed by the HR1a subdomain which was seen to interact only with this form of the GTPase. Suprisingly the HR1b showed a consistent Rho.GDP binding potential. Interestingly, the interaction between endogenous PRK2 and RhoA has been shown to have an almost nucleotide independent character (Vincent and Settleman, 1997), this suggests the $HR1b^{PRK2}$ may contribute to this interaction in a dominant fashion. This is backed up by the observation that a G65A mutation in PRK2 (the GAEN conserved core for the $HR1a^{PRK2}$) is unable to bind Rac1 but retains a Rho binding potential (Jeff Settleman,

personal communication). The same study showed that while the PRK2 autokinase[*1] activity could be increased in association with both Rho.GTP and Rho.GDP, treatment of the samples with C3 toxin blocked both the interaction and associated kinase activity. This suggests that the interaction requires an intact Rho effector domain but not the active GTP conformation. Nucleotide independent binding of GTPases to either upstream or downstream targets has been seen previously: the 68kDa type 1 PI5-kinase activity was seen to associate with either nucleotide bound form of Rho (Tolias, *et al.*, 1995), this interaction was actually enhanced when the Rho was ADP-ribosylated by C3 toxin (Ren, *et al.*, 1996). Thus it may be the case that two mechanisms of GTPase-effector signalling take place: the well characterised effector activation which relies on the interaction with the GTPase only when in the GTP conformation, resulting in a 'hit and run' timed switch. A second effector type may exist where the binding of and activation by a GTPase are separate events i.e where the effector is able to interact with either conformation of the GTPase but is only activated when GDP is exchanged for GTP. As discussed later this second proposed mechanism may have implications with regard to signalling complex formation, where a scaffold protein recruits various members of a particular pathway.

The nucleotide dependent activation of an effector relies upon its interaction with a region of the GTPase which changes conformation upon GTP hydrolysis. Sequence alignments between the structurally characterised bacterial elongation factor EF-Tu and H, K and N-Ras allowed the original observation that the oncogenic mutations, resulting in the constitutive activation of the molecule affect the contacts made with the guanine nucleotides (McCormick, *et al.*, 1985). Subsequent mutational studies in Ras identified residues 30-44 as vital for signalling leading to the transformed phenotype, but not for the intrinsic biochemical activity of the GTPase (Sigal, *et al.*, 1986, Willumsen, *et al.*, 1986).

---

[1] Phosphorylation of PRK in (Vincent and Settleman, 1997) was assumed to be autophosphorylation.

These observations raised the possibility that while other residues were involved in the downstream signalling of Ras via the control of its nucleotide co-ordination, the area most likely to be involved in protein-protein interactions was the so called effector region (residues 30-40). Subsequently, a range of mutation, peptide competition and later structural studies have shown RasGAP, c-Raf1 and the catalytic domain of PI3-kinase to all interact with Ras via this region (Adari, *et al.*, 1988, Cales, *et al.*, 1988, Rodriguez-Viciana, *et al.*, 1994, Scheffzek, *et al.*, 1997, Warne, *et al.*, 1993, Zhang, *et al.*, 1993). The effector loop of Ras overlaps with the switch I region which does indeed go through a conformational change on GTP hydrolysis.

Later studies using Rho-Ras chimeras suggested that although residues in regions flanking the effector loop were important for its full transforming potential, Ras has a single effector binding region required for downstream signalling (Self, *et al.*, 1993). The same study showed that while the homologous region in Rho (residues 32-42) is required for stress fibre formation these residues alone are insufficient to account for the Rho dependent biological readouts or Rho-GAP binding, in fact Rho-GAP displayed no binding to the first 62 residues of the GTPase. Further, chimeric Rho-Rac molecules were used to identify two effector sites on Rac responsible for contacts with the effectors $p65^{PAK}$ and $p67_{phox}$ one including the effector loop and one between residues 143 and 175 (Diekmann, *et al.*, 1995). This study also mapped the bcrGAP binding region to residues 74-90. It is clear that an intact effector loop is required for full biological readout but in the case of Rho family GTPases this may not be the only site of contact for effectors.

The use of Rho/Rac chimeras allowed the regions on Rho involved in the interaction with PRK to be assigned. The HR1a binds between residues 73 and 143 and HR1b binds somewhere in the amino-terminal third of the molecule, but only if the activating V14 mutation is not present. The HR1a binding region overlaps the Switch II loop of Rho and this may well be the determinant of the

GTP-dependent binding. The relative nucleotide independence of the HR1b suggests that its contact with the N-terminus is at a site outside the switch I loop. These findings have subsequently been corroborated by other studies: Fujisawa and colleagues used Rho/Rac chimeras to group Rho effectors into three classes depending upon the region of Rho with which they interact (Fujisawa, *et al.*, 1998). As with previous studies two discrete regions were mapped; amino acids 23-40 and 75-92. While Citron bound only to the first region and Rhophilin to the second, ROCK-I displayed a binding potential for both. The interaction of Rhophilin with the second region is consistent with the PRK data for this effector contains a single HR1a repeat. Consistent with previous findings Zong etal has shown that the first 73 amino acids of Rho can be replaced by Rac without disrupting the $HR1a^{PRK2}$ or ROCK-I Rho binding Domain (RBD) interaction (Zong, *et al.*, 1999). However, a T37A or F39A mutation within the effector loop completely abolishes binding, suggesting that while a functional switch I / effector loop is required, it does not determine the specificity for the effector. Further analysis allowed others to map the residues involved in effector specificity to Asp87 and 90 in loop 6 of Rho (Zong, *et al.*, 1999). The mutation of these residues to Val and Ala, as they are in Rac disrupted binding of the $HR1a^{PRK2}$ and RBD. While the cellular role of PRK2 is still unknown the ROCK kinases have been shown to mediate stress fibre formation. The formation of stress fibres by the microinjection of Rac (Q61L) D85,D88 into epithelial cells coupled to the loss of synergistic transforming potential of Rho (Q61L) V87, A90 with Raf in NIH3T3 cells is convincing evidence for the role of these residues in the specificity of Rho effector binding. It is however noteworthy that the mutation of F39V within the effector loop of RhoA (V14) was seen to be able to interact with ROCK but not PRK1 by two hybrid analysis, once again implicating the effector loop in contributing specificity to the interaction (Sahai, *et al.*, 1998). Figure 7.2 gives a schematic representation of the areas of the Ras, Rac and Rho GTPases that interact with either Effector molecules or GAPs.

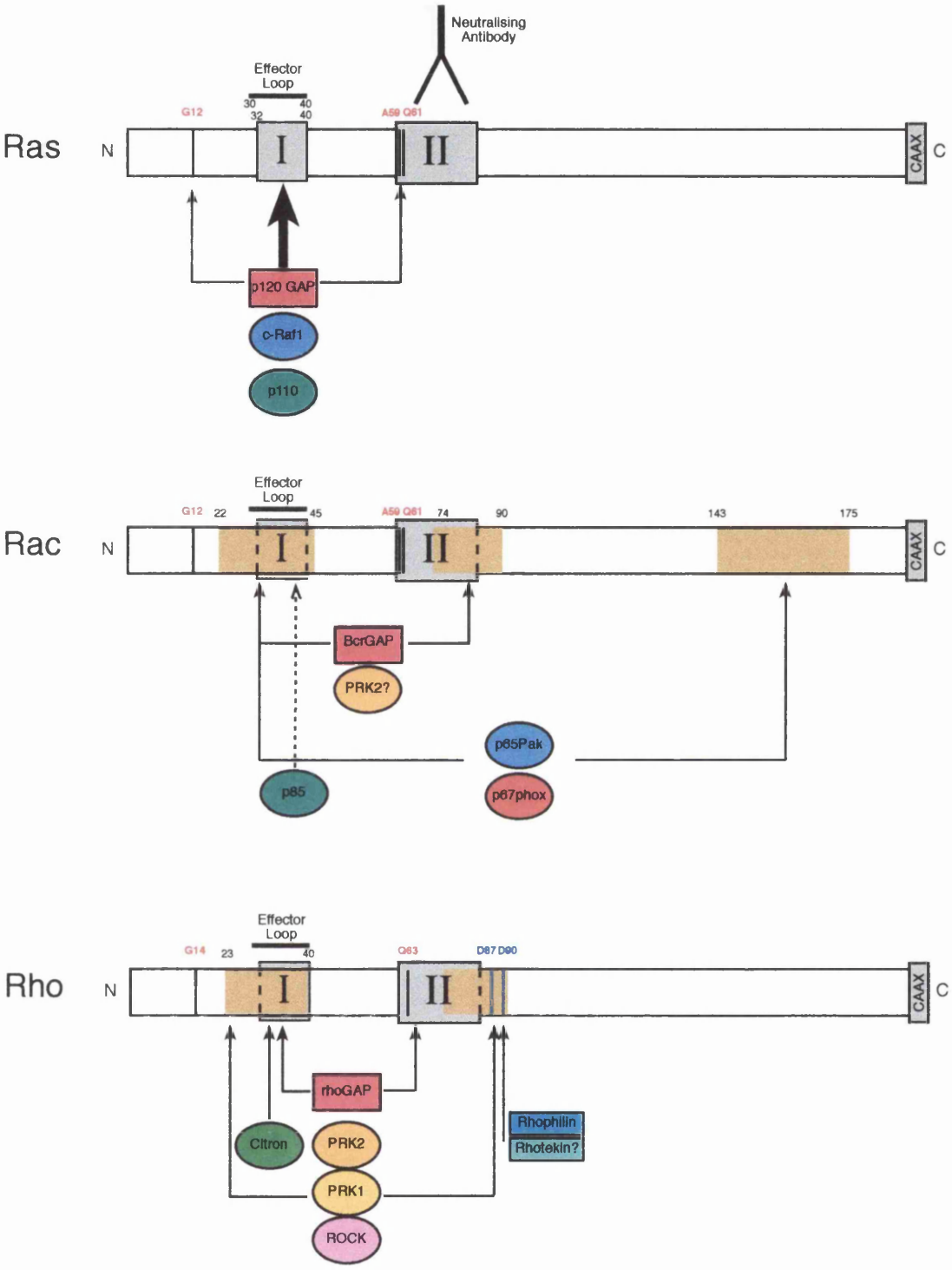

Fig. 7.2: Schematic Representation of the Effector Binding Regions for Ras, Rac and Rho.

The switch I and II loops are shown in *grey* and the key amino acids involved in phosphate co-ordination are in *red*. The amino acid boundaries of the regions implicated in effector binding are shown in normal type and with *sand* boxes. The binding sites of the various effector proteins and GAPs are denoted by the arrows. The epitope of antibody Y13-259, which is seen to neutralise transforming potential of Ras, is mapped to residues in the switch II domain. The Asp residues seen to confer Rho/Rac effector specificity are shown on Rho in *dark blue*.

7.2 Developing a Quantitative Assay for Rho Activation Status.

As described in chapter 4, the use of small G-protein binding domains to selectively pull active GTPase from cultured cells (active refering to the GTP-bound state) has allowed the tracking of Ras activation during cell-cycle progression (Taylor and Shalloway, 1996). Having established that both the full HR1 domain and the HR1a subdomain of PRK1 interact preferentially with the GTP-bound form of RhoA, B and possibly C it was a candidate probe for the assessment of Rho activity. Initial experiments using dominant negative and GTPase deficient mutants of RhoB along with the inactivating *Clostridium* C3 toxin showed the specific purification of active Rho. While further work is required to refine the use of this domain for endogenous systems, it would seem an ideal tool for a number of reasons.

The individual HR1a domain has an absolute dependence for the GTP-bound conformation of Rho. It has also been shown to inhibit the GAP-stimulated and intrinsic GTPase activity of Rho (Reid, *et al.*, 1996, Shibata, *et al.*, 1996) as well as nucleotide exchange (Zong, *et al.*, 1999). It would therefore prevent the loss of active Rho signal on purification due to GTP hydrolysis. It can also be seen that the individual subdomains of the HR1 express to very high levels in *E.coli* and are completely soluble, as is the complete domain. Smart system™ FPLC has demonstrated that while the full HR1 remains monomeric in solution, the HR1b, purified from *E.coli* and cleaved from its GST-tag dimerises (D. Chigadze personal communication). This would suggest that the homologous repeats fold so as to line up against each other, perhaps via the leucine zipper-like region. Both NMR and crystalographic structural studies of the HR1 domain are still underway but a secondary structure prediction method has been used to create the model for HR1a seen in figure 7.3. While this is speculative it displays expected characteristics: the hydrophobic residues are buried between two

helices and a β-strand and the core GAEN of the HR1a is exposed at one end of the finger-like subdomain.

Fig: 7.3 Secondary Structure Prediction of the HR1a Subdomain

The Incite II v97.0 secondary structure prediction software by MSI Biosystems was used to produce the model of $HR1a^{PRK1}$ (amino acids 1-106). The main chain is shown in *blue* as two helices and one β-strand but with connecting loops removed. The hydrophobic residue side chains are depected in *gold* and the core GAEN sequence is in *purple*.

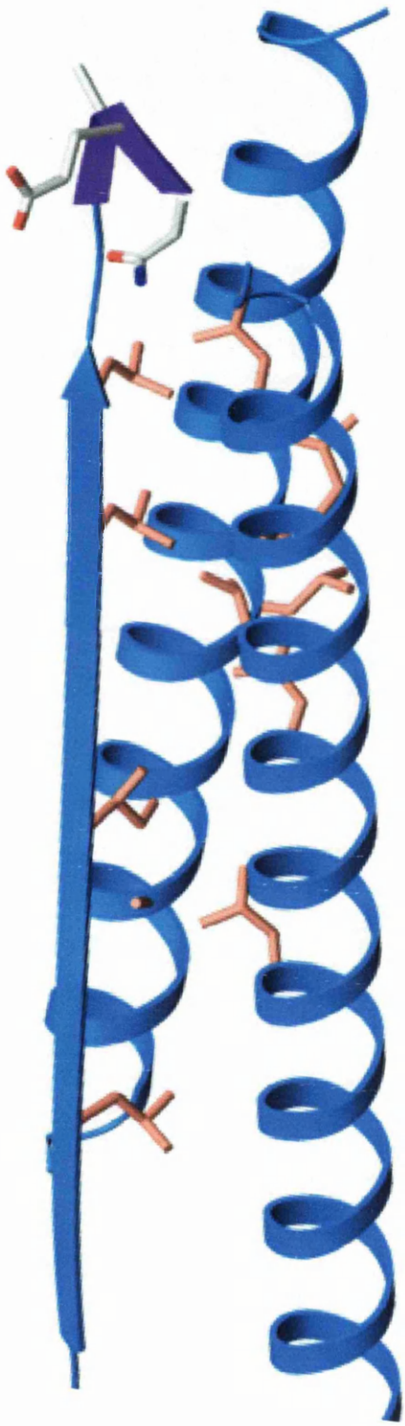

Recently a study analysing the regulation of Rho activity on mitogen stimulation and cell adhesion has been published which utilises the HR1 motif present in Rhotekin to pull down active Rho from fibroblast whole cell lysates (Ren, *et al.*, 1999). Overexpression of Rho mutants allowed the feasibility of the system to be assessed. A 2-6 fold increase in the endogenous RhoA.GTP pulled out was seen after 1 minute of LPA or serum stimulation and a clear biphasic regulation of Rho in response to cells being plated on fibronectin was seen. The purification was completed in 0.5M NaCl RIPA buffer which stripped the Rho of endogenous effectors or GAPs so preventing steric hindrance of the HR1 interaction. The active Rho was detected by western blot which could then be analysed by various software programs. However, this method does not easily allow the detection of the various Rho isoforms due to potential cross reaction of antibodies. An aim of an ongoing study is the refinement of a detection method which will produce absolute quantification of the active Rho.

RhoA has been shown to translocate to the Triton X100 soluble membrane fraction on LPA stimulation in a time and dose dependent manner whereas RhoB is not (Fleming, *et al.*, 1996). Such a translocation event may result in Rho adopting an active conformation i.e. dissociating from the GDI and binding to a membrane localised effector in a GTP-dependent fashion. However, this LPA-stimulated translocation does not seem to be linked to stress fibre formation and it is still unclear at which time point the Rho becomes activated.

The *Clostridium* toxin C3 specifically ADP-ribosylates either nucleotide-bound form of RhoA, B and C at Asn 41, resulting in inactivation of the GTPase by a mechanism presumed to disrupt effector interaction. The use of excess toxin to radiolabel Rho either in a whole cell extract or purified pull-down allows the simple relation of active Rho to total so producing a percentage. The general scheme of the assay can be seen in figure 7.4. The use of 2D electrophoresis would display the differences in the activation profiles of the three Rho isoforms

on agonist stimulation, while the use of a fluorescent labelled HR1 subdomain may allow the detection of active Rho compartment(s) within fixed cells.

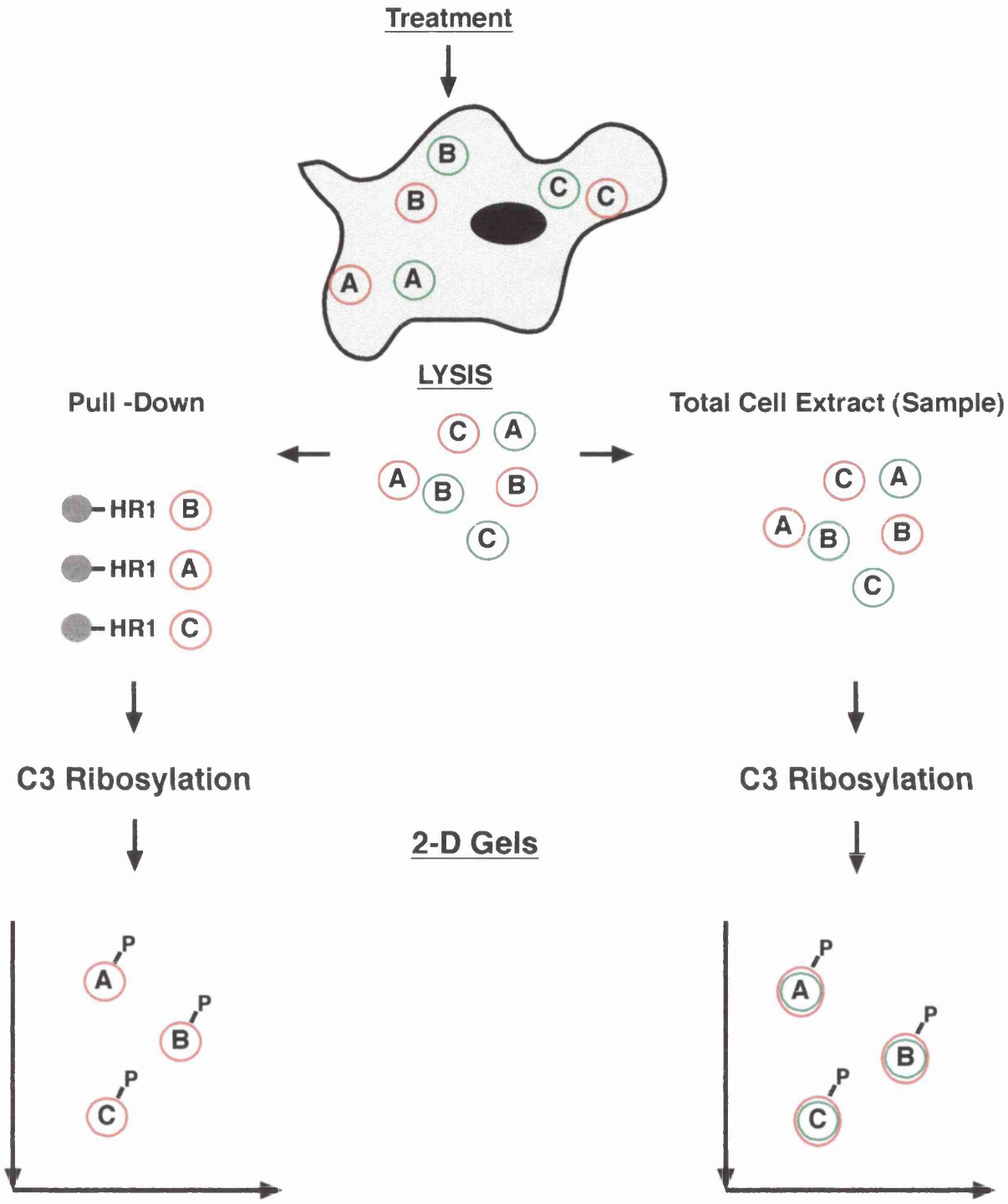

Fig. 7.4: Schematic Representation of the Method Employed to Assess the Percentage of Rho Activity in Cultured Cells.

RhoA, B and C isoforms are represented by the circles where red is Rho.GTP and green is Rho.GDP. The GTP-bound form is specifically extracted from whole cell lysates on a HR1 column; both purified and total Rho is radiolabelled by ADP-ribosylated with C3 toxin and the various isoforms are separated by 2D electrophoresis. The percentage of active to total Rho isoforms can therefore be analysed.

7.3 Multiple Inputs Regulate PRK Activity.

Previous studies have shown an increased PRK autophosphorylation and kinase activity against exogenous substrates on incubation with Rho.GTP *in vitro* (Amano, *et al.*, 1996b, Watanabe, *et al.*, 1996). However the data presented here would suggest that rather than a direct effect *in vitro*, the Rho acts in combination with another cellular component to result in the activation of the kinase. Indeed the discrepancy may be a result of the other cellular component, namely PDK1, being co-purified with the PRK in the previous studies: in both cases the PRK was purified by affinity chromatography on a Rho.GTP column; here we show the co-immunoprecipitation of PDK1 with PRK in a Rho-dependent manner. Further, while the *in vitro* studies presented in chapter 5 are carried out in the presence of Triton X100 concentrations shown to inhibit PDK1 activity, the previous Rho-dependent PRK activations were carried out either in different detergents or in concentrations of Triton X100 that would be ineffective with respect to PDK1 inhibition. Phosphorylation events were shown to be required for both basal and lipid stimulated PRK activity, as judged by PP1 / PP2A pretreatment, and the co-expression of Rho(Q63L) with PRK in 293 cells resulted in an immuoprecipitated kinase with greater autophosphorylation activity. Consistent with these observations previous studies have shown the co-expression of wild-type, and to a greater extent GTPase deficient Rho, with PRK1 results in an immunoprecipitated kinase with increased activity against exogenous substrates (Watanabe, *et al.*, 1996).

PRK phosphorylation *in vitro* was seen to be unchanged in the presence of Triton X100 / phospholipid mixed micelles. Thus the *in vitro* effects of phospholipids on the kinase activity of PRK against MBP are due to a process other that autophosphorylation; possibly the localisation of kinase and substrate on the micelle surface. As mentioned in chapter 5, MBP has been shown to interact with phospholipid micelles through electrostatic and hydrophobic contacts (Boggs, *et al.*, 1981, Palmer and Dawson, 1969). A putative lipid

binding region has been proposed between residues 50-77 of PRK1 (Peng, *et al.*, 1996). The presence of a lipid binding site within this region is backed by analysis of autophosphorylation sites in rat liver-purified PRK1: when the autokinase assay is completed in the presence of cardiolipin a phosphorylation at T64 is not present (Peng, *et al.*, 1996), suggesting a lipid mediated hindrance of the autophosphorylation activity at this site. This is within the now established Rho binding site and the observed Rho inhibition of the PtdIns(4,5)P_2-dependent PRK activation may be explained by a competition for interaction at this site. The unmodified Rho.GTP used in 5.2.2 did not produce an inhibition of the lipid stimulated activity, which may be explained by a simple concentration difference: if more PRK was present within the assays than Rho the remaining free PRK would be able to interact with the PtdIns(4,5)P_2 on the micelle and so come into contact with the substrate at this site. The modified Rho.GTP used in 5.2.6 was in excess with respect to the PRK concentration and completely inhibited the PtdIns(4,5)P_2 effect on kinase activity. The modification would be expected to confer a micelle localisation of the Rho and hence the PRK, however the obvious drop in activity suggests a dislocation of the kinase from the substrate. The Rho.GTP in Triton X100 was mixed with the pre-formed PtdIns(4,5)P_2 mixed micelles, previous work has demonstrated that mixed lipid micelles and pure Triton micelles do not coexist, but rather equilibrate (Hannun, *et al.*, 1985). Thus it was expected that micelles containing both lipid and Rho.GTP would be present in the assay. An obvious way of checking the presence of Rho on the detergent micelle would be by formation, gel filtration and western analysis of both the pelleted micelles and the supernatent. However, discrimination between micelles containing both Rho and PtdIns(4,5)P_2 would be more complicated. Future experiments should be completed in an excess of either modified or unmodified Rho in order to clarify this inhibitory effect. A potential model for these *in vitro* observations is suggested in figure 7.5.

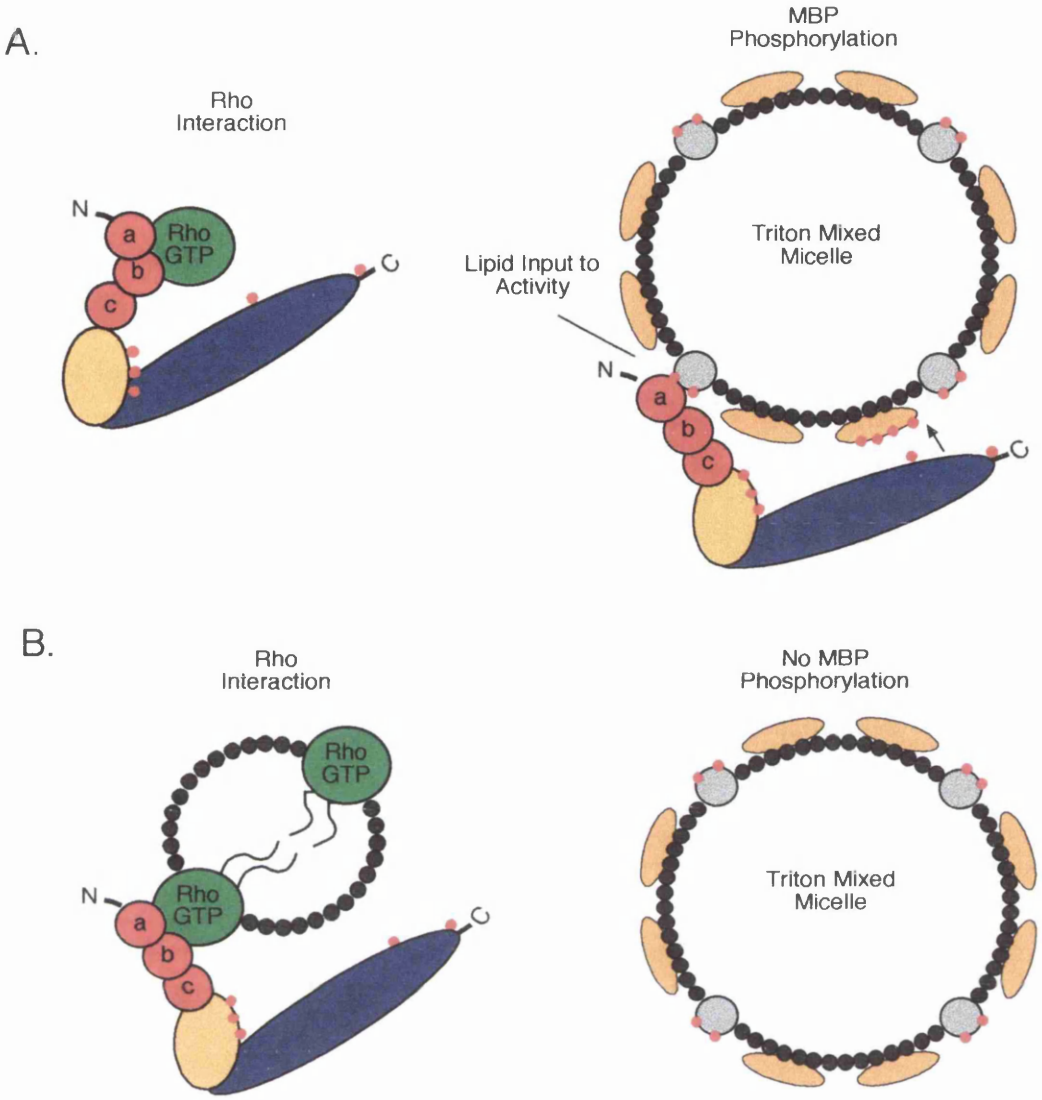

Fig. 7.5 Model for the *in vitro* Lipid and Rho.GTP Dependence of PRK Activity Against MBP.

Representation of putative effect of displaying PtdIns(4,5)P_2 in Triton mixed micelles and Rho to PRK. A.) Unmodified Rho.GTP (green) remains in solution, binding some of the PRK present in the assay; excess PRK is recruited to the Triton mixed micelle by an interaction with PtdIns(4,5)P_2 (grey/red) where the lipid interaction or phosphorylations confers an open active state; the PRK then phosphorylates (phosphate groups small red circles) the MBP (yellow) which is bound to the micelle. B.) Modified Rho may be located within detergent micelles or aggregates seperate from the PtdIns(4,5)P_2 containing micelles and so dislocate the kinase from the substrate.

The *in vitro* data has relevance to the *in vivo* studies using the PI3-kinase inhibitor LY294002. Having established PDK1 as a kinase responsible for PRK activation loop phosphorylation, the treatment of cells with LY294002 blocked this specific phosphorylation event on expression of both full length-PDK1 and ΔPH-PDK1. Previous studies have shown ΔPH-PDK1 to still phosphorylate and activate PKB in a PtdIns(3,4,5)P_3-dependent manner, albeit with a reduction in rate (Alessi, *et al.*, 1997a). This is most likely due to the lipid effects operating through the substrate. The present findings suggest an *in vivo* lipid requirement by PRK that is independent of PDK1. Interestingly another study has been unable to see an effect on the activity of PRK1 immunoprecipitated from adipocytes with a wortmannin treatment (Standaert, *et al.*, 1998). A clear way to resolve whether a direct input of lipid to PRK activation *in vivo* exists is to use a ΔRegulatory-region-PRK in phosphorylation / activity assays in the presence or absence of PI3-kinase inhibitors. However, such a construct has been seen to be unable to translocate to a membrane compartment on RhoB overexpression and may give a negative response for a lipid input purely due to this mislocation. An alternative possibility for the observed input of PI3-kinase products is through the Rho-GTPase. Recent work by Missy *et al* has implicated the PI3-kinase products, especially PtdIns(3,4,5)P_3 in the localisation and nucleotide exchange of RhoA and Rac1 (Missy, *et al.*, 1998). Whether the observed membrane localisation of the GTPases is due to a direct lipid interaction or via a PH domain-containing nucleotide exchange factor has yet to be established. The *in vitro* lipid-dependent PRK activation does not exhibit any particular specificity, whereas the use of PI3-kinase inhibitors would suggest a requirement for either PtdIns(3,4,5)P_3 or PtdIns(3,4)P_2 *in vivo*. Therefore the specificity of the Rho-lipid interaction observed by Missy etal is intriguing with respect to this study.

Ectopically expressed PDK1 has been shown to have a broad cytoplasmic cellular distribution in unstimulated PAE cells (Anderson, *et al.*, 1998) and a

translocation to the plasma membrane on acute PDGF stimulation is seen to be mediated through the resultant increased levels of PtdIns(3,4,5)P_3 produced. This translocation event is associated with the PDK1-dependent PKBα activation. Work completed in collaboration has shown a localisation of a Rho-PRK-PDK1 ternary complex at a previously characterised early endosome compartment that is associated with an accumulation of a hyperphosphorylated form of the PRK (Mellor, *et al.*, 1998). The observation that the ternary complex does not form in the absence of PRK suggests that basal PtdIns(3,4,5)P_3 levels within this compartment are insufficient to cause PDK1 translocation. While the ineffectiveness of a wortmannin treatment demonstrates the maintainence of the complex is dependent upon protein-protein interactions rather than PI3-kinase products. It should be noted that the same inhibitor treatment was previously seen to cause the translocation of PH-domain-containing proteins away from the membrane of adipocytes (Venkateswarlu, *et al.*, 1998).

7.4 PDK1 is the Kinase Responsible for an *in vivo* 'Priming' Event.

AGC-family kinases are highly homologous within their catalytic domains, there are both conserved subdomains and residues that undergo phosphorylation. These phosphorylation events have been shown to effect kinase activity, subcellular localisation and the proteins active lifespan (Bornancin and Parker, 1996, Cazaubon, *et al.*, 1994, Keranen, *et al.*, 1995). A completely conserved threonine residue within the so-called activation loop which lies at the entrance to the catalytic site of the kinases has been shown to be trans-phosphorylated and this phosphorylation event is required to produce and maintain the active conformation (Cazaubon, *et al.*, 1994, Orr and Newton, 1994). Indeed, irrespective of the various regulatory inputs, it is this phosphorylation event which 'primes' the kinases allowing subsequent autophosphorlation and hence activation. With particular reference to PRK, a

study of the autophosphorylation sites of the kinase identified T778 in rat PRK1 (T774 in human) as being phosphorylated *in vivo* and dissociated it from the subsequent autophosphorylation events (Peng, *et al.*, 1996). As mentioned in chapters 1 and 6, PDK1 has been identified as the kinase responsible for this trans-phosphorylation event on many members of the AGC kinase family. And in chapter 6 PDK1 is shown to specifically phosphorylate the equivalent residue in PRK1 and PRK2.

In vitro studies using the truncated GST-PRK1kin indicated the PDK1-dependent phosphorylation event was independent of lipids, although the use of a full length PRK construct may well have resulted in a degree of lipid or Rho dependence. This is also the case for truncated PKB and $p70^{S6K}$ (Alessi, *et al.*, 1997a, Alessi, *et al.*, 1998, Stokoe, *et al.*, 1997). While the *in vitro* phosphorylation resulted in a pronounced activation of the PRK kinase domain, the co-expression of PDK1 in mammalian cells was insufficient to produce increased immunoprecipitated PRK activity. This is not the case for other PDK1 substrates; PKB, $p70^{S6k}$ and PKCζ all show an increased immunoprecipitated activity on co-expression with PDK1 (Chou, *et al.*, 1998, Dong, *et al.*, 1999, Pullen, *et al.*, 1998, Stephens, *et al.*, 1998). Calculating the stoichiometry of PRK phosphorylation may clarify this difference. The Rho and PDK1 co-expression did not act synergistically with respect to PRK activation loop phosphorylation suggesting that either there is another limiting factor or the site of phosphorylation is acutely dephosphorylated. Indeed, the use of phosphatase inhibitors resulted in a much greater activation loop phosphorylation and a mobility shift on SDS-PAGE. Associated with these effects was an increase in immunopurified activity and while the use of point mutations determined the T816 / T774 phosphorylation event to be critical for activation, whether the other modifications were required for the activity increase is uncertain. However, it would seem that activation loop phosphorylation of PRK by PDK1 is a priming event; it is this modification which

renders the kinase catalytically competent, allowing potential autophosphorylation and subsequent further activation.

7.5 PDK1 Specificity is Altered by the PRK Interaction

It is now well characterised that members of the AGC kinase family require the dual phosphorylation of the activation loop threonine as well as a conserved carboxy terminal serine or threoinine residue (labelled FSY-site in figure 6.1) for full activation (Alessi and Cohen, 1998). As demonstrated in the present study, PDK1 is responsible for the activation loop phosphorylation event, but the kinase responsible for the second site modification has until recently remained elusive. The PRK and atypical PKC (ζ and ι) kinases have an acidic residue at this second site and in a recent study by Balendran *et al* this residue has been shown to be critical for the PDK1 interaction (Balendran, *et al.*, 1999). Further, they convincingly demonstrate that when bound to PDK1 a 77 amino acid peptide covering the carboxy-terminus of PRK2 converts the kinase enabling it to phosphorylate both the activation loop (T308) and FSY-site (S473) residues of PKBα. The allosteric effect produced by the peptide contact not only alters the substrate specificity of PDK1 but also results in an *in vitro* lipid dependence not previously seen. It is intriguing that the PRK / atypical PKC class of kinases may act as priming molecules: PDK1 can interact with them directly due to the acidic residue at the FSY site; they are phosphorylated within their activation loops and so activated by PDK1; the contact also converts PDK1 so allowing it to phosphorylate the FSY-site of other AGC kinases, resulting in a potential PDK1 binding site (should a phosphorylated serine / threonine residue confer binding). Further evidence for the involvement of the atypical class of PKCs in the phosphorylation of the FSY-site is offered by the observed role of PKCζ in the phosphorylation of PKCδ at this residue (Ziegler, *et al.*, 1999). The binding of PDK1 to the FSY-site of these other kinases would now allow activation loop

phosphorylation and activation. The lipid dependence of these phosphorylation events suggest membrane localisation is required. However, mutagenesis studies of the T308 and S473 residues would indicate that the S473 phosphorylation is required intrinsically for PKBα activity, beyond a mere PDK1 binding signal: the phosphorylation of a T308D mutant at S473 leads to a substantial increase in catalytic activity (Alessi, *et al.*, 1996). Whether the intact PRK or atypical PKC kinases produce such a change in PDK1 specificity *in vivo* is unclear. The former would implicate the Rho GTPases as potential upstream regulators of PDK1 specificity. The effect of C3 toxin on this specificity would be an obvious first step to characterising this regulation.

7.6 The Mechanism of PRK Activation by Rho.

As outlined in section 5.1, the small GTPases have been shown to act as switches, conferring an active state to their respective effector kinases. While the detailed processes of many of these activation events are yet to be fully elucidated, the translocation of the kinases to a site of co-activators and substrate is thought to be a common mechanism. As seen in both this and other studies, Rho has been implicated in the translocation, phosphorylation and activation of the PRKs (Amano, *et al.*, 1996b, Mellor, *et al.*, 1998, Vincent and Settleman, 1997, Watanabe, *et al.*, 1996). The involvement of the Rho contact with the amino-terminal HR1 domain of PRK in the activation of the kinase would seem to revolve around the possible disruption of an autoinhibitory interaction and the translocation of the kinase to a membrane compartment (Kitagawa, *et al.*, 1996, Mellor, *et al.*, 1998). The RhoB-dependent translocation of PRK is associated with a hyperphosphorylated form. Further, PDK1 is shown to translocate to the same compartment interact with PRK in a Rho-dependent manner and specifically phosphorylate the activation loop, resulting in the catalytic competence of the Rho effector. The *in vitro* PRK-PDK1 complex is

demonstrated to be Rho-dependent and although the constitutive PRK1-PDK1 complex was not inhibited with C3, other small GTPases have been seen to interact specifically with the PRKs (Vincent and Settleman, 1997).

Rho GTPases in the GDP-bound form have been shown to be held in the cytoplasm by an interaction with guanine dissociation inhibitors (GDI) which masks their carboxy-terminal lipid moieties (Sasaki and Takai, 1998). It is the subsequent mitogen activated or cell cycle dependent tranlocation of RhoA to membrane compartments which results in its effective activation. The dissociation of the GDI, induced by an interaction with ERM proteins allows the Rho to bind to the membrane via its modification (Takahashi, *et al.*, 1997) and the subsequent activity of guanine nucleotide exchange factors (GEF) results in a GTP-bound Rho. While the mechanism of the translocation event is unclear the recruitment of the GEFs to sites rich in PI3-kinase products through their PH-domains may act as a specific targeting signal for the Rho GTPases. The GTP-loaded proteins then recruit their relative effectors to the membrane where they can come into contact with both co-activators and substrates. RhoB is seen to be constitutively at the membrane within the early endosomal compartment and thus may be under the control of specific GDI proteins that interact with the membrane. One such GDI has been identified, RhoGDI-3 (Zalcman, *et al.*, 1996). Thus the GTP-loading of this EGF and cell cycle-induced Rho isoform may be controlled *in situ* at the surface of the endosomes.

In chapter 4 of this study an interaction between RhoA.GDP and the HR1b subdomain of PRK was demonstrated. The biological relevance of this is unclear, however, it is plausible that a Rho.GDP - PRK interaction functions *in vivo*. This may be the only contact made between the two proteins in the cytoplasm; should the HR1a be effectively masked by a pseudosubstrate site - catalytic domain interaction. Another nucleotide independent GTPase - effector interaction has seen to take place between Rac and the lipid kinases phosphatidyl-inositol-4-phosphate 5 kinase or diacyl glycerol kinase (Tolias, *et*

al., 1995). More recently RhoGDI was seen to be associated with the Rac - lipid kinase heterodimer but was not necessary for the complex formation (Tolias, *et al.*, 1998) .Thus a putative scenario could be envisaged where a Rho.GDP - GDI heterodimer can interact with inactive PRK within the cytoplasm and the whole complex is then translocated to a membrane compartment upon agonist stimulated PI3-kinase activation. The interaction of Rho with the membrane-bound GEF would result in a Rho.GTP able to interact with HR1a subdomain: it has been seen that the Rho-HR1a interaction is completely dependent on GTP (Flynn, *et al.*, 1998). The subsequent disruption of the autoinhibitory intramolecular interaction would allow PDK1 to bind to PRK's carboxy-terminal 'FSY' site. It is assumed that PDK1 would be present at the same membrane site due to the locally enriched PI3-kinase products, but the subsequent interaction with PRK would be responsible for maintaining it at the membrane. The PDK1 phosphorylation of PRK within the activation loop would prime the Rho effector, allowing subsequent autophosphorylation and hence full activation. Further, the complex formation with PRK may result in a PDK1 capable of causing complete activation of PKBα or other AGC-kinase family members. A model for this scenario can be seen in figure 7.6. The observed interaction between PRK and RhoB at the membrane within the early endosome compartment may follow the same scheme but without the co-translocation event.

While this model for the regulation of PRK activity is highly speculative, many of the proposed events are experimentally accessible. The involvement of the GEFs in the recruitment of both the Rho and PRK to the membrane compartment could be tested through the inducible expression of a membrane targeted protein: a GEFcaax linked to an estrogen receptor would allow the selective expression of the construct by estradiol/tamoxifen treatment. Such a system has been previously used in another context (Hambleton, *et al.*, 1995). A ΔHR1-PRK protein was seen not to translocate to the early endosomal compartment on

RhoB overexpression (Mellor, *et al.*, 1998). The involvement of the HR1b subdomain in this process could be investigated with the use of either a ΔHR1b or double HR1a constructs.

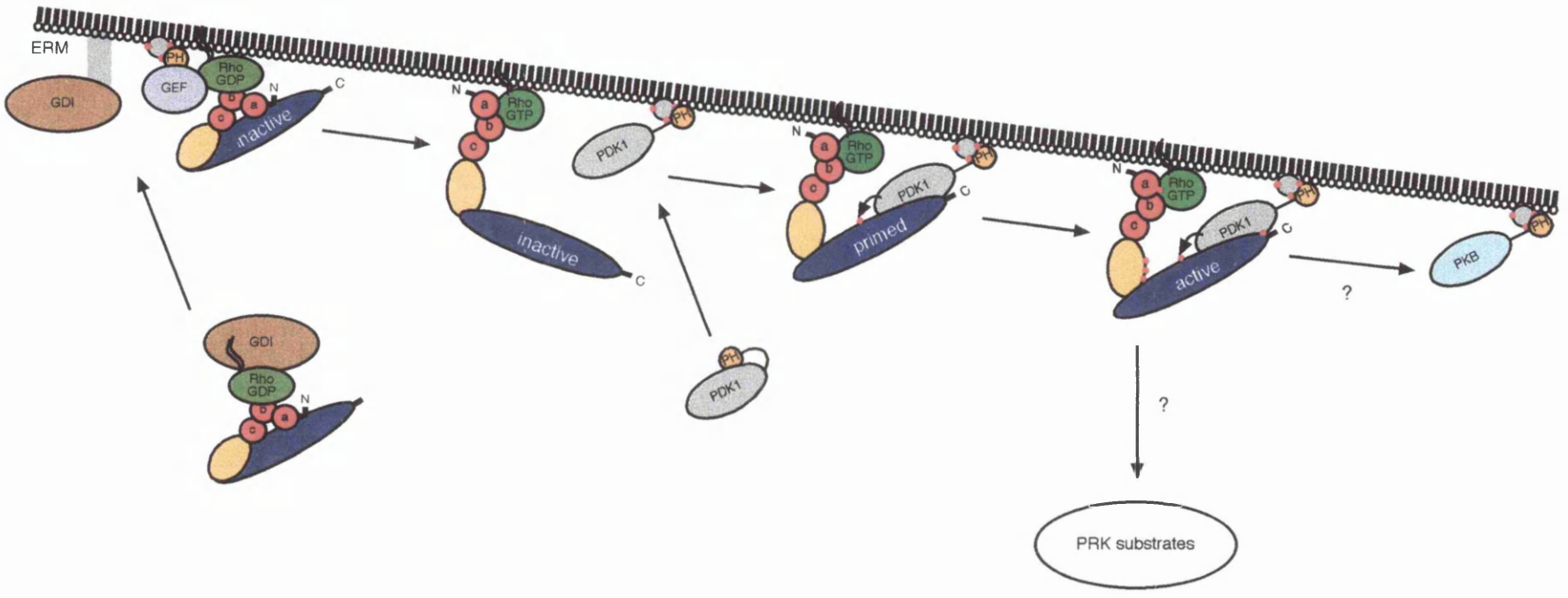

Fig. 7.6: Model of Rho-Regulated PRK Activation.

Putative model of the Rho-dependent activation of PRK *in vivo:* autoinhibited PRK interacts with a Rho.GDP - GDI complex in the cytosol; on mitogenic stimulation of PI3-kinase the localised increase in PtdIns(3,4,5)P_3 causes a translocation of the PRK complex to the membrane. The GDI is displaced by an interaction with ERM proteins and a GEF interaction with Rho. The Rho exchanges GDP for GTP and in now able to interact with PRK's HR1a so disrupting the autoinhibitory contact. PDK1 has tranlocated to the same compartment through a PH-domain - PtdIns(3,4,5)P_3 interaction and is now able to bind PRK's exposed carboxy-terminus. PDK1 phosphorylates PRK within its activation loop, so priming the Rho effector. Subsequent autophosphorylation events result in a fully active kinase capable of activity against *in vivo* substrates. The PDK1-PRK complex may now function to fully activate other AGC-kinase family members in a PtdIns(3,4,5)P_3-dependent manner.

7.7 PRK and the Regulation of Cellular Processes

7.7.1 Cytoskeletal Organisation

The identification of Rho effectors has led to a much greater understanding of this GTPase's involvement in actin stress fibre formation. The Rho dependent increase in ROCK kinase activity results in increased myosin phosphorylation and hence actin-myosin contractility. In a recent study by Watanabe and co-workers the mode of Rho dependent filamentous actin formation through the diaphanous homologue mDia1 has been described (Watanabe, *et al.*, 1999). Further, a co-operation with the ROCK mediated effects results the formation of actin fibres of various thicknesses and densities. Only one study to date has implicated the PRKs in Rho dependent effects on the formation of stress fibres (Vincent and Settleman, 1997). However, the negative effect on stress fibre formation seen with a kinase dead PRK2 could not be reciprocated with the use of a wild type enzyme.

As described in chapter 1 PRK may induce intermediate filament (IF) disassembly through specific phosphorylation events (Matsuzawa, *et al.*, 1997, Mukai, *et al.*, 1996). On reflection of the data presented in this thesis the involvement of PRK in this process would require an input from both Rho and PDK1, hence PI3-kinase. The microinjection of GTPase deficient Rho into sub-confluent Swiss 3T3 cells resulted in the collapse of intermediate filaments into irregular bundles, as visualised with anti-vimentin antibodies (Paterson, *et al.*, 1990). A more recent study in PAE cells has demonstrated a reorganisation of vimentin filaments into a dense coil around the nucleus on acute PDGF stimulation. Further, the expression of a PDGF receptor negative for PI3-kinase binding produced a cell where the vimentin organisation was unaffected on stimulation (Valgeirsdottir, *et al.*, 1998). Thus placing PI3-kinase on a pathway which results in IF reorganisation. However, PRK is not the only Rho effector to be associated with IFs; Rho-kinase has been shown to phosphorylate a unique

site on vimentin (Goto, *et al.*, 1998). This residue was only phosphorylated at the cleavage furrow of late mitotic cells and a later study by the same group shows Rho-kinase to co-localise with IF bundles at this site (Kosako, *et al.*, 1999). It is of interest that intermediate filaments, like PRKs are seen to be proteolytically cleaved by caspases during the apoptotic process (Prasad, *et al.*, 1999). The culmination of direct cleavage of these cytoskeletal components and their disassembly through phosphorylation by an active fragment of PRK may result in the effective disposal of these insoluble structures during cell death.

The characterisation of a loss of function mutant for *Drosophila* PRK homologue Pkn demonstrated a dorsal closure defect most likely resulting from a lack of stretching in the leading edge (LE) cells of the lateral epidermis (Lu and Settleman, 1999). Rho loss of function mutants exhibit the same phenotype as well as other defects, suggesting multiple downstream effectors. Disruption of the JNK kinase cascade, which results in the expression of dpp (a TGFβ receptor ligand), also has the defective dorsal closure phenotype. The apparently normal expression of dpp in Pkn loss-of-function mutants would seemingly discount it from operating downstream of a Rac homologue on this pathway. The mechanism of Rho-dependent LE cell stretching is unknown but the gross cellular morphological changes required ultimately implicate cytoskeletal reorganisation.

7.7.2 Transcriptional Activation

While Rho family members Rac and CDC42 are established as upstream regulators of the SAPK/JNK kinase cascade which leads to transcriptional activation via c-Jun (Coso, *et al.*, 1995, Minden, *et al.*, 1995) Rho itself has only been demonstrated to activate this pathway in one cell type (Teramoto, *et al.*, 1996). More recent evidence of a Rho involvement in this system comes from the observation that the DH domain GEF mNET1 is able to activate the

SAPK/JNK pathway through a C3 toxin-sensitive component (Alberts and Treisman, 1998). However, the lack of effect of V14.RhoA overexpression implicates either RhoB or C in this process. There is no evidence of a direct involvement of PRKs in this signalling pathway. A more intriguing link between PRK and transcription is through the observed Rho-dependent activation of the Serum Response Factor (SRF) (Hill, *et al.*, 1995). The signalling components downstream of Rho on this pathway have remained elusive for several years but several lines of evidence implicate both PRK and ROCK kinases in this process. PRK2 has been shown to synergise with Rho in the activation of a SRF-luciferase reporter gene construct (Quilliam, *et al.*, 1996). The same study also showed a synergy of the kinase with both Rac and CDC42, the latter being surprising considering the lack of evidence for a PRK-CDC42 interaction. The use of Rho effector domain mutants that have differential effector binding patterns showed SRF activation to be inhibited by Rho mutants with reduced binding potential for both PRK1 and ROCK (Sahai, *et al.*, 1998). Further, a ROCK truncation lacking a Rho binding site was seen to cause a SRF reporter gene activation that was still dependent upon active Rho, suggesting the co-operative role of another Rho effector. While this other effector has yet to be identified it is possible that a PRK-PDK1 complex is involved. As mentioned in section 7.5 the interaction of PDK1 with PRK's V_5 region results in the former being able to act as a FSY site kinase as well as a activation loop kinase. ROCK kinases contain a typical V_5 domain sequence and are thus potential effectors of PDK1 activity. ROCK recruitment to the early endosomal compartment seen to contain PRK, PDK1 and RhoB has not been observed, however the co-recruitment of the two Rho effector to another compartment is possible. An obvious method for determining whether PRK acts to potentiate PDK1 activity towards ROCK (or any other AGC-family kinase) would be to mutate the FDF / FDY sequence in PRK seen to be vital for PDK1 interaction. The role of PRK in the activation of ROCK is the subject of an ongoing study.

7.7.3 Glut4 Translocation and Glucose Uptake

Insulin stimulated glucose uptake from the extracellular environment is mediated through the translocation of vesicles containing glucose transporters (Glut4 or the ubiquitously expressed Glut1) from the cytoplasm to the plasma membrane. The mechanism by which insulin produces this translocation has been the subject of intense study and has implicated several signalling components. The translocation event and hence glucose transport can be blocked by the PI3-kinase specific inhibitor LY294002 (Cheatham, *et al.*, 1994). PI3-kinase-IRS1 complexes are seen to be associated with Glut4-containing vesicles and an increase in the detectable levels of p85 at this site on insulin stimulation is associated with increased PI3-kinase activity (Heller, *et al.*, 1996). PKB has been implicated as a potential effector for PI3-kinase products at this site and the expression of a constitutively membrane localised form of this kinase results in increased Glut4 and Glut1 translocation and Glucose uptake (Kohn, *et al.*, 1996). However, a more recent study has shown an inactive PKB (double alanine at residues 308 and 473) has no effect on glucose uptake in 3T3 L1 adipocytes (Kitamura, *et al.*, 1998). The involvement of Rho in these processes has been established through the use of C3 toxin and later GTPase deficient mutants (Karnam, *et al.*, 1997, Standaert, *et al.*, 1998). Thus the two characterised activators of PRK activity would seem to be involved. The stable overexpression of PRK itself is seen to increase glucose transport in 3T3 L1 cells and the transient overexpression of either dominant negative Rho or kinase dead PRK results in a partial inhibition of both insulin and GTPγS stimulated Glut4 translocation (Standaert, *et al.*, 1998). This would suggest that PRK activity is required for these events beyond merely its presence as a scaffold for PDK1 signalling events. However, in the absence of immunohistochemistry data for PRK localisation within adipocytes it is not clear whether a complex of these various components is formed at the surface of the Glut4 vesicles.

7.7.4 Endocytosis

Previous work had demonstrated the association of PRK1 with early endosomes in a RhoB-dependent manner, a translocation event that results in the accumulation of a hyperphosphorylated form of the kinase (Mellor, *et al.*, 1998). The data presented in chapter 6 of this thesis would suggest that the co-localisation of PDK1 with PRK and Rho within this compartment results in the activation of the Rho effector (Flynn, Mellor, Parker, submitted). RhoA has been shown to regulate the clatherin-mediated internalisation of the transferrin receptor (Lamaze, *et al.*, 1996). Different receptors undergo different fates after activation; the transferrin receptor is internalised, processed and recycled to the plasma membrane whereas the greater proportion of EGF receptors are internalised and targeted to the lysosomal compartment for degradation (Sorkin and Water, 1993). In an attempt to define RhoB function within the early endosomal compartment a study by Mellor and co-workers has shown the EGF internalisation to be independent of RhoA but the resulting endosome trafficking dependent upon RhoB (Gampel, Parker and Mellor, submitted). The expression of either a wildtype or GTPase deficient RhoB resulted in the retardation of vesicle movement from early to late endosome compartments. Further, the expression of a wildtype PRK1 potentiated this RhoB effect while kinase dead PRK1 completely inhibited it. Thus the RhoB effect on endosomal traffic is mediated through PRK.

While the mechanism for such an effect is unclear a candidate PRK substrate may be the cytoplasmic linker proteins (CLIPs). As described in chapter 1 the trafficking of endosomes along microtubules is mediated by the dynein motors. However, the binding of the endosomes to the microtubules is also dependent upon other cytoplasmic proteins, namely CLIPs. These proteins consist of a microtubule binding motif, a central coil-coil region and a predicted metal-binding domain which may mediate protein-protein interactions on the surface of endosomes (reviewed by (Rickard and Kreis, 1996)). The CLIPs are highly

phosphorylated on serine residues *in vivo* and these modifications inhibit the proteins association with microtubules. *In vitro* studies have demonstrated CLIP 170 phosphorylation by immunopurified PRK1 although the exact sites of phosphorylation have yet to be confirmed (H. Mellor and T. Kreis unpublished work). Thus a model for the observed PRK effects on endosomal traffic may be: I) PI3-kinase activity results in both the recruitment of PDK1 to the surface of the endosome and RhoB nucleotide exchange; ii) subsequent localisation of PRK with the active Rho results in its activation via PDK1 kinase activity; iii) PRK activity results in the phosphorylation of CLIP resulting in the endosome disengaging from the microtubule.

The retardation of endosomal traffic would result in the prolonged signalling from the EGF receptor prior to degradation within the lysosome. It may also be the case that different signalling systems are activated depending upon the location of the receptor within the cell. Thus RhoB action through PRK could to regulate signalling events from the EGF receptor in both a spatial and temporal manner.

Appendices

I : Calculation of GTPase Loading Capacities.

Theory: pMol GTPase (100% loading) = x dpm expected

$\therefore$ $\frac{\text{Actual cpm X 10}}{\text{1.03 (cpm-dpm conversion)}}$ = y dpm actual

$\therefore$ $\frac{\text{y dpm actual}}{\text{x dpm expected}}$ = % loading

(Actual cpm is multiplied by 10 due to GTP / [α^{32}P] GTP ratio conversion)

Example: 3.27 pMol RhoA is expected to load 3.27 pMol GTP.

1 pMol [α^{32}P] GTP = $0.66X10^6$ dpm

$\therefore$ 3.27 pMol [α^{32}P] GTP = $2.16X10^6$ dpm

$\therefore$ Actual cpm: $\frac{\text{64774 cpm X 10}}{\text{1.03}}$ = $0.629X10^6$ dpm

$\therefore$ % loading: $\frac{0.629X10^6 \text{ dpm}}{2.16X10^6 \text{ dpm}}$ = 29.1 %

II : PCR Primers for the Production of GST-PRK1kin

5' CCCGGATCCACCATGTGCAGCCCTCTGAGGAAG 3'
BamH1 Internal PRK1 sequence

5' GGGGCGGCCGCGGTTCAGCCCCCGGCCACGAA 3'
Not1 Internal PRK1 sequence

III : PCR Primers for the Mutagenesis of PRK2 T816

T816A

Sense: 5' GATAGAACAAGCGCATTTTGTGGCACT 3'

Reverse Complement: 5' AGTGCCACAAAATGCGCTTGTTCTATC 3'
T--A

T816E

Sense: 5' GATAGAACAAGCGAATTTTGTGGCACT 3'

Reverse Complement: 5' AGTGCCACAAAACTTGCTTGTTCTATC 3'
T--E

IV : Immunofluorescence Microscopy Protocol (Dr H. Mellor).

Cells were processed for indirect immunofluorescence microscopy as described previously (Mellor, *et al.*, 1998). The cells were fixed in 4% (w/v)

paraformaldehyde for 15 minutes and permeabilised with 0.2% (v/v) Triton X-100 for 5 minutes. Autofluorescence was quenched by incubation with 0.1% (w/v) sodium borohydride for 10 minutes. Cells were incubated in primary antibody in PBS containing 1% (w/v) BSA for 1h and fluorescent dye-conjugated secondary antibody for 45 minutes. All incubations were performed in PBS. Cells were mounted under MOWIOL 4-88 (Calbiochem) containing 0.6% (w/v) 1,4-diazabicyclo-(2.2.2)octane as an antiphotobleaching agent and were viewed using a Leica DM RBE confocal microscope equipped with a Plan APO x63/1.4 oil immersion lens. Cy2 and Cy3 were excited using the 488nm and 568nm lines of a Kr-Ar laser. Series of images were taken at 0.5mm intervals through the Z-plane of the sample and were processed to form a projected image.

References

Abo, A., Boyhan, A., West, I., Thrasher, A. J. and Segal, A. W., J Biol Chem **267:** 16767-70 (1992)

Adamson, P., Paterson, H. F. and Hall, A., J Cell Biol **119:** 617-27 (1992)

Adari, H., Lowy, D. R., Willumsen, B. M., Der, C. J. and McCormick, F., Science **240:** 518-21 (1988)

Aktories, K., Braun, U., Rosener, S., Just, I. and Hall, A., Biochem Biophys Res Commun **158:** 209-13 (1989)

Alberts, A. S., Bouquin, N., Johnston, L. H. and Treisman, R., J Biol Chem **273:** 8616-22 (1998)

Alberts, A. S. and Treisman, R., Embo J **17:** 4075-85 (1998)

Alessi, D. R., Andjelkovic, M., Caudwell, B., Cron, P., Morrice, N., Cohen, P. and Hemmings, B. A. H., EMBO **15:** 6541-51(1996)

Alessi, D. R. and Cohen, P., Curr Opin Genet Dev **8:** 55-62 (1998)

Alessi, D. R., Deak, M., Casamayor, A., Caudwell, F. B., Morrice, N., Norman, D. G., Gaffney, P., Reese, C. B., MacDougall, C. N., Harbison, D., Ashworth, A. and Bownes, M., Curr Biol **7:** 776-89 (1997a)

Alessi, D. R., James, S. R., Downes, C. P., Holmes, A. B., Gaffney, P. R., Reese, C. B. and Cohen, P., Curr Biol **7:** 261-9 (1997b)

Alessi, D. R., Kozlowski, M. T., Weng, Q. P., Morrice, N. and Avruch, J., Curr Biol **8:** 69-81 (1998)

Amano, M., Chihara, K., Kimura, K., Fukata, Y., Nakamura, N., Matsuura, Y. and Kaibuchi, K., Science **275:** 1308-11 (1997)

Amano, M., Ito, M., Kimura, K., Fukata, Y., Chihara, K., Nakano, T., Matsuura, Y. and Kaibuchi, K., J Biol Chem **271:** 20246-20249 (1996a)

Amano, M., Mukai, H., Ono, Y., Chihara, K., Matsui, T., Hamajima, Y., Okawa, K., Iwamatsu, A. and Kaibuchi, K., Science **271:** 648-50 (1996b)

Anderson, K. E., Coadwell, J., Stephens, L. R. and Hawkins, P. T., Curr Biol **8:** 684-91 (1998)

Anderson, R. A., Boronenkov, I. V., Doughman, S. D., Kunz, J. and Loijens, J. C., J Biol Chem **274:** 9907-10 (1999)

Andjelkovic, M., Alessi, D. R., Meier, R., Fernandez, A., Lamb, N. J., Frech, M., Cron, P., Cohen, P., Lucocq, J. M. and Hemmings, B. A., J Biol Chem **272:** 31515-24 (1997)

Andjelkovic, M., Maira, S. M., Cron, P., Parker, P. J. and Hemmings, B. A., Mol Cell Biol **19:** 5061-72 (1999)

Arellano, M., Duran, A. and Perez, P., Embo J **15:** 4584-91 (1996)

Bagrodia, S., Taylor, S. J., Creasy, C. L., Chernoff, J. and Cerione, R. A., J Biol Chem **270:** 22731-7 (1995)

Balendran, A., Casamayor, A., Deak, M., Paterson, A., Gaffney, P., Currie, R., Downes, C. P. and Alessi, D. R., Curr Biol **9:** 393-404 (1999)

Banfic, H., Tang, X., Batty, I. H., Downes, C. P., Chen, C. and Rittenhouse, S. E., J Biol Chem **273:** 13-6 (1998)

Bellacosa, A., Testa, J. R., Staal, S. P. and Tsichlis, P. N., Science **254:** 274-7 (1991)

Bellanger, J. M., Lazaro, J. B., Diriong, S., Fernandez, A., Lamb, N. and Debant, A., Oncogene **16:** 147-52 (1998)

Bence, K., Ma, W., Kozasa, T. and Huang, X. Y., Nature **389:** 296-9 (1997)

Berridge, M. J. and Irvine, R. F., Nature **312:** 315-321 (1984)

Boggs, J. M., Wood, D. D. and Moscarello, M. A., Biochemistry **20:** 1065-73 (1981)

Boguski, M. S. and McCormick, F., Nature **366:** 643-54 (1993)

Bornancin, F. and Parker, P., Curr. Biol. **VOL: 6:** P: 1114-1123 (1996)

Bos, J. L., Cancer Res **49:** 4682-9 (1989)

Bourne, H. R., Curr Opin Cell Biol **9:** 134-42 (1997)

Bradford, M. M., Anal. Biochem. **72:** 248-254 (1976)

Brown, R. A., Domin, J., Arcaro, A., Waterfield, M. D. and Shepherd, P. R., J Biol Chem **274:** 14529-32 (1999)

Burgering, B. M. and Coffer, P. J., Nature **376:** 599-602 (1995)

Burns, P. F., Campagnoni, C. W., Chaiken, I. M. and Campagnoni, A. T., Biochemistry **20:** 2463-9 (1981)

Cales, C., Hancock, J. F., Marshall, C. J. and Hall, A., Nature **332:** 548-51 (1988)

Campbell, S. L., Khosravi, F. R., Rossman, K. L., Clark, G. J. and Der, C. J., Oncogene 1395-413 (1998)

Castrillon, D. H. and Wasserman, S. A., Development **120:** 3367-77 (1994)

Cazaubon, S., Bornancin, F. and Parker, P. J., Biochem. J. **301:** 443-448 (1994)

Cazaubon, S. M. and Parker, P. J., J. Biol. Chem. **268:** 17559-17563 (1993)

Cerione, R. A. and Zheng, Y., Curr Opin Cell Biol **8:** 216-22 (1996)

Chardin, P., Boquet, P., Madaule, P., Popoff, M. R., Rubin, E. J. and Gill, D. M., Embo J **8:** 1087-92 (1989)

Chardin, P., Madaule, P. and Tavitian, A., Nucleic Acids Res **16:** 2717 (1988)

Cheatham, B., Vlahos, C. J., Cheatham, L., Wang, L., Blenis, J. and Kahn, C. R., Mol Cell Biol **14:** 4902-11 (1994)

Chen, C. A. and Okayama, H., BioTechniques **6:** 632-638 (1988)

Cheng, X., Ma, Y., Moore, M., Hemmings, B. A. and Taylor, S. S., Proc Natl Acad Sci U S A **95:** 9849-54 (1998)

Chong, L. D., Traynorkaplan, A., Bokoch, G. M. and Schwartz, M. A., Cell **79:** 507-513 (1994)

Chou, M. M. and Blenis, J., Cell **85:** 573-583 (1996)

Chou, M. M., Hou, W., Johnson, J., Graham, L. K., Lee, M. H., Chen, C. S., Newton, A. C., Schaffhausen, B. S. and Toker, A., Curr Biol **8:** 1069-77 (1998)

Coffer, P. J. and Woodgett, J. R., Eur. J. Biochem. **201:** 475-481 (1991)

Cooke, F. T., Dove, S. K., McEwen, R. K., Painter, G., Holmes, A. B., Hall, M. N., Michell, R. H. and Parker, P. J., Curr Biol **8:** 1219-22 (1998)

Coso, O. A., Chiariello, M., Yu, J. C., Teramoto, H., Crespo, P., Xu, N., Miki, T. and Gutkind, J. S., Cell **81:** 1137-46 (1995)

Coussens, L., Parker, P. J., Rhee, L., Yang-Feng, T. L., Chen, E., Waterfield, M. D., Francke, U. and Ullrich, A., Science **233:** 859-866 (1986)

Crespo, P., Schuebel, K. E., Ostrom, A. A., Gutkind, J. S. and Bustelo, X. R., Nature **385:** 169-72 (1997)

Cross, D. A. E., Alessi, D. R., Cohen, P., Andjelkovich, M. and Hemmings, B. A., Nature **378:** 785-789 (1995)

Cryns, V. L., Byun, Y., Rana, A., Mellor, H., Lustig, K. D., Ghanem, L., Parker, P. J., Kirschner, M. W. and Yuan, J., J Biol Chem **272:** 29449-53 (1997)

De Camilli. P., Emr, S. D., McPherson, P. S. and Novick, P., Science **271:** 1533-9 (1996)

De Rooij, J., and Bos, J. L., Oncogene **14:** 623-5 (1997)

Denhardt, D., Biochem. J. **: 318:** P: 729-747 (1996)

Diekmann, D., Nobes, C. D., Burbelo, P. D., Abo, A. and Hall, A., EMBO J. **14:** 5297-5305 (1995)

Didichenko, S. A. Tilton, B. Hemmings, B. A. Ballmer, Hofer K. Thelen, M., Curr Biol **10**: 1271-8 (1996)

Domin, J., Pages, F., Volinia, S., Rittenhouse, S. E., Zvelebil, M. J., Stein, R. C. and Waterfield, M. D., Biochem J **326:** 139-47 (1997)

Dong, L. Q., Zhang, R. B., Langlais, P., He, H., Clark, M., Zhu, L. and Liu, F., J Biol Chem **274:** 8117-22 (1999)

Dove, S. K., Cooke, F. T., Douglas, M. R., Sayers, L. G., Parker, P. J. and Michell, R. H., Nature **390:** 187-92 (1997)

Downward, J., Curr Opin Cell Biol **10:** 262-7 (1998)

Drechsel, D. N., Hyman, A. A., Hall, A. and Glotzer, M., Curr Biol **7:** 12-23 (1997)

Dutil, E. M., Toker, A. and Newton, A. C., Curr Biol **8:** 1366-75 (1998)

Evangelista, M., Blundell, K., Longtine, M. S., Chow, C. J., Adames, N., Pringle, J. R., Peter, M. and Boone, C., Science **276:** 118-22 (1997)

Fleming, I. N., Elliott, C. M. and Exton, J. H., J Biol Chem **271:** 33067-73 (1996)
Flint, A. J., Paladini, R. D. and Koshland Jnr, D. E., Science **249:** 408-411 (1990)

Flynn, P., Mellor, H., Palmer, R., Panayotou, G. and Parker, P. J., J Biol Chem **273:** 2698-705 (1998)

Franke, T. F., Yang, S. I., Chan, T. O., Datta, K., Kazlauskas, A., Morrison, D. K., Kaplan, D. R. and Tsichlis, P. N., Cell **81:** 727-36 (1995)

Freeman, J. L., Abo, A. and Lambeth, J. D., J Biol Chem **271:** 19794-801 (1996)

Fujisawa, K., Madaule, P., Ishizaki, T., Watanabe, G., Bito, H., Saito, Y., Hall, A. and Narumiya, S., J Biol Chem **273:** 18943-9 (1998)

Fukami, K., Furuhashi, K., Inagaki, M., Endo, T., Hatano, S. and Takenawa, T., Nature **359:** 150-2 (1992)

Gawler, D. J., Biochim Biophys Acta **1448:** 171-82 (1998)

Gehrmann, T. and Heilmeyer, L. J., Eur J Biochem **253:** 357-70 (1998)

Gibbs, J. B., Marshall, M. S., Scolnick, E. M., Dixon, R. A. and Vogel, U. S., J Biol Chem **265:** 20437-42 (1990)

Goto, H., Kosako, H., Tanabe, K., Yanagida, M., Sakurai, M., Amano, M., Kaibuchi, K. and Inagaki, M., J Biol Chem **273:** 11728-36 (1998)

Gutmann, D. H. and Collins, F. S., Neuron **10:** 335-43 (1993)

Haas, K. D., Shalev, N., Wong, M., Mills, G., Yount, G. and Stokoe, D., Curr Biol **8:** 1195-8 (1998)

Hambleton, J., McMahon, M. and DeFranco, A. L., J Exp Med **182:** 147-54 (1995)

Hamm, H. E., J Biol Chem **273:** 669-72 (1998)

Hamm, H. E. and Gilchrist, A., Curr Opin Cell Biol **8:** 189-96 (1996)

Han, J., Luby, P. K., Das, B., Shu, X., Xia, Y., Mosteller, R. D., Krishna, U. M., Falck, J. R., White, M. A. and Broek, D., Science **279:** 558-60 (1998)

Hanks, S. K. and Hunter, T., Faseb J **9:** 576-96 (1995)

Hannun, Y. A., Loomis, C. R. and Bell, R. M., J. Biol. Chem. **260:** 10039-10043 (1985)

Hart, M. J., Jiang, X., Kozasa, T., Roscoe, W., Singer, W. D., Gilman, A. G., Sternweis, P. C. and Bollag, G., Science **280:** 2112-4 (1998)

Hawkins, P. T., Eguinoa, A., Rong-Guo, Q., Stokoe, D., Cooke, F. T., Walters, R., Wennstrom, S., Claesson-Welsh, L., Evans, T., Symons, M. and Stephens, L., Curr. Biol. **5:** (1995)

Hawkins, P. T., Jackson, T. R. and Stephens, L. R., Nature **358:** 157-9 (1992)

Heldin, C. H., Ostman, A. and Ronnstrand, L., Biochim Biophys Acta **1378:** F79-113 (1998)

Heller, H. R., Morin, M., Guilherme, A. and Czech, M. P., J Biol Chem **271:** 10200-4 (1996)

Herrmann, C., Martin, G. A. and Wittinghofer, A., J Biol Chem **270:** 2901-5 (1995)

Hill, C. S., Wynne, J. and Treisman, R., Cell **81:** 1159-70 (1995)

Hirai, A., Nakamura, S., Noguchi, Y., Yasuda, T., Kitagawa, M., Tatsuno, I., Oeda, T., Tahara, K., Terano, T., Narumiya, S., Kohn, L. D. and Saito, Y., J Biol Chem **272:** 13-6 (1997)

Hodgkin, M. N., Pettitt, T. R., Martin, A., Michell, R. H., Pemberton, A. J. and Wakelam, M. J., Trends Biochem Sci **23:** 200-4 (1998)

House, C. and Kemp, B. E., Science **238:** 1726-1728 (1987)

Hu, K. Q. and Settleman, J., Embo J **16:** 473-83 (1997)

Ihara, K., Muraguchi, S., Kato, M., Shimizu, T., Shirakawa, M., Kuroda, S., Kaibuchi, K. and Hakoshima, T., J Biol Chem **273:** 9656-66 (1998)

Irie, K., Takase, M., Lee, K. S., Levin, D. E., Araki, H., Matsumoto, K. and Oshima, Y., Mol Cell Biol **13:** 3076-83 (1993)

Ishizaki, T., Maekawa, M., Fujisawa, K., Okawa, K., Iwamatsu, A., Fujita, A., Watanabe, N., Saito, Y., Kakizuka, A., Morii, N. and Narumiya, S., Embo J **15:** 1885-93 (1996)

Ishizaki, T., Naito, M., Fujisawa, K., Maekawa, M., Watanabe, N., Saito, Y. and Narumiya, S., Febs Lett **404:** 118-24 (1997)

Jan, L. Y. and Jan, Y. N., Curr Opin Cell Biol **9:** 155-60 (1997)
Jones, P. F., Jakubowicz, T., Pitossi, F. J., Maurer, F. and Hemmings, B. A., Proc. Natl. Acad. Sci. USA **88:** 4171 - 4175 (1991)

Jones, S. M., Klinghoffer, R., Prestwich, G. D., Toker, A. and Kazlauskas, A., Curr Biol **9:** 512-21 (1999)

Jonsson, U., Fagerstam, L., Roos, H., Ronnberg, J., Sjolander, S., Stenberg, E., Stahlberg, C., Urbaniczky, C., Ostlin, H. and Malmqvist, M., Biotechniques **11:** 620-527 (1991)

Karnam, P., Standaert, M. L., Galloway, L. and Farese, R. V., J Biol Chem **272:** 6136-40 (1997)

Katayama, S., Hirata, D., Arellano, M., Perez, P. and Toda, T., J Cell Biol **144:** 1173-86 (1999)

Kavran, J. M., Klein, D. E., Lee, A., Falasca, M., Isakoff, S. J., Skolnik, E. Y. and Lemmon, M. A., J Biol Chem **273:** 30497-508 (1998)

Keranen, L. M., Dutil, E. M. and Newton, A. C., Curr. Biol. **5:** 1394-1403 (1995)

Kimura, K., Ito, M., Amano, M., Chihara, K., Fukata, Y., Nakafuku, M., Yamamori, B., Feng, J. H., Nakano, T., Okawa, K., Iwamatsu, A. and Kaibuchi, K., Science **273:** 245-248 (1996)

Kitagawa, M., Shibata, H., Toshimori, M., Mukai, H. and Ono, Y., Biochem Biophys Res Commun **220:** 963-8 (1996)

Kitamura, T., Ogawa, W., Sakaue, H., Hino, Y., Kuroda, S., Takata, M., Matsumoto, M., Maeda, T., Konishi, H., Kikkawa, U. and Kasuga, M., Mol Cell Biol **18:** 3708-17 (1998)

Klippel, A., Reinhard, C., Kavanaugh, W. M., Apell, G., Escobedo, M. A. and Williams, L. T., Mol Cell Biol **16:** 4117-27 (1996)

Knighton, D., Zheng, J., Teneyck, L., Ashford, V., Xuong, N., Taylor, S. and Sowadski, J., Science **253:** 407-414 (1991)

Koelle, M. R., Curr Opin Cell Biol **9:** 143-7 (1997)

Kohn, A. D., Summers, S. A., Birnbaum, M. J. and Roth, R. A., J Biol Chem **271:** 31372-8 (1996)

Kohno, H., Tanaka, K., Mino, A., Umikawa, M., Imamura, H., Fujiwara, T., Fujita, Y., Hotta, K., Qadota, H., Watanabe, T., Ohya, Y. and Takai, Y., Embo J **15:** 6060-8 (1996)

Kosako, H., Goto, H., Yanagida, M., Matsuzawa, K., Fujita, M., Tomono, Y., Okigaki, T., Odai, H., Kaibuchi, K. and Inagaki, M., Oncogene **18:** 2783-8 (1999)

Kozma, R., Ahmed, S., Best, A. and Lim, L., Mol Cell Biol **16:** 5069-80 (1996)

Ktistakis, N. T., Bioessays **20:** 495-504 (1998)

Kumagai, N., Morii, N., Fujisawa, K., Nemoto, Y. and Narumiya, S., J Biol Chem **268:** 24535-24538 (1993)

Laemmli, U. K., Nature **227:** 680-685 (1970)

Lamaze, C., Chuang, T. H., Terlecky, L. J., Bokoch, G. M. and Schmid, S. L., Nature **382:** 177-9 (1996)

Lang, P., Gesbert, F., Delespinecarmagnat, M., Stancou, R., Pouchelet, M. and Bertoglio, J., Embo J **15:** 510-519 (1996)

Langhans, R. S., Wan, Y. and Huang, X. Y., Proc Natl Acad Sci U S A **92:** 8601-5 (1995)

Le Good. J., Ziegler, W. H., Parekh, D. B., Alessi, D. R., Cohen, P. and Parker, P. J., Science **281:** 2042-5 (1998)

Leevers, S. J., Paterson, H. F. and Marshall, C. J., Nature **369:** 411-414 (1994)

Lehninger, Principles of Biochemistry 730-735 (1988)

Leung, T., Manser, E., Tan, L. and Lim, L., J Biol Chem **270:** 29051-29054 (1995)

Leung, T., Chen, X. Q., Manser, E. and Lim, L., Mol Cell Biol **16:** 5313-27 (1996)

Leung, T., Chen, X. Q., Tan, I., Manser, E. and Lim, L., Mol Cell Biol **18:** 130-40 (1998)

Lu, Y. and Settleman, J., Genes Dev **13:** 1168-80 (1999)

Luberto, C. and Hannun, Y. A., J Biol Chem **273:** 14550-9 (1998)

Madaule, P., Eda, M., Watanabe, N., Fujisawa, K., Matsuoka, T., Bito, H., Ishizaki, T. and Narumiya, S., Nature **394:** 491-4 (1998)

Maniatis, T., Sambrook, J., Fritsch, E.F. Molecular Cloning, a Laboratory Manual (1989)

Manser, E., Leung, T., Salihuddin, H., Zhao, Z. S. and Lim, L., Nature **367:** 40-6 (1994)

Manser, E., Chong, C., Zhao, Z. S., Leung, T., Michael, G., Hall, C. and Lim, L., J Biol Chem **270:** 25070-25078 (1995a)

Manser, E., Leung, T. and Lim, L., Methods in Enzymology **256:** 130-135 (1995b)

Manser, E., Loo, T. H., Koh, C. G., Zhao, Z. S., Chen, X. Q., Tan, L., Tan, I., Leung, T. and Lim, L., Mol Cell **1:** 183-92 (1998)

Markby D.W., Onrust R., Bourne H.R. Science **262**: 1895-901 (1993)

Marshall, C. J., Curr Opin Cell Biol **8:** 197-204 (1996)

Martin, G. A., Bollag, G., McCormick, F. and Abo, A., Embo J **14:** (1995)

Matsui, T., Amano, M., Yamamoto, T., Chihara, K., Nakafuku, M., Ito, M., Nakano, T., Okawa, K., Iwamatsu, A. and Kaibuchi, K., Embo J **15:** 2208-16 (1996)

Matsuzawa, K., Kosako, H., Inagaki, N., Shibata, H., Mukai, H., Ono, Y., Amano, M., Kaibuchi, K., Matsuura, Y., Azuma, I. and Inagaki, M., Biochem Biophys Res Commun **234:** 621-5 (1997)

McCormick, F., Clark, B. F., la, C. T., Kjeldgaard, M., Norskov, L. L. and Nyborg, J., Science **230:** 78-82 (1985)

Mellor, H., Flynn, P., Nobes, C. D., Hall, A. and Parker, P. J., J Biol Chem **273:** 4811-4 (1998)

Mellor, H. and Parker, P. J., Biochem J **332**: 281-92 (1998)

Michiels, F., Stam, J. C., Hordijk, P. L., van, der, Kammen, Ra, Ruuls, Van, S. L., Feltkamp, C. A. and Collard, J. G., J Cell Biol **137:** 387-98 (1997)

Minden, A., Lin, A., Claret, F. X., Abo, A. and Karin, M., Cell **81:** 1147-1157 (1995)

Misra, S. and Hurley, J. H., Cell **97:** 657-66 (1999)

Missy, K., Van, P. V., Raynal, P., Viala, C., Mauco, G., Plantavid, M., Chap, H. and Payrastre, B., J Biol Chem **273:** 30279-86 (1998)

Moores, S. L., Schaber, M. D., Mosser, S. D., Rands, E., O'Hara, M. B., Garsky, V. M., Marshall, M. S., Pompliano, D. L. and Gibbs, J. B., J Biol Chem **266:** 14603-10 (1991)

Morrice, N. A., Fecondo, J. and Wettenhall, R. E. H., FEBS Letts. **351:** 171-175 (1994a)

Morrice, N. A., Gabrielli, B., Kemp, B. E. and Wettenhall, R. E., J Biol Chem **269:** 20040-6 (1994b)

Morrison, D. K. and Cutler, R. E., Curr Opin Cell Biol **9:** 174-9 (1997)

Mosch, H. U., Roberts, R. L. and Fink, G. R., Proc Natl Acad Sci U S A **93:** 5352-6 (1996)

Mukai, H., Kitagawa, M., Shibata, H., Takanaga, H., Mori, K., Shimakawa, M., Miyahara, M., Hirao, K. and Ono, Y., Biochem Biophys Res Commun **204:** 348-356 (1994)

Mukai, H. and Ono, Y., Biochem Biophys Res Commun **199:** 897-904 (1994)

Mukai, H., Toshimori, M., Shibata, H., Kitagawa, M., Shimakawa, M., Miyahara, M., Sunakawa, H. and Ono, Y., J Biol Chem **271:** 9816-22 (1996)

Mukai, H., Toshimori, M., Shibata, H., Takanaga, H., Kitagawa, M., Miyahara, M., Shimakawa, M. and Ono, Y., J Biol Chem **272:** 4740-6 (1997)

Murphy, C., Saffrich, R., Grummt, M., Gournier, H., Rybin, V., Rubino, M., Auvinen, P., Lutcke, A., Parton, R. G. and Zerial, M., Nature **384:** 427-32 (1996)

Nakagawa, O., Fujisawa, K., Ishizaki, T., Saito, Y., Nakao, K. and Narumiya, S., Febs Lett **392:** 189-93 (1996)

Nimnual, A. S., Yatsula, B. A. and Bar, S. D., Science **279:** 560-3 (1998)

Nishizuka, Y., Nature **308:** 693-695 (1984)

Nobes, C. D. and Hall, A., Cell **81:** 53-62 (1995)

Nobes, C. D., Hawkins, P., Stephens, L. and Hall, A., J Cell Sci 225-33 (1995)
Nonaka, H., Tanaka, K., Hirano, H., Fujiwara, T., Kohno, H., Umikawa, M., Mino, A. and Takai, Y., Embo J **14:** 5931-8 (1995)

Novick, P. and Zerial, M., Curr Opin Cell Biol **9:** 496-504 (1997)

Olson, M. F., Ashworth, A. and Hall, A., Science **269:** 1270-2 (1995)

Olson, M. F., Paterson, H. F. and Marshall, C. J., Nature **394:** 295-9 (1998)

Ono, Y., Fujii, T., Ogita, K., Kikkawa, U., Igarishi, K. and Nishizuka, Y., J. Biol. Chem. **263:** 6927-6932 (1988)

Ono, Y., Fujii, T., Ogita, K., Kikkawa, U., Igarashi, K. and Nishizuka, Y., Proc. Natl. Acad. Sci. USA **86:** 3099-3103 (1989)

Orr, J. W. and Newton, A. C., J. Biol. Chem. **269:** 27715-27718 (1994)

Palmer, F. B. and Dawson, R. M., Biochem J **111:** 629-36 (1969)

Palmer, R., Ridden, J. R. and Parker, P. J., FEBS Letts **356:** 5-8 (1994)

Palmer, R. H., Dekker, L. V., Woscholski, R., Le Good, A., Gigg, R. and Parker, P. J., J. Biol. Chem. **270:** 22412-22416 (1995a)

Palmer, R. H. and Parker, P. J., Bioch. J. **309:** 315-320 (1995)

Palmer, R. H., Ridden, J. and Parker, P. J., Eur. J. Biochem. **227:** 344-351 (1995b)

Parker, P. J., Coussens, L., Totty, N., Rhee, L., Young, S., Chen, E., Stabel, S., Waterfield, M. D. and Ullrich, A., Science **233:** 853-859 (1986)

Paterson, H. F., Self, A. J., Garrett, M. D., Just, I., Aktories, K. and Hall, A., J Cell Biol **111:** 1001-7 (1990)

Pawson, T., Nature **373:** 573-80 (1995)

Pawson, T. and Scott, J. D., Science **278:** 2075-80 (1997)

Peng, B., Morrice, N. A., Groenen, L. C. and Wettenhall, R. E., J Biol Chem **271:** 32233-40 (1996)

Peppelenbosch, M. P., Qiu, R. G., de, V., Smits, A. M., Tertoolen, L. G., de, L. S., McCormick, F., Hall, A., Symons, M. H. and Bos, J. L., Cell **81:** 849-56 (1995)

Perona, R., Montaner, S., Saniger, L., Sanchez, P. I., Bravo, R. and Lacal, J. C., Genes Dev **11:** 463-75 (1997)

Ponting, C. P. and Parker, P. J., Protein Sci **5:** 162-166 (1996)

Prasad, S., Soldatenkov, V. A., Srinivasarao, G. and Dritschilo, A., Int J Oncol **14:** 563-70 (1999)

Prive, G. G., Milburn, M. V., Tong, L., de, V. A., Yamaizumi, Z., Nishimura, S. and Kim, S. H., Proc Natl Acad Sci U S A **89:** 3649-53 (1992)

Pullen, N., Dennis, P. B., Andjelkovic, M., Dufner, A., Kozma, S. C., Hemmings, B. A. and Thomas, G., Science **279:** 707-10 (1998)

Pumiglia, K. M., LeVine, H., Haske, T., Habib, T., Jove, R. and Decker, S. J., J Biol Chem **270:** 14251-4 (1995)

Qadota, H., Python, C. P., Inoue, S. B., Arisawa, M., Anraku, Y., Zheng, Y., Watanabe, T., Levin, D. E. and Ohya, Y., Science **272:** 279-81 (1996)

Qiu, R. G., Chen, J., Kirn, D., McCormick, F. and Symons, M., Nature **374:** 457-9 (1995a)

Qiu, R. G., Chen, J., McCormick, F. and Symons, M., Proc Natl Acad Sci U S A **92:** 11781-5 (1995b)

Quilliam, L. A., Lambert, Q. T., Mickelson, Y. L., Westwick, J. K., Sparks, A. B., Kay, B. K., Jenkins, N. A., Gilbert, D. J., Copeland, N. G. and Der, C. J., J Biol Chem **271:** 28772-6 (1996)

Rameh, L. E., Tolias, K. F., Duckworth, B. C. and Cantley, L. C., Nature **390:** 192-6 (1997)

Reid, T., Furuyashiki, T., Ishizaki, T., Watanabe, G., Watanabe, N., Fujisawa, K., Morii, N., Madaule, P. and Narumiya, S., J Biol Chem **271:** 13556-60 (1996)

Reif, K., Nobes, C. D., Thomas, G., Hall, A. and Cantrell, D. A., Curr Biol **6:** 1445-55 (1996)

Reinstein, J., Schlichting, I., Frech, M., Goody, R. S. and Wittinghofer, A., J Biol Chem **266:** 17700-6 (1991)

Reiss, Y., Stradley, S. J., Gierasch, L. M., Brown, M. S. and Goldstein, J. L., Proc Natl Acad Sci U S A **88:** 732-6 (1991)

Ren, X. D., Bokoch, G. M., Traynor, K. A., Jenkins, G. H., Anderson, R. A. and Schwartz, M. A., Mol Biol Cell **7:** 435-42 (1996)

Ren, X. D., Kiosses, W. B. and Schwartz, M. A., Embo J **18:** 578-85 (1999)

Rickard, J. and Kreis, T., Trends in Cell Biology **6:** 178-183 (1996)

Ridley, A. J. and Hall, A., Cell **70:** 389-99 (1992)

Ridley, A. J., Paterson, H. F., Johnston, C. L., Diekmann, D. and Hall, A., Cell **70:** 401-10 (1992)

Ridley, A. J., Self, A. J., Kasmi, F., Paterson, H. F., Hall, A., Marshall, C. J. and Ellis, C., Embo J **12:** 5151-60 (1993)

Ridley, A. J. and Hall, A., Embo J **13:** 2600-2610 (1994)

Rodbell, M., Nature **284:** 17-22 (1980)

Rodriguez, V. P., Warne, P. H., Khwaja, A., Marte, B. M., Pappin, D., Das, P., Waterfield, M. D., Ridley, A. and Downward, J., Cell **89:** 457-67 (1997)

Rodriguez-Viciana, P., Warne, P. H., Dhand, R., VanHaesebroeck, B., Gout, I., Fry, M. J., Waterfield, M. D. and Downward, J., Nature **370**: 527-32 (1994)

Roof, R. W., Haskell, M. D., Dukes, B. D., Sherman, N., Kinter, M. and Parsons, S. J., Mol Cell Biol **18:** 7052-63 (1998)

Roth, M. G., Cell **97:** 149-52 (1999)

Rush, M. G., Drivas, G. and D'Eustachio, P., Bioessays **18:** 103-12 (1996)

Sahai, E., Alberts, A. S. and Treisman, R., Embo J **17:** 1350-61 (1998)

Sahai, E., Ishizaki, T., Narumiya, S. and Treisman, R., Curr Biol **9:** 136-45 (1999)

Salinovich, O. and Montelaro, R. C., Anal Biochem **156:** 341-7 (1986)

Sasaki, T. and Takai, Y., Biochem Biophys Res Commun **245:** 641-5 (1998)

Scheffzek, K., Ahmadian, M. R., Kabsch, W., Wiesmuller, L., Lautwein, A., Schmitz, F. and Wittinghofer, A., Science **277:** 333-8 (1997)

Scheffzek, K., Ahmadian, M. R. and Wittinghofer, A., Trends Biochem Sci **23:** 257-62 (1998)

Schmidt, A., Bickle, M., Beck, T. and Hall, M. N., Cell **88:** 531-42 (1997)

Schonwasser, D. C., Marais, R. M., Marshall, C. J. and Parker, P. J., Mol Cell Biol **18:** 790-8 (1998)

Sekine, A., Fujiwara, M. and Narumiya, S., J Biol Chem **264:** 8602-5 (1989)

Self, A., Paterson, H. and Hall, A., Oncogene **8:** 655-661 (1993)

Self, A. and Hall, A., Methods in Enzymology **256:** 67-76 (1995a)

Self, A. and Hall, A., Methods in Enzymology **256:** 1-13 (1995b)

Shaw, G., Bioessays **18:** 35-46 (1996)

Sheetz, M. P., Eur J Biochem **262:** 19-25 (1999)

Shibata, H., Mukai, H., Inagaki, Y., Homma, Y., Kimura, K., Kaibuchi, K., Narumiya, S. and Ono, Y., Febs Lett **385:** 221-4 (1996)

Sigal, I. S., Gibbs, J. B., D'Alonzo, J. S. and Scolnick, E. M., Proc Natl Acad Sci U S A **83:** 4725-9 (1986)

Simon, M. N., De, V. C., Souza, B., Pringle, J. R., Abo, A. and Reed, S. I., Nature **376:** 702-5 (1995)

Sorkin, A. and Water, C. M., BioEssays **15:** 375-381 (1993)

Stambolic, V., Suzuki, A., de, la, Pompa, Jl, Brothers, G. M., Mirtsos, C., Sasaki, T., Ruland, J., Penninger, J. M., Siderovski, D. P. and Mak, T. W., Cell **95:** 29-39 (1998)

Standaert, M., Bandyopadhyay, G., Galloway, L., Ono, Y., Mukai, H. and Farese, R., J Biol Chem **273:** 7470-7 (1998)

Stephens, L., Anderson, K., Stokoe, D., Erdjument, B. H., Painter, G. F., Holmes, A. B., Gaffney, P. R., Reese, C. B., McCormick, F., Tempst, P., Coadwell, J. and Hawkins, P. T., Science **279:** 710-4 (1998)

Stephens, L. R., Eguinoa, A., Erdjument, B. H., Lui, M., Cooke, F., Coadwell, J., Smrcka, A. S., Thelen, M., Cadwallader, K., Tempst, P. and Hawkins, P. T., Cell **89:** 105-14 (1997)

Stephens, L. R., Hughes, K. T. and Irvine, R. F., Nature **351:** 33-39 (1991)

Stephens, L. R., Jackson, T. R. and Hawkins, P. T., Biochim Biophys Acta **1179:** 27-75 (1993)

Stokoe, D. Macdonald, S. G.Cadwallader, K.Symons, M.Hancock, J. F., Science **264**: 1463-7 (1994)

Stokoe, D. and McCormick, F., Embo J **16:** 2384-96 (1997)

Stokoe, D., Stephens, L. R., Copeland, T., Gaffney, P. R., Reese, C. B., Painter, G. F., Holmes, A. B., McCormick, F. and Hawkins, P. T., Science **277:** 567-70 (1997)

Stoyanov, B., Volinia, S., Hanck, T., Rubio, I., Loubtchenkov, M., Malek, D., Stoyanova, S., Vanhaesebroeck, B., Dhand, R., Nurnberg, B. and et, a. I., Science **269:** 690-3 (1995)

Sudol, M., Oncogene **17**: 1469-74 (1998)

Takahashi, K., Sasaki, T., Mammoto, A., Takaishi, K., Kameyama, T., Tsukita, S. and Takai, Y., J Biol Chem **272:** 23371-5 (1997)

Takahashi, M., Mukai, H., Toshimori, M., Miyamoto, M. and Ono, Y., Proc Natl Acad Sci U S A **95:** 11566-71 (1998)

Tapon, N. and Hall, A., Curr Opin Cell Biol **9:** 86-92 (1997)

Tapon, N., Nagata, K., Lamarche, N. and Hall, A., Embo J **17:** 1395-404 (1998)

Taylor, S. J. and Shalloway, D., Curr Biol **6:** 1621-7 (1996)

Taylor, S. S. and Radzio-Andzelm, E., Structure **2:** 345-355 (1994)

Teramoto, H., Crespo, P., Coso, O. A., Igishi, T., Xu, N. and Gutkind, J. S., J Biol Chem **271:** 25731-4 (1996)

Toda, T., Dhut, S., Superti, F. G., Gotoh, Y., Nishida, E., Sugiura, R. and Kuno, T., Mol Cell Biol **16:** 6752-64 (1996)

Toda, T., Shimanuki, M. and Yanagida, M., Embo J **12:** 1987-95 (1993)

Toker, A., Curr Opin Cell Biol **10:** 254-61 (1998)

Tolias, K. F., Cantley, L. C. and Carpenter, C. L., J Biol Chem **270:** 17656-9 (1995)

Tolias, K. F., Couvillon, A. D., Cantley, L. C. and Carpenter, C. L., Mol Cell Biol **18:** 762-70 (1998)

Traverse, S., Cohen, P., Paterson, H., Marshall, C., Rapp, U. and Grand, R. J., Oncogene **8:** 3175-81 (1993)

Treisman, R., Embo J **14:** 4905-13 (1995)

Treisman, R., Curr Opin Cell Biol **8:** 205-15 (1996)

Uehata, M., Ishizaki, T., Satoh, H., Ono, T., Kawahara, T., Morishita, T., Tamakawa, H., Yamagami, K., Inui, J., Maekawa, M. and Narumiya, S., Nature **389:** 990-4 (1997)

Valgeirsdottir, S., Claesson, W. L., Bongcam, R. E., Hellman, U., Westermark, B. and Heldin, C. H., J Cell Sci **111**: 1973-80 (1998)

Van, A. L. and D'Souza, S. C., Genes Dev **11:** 2295-322 (1997)

Vanhaesebroeck, B., Leevers, S. J., Panayotou, G. and Waterfield, M. D., Trends Biochem. Sciences **22:** 267-72 (1997)

Venkateswarlu, K., Oatey, P. B., Tavare, J. M. and Cullen, P. J., Curr Biol **8:** 463-6 (1998)

Vincent, S. and Settleman, J., Mol Cell Biol **17:** 2247-56 (1997)

Vlahos, C. J., Matter, W. F., Hui, K. Y. and Brown, R. F., J Biol Chem **269:** 5241-8 (1994)

Volinia, S., Dhand, R., Vanhaesebroeck, B., MacDougall, L. K., Stein, R., Zvelebil, M. J., Domin, J., Panaretou, C. and Waterfield, M. D., Embo J **14:** 3339-48 (1995)

Warne, P. H., Viciana, P. R. and Downward, J., Nature **364:** 352-5 (1993)

Watanabe, G., Saito, Y., Madaule, P., Ishizaki, T., Fujisawa, K., Morii, N., Mukai, H., Ono, Y., Kakizuka, A. and Narumiya, S., Science **271:** 645-8 (1996)

Watanabe, N., Kato, T., Fujita, A., Ishizaki, T. and Narumiya, S., Nature Cell Biology **1:** 136-143 (1999)

Watanabe, N., Madaule, P., Reid, T., Ishizaki, T., Watanabe, G., Kakizuka, A., Saito, Y., Nakao, K., Jockusch, B. M. and Narumiya, S., Embo J **16:** 3044-56 (1997)

Wennstrom, S., Hawkins, P., Cooke, F., Hara, K., Yonezawa, K., Kasuga, M., Jackson, T., Claesson, W. L. and Stephens, L., Curr Biol **4:** 385-93 (1994)

Westwick, J. K., Lambert, Q. T., Clark, G. J., Symons, M., Van, A. L., Pestell, R. G. and Der, C. J., Mol Cell Biol **17:** 1324-35 (1997)

Whiteford, C. C., Brearley, C. A. and Ulug, E. T., Biochem J **323**: 597-601 (1997)

Willumsen, B. M., Papageorge, A. G., Kung, H. F., Bekesi, E., Robins, T., Johnsen, M., Vass, W. C. and Lowy, D. R., Mol Cell Biol **6:** 2646-54 (1986)

Woscholski, R. and Parker, P. J., Trends Biochem Sci **22:** 427-31 (1997)

Yamada, K. M. and Geiger, B., Curr Opin Cell Biol **9:** 76-85 (1997)

Yamamoto, M., Marui, N., Sakai, T., Morii, N., Kozaki, S., Ikai, K., Imamura, S. and Narumiya, S., Oncogene **8:** 1449-55 (1993)

Yamochi, W., Tanaka, K., Nonaka, H., Maeda, A., Musha, T. and Takai, Y., J Cell Biol **125:** 1077-93 (1994)

Yeargin, J. and Haas, M., Curr Biol **5:** 423-31 (1995)

Yeramian, P., Chardin, P., Madaule, P. and Tavitian, A., Nucleic Acids Res **15:** 1869 (1987)

Zalcman, G., Closson, V., Camonis, J., Honore, N., Rousseau, M. M., Tavitian, A. and Olofsson, B., J Biol Chem **271:** 30366-74 (1996)

Zalcman, G., Closson, V., Linares, C. G., Lerebours, F., Honore, N., Tavitian, A. and Olofsson, B., Oncogene **10:** 1935-45 (1995)

Zhang, X. F., Settleman, J., Kyriakis, J. M., Takeuchi, S. E., Elledge, S. J., Marshall, M. S., Bruder, J. T., Rapp, U. R. and Avruch, J., Nature **364:** 308-13 (1993)

Zhao, Z. S., Leung, T., Manser, E. and Lim, L., Mol Cell Biol **15:** 5246-57 (1995)

Zheng, Y., Zangrilli, D., Cerione, R. A. and Eva, A., J Biol Chem **271:** 19017-20 (1996)

Ziegler, W. H., Parekh, D. B., Le, G. J., Whelan, R. D., Kelly, J. J., Frech, M., Hemmings, B. A. and Parker, P. J., Curr Biol **9:** 522-9 (1999)

Zong, H., Raman, N., Mickelson, Y. L., Atkinson, S. J. and Quilliam, L. A., J Biol Chem **274:** 4551-60 (1999)